TECHNISCHE UNIVERSITÄT MÜNCHEN

TUM School of Natural Sciences

Tunable polymer architectures for aliphatic polycarbonates *via* co- and terpolymerization of epoxides and CO_2

Alina Constanze Denk

Vollständiger Abdruck der von der TUM School of Natural Sciences der Technischen Universität München zur Erlangung einer

Doktorin der Naturwissenschaften (Dr. rer. nat.)

genehmigten Dissertation.

Vorsitz:	Prof. Dr. Martin Elsner
Prüfer*innen der Dissertation:	1. Prof. Dr. Dr. h.c. Bernhard Rieger
	2. Prof. Dr. Tom Nilges

Die Dissertation wurde am 28.07.2023 bei der Technischen Universität München eingereicht und durch die TUM School of Natural Sciences am 26.09.2023 angenommen.

Die vorliegende Arbeit wurde in der Zeit von Dezember 2019 bis Dezember 2023 am WACKER-Lehrstuhl für Makromolekulare Chemie, Technische Universität München, unter der Betreuung von Herrn Prof. Dr. Dr. h.c. Bernhard Rieger angefertigt.

Danksagung

An erster Stelle danke ich Herrn Prof. Dr. Dr. h.c. Bernhard Rieger für die Möglichkeit, meine Doktorarbeit am WACKER-Lehrstuhl für Makromolekulare Chemie der Technischen Universität München unter seiner Leitung anzufertigen. Vielen Dank für die wertvollen Diskussionen, die Freiheiten in der Arbeit am Lehrstuhl und vor allem für das entgegengebrachte Vertrauen im Rahmen der Industriekooperation.

Dr. Carsten Troll möchte ich sowohl für die allgemeine Organisation des Lehrstuhls als auch für die Unterstützung bei sämtlichen technischen Problemen danken. Ohne ihn wäre weder der Aufbau noch der Betrieb des Dosiersystems oder einer der legendären Makro-Grillabende möglich gewesen. Außerdem danke ich Dr. Sergei Vagin für das Teilen seines unerschöpflichen Wissens und für seine Zeit und Geduld, wenn es darum ging, mal wieder etwas an der GPC zu reparieren. Weiterhin danke ich Dr. Sebastian Kernbichl für die herzliche Aufnahme am Lehrstuhl in meiner Masterarbeit, der wertvollen Vorarbeit und der hervorragenden Einarbeitung in mein Promotionsthema.

Vielen Dank auch den Studentinnen und Studenten, die ich in dieser Zeit in ihren Abschlussarbeiten und Forschungspraktika betreuen durfte und die mich mit ihrer praktischen Arbeit im Labor fleißig unterstützt haben. Vor allem meiner Masterandin Emilia Fulajtar, die durch ihre Ausdauer und Eigeninitiative jede noch so große Herausforderung und all die kniffligen Probleme ihres Masterarbeitsthemas angegangen ist. Es hat mir sehr viel Freude bereitet ihren Weg ein Stück weit zu begleiten.

Besonders gerne werde ich mich an die schönen Lehrstuhl-Grillabende, Hüttenwochenenden und gemeinsamen Aktivitäten erinnern. Vielen Dank dabei an den gesamten Lehrstuhl, aber vor allem an Dr. Christopher Thomas, Dr. Andreas Schaffer, Magdalena Kleybolte und Moritz Kleybolte für Tennis Matches, Spezi-Exzesse und eine unvergessliche Zeit in San Diego.

Ein besonderer Dank gilt meinen Eltern, die mir immer wieder das Vertrauen an mich selbst zurückgeben, wenn ich glaube es verloren zu haben.

Zu guter Letzt: Danke, Michi, dass du es schaffst mich am tiefsten Punkt noch zum Lachen zu bringen und mich motivierst immer weiterzumachen.

Abbreviations

Symbol	Description
AIBN	azobisisobutyronitrile
BDI	*β*-diiminate
BPA	bisphenol A; 2,2-bis(4-hydroxyphenyl)propane
BPZ	bisphenol Z; 1,1-bis(4-hydroxyphenyl)cyclohexane
cat.	catalyst
CHO	cyclohexene oxide
cPC	cyclic propylene carbonate
CTA	chain transfer agent
DEVP	diethyl vinylphosphonate
ΔG_f	free energy of formation
DMAP	(4-dimethylamino)pyridine
DOSY	diffusion ordered spectroscopy
DSC	differential scanning calorimetry
Et	ethyl
et al.	and others (Latin *et alii*)
GPC	gel permeation chromatography
GTP	group-transfer polymerization
IPOx	2-isopropenyl-2-oxazoline
IR	infrared
LCST	lower critical solution temperature
LO	limonene oxide
MALDI	matrix-assisted laser desorption/ionization
*m*CPBA	*meta*-chloroperoxybenzoic acid
Me	methyl

MMA	methyl methacrylate
MS	mass spectrometry
MTP	methanol-to-propylene
NBS	*N*-bromosuccinimide
NMR	nuclear magnetic resonance spectroscopy
PCHC	poly(cyclohexene carbonate)
PDEVP	poly(diethyl vinylphosphonate)
PDMS	poly(dimethylsiloxane)
Ph	phenyl
PHB	poly(3-hydroxybutyrate)
PLA	poly(lactic acid)
PLC	poly(limonene carbonate)
P_m	propability of a diad being *meso*
PMMA	poly(methyl methacrylate)
PO	propylene oxide
PPC	poly(propylene carbonate)
PPNCl	bis(triphenylphosphine)iminium chloride
P_r	propability of a diad being *racemo*
PS	poly(styrene)
PVC	poly(vinyl chloride)
P2VP	poly(2-vinylpyridine)
RAFT	reversible addition-fragmentation chain transfer
REM-GTP	rare earth metal-mediated group-transfer polymerization
ROCOP	ring-opening copolymerization
sym-collidine	2,4,6-trimethylpyridine
T_g	glass transition temperature
TGA	thermogravimetric analysis

THF	tetrahydrofuran
TMS	trimethylsilyl
TOF	turn-over frequency
TPP	tetraphenyl porphyrin
2VP	2-vinylpyridine
ZnGA	zinc glutarate

Publication list

- A. Denk, P. Großmann, B. Rieger*. The soft side of aliphatic polycarbonates: with PCHC-b-PDMS copolymers towards ductile materials. *Macromolecules*, *56* (11), 4318–4324, (10.1021/acs.macromol.2c02433).

- A. Denk, E. Fulajtar, C. Troll, B. Rieger*. Controlled synthesis of statistical polycarbonates based on epoxides and CO_2. Macromolecular Materials and Engineering, 2300097, (10.1002/mame.202300097).
- A. Denk‡, S. Kernbichl‡, A. Schaffer, M. Kränzlein, T. Pehl, B. Rieger*. Heteronuclear, monomer-selective Zn/Y catalyst combines copolymerization of epoxides and CO_2 with group-transfer polymerization of Michael-type monomers. *ACS Macro Letters* **2020**, *9* (4), 571–575, (10.1021/acsmacrolett.9b01025).

- A. Denk, B. Rieger*, Book chapter in: *Advances in Polymer Science*. Springer, Berlin, Heidelberg. **2022**, 1–19 “Biobased Synthesis and Biodegradability of CO_2-Based Polycarbonates”.

‡These authors contributed equally; *Corresponding authors

Conference contributions

- A. Denk, S. Kernbichl, A. Schaffer, M. Kränzlein, T. Pehl, B. Rieger, *ACS Spring* **2022** (conference), San Diego, oral presentation: “Think and link in two directions: A monomer-selective heteronuclear Zn/Y catalyst for block polymers from aliphatic polycarbonates and functional polyolefins”.

In this Dissertation selected results of my Master’s thesis are included.

Index

1. Introduction

Biopolymers, such as polypeptides (proteins) in wool or silk, have a long history of being deployed as materials for humanity.[1] With time the growing industrial processing also extends to artificially manipulated polymeric materials from natural feeds. Caoutchouc, a naturally derived polymer, was further processed by vulcanization with sulfur giving a cross-linked, elastic product and has great industrial relevance until today.[2] Another biopolymer being applied in further reactions towards an industrial polymer was cellulose. Nitration of this biopolymer resulted in nitrocellulose, which was used as an explosive, coating, or celluloid film.[3] With the development of synthetic polymers, it was possible to enlarge the selection of available materials and allowed a targeted variation of polymer properties. Bakelite,[4] polystyrene (PS),[2] and poly(vinyl chloride) (PVC)[5] are only a few examples developed in the 19th century with partly even high importance for industry and everyday life until today (Figure 1).

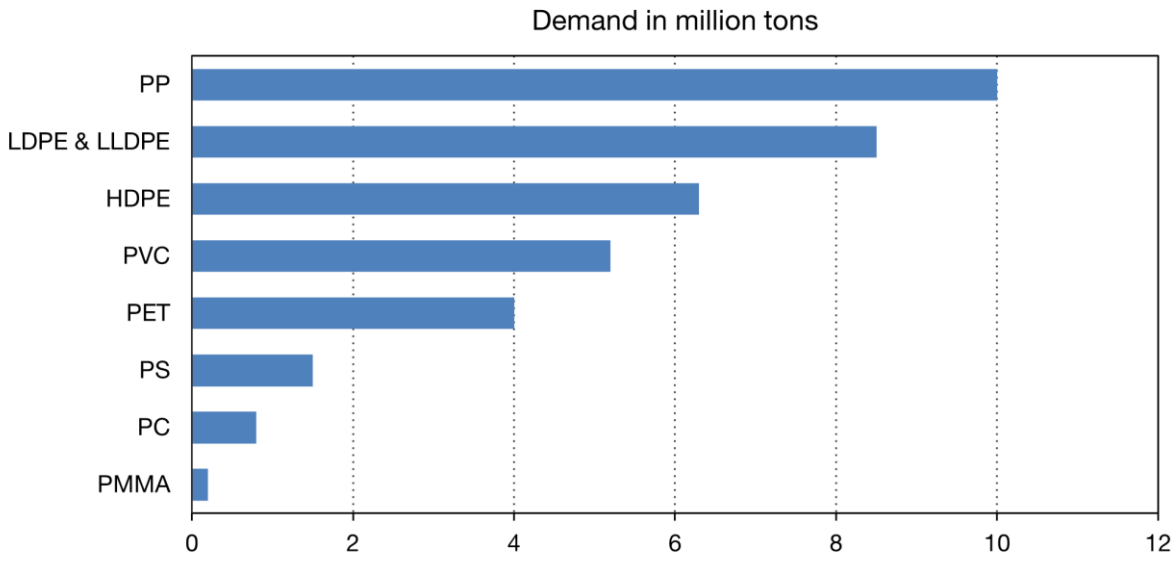

Figure 1. Plastic demand in the European Union in 2021 by polymer type, adapted from "Plastics – the Facts 2022" by PlasticsEurope.[6]

In 1956 *H. Schnell* developed the synthesis of high molecular weight polycarbonate (PC) and two years later their industrial production was launched.[7-8] As of 2022, over 7.1 Mt of bisphenol A-based PCs are produced worldwide per year and the demand is growing continuously.[9] They find application mainly in the automotive and electronics industry (Figure 2) due to their toughness in combination with transparency and flame-retardancy.[10]

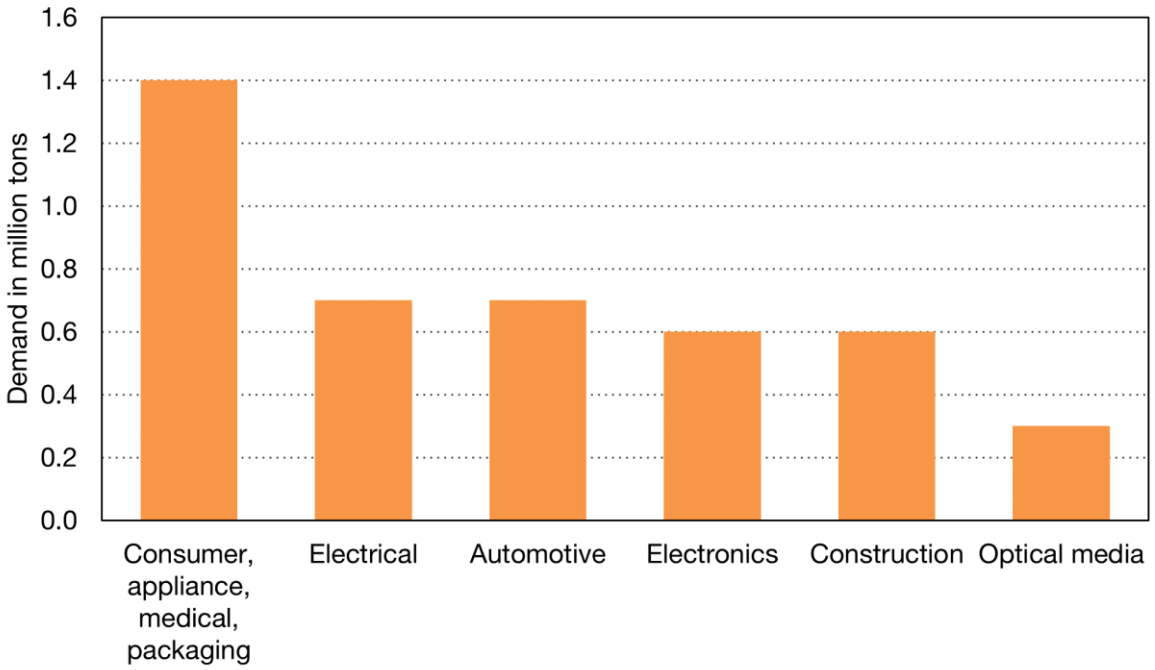

Figure 2. Worldwide PC demand in 2017 by application, adapted from "Capital Markets Day 2018 Presentation" by Covestro.[11]

However, the majority of synthetic polymers, including polycarbonate, is based on fossil resources, which are limited.[6] Even though it is expected that their limit will not be reached before 2050 with the current rate of consumption, the interest in renewable resources is growing.[12] For 2021 the world market share of bio-based plastics was 1.5%, but studies expect the production of bioplastics to continuously increase in the next years (Figure 3).[6, 13] In this context the term *bioplastic* is often used, but rarely defined precisely. One part of the definition is concerning the origin of the raw materials, where polymers extracted from biomass or synthesized from monomers originating from renewable resources are called biopolymers. Furthermore, polymers fall into the category bioplastic, which are synthesized *via* a biological process, but not necessarily from renewable sources. The third reason why a polymer can be called a biopolymer is based on the polymer's degradability in the environment.[14] It must be mentioned that these properties are not necessarily going hand in hand. For example polyethylene can be synthesized from dehydrated bioethanol as sustainable resource, but is not biodegradable.[15-16] The industrially most important biodegradable polymer is poly(lactic acid) (PLA), which is mainly used as packaging materials.[13] Utilization and incorporation of CO_2 does not necessarily end in a biodegradable plastic but provides an interesting opportunity to make use of an abundant and non-toxic greenhouse gas. Its application as a monomer for polycarbonate synthesis is a part of this work. Exemplarily, its copolymerization with limonene oxide yields a bio-based material,

which is an especially captivating case as the epoxide can be synthesized from limonene extracted from citrus fruit waste.[17-18] The related poly(propylene carbonate) is another example for a biodegradable polymer and features an impressive CO_2 content of 43wt%.[19-20]

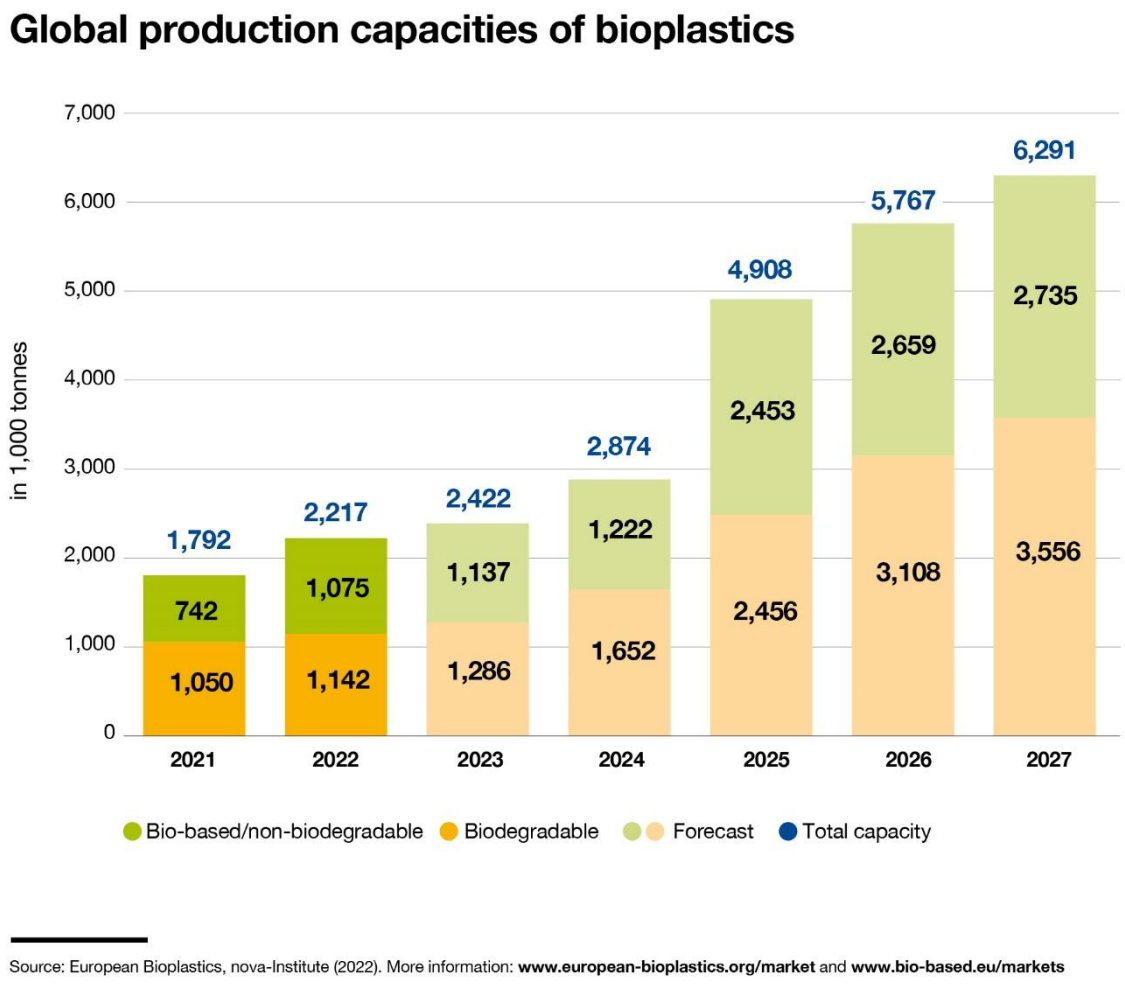

Figure 3. Global production capacities in 2021, and 2022, and a forecast for 2023 – 2027, adopted from "Bioplastics market data" by European Bioplastics e.V.[13]

The focus of this dissertation is the continuous improvement of material properties *via* tuning the polymer structure and extending the combination of different monomer and polymer types.

2. Theory

2.1 Polycarbonates

In the developing polymer industry of the 20th century, a groundbreaking innovation was the development of polycarbonates (PCs), where in 1958 *Bayer AG* began with a large-scale production under the brand name Makrolon®.[8] These polymers were synthesized *via* polycondensation of bisphenol A (BPA) and phosgene in the presence of sodium hydroxide (Scheme 1, (A)).[7] An alternative for phosgene is diphenyl carbonate, which reacts with BPA in a melt transesterification process (see Scheme 1, (B)). In this pathway phenol is formed as a byproduct and needs to be removed from the reaction *via* distillation.[10]

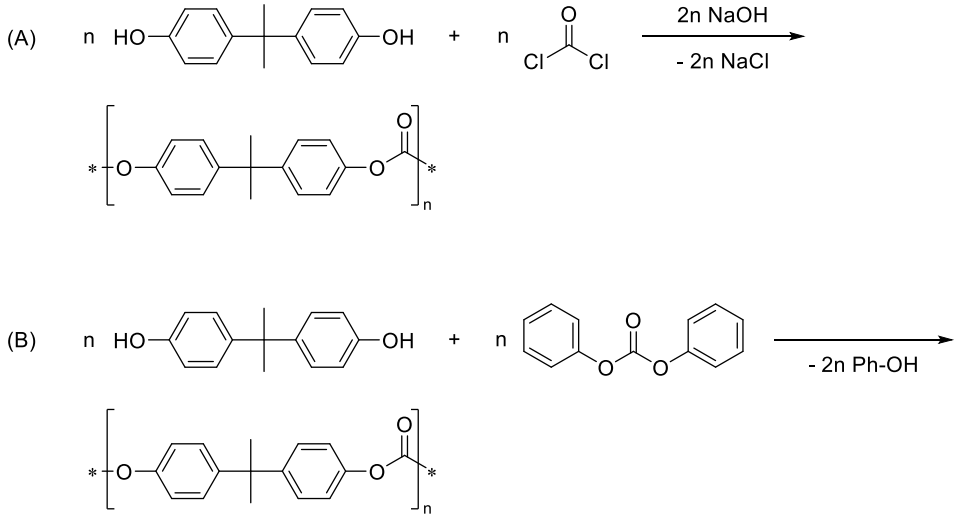

Scheme 1. Synthesis of BPA-based aromatic PC from BPA and phosgene (A) or from BPA and diphenyl carbonate (B).

With the variation of the bisphenol monomer the properties of the resulting PC can be adjusted. The incorporation of 1,1-bis(4-hydroxyphenyl)cyclohexane (BPZ) as comonomer besides BPA results in a reduced crystallinity of the PC. Another comonomer is 1,4'-dihydroxydiphenyl, which improves the product's notched impact strength.[10] Properties like toughness and tensile strength, heat-resistance and flame-retardancy, together with transparency are the reason for the growth of this thermoplastic into a key engineering plastic in the industry.[21] The incorporation of other polymer units allows further tuning of the mechanical or thermal properties of the polymer. A block copolymer from PC and polyether combines the tensile strength of PCs with elastic segments of polyethers.[22] Another example for such a thermoplastic elastomer is a copolymer from PC with polysiloxanes. These siloxane blocks improve the impact toughness of the product even at low temperatures.[22-23]

The health hazards posed by phosgene[24] and BPA[25] lead to an inevitable development of aromatic PCs avoiding these educts. Furthermore, the synthesis of novel polymers from sustainable resources is of high interest. Having a look at the class of aliphatic PCs, it stands out that they offer both high variability in their starting materials and the possibility of using CO_2 as a C1 building block for polymer synthesis. One example for a monomer from renewable resources is isosorbide. Its copolymerization with diacids or diols and a diarylcarbonate forms Durabio®, an industrially applicable material, sold by *Mitsubishi Chemical Performance Polymers*.[26] Another pathway to sustainable PCs is the copolymerization of epoxides, that can be obtained from petroleum-free sources, and CO_2, a non-toxic and abundant greenhouse gas.[27-28] The resulting polymer is an aliphatic PC due to the alternating incorporation of CO_2 and the epoxide leads to carbonate junctions between the aliphatic motifs (Scheme 2).

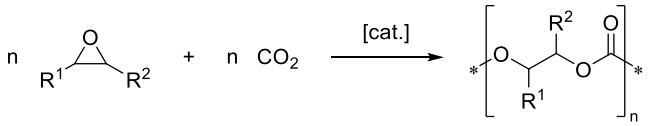

Scheme 2. General synthesis of aliphatic PCs from epoxides and CO_2.

Initially, aliphatic PCs were unable to compete regarding thermal stability and hydrolysis resistance with PCs derived from aromatic monomers.[29],[30] An important example of an aliphatic PC with commercial relevance as material for optical lenses is CR-39®, a polymer based on diethylene glycol bis(allyl carbonate).[10] Aliphatic PCs are furthermore promising materials in medicinal engineering due to their good biocompatibility and are applied in tissue engineering and drug delivery systems.[30],[31]

2.1.1 Catalysts for the copolymerization of epoxides with CO_2

The opportunity to use a non-toxic and widely abundant greenhouse gas in syntheses makes CO_2 an attractive molecule, but its thermodynamic stability (ΔG_f = -394 kJ mol^{-1}) causes challenges in its application as monomer.[32] To enable its use, a catalytic system is required to overcome this energy barrier. In this context, *Inoue et al.* developed in 1969 a heterogeneous catalyst system for the copolymerization of epoxides and CO_2 based on diethyl zinc and water.[33] Following these findings *Soga et al.* combined $Zn(OH)_2$ and aliphatic dicarboxylic acids for the catalysis of the copolymerization. Thereof the combination of $Zn(OH)_2$ and glutaric acid (ZnGA) showed the highest activity in the copolymerization of propylene oxide (PO) and CO_2 and is used in the industrial production of poly(propylene

carbonate) (PPC).[34] The bimetallic mechanism of this air-stable catalytic system, was reported by the group of *Rieger*. They stated that the interaction of two zinc centers on the catalyst surface is crucial for the alternating insertion of PO and CO_2 into the polymer. The distance between these adjacent catalytic centers has a direct influence on the activity of the catalyst in the copolymerization.[35]

Even though the heterogeneous catalysis system has a dominating relevance in the epoxide/CO_2 copolymerization, the interest in homogeneous catalysts is high as they offer a high variability in their structure. The defined active site of a homogeneous catalyst can be altered by exchanging the metal center, modification of the ligand or variation of the initiating group. Thereby the catalyst's characteristics, for example selectivity or activity, in a specific reaction can be tailored. The first homogeneous catalyst that allowed the synthesis of PPC with defined molecular weights was an aluminum porphyrin catalyst ((TPP)AlCl/$EtPh_3PBr$, Figure 4). The copolymers featured narrow polydispersities (< 1.1) and could furthermore be combined with polyesters towards AB or ABA block copolymers.[36] One challenge in the copolymerization of PO and CO_2 is the competing back-biting of the chain end coordinated to the metal center into the polymer chain. Calculations of *Luinstra et al.* showed that back-biting of a carbonate end group has lower activation energies than of an alkoxy chain end and is therefore more likely.[37] The unwanted side reaction generates cyclic carbonate as a byproduct (Scheme 3) and is especially dominating with zinc phenoxide complexes (Figure 4) as catalysts.[38-39] Additionally, not only cyclic propylene carbonate (cPC) is produced, but often a part of the CO_2 is released again as well, which can lead to an increased number of polyether moieties in the polycarbonate chain.[40]

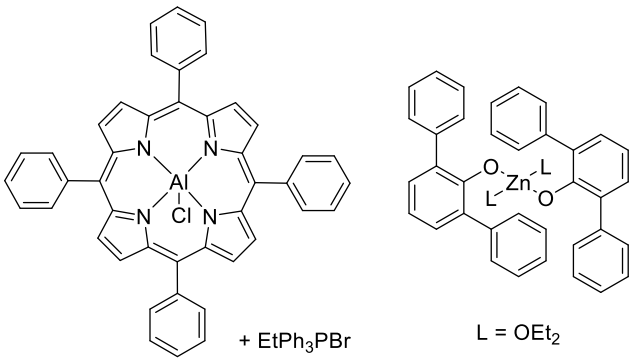

Figure 4. Aluminum porphyrine (left) and zinc phenoxide complexes (right) as used by *Aida et al.* and *Darensbourg et al.* as catalysts for PO/CO_2 copolymerization.[36, 38]

Although the cyclic carbonate can be used as a monomer in the synthesis of PCs *via* a different pathway, the side-reaction lowers the efficiency of the direct copolymerization of epoxide and CO_2 and should therefore be reduced to a minimum. An increased selectivity for

the polymer over the cyclic carbonate can be achieved by tuning the applied catalyst for this reaction, for example with sterically demanding groups.[41],[42] Lowering the temperature can also lead to a favored generation of the polymer as its rate is less dependent on temperature than the rate of cyclic carbonate formation.[39]

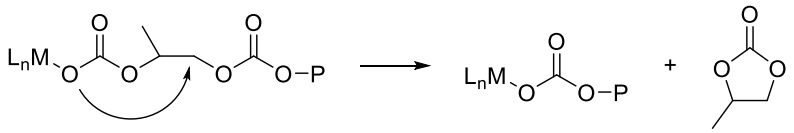

Scheme 3. Back-biting of a carbonate end group into the polymer chain (P = PPC chain) leading to the generation of a thermodynamically stable cPC during copolymerization of PO and CO_2.[37]

The probability of cyclic carbonate formation is less likely in the copolymerization of cyclohexene oxide (CHO) and CO_2, because cyclic cyclohexene carbonate is thermodynamically less stable than cPC.[38-39] Catalysts based on porphyrin or phenoxide ligands were also applied in the synthesis of poly(cyclohexene carbonate) (PCHC).[36, 38, 43] *Mang et al.* reported an own catalyst system with chromium as metal center, which employed supercritical CO_2 in the copolymerization towards PCHC.[44] Besides chromium also aluminum and especially zinc are used as active sites.[39, 45] In their work with phenoxide complexes the group of *Darensbourg* reported not only copolymers from PO and CHO with CO_2, but also terpolymers with both epoxides as mixed feedstock.[38] A more prominent side reaction in the PCHC synthesis is the subsequent insertion of two or more epoxide molecules, which leads to ether instead of carbonate linkages in the polymer. Especially the phenoxide system can catalyze the homopolymerization of the epoxide, which is why one strategy to overcome the generation of polyether units during copolymerization is the addition of the catalyst after pressurizing the reaction vessel with CO_2.[39]

Another catalyst class are salicylaldimine (salen) complexes, which can work at mild temperatures and CO_2 pressures as low as 1 bar.[46] The high variability of the catalytic system allows tuning it towards a selective synthesis of the alternating polymer.[47] A fully conjugated ligand backbone leads to a favored formation of polymer instead of cyclic carbonate in the reaction of PO and CO_2.[48] *Darensbourg et al.* could furthermore show that the introduction of electron donating substituents results in an increase of turn-over frequency (TOF = 1150 h^{-1}) for the copolymerization of CHO and CO_2. At the same time though these complexes reduced the selectivity for polymer formation in the PO/CO_2 reaction.[49] The mentioned catalysts consist of a salen ligand coordinating to a metal center, which can be varied from Al(III) over Cr(III) to Co(III), and are accompanied by a nucleophilic co-catalyst. Ring-opening of the epoxide monomer requires pre-activation since the carbonate chain end is a weak

nucleophile. The pre-coordination of a second catalyst molecule or a co-catalyst to the epoxide activates the oxirane for the copolymerization towards PCs. A system with bis(triphenylphosphine)-iminium chloride (PPNCl) or (4-dimethylamino)pyridine (DMAP) as co-catalyst shows an increased activity in the copolymerization.[50] To select a suitable co-catalyst it is again necessary to match the compound to the used epoxide. While a salen complex accompanied with PPNCl as a co-catalyst leads to an increase in activity in the copolymerization of CHO and CO_2, the selectivity of the PO/CO_2 copolymerization shifts towards the generation of cPC when PPNCl is used.[51] At the same time the co-catalyst can also coordinate to the catalyst, where it is competing with the monomer and can lead to a longer initiation phase of the reaction.[48] This initiation time is reduced when a more nucleophilic initiation group, as for example an azide group, is introduced at the catalyst center.[52] A high selectivity of the cobalt salen complex by *Seong et al.* resulted in the formation of high molecular weight PC terpolymers from two epoxides and CO_2. The epoxide monomer feedstock consisted of PO, CHO, 1-hexene oxide, and 1-butene oxide and the combination of monomers together with their ratio in the final terpolymer allowed tuning of the thermal properties of the product.[53] The group of *Lee* conducted detailed studies on the variability of salen ligands. By introducing quaternary ammonium salts into the ligand (Figure 5) TOFs of up to 26,000 h^{-1} for the copolymerization of PO and CO_2 were reported, which are, to the best of our knowledge, the highest until today.[54-55]

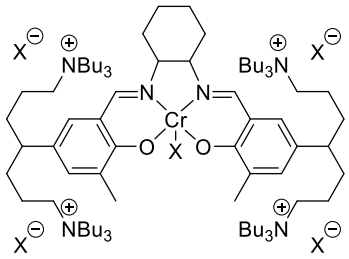

Figure 5. Highly active chromium salen complex containing quaternary ammonium salts in the ligand structure (X = BF_4).[54]

Commonly, the standard reaction to compare catalyst activities is the copolymerization of CHO and CO_2. With the development of *β*-diiminate (BDI) zinc complexes by the group of *Coates* copolymerizations at low temperatures (20–50 °C) and low CO_2 pressures (< 10 bar) were possible without the need for a co-catalyst. At the same time the activity of the catalysis could be increased significantly (TOF = 235–247 h^{-1}).[56] The variability of the ligand system allows the introduction of electron withdrawing groups at the diimine backbone, as for example trifluoromethyl or cyano groups, leading to an increased Lewis acidity at the zinc center and thus further increase in activity of the catalyst.[57] However, a combination of

electron withdrawing groups for maximum electron deficiency at the zinc center results in inactivation of the complex.[41] A complex with electron withdrawing trifluoromethyl groups at the backbone and ethyl substituents at the aromatic rings shows a TOF of 4800 h^{-1},[58] and with bis(trimethylsilyl)amido ($N(TMS)_2$) as initiation group the activity of the catalyst increased further up to 5520 h^{-1}.[59] The BDI^{CF3}-Zn-$N(TMS)_2$ catalyst (Figure 6) enabled the copolymerization of a broad feedstock of epoxide monomers with CO_2 and furthermore the terpolymerization of two epoxides with CO_2.[59]

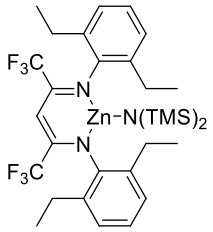

Figure 6. BDI zinc complex with electron withdrawing CF_3 groups at the ligand and $N(TMS)_2$ as initiating group as developed by *Reiter et al.* for epoxide/CO_2 co- and terpolymerization.[59]

Bridging initiating groups, as for example acetate, can lead to a dimerization of BDI zinc complexes. In this case the steric bulk of the substituents on the aryl group is decisive for dimerization, which is important since the mechanism of the ring-opening copolymerization (ROCOP) of epoxides and CO_2 most likely proceeds *via* a bimetallic mechanism.[50, 60] Sterically demanding groups like phenyl substituents hinder the dimerization and thus result in inactive complexes.[61] On the other side with a minimum steric bulk from methyl substituents tightly bound dimers are generated, which are unreactive while the distance between the zinc centers (3.81 Å) is too low for coordination and insertion of the monomers as well.[61] With a medium sterically demanding substituent, i.e. ethyl or isopropyl dimerizing catalysts with good catalytic activities are synthesized.[61-62] In these active catalyst dimers the optimized zinc-zinc distance measures about 4 Å.[63]

Applying the knowledge from mechanistic studies, which show a dinuclear nature of the ROCOP, bridged complexes with two active sites have been developed.[35, 61] Based on the reduced *Robson*-type ligand the group of *Williams* developed a variety of dinuclear catalysts (Figure 7, left). These are already active at low CO_2 pressures (1–10 bar) and with two zinc centers in close proximity TOFs of 25 to 140 h^{-1} were reported for the copolymerization of CHO and CO_2.[64] Other metals used as active centers in these complexes are magnesium, iron, or cobalt resulting in similar activities of 29 to 172 h^{-1} for the CHO/CO_2 copolymerization.[65-67] The group of *Rieger* based their design of a bridged catalyst on their previous work with BDI zinc complexes. The two BDI ligand moieties in these complexes are

connected *via* their aryl substituents and the distance between the zinc centers can be adjusted with the length and rigidity of the bridging units. With the introduction of electron-withdrawing trifluoromethyl groups a TOF of up to 155,000 h^{-1} in the copolymerization of CHO and CO_2 was reported (Figure 7, right).[68] This is, to the best of our knowledge, the highest activity for a catalyst in this reaction until today.

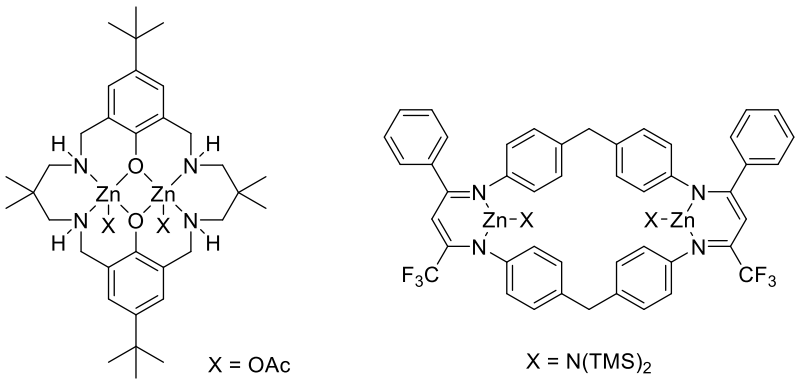

Figure 7. Dinuclear zinc complexes based on Robson-type (left) and BDI ligand (right).[64, 68]

The crystal structure of the bridged catalyst based on the BDI ligand (Figure 7, right) revealed a distance around 8 Å between both zinc centers.[68] Compared to that the zinc-zinc distance in the dimerized form of mononuclear BDI complexes measures about 4 Å.[69] Despite this massive difference in zinc distances the activity has not decreased but is instead surprisingly high. This can be explained by the flexibility of the ligand structure as quantum chemical calculations of *Kissling et al.* show. During copolymerization the two centers approach each other to a distance of 4.5 Å.[63] While the dinuclear BDI zinc complex exhibits the highest measured activity of a catalyst for copolymerizing CHO with CO_2 it is inactive in the coupling of PO and CO_2. Theoretical calculations revealed a six-membered transition state for the insertion of CO_2 into the bond between a zinc center and the coordinated alkoxide chain end of the growing PC. Overcoming this energy barrier is rate-limiting and for PO/CO_2 copolymerization this barrier is significantly higher than for reaction of CO_2 with CHO.[63]

So far catalysts for the copolymerization of PO and CHO with CO_2 were described. In comparison to these, the catalysis of the copolymerization with limonene oxide (LO) as epoxide monomer is more complex due to the sterically demanding structure of LO, thus only a few complexes were found to be active in this reaction. In 2004 the group of *Coates* described the first active catalyst for the copolymerization of LO and CO_2, which was built from a BDI ligand with zinc as active metal center and an acetate initiating group.[70] The *Lewis* acidity of the zinc center and therefore activity of the catalyst can be increased *via* the introduction of electron withdrawing substituents like trifluoromethyl groups (TOF = 37 h^{-1}).

Experiments with *cis*-LO show no conversion of this isomer as BDI zinc catalysts are selective towards *trans*-LO.[71] Another active catalyst is the amino-trisphenolate aluminum catalyst of the group of *Kleij* (Figure 8). With this catalyst both isomers of LO are accessible for the copolymerization with CO_2. Other than the BDI zinc catalyst this complex requires a co-catalyst, as for example PPNCl. Copolymerization of pure *cis*-LO with this catalyst system results in poly(limonene carbonate) (PLC) of moderate molecular weight (7.0–11 kg mol^{-1}) and low polydispersity (< 1.5).[72] With turnover frequencies of 2–3 h^{-1} the aluminum catalyst has a remarkably lower activity[72] compared to the BDI catalyst (37 h^{-1})[71] described previously.

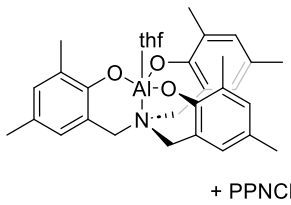

+ PPNCl

Figure 8. Aluminum complex with PPNCl as co-catalyst active in the polymerization of CO_2 with both *cis*- as well as *trans*-LO.[72]

The incorporation of electron withdrawing trifluoromethyl substituents and $N(TMS)_2$ as initiating group in a BDI-zinc complex resulted in TOFs of 310 h^{-1} in the *trans*-LO/CO_2 copolymerization (Figure 6). To the best of our knowledge, this is the most active catalyst in this reaction until today.[59]

Besides the previously discussed heterogenous und homogenous metal-based catalysts *Zhang et al.* reported the utilization of organocatalysts in the copolymerization of epoxides and CO_2. These alternative catalysts are based on *Lewis* acidic activators, like triethyl borane to ring-open the epoxide, in combination with cationic initiators which enable the alternating copolymerization of epoxides and CO_2.[73] Due to a high variability in the combination of *Lewis* acid and cationic initiator these systems can be optimized towards highly active organocatalysts. With the combination of an activator and an initiator moiety in one molecule *Yang et al.* were able to increase the activity of the catalyst up to a TOF of 4,900 h^{-1} in the copolymerization of CHO and CO_2.[74]

2.1.2 Mechanism of the ring-opening copolymerization

The alternating copolymerization of epoxides with CO_2 proceeds *via* a coordination-insertion mechanism. In Scheme 4 this mechanism as proposed by *Coates et al.* is shown exemplarily with a catalyst containing zinc as active metal center.[75] In the copolymerization of epoxides

and CO_2 two reaction steps are substantial: the insertion of CO_2 into a zinc-alkoxide bond, which is kinetically favored, and the insertion of an epoxide into a zinc-carbonate bond, which is usually the rate-determining step due to its high kinetic energy barrier.[76] The active form of BDI-zinc complexes in the copolymerization of epoxides and CO_2 are dimeric species.[62] A comparison of different substituents on the BDI ligand published by *Moore et al.* showed a correlation between the dimeric nature, zinc-zinc distance, and reactivity of these catalysts. With increased steric bulk the complex is unable to dimerize and showed no reactivity in the copolymerization of CHO and CO_2. On the other side a low steric bulk leads to tightly bound dimers, which result in unreactive complexes again. Only ligands leading to loosely bound dimers resulted in high activities of the complexes.[61] These catalysts can activate the epoxide prior to insertion into the growing polymer, which is necessary since the carbonate group is a weak nucleophile.[50] Observations of a decreasing reactivity of these homogenous catalysts with increasing dilutions support the theory of a bimetallic mechanism. In such diluted environments the probability of two complexes being in close proximity and able to dimerize is reduced.[50, 77]

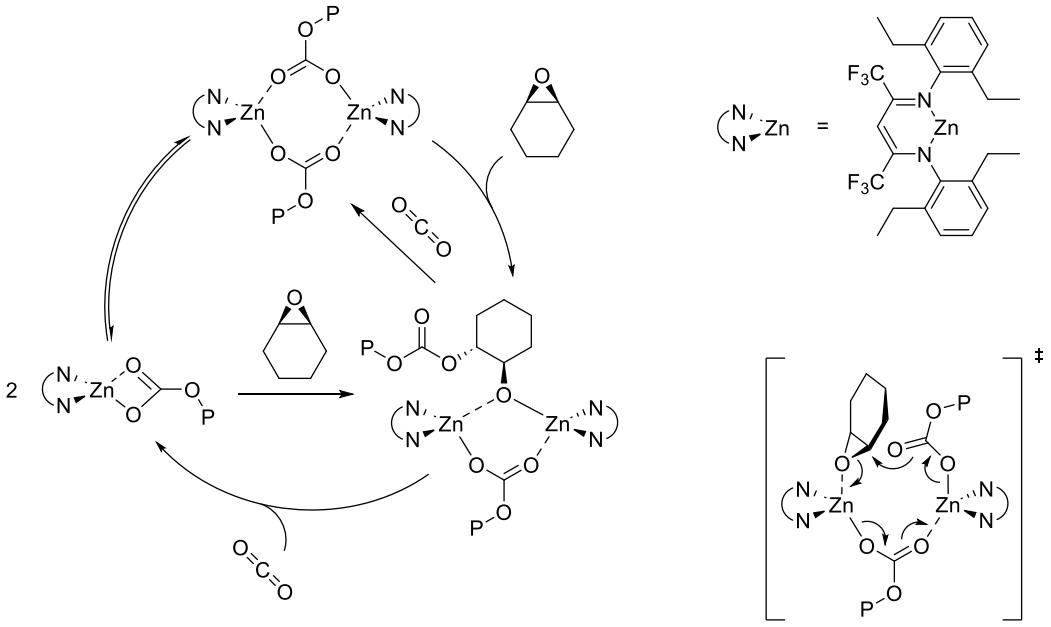

Scheme 4. Bimetallic mechanism with BDI-Zn complexes in the copolymerization of CHO and CO_2 (left) and transition state during ring-opening of the epoxide (right) as proposed by *Coates et al*. (P = polymer chain).[75]

The incorporation of two successive epoxides into the polymer chain leads to ether instead of carbonate linkages in the chain and can be another unwanted side reaction besides formation of cyclic carbonates. Tuning the catalytic system or adjusting the temperature and CO_2 pressure can drive the selectivity of the reaction towards the alternating incorporation of epoxides and CO_2 and therefore a low polyether content. The opposite process, a

consecutive incorporation of two CO_2 molecules, is reversible and enthalpic barriers prevent the formation of such dicarbonate linkages.[76] Water, alcohol, or other impurities can act as chain transfer agents (CTAs).[42, 78] As a consequence unwanted side reactions can originate from these substances resulting in low molecular weights of the polymer and bimodal molecular weight distribution. However, if applied systematically as CTA a targeted synthesis of polymers with well-defined molecular weights can be achieved.[79]

The initiation and propagation in the copolymerization of LO and CO_2 with a BDI zinc catalyst was studied by the groups of *Greiner* and *Rieger* in 2016.[80] Again, a bimetallic mechanism is proposed, where a LO monomer is pre-coordinated by one metal center followed by coordination of a second LO molecule at the other metal center and an intramolecular nucleophilic attack (Scheme 5).

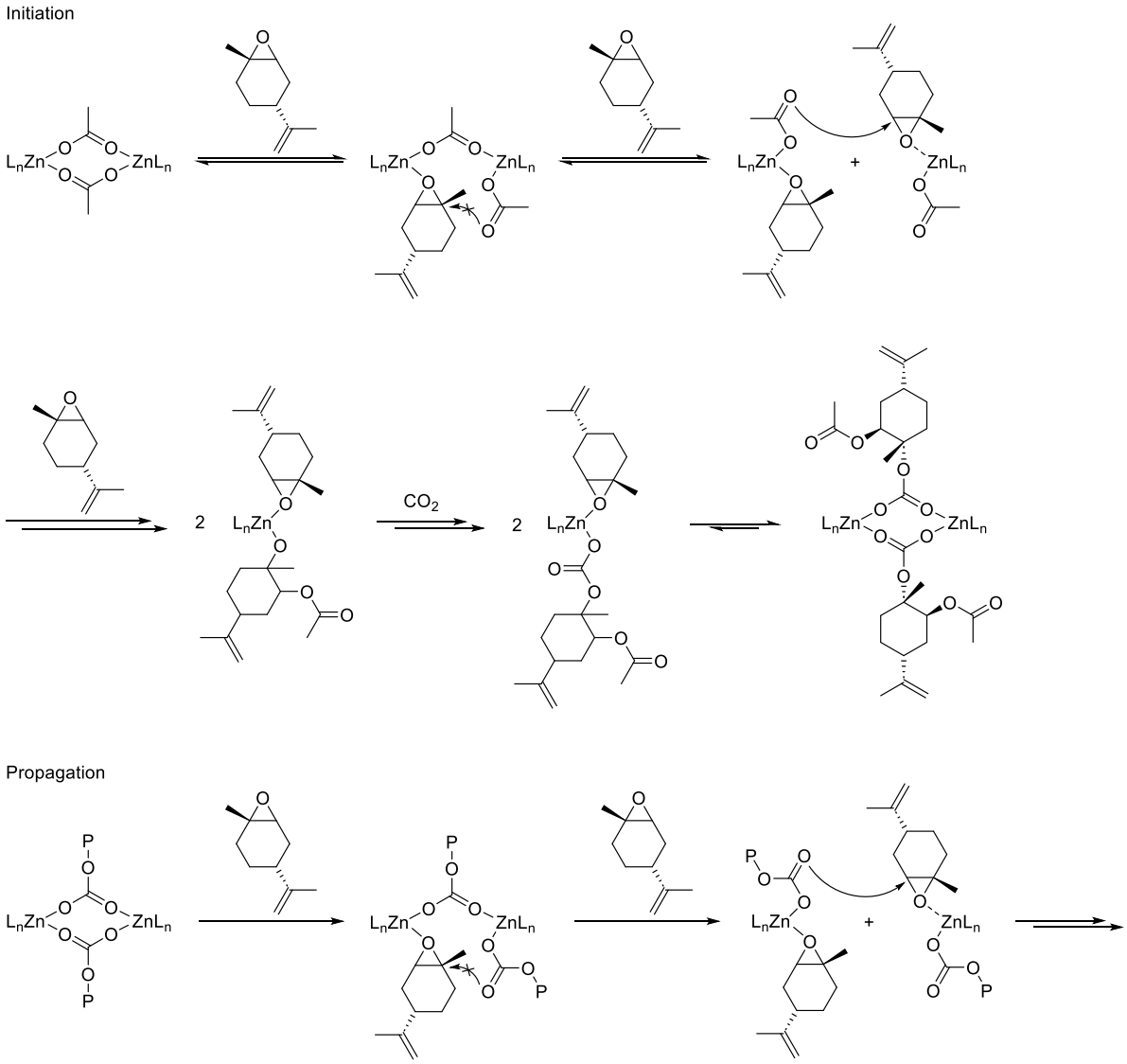

Scheme 5. Mechanism of the initiation and propagation of LO/CO_2 copolymerization with a BDI zinc catalyst as proposed by *Hauenstein et al.* (L_n = BDI, P = polymer chain).[80]

A difference in the copolymerization mechanism for CHO compared to LO is indicated when the rate equations of both copolymerizations are considered. Here the reaction order for CHO is one while in the case of the LO/CO_2 copolymerization the reaction order of LO is two.[80] In contrast to the mechanism postulated by *Coates et al.* for the copolymerizations of CHO and CO_2[75] no attack at the LO can take place as long as the two metal centers are still connected *via* the acetate group or carbonate chain end. Only when a second LO is coordinated the now monomeric catalyst molecules can rearrange to allow the nucleophilic attack at the coordinated LO.[80] *Byrne et al.* reported the observation of a strong temperature dependency of the catalyst's activity in LO/CO_2 copolymerization so that above 35 °C the TOF of the complex decreased significantly from 33 h^{-1} (35 °C) to 1 h^{-1} (50 °C).[71] Contrary to earlier assumptions, *Reiter et al.* were able to show that neither the double bond in LO nor the *cis*-isomer of LO act as catalyst poisons. They furthermore reported *in situ* IR measurements of LO/CO_2 copolymerizations at different temperatures indicating that the equilibrium between polymerization and depolymerization is influenced by temperature and shifted towards the latter with increasing temperature.[59]

2.1.3 Synthesis strategies for epoxide monomers

An intensely investigated epoxide, that is used in the copolymerization with CO_2, is PO. It is synthesized *via* two main routes, the chlorohydrin process and the hydrogen peroxide propylene oxide (HPPO) process. The synthesis of PO *via* propylene chlorohydrin developed a growing industrial relevance over the years after its first report in 1859. It proceeds *via* two steps: First propylene is chlorinated to propylene chlorohydrin, which is then dehydrochlorinated in a saponification reaction with sodium or calcium hydroxide (Scheme 6, (A)).[81-82] Another approach towards PO is the HPPO process. This route uses hydrogen peroxide to epoxidize propylene with the help of a titanium silicalite catalyst (TS-1) (Scheme 6, (B)). Compared to the chlorohydrin process this approach is more sustainable since it is chlorine-free and the main byproduct is water.[83-84]

(A) chlorohydrin process

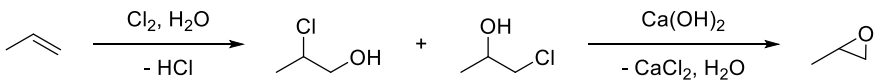

(B) HPPO process

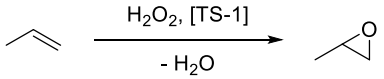

Scheme 6. Synthesis of PO *via* (A) the chlorohydrin process or (B) the HPPO process.[81-84]

Both processes have in common that they start from propylene, which is commonly petroleum-based. To enable the sustainable synthesis of PO an alternative source for the olefin is crucial. In most routes methanol is used to synthesize propylene from sustainable resources. The hydrogenation of carbon monoxide towards methanol can be catalyzed by a variety of supported metal oxides.[27-28] Even more attractive is the synthesis of methanol from CO_2 as it is an abundant and non-toxic waste and greenhouse gas.[85] Here the difficulty arises from the chemical inertness of CO_2, which requires powerful and selective catalytic processes for the reaction towards methanol.[86-87] The synthesized alcohol can then be converted further into propylene *via* the methanol-to-propylene (MTP) route using zeolites as catalysts (Scheme 7).[28, 88-89]

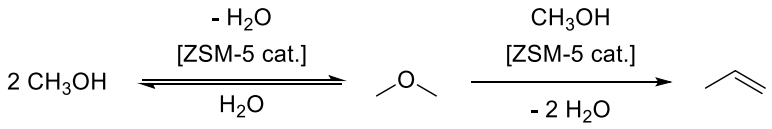

Scheme 7. Methanol-to-propylene route using ZSM-5 zeolithe catalysts.

A third alternative approach was published by *Yu et al.*, where PO can be synthesized from glycerol without the need of propylene as starting material. After hydrogenation and dehydration of glycerol the resulting propylene glycol is further dehydrated to result in PO (Scheme 8).[90] This is an interesting approach in terms of sustainability, but due to moderate yield and selectivity it is so far not industrially competitive to the two previously mentioned main routes.

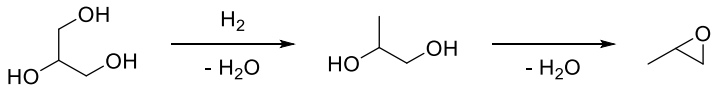

Scheme 8. Synthesis of PO by hydrogenation and dehydration of glycerol.[90]

Another central epoxide monomer in the copolymerization with CO_2 is CHO. The common pathway towards CHO is starting with benzene, which is derived from crude oil. After dehydrogenation of benzene[91-92] the resulting cyclohexene can be epoxidized towards CHO using different peroxides, for example hydrogen peroxide or *tert*-butyl hydroperoxide (Scheme 9, (A)).[93-94] Addressing the interest in sustainable alternatives for petrochemicals a route towards CHO makes use of plant-based triglycerides (Scheme 9, (B)). The product 1,4-cyclohexadiene from self-metathesis of the triglycerides is epoxidized in the next step.[95] After hydrogenation of the remaining double bond CHO is formed.[96]

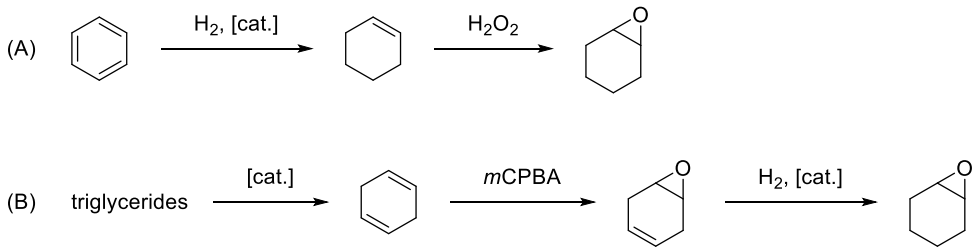

Scheme 9. CHO synthesis from (A) crude oil-based benzene or (B) triglycerides.[91-96]

A broad and diverse group of bio-based molecules, which are important building blocks for various sustainable syntheses are terpenes. One prominent representative among them is (+)-limonene, a monoterpene, that can be extracted from peels of citrus fruits.[18] Its synthesis is therefore not competing with food production as the peels are accruing as waste from juice production. With its two double bonds limonene has two positions for potential epoxidation. A less selective oxidizing agent results in the generation of the diepoxide or other alcohol or ketone by-products.[97-98] In case of the diepoxide, the ring-opening copolymerization could take place on both functionalities and instead of the targeted linear polymer a cross-linked product would be obtained. The synthesis of 1,2-limonene oxide (LO) requires epoxidation of the endocyclic double bond. *Via* the epoxidation a stereo center is introduced into the molecule and a *cis*- and a *trans*-product can be generated. Using peracetic acid for the epoxidation the isomer ratio of the product is 46:54 (*cis*:*trans*), which is the common ratio of commercially available LO.[17] As explained in Chapter 2.1.1 most catalysts that are active in the copolymerization of LO and CO_2 are exclusively incorporating *trans*-LO. A route for the *trans*-enriched synthesis of LO is therefore of high interest and can proceed *via* bromination with *N*-bromosuccinimide (NBS) followed by a nucleophilic attack and ring closure (Scheme 10). With this method a content of 85% *trans*-LO could be achieved by *Hauenstein et al*.[80]

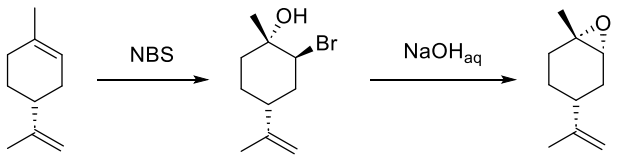

Scheme 10. *Trans*-enriched synthesis of LO as published by *Hauenstein et al*.[80]

The feedstock for bio-based monomers became even more divers when *Zhang et al.* added epoxidized vegetable oils to them. In their work from 2014 they use 10-undecenoic acid from castor oil, which is nonedible and derived from the castor bean plant. The unsaturated fatty

acid is methylated followed by the epoxidation of the terminal double bond with *meta*-chloroperoxybenzoic acid (*m*CPBA, see Scheme 11). The resulting epoxide can then be copolymerized with CO_2.[99]

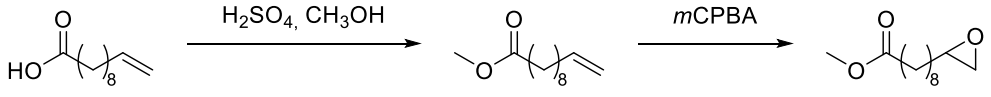

Scheme 11. Synthesis of bio-based epoxides from 10-undecenoic acid *via* esterification, followed by epoxidation.[99]

2.2 Polysiloxanes

Polyorganosiloxanes, also called polysiloxanes or silicones, are polymers with an inorganic backbone of alternating silicon and oxygen with organic groups attached to the silicon. In case of the organic substituents being methyl groups only, the polymer is called a poly(dimethylsiloxane) (PDMS).[100] Four structural motives build the basis of a polysiloxane: Monofunctional (M), difunctional (D), trifunctional (T) and tetrafunctional (Q) units (Figure 9).[101] Monofunctional units are terminal units in polymer chains or networks and allow to control the length and molecular weight of polymers by adjusting their share in the monomer feed. The classic linear polymer is built from difunctional monomer units, and the length of the resulting polymer chain defines the viscosity of linear polysiloxanes. Branched or cross-linked polysiloxane structures can be formed with tri- or tetrafunctional units, often in combination with difunctional units to build a more loosely connected network.[21, 101]

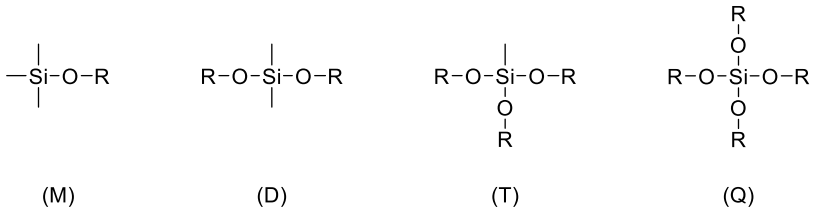

Figure 9. Structural motives in PDMS: Monofunctional (M), difunctional (D), trifunctional (T), and tetrafunctional (Q) units.[101]

The *Müller-Rochow* process, also known as the direct process, generates organo(chloro)silanes, typically methyl chlorosilanes, from silicon and organochlorides (Scheme 12). At 260–310 °C and in the presence of a copper catalyst a mixture of dimethyldichlorosilane (80–90%), methyltrichlorosilane (3–15%), trimethylsilyl chloride (2–5%), tetramethylsilane (0.1–1%), silicon tetrachloride (<0.1%), and other silanes is produced and separated by fractional distillation.[102]

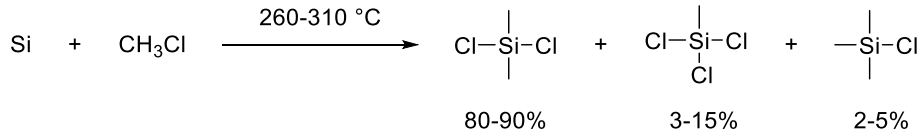

Scheme 12. Synthesis of methyl chlorosilanes *via* the *Müller-Rochow* process.[102]

These organochlorosilanes react with water to silanols releasing hydrogen chloride as by-product. These silanols can be directly polymerized in a polycondensation reaction releasing water in this process (Scheme 13). Cyclic siloxanes, which occur as a by-product in the hydrolysis of dimethyldichlorosilane can be again converted into linear siloxanes by ring-opening them with the help of dimethyldichlorosilane.[100]

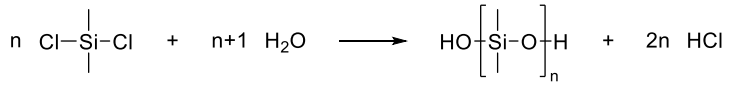

Scheme 13. Polycondensation of dimethyldichlorosilane.[21]

The performance of polysiloxanes varies strongly depending on their structural design. By controlling the chain length, number of linking points and substituents at the silicone the properties of the product can be tuned to meet the individual application requirements. Linear polysiloxanes are fluids even up to high molecular weights. In PDMS the methyl groups can rotate easily around the backbone leading to the typical low surface tension of siloxanes while the non-polar organic side groups determine the hydrophobic character of siloxanes.[21] Polymers with a high degree of tri- and tetrafunctional units can build up a highly cross-linked network. The degree of crosslinking defines the distinction between rubbers and resins. Rubbers are more loosely inter-connected elastomers cross-linked *via* curing. Resins contain mainly tri- and tetrafunctional units and stand out for their temperature resistance. A network containing only tetrafunctional units is a silicate.[100]

2.3 Group-transfer polymerization

In a publication from 1983 *Webster et al.* introduced the term “group-transfer polymerization” (GTP) in the course of their work on silyl ketene actetal-initiated polymerizations of *Michael*-type monomers. The name of this polymerization mechanism is based on the proposed associative mechanism in which a silyl group is transferred to a free monomer during incorporation into the growing polymer chain (Scheme 14, (A)).[103] Later studies revealed that the polymerization proceeds *via* a dissociative propagation mechanism instead. The

complexation of the silyl group by a nucleophilic catalyst leads to its dissociation from the polymer and the resulting enolate chain end attacks a free monomer (Scheme 14, (D)).[104-105]

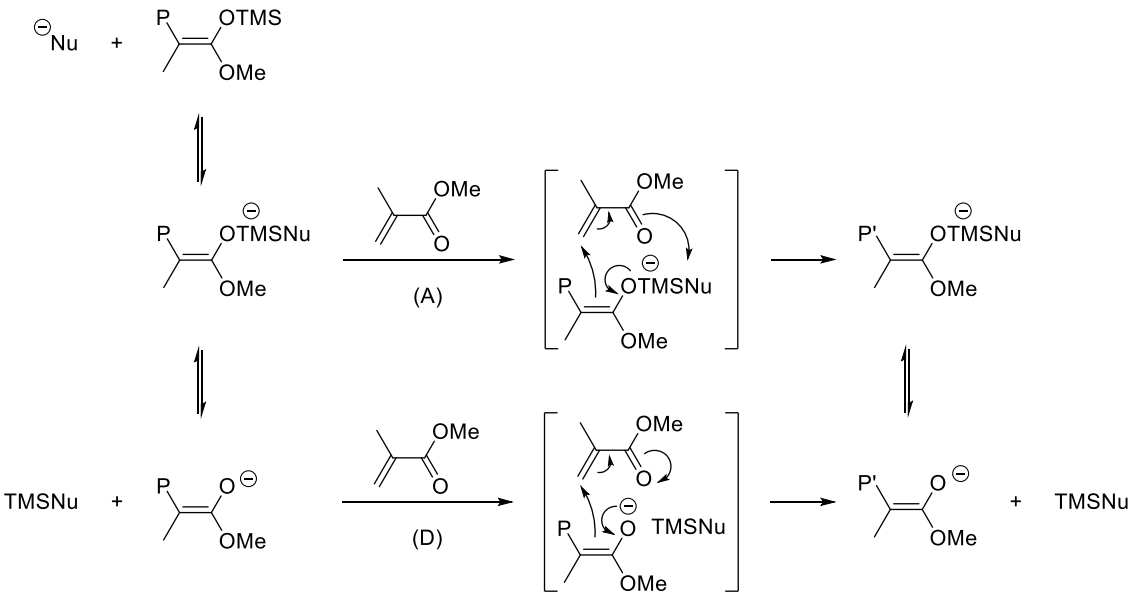

Scheme 14. The associative (A) and dissociative (D) propagation in silyl ketene actetal-initiated GTP of MMA (Nu = nucleophile, P/P' = polymer chain).**[106-107]**

In the independent reports of *Yasuda et al.* and *Collins et al.* the first rare earth metal-mediated GTP (REM-GTP) approaches were published in 1992.[108-109] Transition metal complexes were developed to synthesize poly(methyl methacrylate) (PMMA) of high molecular weights and narrow polydispersities. The catalyst system by *Collins et al.* is composed of a cationic and a neutral zirconocene complex, which are both active in the bimetallic propagation step.[109] The catalyst investigated by *Yasuda et al.* is a dimer of a neutral samarocene hydride complex, which produces PMMA with a high syndiotacticity (95% rr) and molecular weights greater than 100 kg mol^{-1} while maintaining low polydispersities (< 1.05).[108] In the initiation step methyl methacrylate (MMA) is coordinated to the samarocene complex, cleaving the dimeric complex. Then a hydrid of the catalyst is transferred to the MMA followed by coordination and insertion of another MMA molecule *via* an eight-membered ring transition state (Scheme 15).[108]

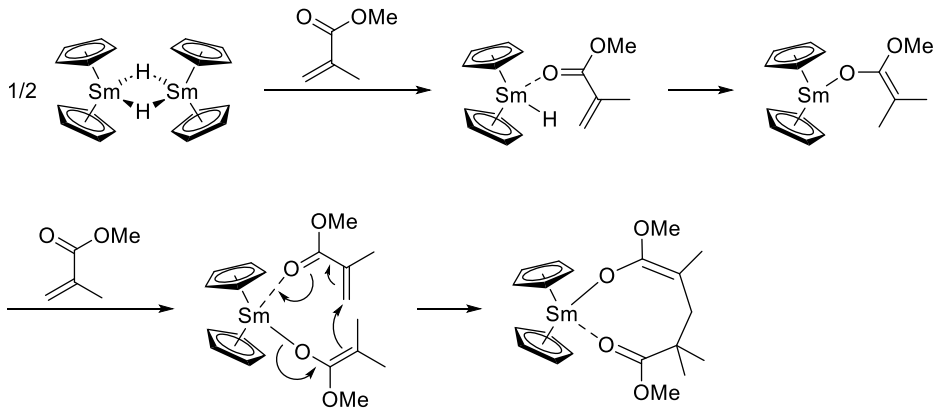

Scheme 15. Initiation step of MMA polymerization with a samarocene hydrid catalyst.[108, 110]

Depending on the applied metallocene the polymerization proceeds either *via* a mono- or a bimetallic propagation step. The samarocene complex of *Yasuda et al.* shows a monometallic propagation step similar to the initiation step. After the coordination of a free MMA to the metal the enolate chain end of the growing polymer attacks the MMA forming an eight-membered ring transition state of the insertion (Scheme 16, (A)).[108, 110] In the bimetallic mechanism the stabilization of the polymer chain end and the activation of a new monomer molecule is realized by two individual metal complexes. The zirconocene catalyst system of *Collins et al.* proceeds *via* such a bimetallic mechanism (Scheme 16, (B)).[110-111]

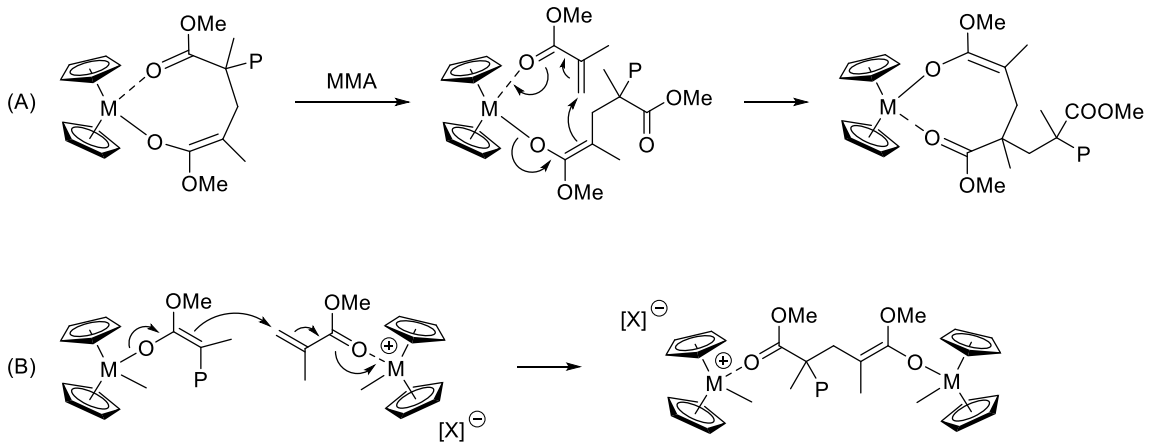

Scheme 16. Monometallic (a) and bimetallic (b) propagation in MMA polymerization with different metallocene complexes (M = metal, P = polymer chain).[107]

High molecular weight (> 1000 kg mol^{-1}) polymers of diethyl vinylphosphonate (DEVP) were reported by the group of *Rieger*. The catalyst used in these reactions was a metallocene complex based on ytterbium as rare-earth metal center (Figure 10, left). Besides the homopolymerization, also copolymerizations of DEVP and MMA towards polymers of high molecular weights (29–46 kg mol^{-1}) and low polydispersities (1.1–1.2) were reported.[112]

Based on bisphenolate ligands a new group of catalysts for REM-GTP was developed (Figure 10, right). They not only showed promising activity in the REM-GTP of a broad variety of polar monomers, but also in the ring-opening polymerization of *β*-butyrolactone.[113] Highly stereoselective syntheses towards isotactic poly(2-vinylpyridine) (P2VP) (P_m = 92%)[114] or syndiotactic poly(3-hydroxybutyrate) (PHB) (P_r = 88%)[113] are enabled by the application of this tunable catalyst. Such a high control over stereoregularity as well as molecular weight distribution is typical for REM-GTP catalysts.

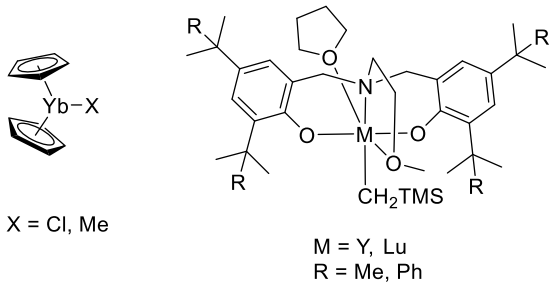

Figure 10. Catalysts active in the GTP of *Michael*-type monomers based on a metallocene (left) or a bisphenolate ligand (right).[112-113, 115]

2.3.1 C-H bond activation

The initiation in REM-GTP with rare-earth metal metallocene catalysts can proceed either *via* deprotonation or *via* nucleophilic transfer of the initiating group (Scheme 17). Hereby, the nucleophilicity of the ligand determines which reaction pathway is preferred.[116]

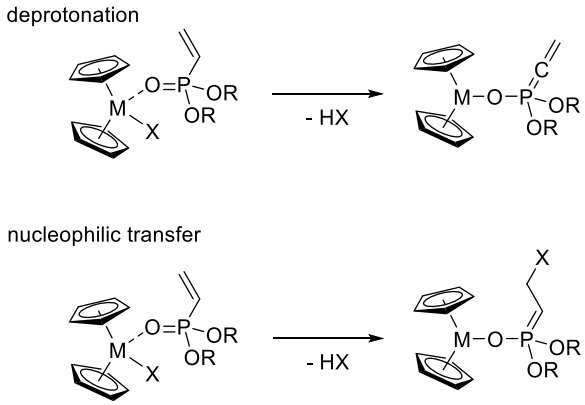

Scheme 17. Initiation pathways in GTP with metallocenes as exemplified with vinyl phosphonate monomers.[116]

The deprotonation step is rather slow compared to the nucleophilic transfer, which is why catalysts were tuned towards the latter to improve the activity and initiator efficiency of the complexes. Heteroaromatic initiating groups, like 2,4,6-trimethylpyridine (*sym*-collidine) are

successfully introduced *via* σ-bond metathesis, which proceeds *via* C-H-bond activation of the *N*-adjacent methyl group.[116] By suppressing unwanted side-reactions not only the activity and initiator efficiency is increased, but also the controlled nucleophilic transfer in the initiation enables the selective introduction of a functional group at the end of the polymer chain. This principle of an initiating group exchange *via* C-H bond activation can be used with bisphenolate lanthanides as well (Scheme 18). [117-118] *Via* the conjugation of more than one metal center to a central, multinuclear initiating group linear or even more complex star-shaped polymer structures can be synthesized with the transferred initiating group connecting the polymer chains.[119-120]

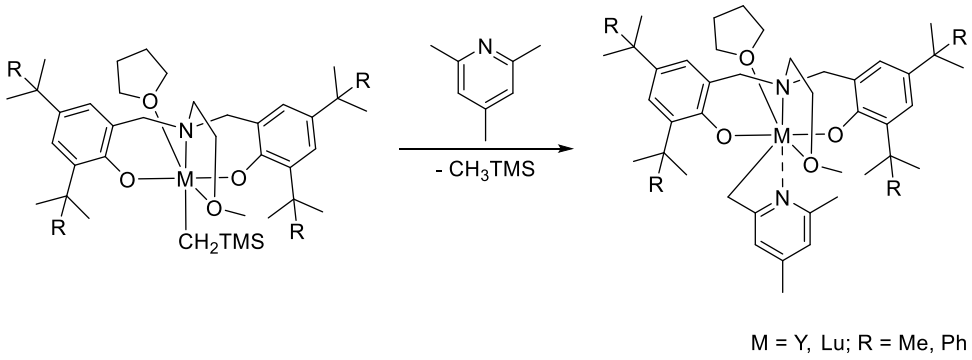

Scheme 18. C-H bond activation of a bisphenolate complex with *sym*-collidine.[117-118]

2.3.2 *Michael*-type monomers and their corresponding polymers

The catalysts described in the previous chapter are active in the polymerization of polar unsaturated molecules. These monomers are characterized by conjugated double bonds and electron withdrawing substituents which is why they are also called *Michael*-type monomers (Figure 11).[117]

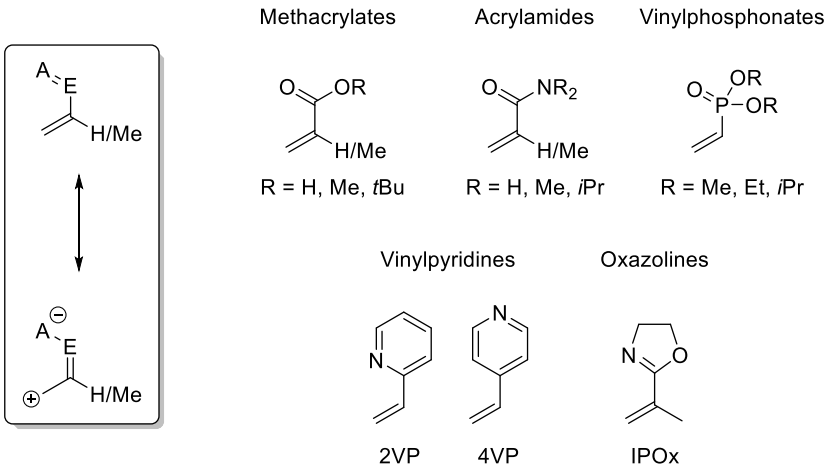

Figure 11. Selected *Michael*-type monomers and their general resonance structure.[117-118, 121]

The polymerization products of these monomers have diverse properties, making them suitable for a variety of different applications. The engineering plastic PMMA is known for its high impact strength and due to its light weight and transparency it is widely used as alternative for glass.[122] Poly(diethyl vinylphosphonate) (PDEVP) is soluble in water and possesses amphiphilic properties. It furthermore shows thermoresponsive behavior in water, so that below its lower critical solution temperature (LCST) the polymer is completely dissolved in the solvent at all compositions. These properties and its biological compatibility makes PDEVP especially attractive for medical applications.[115, 123] The pH-dependent solubility of the amphiphilic P2VP makes it interesting for high-performance applications.[117] By copolymerization of 2-vinylpyridine (2VP) with water-soluble monomers copolymers can be formed, which can arrange *via* self-assembly to build micelles.[124]

2.4 Advanced polymer structures *via* co- and terpolymerization

The most basic polymer structure is built from one monomer only and is therefore called a homopolymer. When more than one monomer is polymerized into a polymer chain the term copolymer is used.[125] Depending on the reactivity of the monomers, the polymerization mechanism, or catalyst used a variety of different polymer microstructures can be generated. In general, four main structural motives – alternating, block, statistical and gradient – are used to categorize linear copolymers.[125] In alternating copolymers the monomers are incorporated in a strictly alternating manner (Figure 12, (A)). One example for this copolymer type is poly(ethylene terephthalate) (PET), where terephthalic acid and ethylene glycol are incorporated alternatingly.[21] Epoxide and CO_2 copolymerization towards PCs is another example whereby the alternating combination results in carbonate linkages. As discussed earlier also a consecutive incorporation of two or more epoxides can happen as a side reaction resulting in ether linkages and an interruption of the alternating structure of the polymer.[44, 126] Block copolymers are structures, where several units of one monomer are incorporated consecutively (Figure 12, (B)). This leads to homopolymer segments within the copolymer, where each segment is clearly separated from another.[125] Multiblock structures as well as a simple AB block copolymers can be the resulting motive.[127-128] If no order in the copolymerization pattern can be observed the structure is called random or statistical (Figure 12, (C)).[125] A gradient copolymer can be seen as a mixture of block and statistical polymers (Figure 12, (D)). The concentration of each monomer is higher on only one side of the polymer chain and decreases over the chain length. Between the two chain ends monomer concentrations change continuously, either symmetrical or asymmetrical.[125, 129]

The probability for the generation of these different copolymer structures resulting from a one pot reaction can be predicted by determining the copolymerization parameters. These express the probability of a monomer to form a homopolymer or a copolymer with a second monomer and are specific for each monomer combination.[125, 130] A high copolymerization parameter indicates a high probability of the monomer to form homopolymers from the reaction mixture. If both copolymerization parameters for a monomer mixture are significantly higher than 1, it is most likely that block copolymers or even two separate homopolymers are formed. The other extreme, with a value of 0 for both parameters a strictly alternating copolymer is formed as the homopolymerization is very unlikely. In the unusual case of both parameters being determined with a value of 1 a statistical copolymer is formed, because neither homo- nor copolymerization is preferred.[125] These values can be determined with the help of copolymerization experiments and calculations according to *Mayo* and *Lewis* or *Fineman* and *Ross*, where the ratio between the monomers in the feed is compared with the ratio of the monomers incorporated into the polymer chain.[125, 130]

Besides the synthesis of linear copolymers another structure worth mentioning is the generation of graft copolymers (Figure 12, (E)). In these macromolecules a linear polymer chain contains reactive groups along the chain, which can be used as connection points for another polymer forming branched structures.[125, 131]

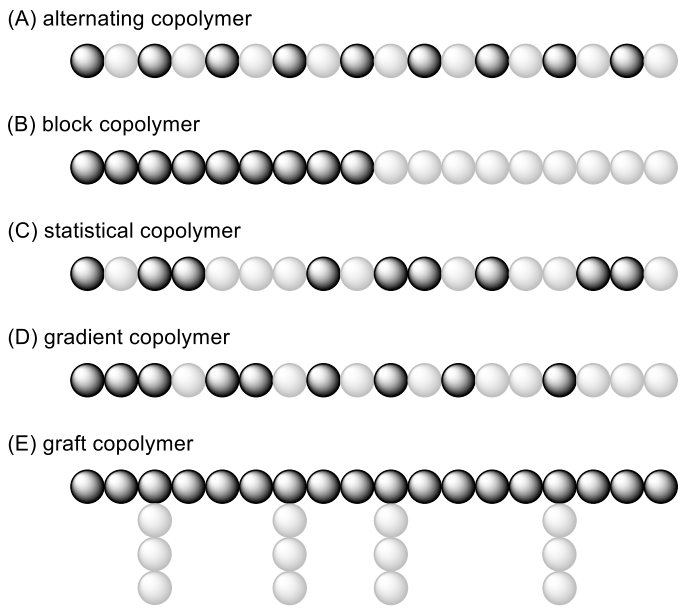

Figure 12. Block copolymer structures.

The synthesis of defined copolymer structures requires different approaches depending on the targeted copolymer type. The simplest one is to polymerize all monomers from one feed, a classical one pot reaction. However, if a block structure is targeted, but the one pot pathway

results in alternating or statistical copolymers a sequential addition of the monomers can be used to overcome the intrinsic reactivity and lead to generation of defined (multi)block polymers.[132] This is also a helpful pathway if a change between the catalytic system is necessary for the polymerization of the monomers. After the epoxide is completely consumed *Zhang et al.* added the vinyl monomer and azobisisobutyronitrile (AIBN) for the polymerization of the second monomer. This way the ROCOP of epoxides and CO_2 could be combined with the reversible addition-fragmentation (RAFT) polymerization of vinyl monomers.[133] If the reaction *via* sequential addition is not possible two polymer chains can also be connected in a post-polymerization reaction. For the synthesis of biomedical materials poly(L-lactide) was used as macroinitiator in the polymerization of L-lysine resulting in block copolymers, which can provide useful connection properties based on their functional groups and hydrophilic or hydrophobic behavior.[134]

2.4.1 Extension of aliphatic polycarbonate copolymers

The catalyst used in the present work is the previously discussed BDI^{CF3}-Zn-$N(TMS)_2$ complex developed by the group of *Rieger*. This catalyst is capable of copolymerizing a broad variety of epoxide monomers with CO_2. Besides the epoxides PO, and CHO, mentioned before the pool of polymerizable monomers also contains LO, styrene oxide and octene oxide. This versatility of the catalyst allows even a mixed feed of epoxide monomers like PO and CHO or PO and LO to be polymerized with CO_2 towards terpolymers.[59] Starting with more than one monomer present in the reaction mixture the control over the microstructure is not given and most likely a statistical or rather gradient type polymer is generated. Sequential addition of PO, CHO and vinylcyclohexene oxide was used by *Darensbourg et al.* to synthesize triblock copolymers with the help of a chromium salan complex. These copolymers show separated glass transition temperatures (T_g) in contrast to the mixed T_g that gradient or statistical copolymers usually feature.[135]

2.4.2 Siloxanes as complements to polycarbonates

With the intention of improving the mechanical properties of BPA-PC at low temperature, a blend with PDMS was prepared in the work by The *Dow Chemical Company*. In the presence of KOH, transesterification reactions took place, which covalently linked BPA-PC with PDMS while reducing the molar mass of the PC. The block copolymers formed in this reactive blending also contribute to an increase in miscibility of both polymers in the blend. As a result, products with an enhanced impact toughness at temperatures down to -40 °C are

produced.[23] A selective combination of siloxanes and BPA-PC is possible *via* cophosgenation of BPA and siloxane oligomers or by linking blocks of carbonate and siloxane oligomers alternatingly using different end groups at the oligomers.[22] In a work of *Reiter et al.* PDMS was used as a chain transfer agent in the polymerization of epoxides and CO_2. The hydroxy end groups of the siloxane can exchange the initiator at the catalyst center and the PDMS initiator is therefore transferred to the end of the growing aliphatic polycarbonate chain.[58]

2.4.3 Combination of polymerization mechanisms

The variety of polymerizable molecules is so diverse, which is why they often need special catalysts tailored to the respective monomer types. Some monomers can readily be copolymerized with each other, but others react *via* such different mechanisms that they cannot be incorporated into one polymer chain. As described before, an yttrium bisphenolate complex enables homopolymerization of BBL or 2VP, but a combination of both monomers into one copolymer was not possible.[113] Successful examples are the polymerization of MMA and lactones towards block copolymers using a lanthanocene catalyst. In this reaction the sequence of monomer addition is crucial as the polymerization of MMA does not take place when the lactone is added first to the reaction mixture.[136] With the help of organoaluminum catalysts a mixture of the two homopolymers could be obtained polymerizing directly from a mixture of MMA and lactones. In this case the monomers are not inhibiting each other in the polymerization, however a successful combination in one polymer chain could not be achieved.[137] In the context of the combination of GTP with ring-opening polymerization the question about how GTP can be combined with ROCOP caught increasing interest. *Wang et al.* reported the combination of the polymerization of MMA with the copolymerization of PO and CO_2 by using a bifunctional CTA. For the ROCOP of PO and CO_2 an aluminum porphyrin catalyst was applied and the radical polymerization of MMA was performed with PPNCl/AIBN. In the resulting block copolymer the CTA is the connection between the two polymer blocks.[138]

3. Aim of the thesis

Aliphatic PCs based on epoxides and CO_2 are materials of high interest, especially as a possible replacement for BPA-PC. They are integrated particularly well in the field of sustainable materials by making use of CO_2 as a monomer. Furthermore, the absence of aromaticity in the backbone indicates an increased UV stability. However, the outstanding performance of BPA-PC, especially in terms of impact toughness is yet to be met.[126, 139] The aim of this thesis is to upgrade the material properties of aliphatic PCs by tuning the polymer structure and extending the combinations of different monomer and polymer types.

The first part of this work is focused on the structural modification to improve the mechanical performance of aliphatic PCs. In the previous work of this group, but also by the group of *Williams* a combination of epoxide/CO_2 ROCOP and lactone ring-opening copolymerization resulted in terpolymers with an increased elongation at break.[140-142] In this work, PDMS is incorporated as soft block into the chain of PCHC to improve its mechanical properties. PDMS impresses with low interactions between the chains while being non-toxic and colorless at the same time.[143] The successful incorporation of short siloxane blocks into the PCHC chain was achieved by *Reiter et al.* using hydroxy-terminated molecules as CTAs.[58] With the help of the same BDI^{CF3}-Zn-$N(TMS)_2$ catalyst the principle of initiator exchange shall be applied to our work. It is expected that the utilization of α,ω-hydroxy-terminated PDMS of high molecular weight as CTA leads to synthesis of PCHC-PDMS block copolymers with improved mechanical properties. At the same time the high T_g, transparency and thermal stability of PCHC should not be influenced negatively. Upscaling of the polymerization can show the stability of the reaction pathway and enable an in-depth analysis of the product regarding mechanical, thermal, and rheological properties.

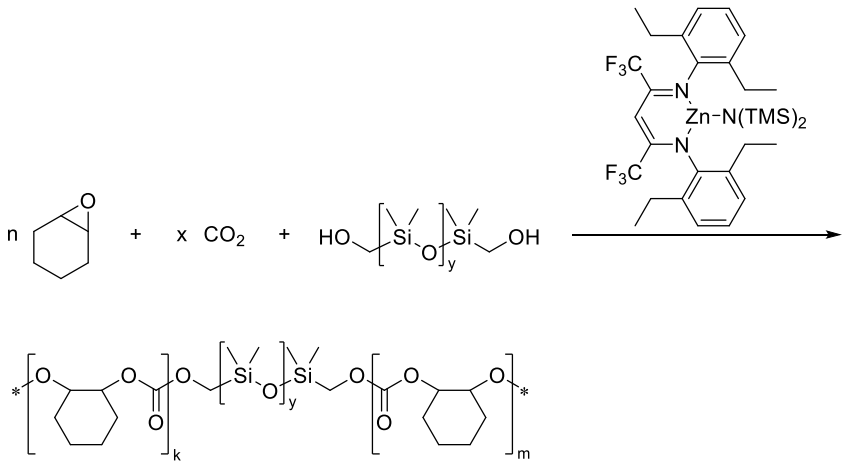

Scheme 19. Synthesis of PCHC-PDMS block copolymers with hydroxy-terminated PDMS as CTA and a BDI zinc complex as catalyst for the CHO/CO_2 copolymerization.[144]

The second part of this thesis covers the power of a mixed monomer feedstock to allow selective tuning of polymer properties. PO, CHO, and LO all have in common that they belong to the most intensively studied epoxides for the copolymerization with CO_2.[145-146] At the same time the corresponding PCs differ fundamentally in their mechanical and thermal properties. PCHC and PLC are well known for their high T_g of 115 °C and 130 °C, respectively, but also a high brittleness.[80, 147] Contrary to this, PPC is known for its low modulus of elasticity (831 MPa)[148] and low T_g (25-45 °C)[19]. A combination of these contrasting polymers could allow the merger of their advantageous properties and a high control over them with adjustment of the ratios between them. In this project the previously mentioned BDI zinc catalyst is used again, because it is not only capable of catalyzing all three monomers at high TOFs, but also enabling the use of a mixed epoxide feedstock to synthesize terpolymers.[59] However, the epoxides are polymerized with TOFs between 120 and 5520 h^{-1},[59] indicating different activities of the catalyst in their respective homopolymerizations. This reactivity difference influences the microstructure of the resulting polymer. Starting from a mixed feed of two epoxides with such different reactivities will most likely result in the generation of gradient copolymers, because the epoxide, which is incorporated faster will dominate in the beginning of the copolymerization. With the progression of the reaction its concentration and therefore probability of incorporation decreases resulting in a growing ratio of the other monomer. This work has the synthesis of terpolymers from two epoxides and CO_2 with a high control over the microstructure as a target. With the help of a dosing system the faster incorporated monomer will be added continuously into the reactor keeping its concentration low and allowing the synthesis of statistical terpolymers with defined polymer ratios.

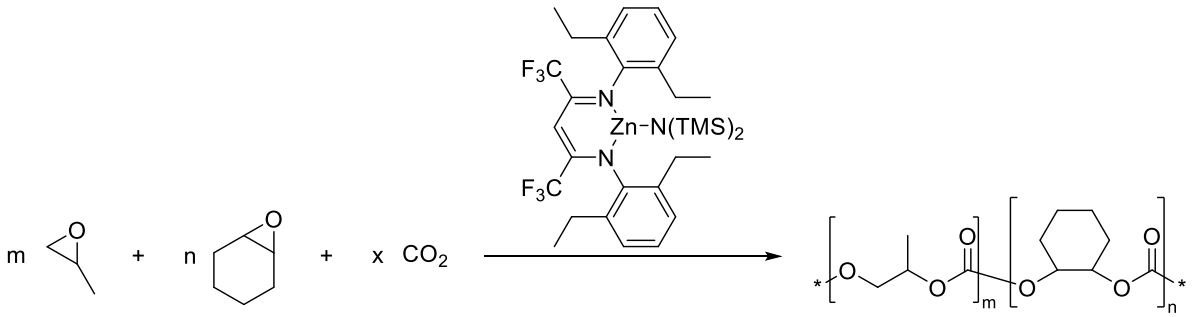

Scheme 20. Polymerization of PO, CHO, and CO_2 with a BDI zinc complex as catalyst towards terpolymers.[149]

The third part of the thesis deals with the combination of polymerization mechanisms demanding different complexes for their catalysis. GTP is a beneficial method to polymerize *Michael*-type monomers towards polymers with a high degree of precision in their molecular weight distribution and end group functionality.[150] To combine GTP of 2VP and

2-isopropenyl-2-oxazoline (IPOx) with ROCOP of CHO and CO_2 a dinuclear catalyst shall be developed. The idea is to design each active site specifically to catalyze one of the polymerization types. ROCOP should be catalyzed at the BDI zinc center, which can be connected *via* a linker with the yttrium metallocene center active in GTP. The linker between the active centers will then be transferred as an end group to the growing polymer chains and serve also as the connection between the two polymer blocks. Connecting two polymerization mechanisms as controlled, but also as diverse as GTP and ROCOP enables the generation of a broad variety of novel block copolymers with tunable properties *via* a one pot reaction.

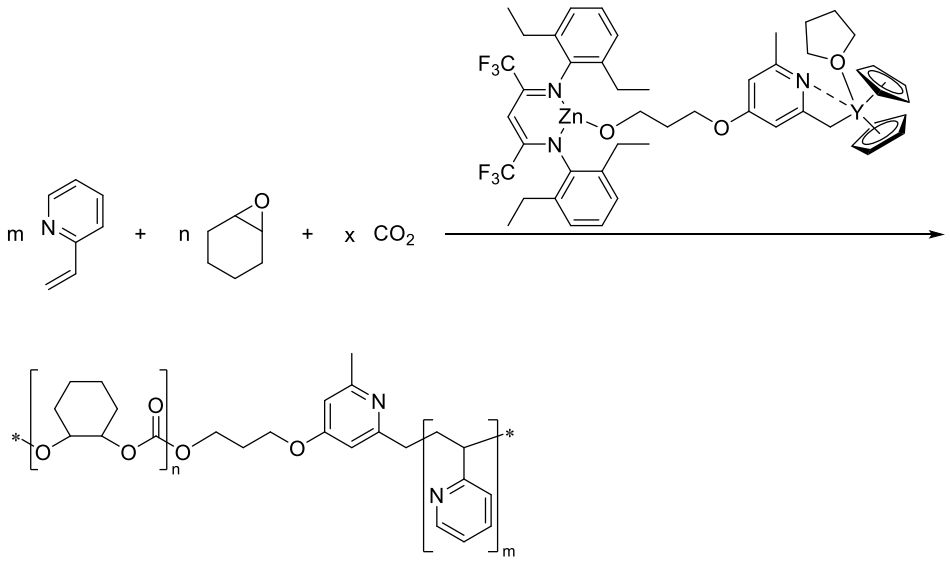

Scheme 21. Terpolymerization of 2VP, CHO and CO_2 with a dinuclear complex containing a zinc and an yttrium center, connected *via* a pyridyl alcohol initiating group.[151]

4. The soft side of aliphatic polycarbonates: with PCHC-*b*-PDMS copolymers towards ductile materials

Title: The soft side of aliphatic polycarbonates: with PCHC-*b*-PDMS copolymers towards ductile materials

Status: Full paper, published May 15, 2023

Journal: Macromolecules, 56, 11, 4318–4324

Publisher: American Chemical Society

DOI: 10.1021/acs.macromol.2c02433

Authors: Alina Denk, Paula Großmann, Bernhard Rieger*

Content

The utilization of CO_2 as a building block makes aliphatic polycarbonates a promising group of polymers in the fields of sustainable materials. To improve the mechanical properties of aliphatic polycarbonates block copolymers with siloxanes are synthesized. The poly(dimethyl siloxane) block is incorporated into the polycarbonate with the help of a *β*-diiminate zinc catalyst, where the polysiloxane exchanges the initiating group at the zinc center and is transferred to the end of the growing polycarbonate chain. The successful synthesis of block copolymers is indicated by diffusion-ordered nuclear magnetic resonance spectroscopy. Upscaling of the copolymerization showed the stability of the reaction and enabled an in-depth analysis of the polymers. Those show a significant increase in elongation at break in tensile testing experiments and an improved mechanical stability in deformation experiments. The analysis *via* atomic force microscopy and transmission electron microscopy visualizes the phase separation of the polycarbonate and the polysiloxane on a nanometer scale and their different soft and hard characteristics.

*A. Denk carried out all experiments and wrote the manuscript. P. Großmann recorded the TEM images and gave advice on the manuscript. All work was carried out under the supervision of B. Rieger.

Macromolecules

pubs.acs.org/Macromolecules Article

Soft Side of Aliphatic Polycarbonates: with PCHC-*b*-PDMS Copolymers toward Ductile Materials

Alina Denk, Paula Großmann, and Bernhard Rieger*

Cite This: *Macromolecules* 2023, 56, 4318−4324 Read Online

ACCESS | Metrics & More | Article Recommendations | Supporting Information

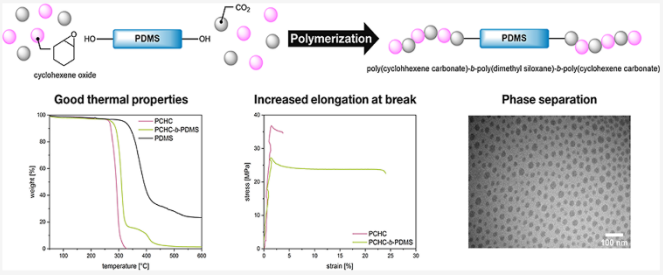

ABSTRACT: Aliphatic polycarbonates based on CO_2 and epoxides are a promising group of polymers due to the utilization of CO_2 as a monomer combined with a versatile epoxide feedstock. To increase the attractiveness of these polymers as a material, the poor mechanical properties have to be improved. Herein, we present the synthesis of block copolymers from poly(cyclohexene carbonate) and poly(dimethyl siloxane) (PDMS), where diffusion-ordered NMR spectroscopy measurements indicate a successful synthesis of block structures. The resulting material shows an elongation at break of up to 24% in tensile testing with an incorporation ratio of only 27% PDMS in the copolymer. At the same time, a high tensile strength (27.9 MPa) and modulus of elasticity (1726 MPa) are observed.

■ INTRODUCTION

In a world in constant flux, aliphatic polycarbonates (PCs) are promising materials that are likely to become increasingly relevant in the future. They have been studied by many research groups for decades, especially as a possible replacement for bisphenol A-based PCs (BPA-PCs).[1−3] So far, the current standard for industrially produced PCs is still BPA-PC, which is impressive because of its high impact strength and good transparency at the same time.[4,5] The use of aliphatic PCs based on epoxides and CO_2 is expected to have positive effects on UV stability due to the lack of aromaticity. In addition, the abundant, non-toxic, climate-damaging CO_2 is used as the C1 building block, which will make the resulting materials increasingly interesting in the fields of sustainable materials.

The properties of aliphatic PCs can be influenced by the epoxy monomers used.[6] Among these, the most commonly used epoxides are propylene oxide (PO), cyclohexene oxide (CHO), and limonene oxide (LO).[7,8] The polymers resulting from ring-opening copolymerization (ROCOP) with CO_2 have good transmission properties [e.g. poly(limonene carbonate) (PLC)] with a transmission of 94%[9]). However, they differ fundamentally in terms of their thermal and mechanical properties. Poly(propylene carbonate) (PPC) is known for its relatively low modulus of elasticity (831 MPa)[10] and low glass transition temperature (T_g) (25−45 °C).[11] As a result, this aliphatic PC is unlikely to be a suiting substitute for BPA-PC. In contrast, PLC shows higher tensile strength and T_g (130 °C) than PPC.[9] The epoxy monomer LO makes aliphatic PCs interesting for current research due to its bio-based nature, but it exhibits much higher brittleness than BPA-PC.[9] Furthermore, only few catalysts can catalyze the ROCOP of LO and CO_2.[1,6,12] Poly(cyclohexene carbonate) (PCHC) also has a high T_g (115 °C)[13] and a relatively high modulus of elasticity (3600 MPa).[4] CHO is often used in research as a benchmark monomer for initial experiments with new systems because it polymerizes reliably and quickly.[14] For comparability reasons, it will be used in this work.

Structural modifications are a promising way to address the lacking mechanical performance of most aliphatic PCs

Received: December 1, 2022
Revised: April 3, 2023
Published: May 15, 2023

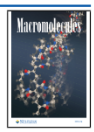

https://doi.org/10.1021/acs.macromol.2c02433
Macromolecules 2023, 56, 4318−4324

Scheme 1. In Situ Exchange of the Initiating Group $-N(TMS)_2$ with the α,ω-hydroxy-methylene-terminated PDMS

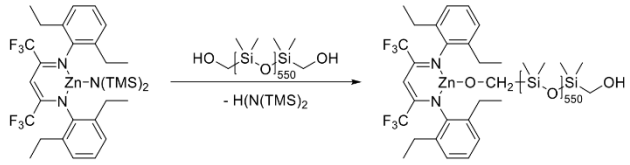

Table 1. Polymerizations of CHO/CO_2 With and Without PDMS Toward PCHC and PCHC-*b*-PDMS[a]

entry	equiv CHO/PDMS/cat	m(CHO) [g]	X [%][b]	$M_{n,calc}$ [kg/mol][c]	$M_{n,meas}$ [kg/mol][d]	$M_{w,meas}$ [kg/mol][d]	$Đ$[d]	PCHC/PDMS [%][e]
1	1000:0:1	2.50	93	132	114	134	1.2	100:0
2*	2500:0:1	90.0	95	337	188	248	1.3	100:0
3	1000:1:1	1.50	98	139	82.2	106	1.3	64:36
4	1000:1:2	1.50	99	140	89.4	118	1.3	68:32
5	2000:1:2	3.00	99	281	133	176	1.3	77:23
6*	1500:1:1	51.7	97	248	99.5	134	1.3	73:27
7*	2500:1:1	86.2	99	392	133	166	1.2	81:19
8*	3500:1:1	121	97	523	157	199	1.3	84:16

[a]Polymerizations in toluene, 25−30 bar CO_2 pressure, 40−60 °C, stirred at 500 rpm. [b]Conversion calculated from the respective polymer and monomer integrals in ^{1}H NMRs. [c]$M_{n,calc}$ = equivalents (CHO)·142 g/mol·X. [d]Measured via GPC in $CHCl_3$ relative to poly(styrene) standards. [e]Calculated from the respective polymer integrals in the ^{1}H NMR from the precipitated polymer products. *Upscaling experiments performed in a 1.1 L-autoclave.

compared to BPA-PC. In this context, Rieger et al. reported the synthesis of statistical and block terpolymers from CHO, CO_2, and β-butyrolactone.[15] These show an increase in the elongation at break due to the incorporation of the soft poly(3-hydroxybutyrate) into the PC chain.[16] A similar approach was published by the group of Williams, who combined PLC and poly(ε-decalactone) in ABA block structures resulting in an enhanced elongation at break.[17] In both cases, however, the modulus of elasticity (E-modulus) decreased with increasing content of the respective soft polymer.[16,17] In another work by the group of Williams, ABA block copolymers from PCHC and poly(ε-decalactone) showed not only an increase in elongation at break but also an increase in E-modulus and tensile strength for block copolymers with a comparable weight percentage of the respective PC.[18] By using ethyl oleate (EtOL) as an additive for PLC, Greiner et al. were able to reduce the melt viscosity of their product. With EtOL contents of up to 15 wt %, they could also improve the elongation at break while retaining the optical properties of the PC. The thermal properties are also altered by the additive. Greiner et al. reported a decrease in T_g with increasing EtOL incorporation into the polymer.[19]

In this work, we introduce a soft polymer block into the PCHC chain to improve its mechanical properties. We choose poly(dimethyl siloxane) (PDMS) as a building block because it is non-toxic and colorless and, at the same time, has the potential to act as a soft block in a copolymer with PCHC due to low interactions between the PDMS chains.[20] Thus, we hope to influence the mechanical properties of the polymer positively without losing the high T_g, transparency, and thermal stability of PCHC. The catalyst used in the present work consists of a β-diimine (BDI) ligand to which zinc coordinates as the catalytic active site. Also coordinating to the zinc is the initiating group $N(TMS)_2$ (Scheme 1). This structure was developed by our group[6] based on the catalysts of Coates et al.[21] The potential of our catalyst system is shown by the variability of the polymerized epoxides. In addition to the aforementioned PO, CHO, and LO, styrene oxide and octene oxide, for example, can also be copolymerized with CO_2 using the described catalyst.[6] However, a main hindrance for large-scale industrial applications of PCHC is its high brittleness. In a previous publication by our group, we could show that siloxane building blocks can be incorporated into the PC chain either as an end group or using bifunctional structures as a block in ABA block copolymers.[22] The principle of initiator exchange was used, whereby the hydroxy-terminated siloxanes as chain transfer reagents exchanged the $N(TMS)_2$ initiating group. It could be observed that with a short siloxane, selective ABA structures can be generated, while the main focus was placed on the investigation of the catalysis. Using this principle in our current work, α,ω-hydroxy-terminated PDMS building blocks, with a significantly increased chain length, are incorporated into the growing PCHC chains. In this work, the main focus besides the synthesis of block copolymers is the detailed analysis of their properties. After upscaling of the polymerization, the resulting block copolymers are thoroughly characterized using various thermal, mechanical, rheological, and spectroscopic methods.

INITIATOR EXCHANGE WITH PDMS

For the soft block in the copolymer structure, we chose an α,ω-hydroxy-terminated PDMS with a relatively high molecular weight (41.0 kg/mol) to allow the synthesis of high-molecular-weight polymer products while maintaining a positive influence of the PDMS on the overall mechanical properties of the resulting copolymer. To avoid condensation of the Si−OH end groups of the PDMS in the drying process, $Si-CH_2-OH$ end groups were introduced (Figure S1). In the polymerization of CHO with CO_2, we applied the BDI^{CF_3}–Zn–$N(TMS)_2$ catalyst (**1**) known from previous publications of our group,[15,23] which allows the in situ exchange of the

https://doi.org/10.1021/acs.macromol.2c02433
Macromolecules 2023, 56, 4318−4324

−N(TMS)$_2$ initiating group by addition of hydroxy-terminated siloxanes (Scheme 1).[22]

These chain transfer agents are then transferred to the end of the growing PC chain upon addition of CHO and CO_2 to the reaction mixture. We could observe the initiator exchange by ^{1}H NMR monitoring over 2 h (Figure S2), where signals of free HN(TMS)$_2$ can be observed over time while the signals of the catalyst's ligand become broader due to the addition of the polymeric initiating group. No signals of the uncoordinated ligand and, therefore, decomposition of the catalyst could be observed, which emphasizes the stability of this in situ generated catalytic species. The second hydroxy-methylene end group can react in such an exchange of the initiating group or of a growing chain at the active center as well. Since we are working with a polymeric initiating group, both options are possible: polymerization on both end groups and only on one. The resulting copolymers can, therefore, be either of an AB or a BAB structure depending on the reaction of the second end group of the PDMS.

Synthesis of PCHC-*b*-PDMS. Copolymerizations without PDMS as the chain transfer agent are shown in Table 1, entries 1 and 2. To test the principle of PDMS incorporation into the PCHC chain via initiator exchange, we performed copolymerizations with varying equivalents of CHO, PDMS, and catalyst **1** (see Table 1, entries 3−5). The conversion of CHO was selective toward the corresponding PC without the formation of unwanted cyclic carbonate or polyether by-products (Scheme 2).

Scheme 2. Polymerization of CHO and CO_2 with the Chain Transfer Agent PDMS and Catalyst 1 toward PCHC-*b*-PDMS-*b*-PCHC

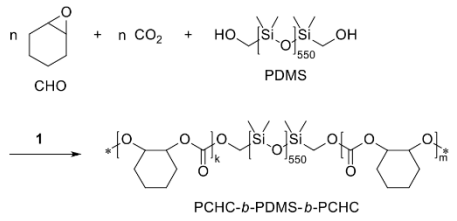

A twofold amount of catalyst as in entry 4, resulted in similar molecular weights and, therefore, similar chain lengths as in entry 3. The reason for this observation is the two hydroxy end groups of the PDMS building block, which allow a reaction with the catalyst center and the following copolymerization on both chain ends either sequentially or simultaneously. The difference in reaction speed of the polymerization is monitored via in situ IR measurements (Figure S4). With double the amount of catalyst, the reaction proceeds faster since the PCHC chain can grow on both chain ends of the PDMS while still the same block copolymer ratio (64:36 and 68:32) could be obtained in the polymer products. An increase of the CHO equivalents as in entry 5 leads to longer PCHC chains and, therefore, to polymers with an overall higher molecular weight, as expected. This way, the ratio of PDMS and PCHC in the copolymer can be controlled with the equivalents of CHO. The resulting GPC traces (Figures S10−S12) show bimodality and a low polydispersity (1.3), similar to the polymer from the polymerization of CHO/CO_2 without PDMS (Table 1, entry 1 and Figure S8). After the exchange of the initiating group at the catalyst with PDMS, the PC chain can grow not only on one chain end of the PDMS but also on both chain ends simultaneously, which leads to a statistical generation of AB and BAB block copolymers and therefore to bimodality in the GPC traces. Here, the term PCHC-*b*-PDMS is used for both types of block copolymers. The bimodality of GPC traces from pure PCHC, as shown in Figures S8 and S9, is also well known in the literature and explained there with traces of water or cyclohexene diols acting as chain transfer agents.[24]

The ^{1}H NMR measurements of the polymerizations show a high conversion of the epoxide monomer (≥95%) for all performed polymerizations. Analysis of the polymer products via diffusion-ordered NMR spectroscopy (DOSY-NMR) shows that the corresponding polymer signals share one diffusion coefficient (Figures S16−S18), indicating the connection of the PDMS and the PCHC block. Further support of a successful block copolymer synthesis can be drawn from the comparison of these DOSY-NMR spectra with measurements of a blend from PCHC and PDMS (Figure S19). The polymers used in the blend are of molecular weights comparable to that of the individual PCHC and PDMS block of a copolymer. In this case, two different diffusion coefficients can be observed for PCHC and PDMS as the two polymers are not connected to each other.

To show the potential applications of our approach on a larger scale, we performed copolymerization reactions in a 1.1 L Büchi steel autoclave with a 30- to 80-fold increase in the used monomer (see Table 1, entries 2, 6−8). Despite the more complex preparation of the reaction in the large autoclave, similarly high conversions of the epoxide could be achieved (≥97%). In the GPC measurements, bimodal distributions could be observed (Figures S13−S15) with low polydispersities (1.2−1.3). All polymers were purified by washing with an aqueous ethylenediaminetetraacetic acid solution, precipitation from methanol, and drying under vacuum. For an in-depth study of the copolymers' thermal, mechanical, and rheological properties, the polymers from the large-scale polymerizations were used.

Thermal Properties. Table 2 summarizes the results of the thermal and mechanical characterization of the polymer products. Using thermogravimetric analysis (TGA), we could observe a two-step decomposition of the block copolymers (Figure 1A). The first weight loss occurs at around 300 °C,

Table 2. Thermal Properties of the Synthesized Polymers

Entry	PCHC/PDMS [%][a]	M_n ($Đ$) [kg/mol][b]	T_{gDSC} [°C][c]	$T_{gtan\delta}$ [°C][d]	T_{donset} [°C][e]
1	100:0	114 (1.2)	111		280
2*	100:0	188 (1.3)	113	117	279
3	64:36	82.2 (1.3)	124		281/391
4	68:32	89.4 (1.3)	122		290/383
5	77:23	133 (1.3)	120		282/377
6*	73:27	99.5 (1.3)	117	−127/120	300/407
7*	81:19	133 (1.2)	112	−127/120	302/398
8*	84:16	157 (1.3)	112	−126/122	296/392

[a]Calculated from the respective polymer integrals in the ^{1}H NMR from the precipitated polymer products. [b]Measured via GPC in $CHCl_3$ relative to poly(styrene) standards. [c]Determined via DSC. [d]Derived from the maximum of the loss factor (tan δ) measured via DMA. [e]Determined via TGA. *Upscaling experiments performed in a 1.1 L-autoclave.

https://doi.org/10.1021/acs.macromol.2c02433
Macromolecules 2023, 56, 4318−4324

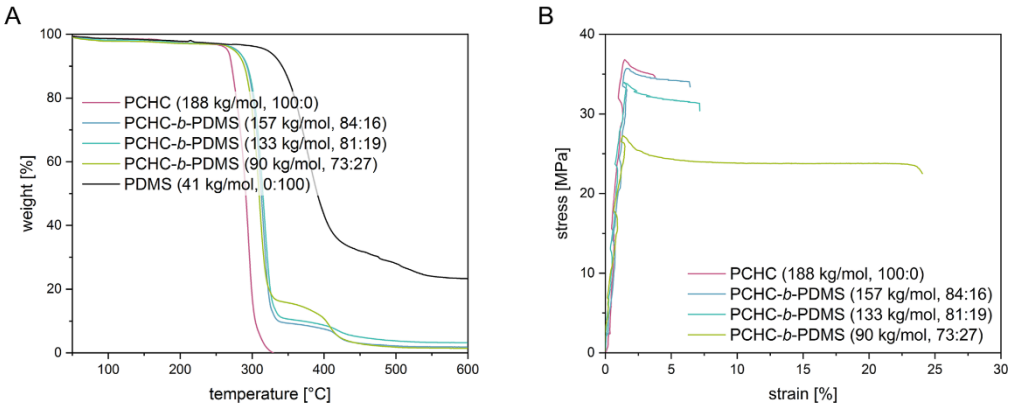

Figure 1. (A) TGA of PCHC (Table 1, entry 2), PDMS, and PCHC-*b*-PDMS copolymers of varying compositions (Table 1, entry 6–8). (B) Tensile testing of polymer specimen from PCHC (Table 1, entry 2) and PCHC-*b*-PDMS copolymers (Table 1, entry 6–8).

Table 3. Mechanical Properties of the Synthesized Polymers

Entry	PCHC/PDMS [%][a]	M_n ($Đ$) [kg/mol][b]	*E*-modulus [MPa][c]	tensile strength [MPa][c]	elongation at break [%][b]	max. force [N][d]	deformation [mm][d]
1	100:0	114 (1.2)					
2*	100:0	188 (1.3)	2473 ± 155	35.3 ± 1.5	2.7 ± 1.0	239 ± 8.5	2.9 ± 0.6
3	64:36	82.2 (1.3)					
4	68:32	89.4 (1.3)					
5	77:23	133 (1.3)					
6*	73:27	99.5 (1.3)	1726 ± 152	27.9 ± 1.2	17.5 ± 6.5	1062 ± 149	8.9 ± 1.2
7*	81:19	133 (1.2)	1977 ± 15.0	33.7 ± 0.6	4.9 ± 2.3	796 ± 171	5.7 ± 1.0
8*	84:16	157 (1.3)	2041 ± 114	37.1 ± 1.4	5.6 ± 0.9	864 ± 166	5.8 ± 0.7

[a]Calculated from the respective polymer integrals in the ^{1}H NMR from the precipitated polymer products. [b]Measured via GPC in $CHCl_3$ relative to poly(styrene) standards. [c]Measured via tensile testing, mean values. [d]Measured via multi-axial pressure tests, mean values. *Upscaling experiments performed in a 1.1 L-autoclave.

which is where PCHC is decomposed. This temperature is slightly higher than the decomposition temperature ($T_{d,onset}$) measured for pure PCHC (279 °C, Table 2, entry 2), and the values are reported in the literature.[25] The second $T_{d,onset}$ is observed at around 400 °C and in accordance to the decomposition of the siloxane (>350 °C).[26]

In the differential scanning calorimetry (DSC) measurements, we could only detect one glass-transition temperature ($T_{g,DSC}$). The observed glass transition $T_{g,DSC}$ occurs at 112–124 °C (Figure S21), which is close to the determined $T_{g,DSC}$ of pure PCHC at 113 °C (Table 2, entry 2) and in accordance with the literature (115 °C).[13] As the T_g of PDMS was not pronounced enough for the DSC measurement, we decided to conduct dynamic mechanical analysis (DMA) with our samples (Figures S22–S25). These measurements showed both the $T_{g,tan\delta}$ of PCHC at around 120 °C and the $T_{g,tan\delta}$ of PDMS at around −127 °C, derived from the maxima of the measured loss factor (tan δ).

Mechanical and Rheological Characterization. To determine the impact of the incorporated PDMS building blocks on the overall mechanical properties of the PCHC-*b*-PDMS polymers, we performed tensile testing (Figure 1B) and multi-axial pressure tests (Figure S27). The summarized results can be found in Table 3. For the tensile testing experiments, dog-bone-shaped specimens were strained until fracture, while the applied force and the elongation of the sample were constantly measured. An important value derived from these measurements is the modulus of elasticity (E-modulus), which is around 2473 MPa for the pure PCHC (Table 3, entry 2). Matching our observations (Table 3 entry 2), an elongation at break of 1–2% is reported in the literature caused by the brittleness of PCHC.[1] The incorporation of a PDMS block into the PCHC chain, at a PCHC/PDMS composition of 84:16 leads to an increased strain of 5.6% until the specimen breaks (Table 3, entry 8). With an even higher siloxane content of 27%, it was possible to reach elongations of 17.5% (Table 3, entry 6). At the same time, the E-moduli for all three block copolymers decrease with an increasing PDMS content. However, the material is still relatively stiff with moduli between 1700 and 2000 MPa.

The results from the multi-axial pressure tests are in correspondence with this tendency (Figure S27). With a higher PDMS content, the specimens withstand higher forces applied to them over a longer deformation way until fracture occurs. The maximum applied forces increased from 247 N (0% PDMS) over 1030 and 966 N (16 and 19% PDMS) to 1210 N (27% PDMS) (see Table S4). The copolymer with a PDMS content of 16% shows an increased deformation up to 6.4 mm until the specimen fails (see Table S4s), whereas with a PDMS content of 27%, it was even possible to reach deformations of 10 mm.

https://doi.org/10.1021/acs.macromol.2c02433
Macromolecules 2023, 56, 4318–4324

The rheology experiments performed with a plate−plate rheometer show a significant increase in storage modulus for all PDMS containing polymers compared to the pure PCHC (see Figure S28). These results go hand in hand with the mechanical data obtained. Overall, these findings clearly demonstrate the impact of the incorporated soft block on the mechanical behavior of the polymer. The brittleness could be reduced, leading to a more ductile polymer product while maintaining the toughness of a PC.

Atomic Force Microscopy. With the improvements in the mechanical performance and the observed thermal properties it is to discuss whether microphase separation of the two polymer blocks is present. Using atomic force microscopy (AFM) we could not only measure the topology of our samples, but also analyze the samples regarding their mechanical characteristics. A phase resolved analysis reveals soft and hard properties in different phases within the material. The phase diagram of pure PCHC (Figure S29) shows uniformity in hardness throughout the sample whereas the diagrams of the PCHC-*b*-PDMS copolymers (Figures S30−S32) show a clear increase in soft (dark) segments with increasing PDMS-content of the material. These two phases present in the copolymer can be attributed to non-miscibility of the PDMS and the PCHC leading to the observed phase separation (Figure 2). This phase separation is, however, in micro scale, because the polymers in the block copolymer are—in difference to a blend—connected to each other. The small size of the phases is the reason for the contained transparency of the product.

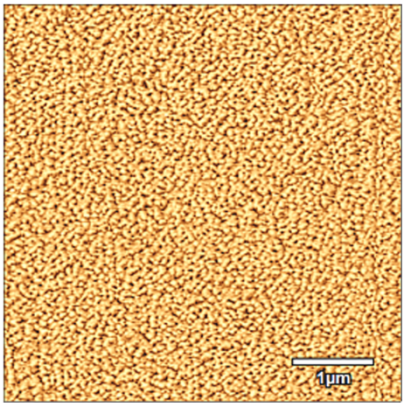

Figure 2. AFM phase imaging from PCHC-*b*-PDMS (Table 1, entry 6), where harder segments are displayed with a lighter color.

Transmission Electron Microscopy. Concerning the soft and hard phases shown in the AFM measurements, we were able to make similar observations via transmission electron microscopy (TEM). Figure 3 shows an enlarged picture of a polymer sample with incorporated PDMS. In comparison to the homogenous sample of pure PCHC (Figures S33), the copolymer samples show two phases interacting differently with the electrons (Figures S34−S36). This is due to the fact that the backbone of the PCHC and PDMS is fundamentally different. The heavier silicon in the siloxane backbone scatters the electrons differently compared to the carbon in the PC polymer, resulting in a darker appearance of the siloxane phases.[27] In line with a decreasing content of PDMS in the copolymers, the darker siloxane phases appear less frequently.

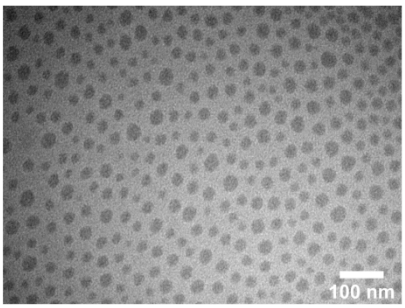

Figure 3. TEM from PCHC-*b*-PDMS (Table 1, entry 6).

The PDMS phases in the copolymers show an even size distribution with diameters around 20 nm, which indicates the generation of block copolymers and is in alignment with the previously discussed analytical data. In the case of a blend of PCHC with PDMS, the phases of both polymers would be larger, approximately in the micrometer scale.[28,29] Overall, this separation of the PC and the siloxane phases within the copolymer is presumably leading to the enhanced mechanical properties of the material. At the same time, the copolymer stays transparent due to the small size of the phases (<30 nm), which makes this approach especially interesting to tune the properties of aliphatic PCs.

■ CONCLUSIONS

In this work, we presented the straightforward synthesis of block copolymers from CHO, CO_2, and a hydroxy-terminated PDMS. By exchanging the initiating group at our BDI^{CF_3}−Zn−N(TMS) catalyst in situ with the hydroxy-methylene siloxane, the PDMS block could be incorporated into the growing PCHC chain. The successful synthesis of block structures is supported by DOSY-NMR measurements, where the two polymers share one diffusion coefficient. To show the robustness and versatility of the presented concept, upscaling reactions with 30- to 80-fold amount of monomer were successfully conducted. In TGA measurements, two decomposition temperatures could be observed, corresponding to the two polymer blocks in the PCHC-*b*-PDMS copolymers. The T_g of the PCHC block could be measured via DSC and was close to the literature value. However, due to a lack of intensity in the DSC, the T_g of the PDMS block was determined via DMA measurements. The observed glass transition temperatures for the respective copolymer were in good accordance with the ones of the individual polymers. While the specimen shows an increased ductility with elongation at break of up to 24%, the tensile strength remained high (27.9−37.1 MPa). The mechanical properties changed with the ratio between PCHC and PDMS in the copolymers as a higher PDMS content led to an increased elongation at break. The same tendency could be observed in pressure tests, where the specimen showed a greater deformability and maximum force for these copolymers. AFM and TEM measurements showed phase separation with PDMS phases not larger than 30 nm, whereby the transparency of the polymer product is not

https://doi.org/10.1021/acs.macromol.2c02433
Macromolecules 2023, 56, 4318−4324

affected. Overall, this work shows the potential to combine a soft block like PDMS with the brittle PC PCHC in block copolymers. With this approach, we could improve the mechanical properties of PCHC while preserving the thermal performance and transparency of the PC.

■ ASSOCIATED CONTENT

Supporting Information

The Supporting Information is available free of charge at https://pubs.acs.org/doi/10.1021/acs.macromol.2c02433.

Synthesis procedures, NMR spectra, GPC traces, and data from thermal, mechanical, rheological, and microscopic analyses (PDF)

■ AUTHOR INFORMATION

Corresponding Author

Bernhard Rieger − *WACKER-Chair of Macromolecular Chemistry, TUM School of Natural Sciences, Catalysis Research Center, Technical University Munich, 85748 Garching, Germany;* orcid.org/0000-0002-0023-884X; Email: rieger@tum.de

Authors

Alina Denk − *WACKER-Chair of Macromolecular Chemistry, TUM School of Natural Sciences, Catalysis Research Center, Technical University Munich, 85748 Garching, Germany*

Paula Großmann − *WACKER-Chair of Macromolecular Chemistry, TUM School of Natural Sciences, Catalysis Research Center, Technical University Munich, 85748 Garching, Germany*

Complete contact information is available at: https://pubs.acs.org/10.1021/acs.macromol.2c02433

Notes

The authors declare no competing financial interest.

■ ACKNOWLEDGMENTS

The authors would like to thank Moritz Kränzlein for the valuable discussions on the manuscript.

■ REFERENCES

(1) Peña Carrodeguas, L.; González-Fabra, J.; Castro-Gómez, F.; Bo, C.; Kleij, A. W. AlIII-Catalysed Formation of Poly(limonene)-carbonate: DFT Analysis of the Origin of Stereoregularity. *Chem.—Eur. J.* **2015**, *21*, 6115−6122.

(2) Winkler, M.; Romain, C.; Meier, M. A. R.; Williams, C. K. Renewable polycarbonates and polyesters from 1,4-cyclohexadiene. *Green Chem.* **2015**, *17*, 300−306.

(3) Nelson, A. M.; Long, T. E. A perspective on emerging polymer technologies for bisphenol-A replacement. *Polym. Int.* **2012**, *61*, 1485−1491.

(4) Koning, C.; Wildeson, J.; Parton, R.; Plum, B.; Steeman, P.; Darensbourg, D. J. Synthesis and physical characterization of poly(cyclohexane carbonate), synthesized from CO2 and cyclohexene oxide. *Polymer* **2001**, *42*, 3995−4004.

(5) Freitag, D.; Fengler, G.; Morbitzer, L. Routes to New Aromatic Polycarbonates with Special Material Properties. *Angew. Chem., Int. Ed.* **1991**, *30*, 1598−1610.

(6) Reiter, M.; Vagin, S.; Kronast, A.; Jandl, C.; Rieger, B. A Lewis acid β-diiminato-zinc-complex as all-rounder for co- and terpolymerisation of various epoxides with carbon dioxide. *Chem. Sci.* **2017**, *8*, 1876−1882.

(7) Wang, Y.; Darensbourg, D. J. Carbon dioxide-based functional polycarbonates: Metal catalyzed copolymerization of CO2 and epoxides. *Coord. Chem. Rev.* **2018**, *372*, 85−100.

(8) Hauenstein, O.; Agarwal, S.; Greiner, A. Bio-based polycarbonate as synthetic toolbox. *Nat. Commun.* **2016**, *7*, 11862.

(9) Hauenstein, O.; Reiter, M.; Agarwal, S.; Rieger, B.; Greiner, A. Bio-based polycarbonate from limonene oxide and CO2 with high molecular weight, excellent thermal resistance, hardness and transparency. *Green Chem.* **2016**, *18*, 760−770.

(10) Du, L.; Qu, B.; Meng, Y.; Zhu, Q. Structural characterization and thermal and mechanical properties of poly(propylene carbonate)/MgAl-LDH exfoliation nanocomposite via solution intercalation. *Compos. Sci. Technol.* **2006**, *66*, 913−918.

(11) Luinstra, G. A.; Borchardt, E. *Synthetic Biodegradable Polymers*; Rieger, B., Künkel, A., Coates, G. W., Reichardt, R., Dinjus, E., Zevaco, T. A., Eds.; Springer Berlin Heidelberg: Berlin, Heidelberg, 2012; pp 29−48.

(12) Byrne, C. M.; Allen, S. D.; Lobkovsky, E. B.; Coates, G. W. Alternating copolymerization of limonene oxide and carbon dioxide. *J. Am. Chem. Soc.* **2004**, *126*, 11404−11405.

(13) Li, G.; Qin, Y.; Wang, X.; Zhao, X.; Wang, F. Study on the influence of metal residue on thermal degradation of poly(cyclohexene carbonate). *J. Polym. Res.* **2011**, *18*, 1177−1183.

(14) Cao, H.; Wang, X. Carbon dioxide copolymers: Emerging sustainable materials for versatile applications. *SusMat* **2021**, *1*, 88−104.

(15) Kernbichl, S.; Reiter, M.; Adams, F.; Vagin, S.; Rieger, B. CO2-Controlled One-Pot Synthesis of AB, ABA Block, and Statistical Terpolymers from β-Butyrolactone, Epoxides, and CO2. *J. Am. Chem. Soc.* **2017**, *139*, 6787−6790.

(16) Kernbichl, S.; Reiter, M.; Mock, J.; Rieger, B. Terpolymerization of β-Butyrolactone, Epoxides, and CO2: Chemoselective CO2-Switch and Its Impact on Kinetics and Material Properties. *Macromolecules* **2019**, *52*, 8476−8483.

(17) Carrodeguas, L. P.; Chen, T. T. D.; Gregory, G. L.; Sulley, G. S.; Williams, C. K. High elasticity, chemically recyclable, thermoplastics from bio-based monomers: carbon dioxide, limonene oxide and ε-decalactone. *Green Chem.* **2020**, *22*, 8298−8307.

(18) Sulley, G. S.; Gregory, G. L.; Chen, T. T. D.; Peña Carrodeguas, L.; Trott, G.; Santmarti, A.; Lee, K.-Y.; Terrill, N. J.; Williams, C. K. Switchable Catalysis Improves the Properties of CO2-Derived Polymers: Poly(cyclohexene carbonate-b-ε-decalactone-b-cyclohexene carbonate) Adhesives, Elastomers, and Toughened Plastics. *J. Am. Chem. Soc.* **2020**, *142*, 4367−4378.

(19) Neumann, S.; Leitner, L.-C.; Schmalz, H.; Agarwal, S.; Greiner, A. Unlocking the Processability and Recyclability of Biobased Poly(limonene carbonate). *ACS Sustainable Chem. Eng.* **2020**, *8*, 6442−6448.

(20) Owen, M. J. Why silicones behave funny. *Chem. Tech.* **1981**, *11*, 288−292.

(21) Cheng, M.; Moore, D. R.; Reczek, J. J.; Chamberlain, B. M.; Lobkovsky, E. B.; Coates, G. W. Single-Site β-Diiminate Zinc Catalysts for the Alternating Copolymerization of CO2 and Epoxides: Catalyst Synthesis and Unprecedented Polymerization Activity. *J. Am. Chem. Soc.* **2001**, *123*, 8738−8749.

(22) Reiter, M.; Kronast, A.; Kissling, S.; Rieger, B. In Situ Generated ABA Block Copolymers from CO2, Cyclohexene Oxide, and Poly(dimethylsiloxane)s. *ACS Macro Lett.* **2016**, *5*, 419−423.

(23) Kernbichl, S.; Rieger, B. Aliphatic polycarbonates derived from epoxides and CO2: A comparative study of poly(cyclohexene carbonate) and poly(limonene carbonate). *Polymer* **2020**, *205*, 122667.

(24) Darensbourg, D. J. Chain transfer agents utilized in epoxide and CO2 copolymerization processes. *Green Chem.* **2019**, *21*, 2214−2223.

(25) Thorat, S. D.; Phillips, P. J.; Semenov, V.; Gakh, A. Physical properties of aliphatic polycarbonates made from CO2 and epoxides. *J. Appl. Polym. Sci.* **2003**, *89*, 1163−1176.

(26) Rupasinghe, B.; Furgal, J. C. Degradation of silicone-based materials as a driving force for recyclability. *Polym. Int.* **2022**, *71*, 521−531.
(27) McDowell, M. T.; Lee, S. W.; Harris, J. T.; Korgel, B. A.; Wang, C.; Nix, W. D.; Cui, Y. In Situ TEM of Two-Phase Lithiation of Amorphous Silicon Nanospheres. *Nano Lett.* **2013**, *13*, 758−764.
(28) Megevand, B.; Pruvost, S.; Lins, L. C.; Livi, S.; Gérard, J.-F.; Duchet-Rumeau, J. Probing nanomechanical properties with AFM to understand the structure and behavior of polymer blends compatibilized with ionic liquids. *RSC Adv.* **2016**, *6*, 96421−96430.
(29) Zhang, H.; Wang, H.; Zhong, W.; Du, Q. A novel type of shape memory polymer blend and the shape memory mechanism. *Polymer* **2009**, *50*, 1596−1601.

https://doi.org/10.1021/acs.macromol.2c02433
Macromolecules 2023, 56, 4318−4324

5. Controlled synthesis of statistical polycarbonates based on epoxides and CO_2

Title: Controlled synthesis of statistical polycarbonates based on epoxides and CO_2

Status: Communication, accepted June, 2023

Journal: Macromolecular Materials and Engineering, 2300097

Publisher: John Wiley & Sons, Inc.

DOI: 10.1002/mame.202300097

Authors: Alina Denk, Emilia Fulajtar, Carsten Troll, Bernhard Rieger*

Content

The controlled polymerization of a mixed epoxide feedstock towards CO_2 based polycarbonates is enabled by the application of a dosing system. This setup allows the synthesis of statistical terpolymers despite significantly different reactivities of the epoxide monomers. With the continuous addition of the more reactive monomer into the reaction mixture over the whole time of the reaction it is possible to produce statistical terpolymers of defined monomer compositions by adjusting the monomer feed. The successful synthesis of terpolymers with the desired microstructure is analytically proven by diffusion-ordered nuclear magnetic resonance spectroscopy, gel permeation chromatography and differential scanning calorimetry measurements. The versatile concept can be transferred to other monomer mixtures as well.

*A. Denk carried out most of the experiments and wrote the manuscript. E. Fulajtar carried out experiments and gave advice on the manuscript. C. Troll designed the setup of the dosing system. All work was carried out under the supervision of B. Rieger.

RESEARCH ARTICLE

Macromolecular Materials and Engineering
Open Access
www.mame-journal.de

Controlled Synthesis of Statistical Polycarbonates Based on Epoxides and CO_2

*Alina Denk, Emilia Fulajtar, Carsten Troll, and Bernhard Rieger**

The controlled synthesis of terpolymer structures is often limited by the intrinsic reactivities of the monomers. For the synthesis of a statistical terpolymer from cyclohexene oxide (CHO) and propylene oxide (PO) with CO_2, an instrumental solution is demanded. Implementing a setup where one monomer can be added to the reaction mixture over the whole course of the reaction, the random distribution of the epoxides over the whole chain is realized. The successful terpolymerization can be determined with diffusion-ordered nuclear magnetic resonance spectroscopy and gel permeation chromatography measurements while the statistical microstructure of the generated polymers is indicated in NMR spectroscopy and differential scanning calorimetry measurements. Furthermore, the concept is transferred to the terpolymerization of limonene oxide with PO and CO_2 underlining the versatility of the setup.

1. Introduction

The development of CO_2-based aliphatic polycarbonates (PCs) in 1969 by the group of Inoue[1] set the starting point for research ambitions on this class of polymer materials which has not decreased since then. Until today, the range of monomers that can be used in the reaction is extended constantly. While bisphenol A-based polycarbonates (BPA-PCs) depend on fossil sources, the group of aliphatic PCs provide the opportunity to utilize sustainable feedstocks for epoxide monomers and furthermore the incorporation of CO_2 as a C1 building block.[2,3] The catalyst used in this work is based on the catalysts of Coates et al., a β-diimine (BDI) zinc complex.[4] In the improved complex from Rieger et al. CF_3 groups increase the Lewis acidity of the zinc center and $N(TMS)_2$ is used as initiating group.[5] With this catalyst a broad variety of epoxides can be copolymerized with CO_2 to the corresponding PCs. Through the combination of two different epoxides in the reaction solution even terpolymers can be synthesized (**Scheme 1**).[5]

In this work, we strive for the synthesis of terpolymers based on two different epoxides and CO_2. Thus, we want to control the microstructure of the polymers and combine the mechanical and thermal properties of the individual copolymers via terpolymerization.

2. Results and Discussion

2.1. Differences in Reaction Speed

While the catalyst allows to copolymerize a broad variety of epoxides with CO_2, they show strong differences in their reaction speed. This is clearly visible in the direct comparison of the copolymerizations of cyclohexene oxide (CHO), limonene oxide (LO), and propylene oxide (PO) each with CO_2, which can be followed using in situ IR. The signal of the respective PCs formed is plotted against time in Figure S1 (Supporting Information). While CHO is completely converted after only 40 min, the copolymerization of PO takes more than 20 h. The polymerization speed of these monomers depends on the catalyst and can vary for different catalytic systems. In the case of standard one pot terpolymerizations two epoxides would be placed in the reactor together with the catalyst and pressurized with CO_2. Due to the strong difference in reaction speed the more reactive epoxide would then be incorporated into the growing polymer chain more frequently than the other, less reactive, epoxide. Over the course of the reaction the concentration of the faster incorporated monomer in the reaction mixture would therefore decrease more rapidly and with this the probability to incorporate this monomer would also decrease over time. The resulting terpolymer microstructure is therefore of a gradient type (see Figure S3, Supporting Information). In our work we target a controlled incorporation of both monomers resulting in a statistical copolymer structure. In such a statistical copolymer no segment of measurably different composition is observed.[6] Such a uniform monomer distribution can result in consistent properties over the whole polymer chain. In this case no microphase separation or amphiphilic behavior is observed as it is possible for block or gradient copolymers. Statistical polymers from monomers with such different reactivities as for our reaction system can only be realized by controlling the polymerization process and incorporation of each monomer by means

A. Denk, E. Fulajtar, C. Troll, B. Rieger
WACKER-Chair of Macromolecular Chemistry
TUM School of Natural Sciences
Catalysis Research Center
Technical University Munich
Lichtenbergstr. 4, 85748 Garching, Germany
E-mail: rieger@tum.de

The ORCID identification number(s) for the author(s) of this article can be found under https://doi.org/10.1002/mame.202300097

DOI: 10.1002/mame.202300097

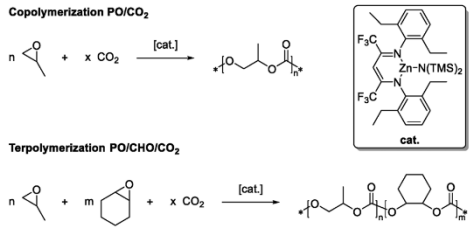

Scheme 1. Copolymerization of propylene oxide (PO) with CO_2 and terpolymerization of PO, cyclohexene oxide (CHO), and CO_2 with a β-diimine zinc complex as catalyst (cat.).

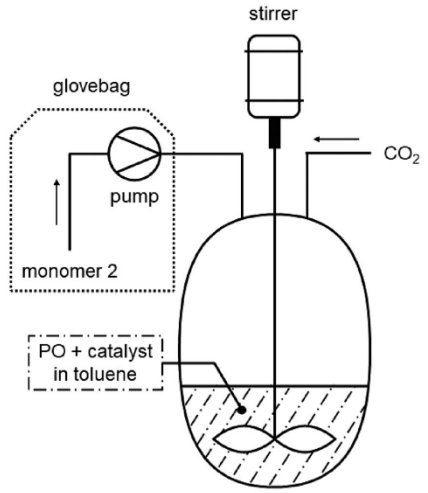

Figure 1. Setup of the dosing system for the synthesis of statistical terpolymerization of two epoxides and CO_2.

of instrumental modifications. Regulating the concentration of both monomers in the reaction mixture during the whole terpolymerization time, the generated microstructure of the evolving polymer chain can be controlled. A reduced concentration of the faster incorporated epoxide allows the other monomer to insert into the growing chain more frequently. This can be achieved by dosing the faster epoxide into the reaction mixture, keeping its concentration low for less dominance in the terpolymerization process.

2.2. Setup Dosing System

The instrumental layout for this controlled terpolymerization resembles a semi-batch setup (**Figure 1**). A pump is used to constantly dose the second monomer against a CO_2 pressure of 30 bar into the autoclave. The mass flow is monitored with a mass flow meter which is installed between the pump and the autoclave. With the in situ IR of the autoclave system the progress of the polymerization can be tracked. To ensure a water-free storage and transfer of the second monomer into the autoclave the storage flask and pump are placed in a glove bag under nitrogen and connected via steel capillaries with the autoclave. The atmosphere in the glove bag is furthermore dried with phosphorus pentoxide (P_4O_{10}) as desiccant.

2.3. Statistical Terpolymerization of PO, CHO, and CO_2

In the terpolymerization procedure PO and catalyst solution are introduced into the reactor and pressurized with CO_2. The second monomer is then added via the dosing system at a constant feed rate. **Table 1** shows terpolymerizations with different feeds of PO and CHO. Since CHO is dosed into the reaction mixture with a constant rate until stopping the reaction, the conversion is never 100%. At the same time the conversion of PO should stay below 100% as well to have both monomers present in the reaction mixture during the whole polymerization time. The difference between the classic batch approach and the herein presented semi-batch process can be observed via in situ IR (Figure S2, Supporting Information). The constant dosing of the second monomer ensures a constant reaction of both monomers and therefore also a linear growth of the intensity of the polymer signal. CHO reacts with CO_2 selectively towards the polymer product, PO forms besides poly(propylene carbonate) (PPC) also cyclic propylene carbonate (cPC) as a thermodynamically stable side product.[7] The selectivity of cPC formation could be decreased to around 20% by reducing the reaction temperature to 25 °C.[8] With an increasing CHO feed (Table 1, entries 4 and 5) the backbiting during the ongoing polymerization forming cPC (Scheme S1, Supporting Information),[9] is suppressed since CHO is inserted rapidly into the end of the growing chain. The composition and molecular weight of the generated terpolymers can be controlled by the feed rate and time and by adjusting the ratio between PO, CHO, and catalyst. A high amount of PO in the reactor together with the dosing rate of CHO reduced to a minimum result in a terpolymer with a PPC content of 76% (Table 1, entry 1). With the same dosing rate, but a longer reaction time (Table 1, entries 2 and 3) or with a higher rate and short reaction time (Table 1, entries 4 and 5) the amount of poly(cyclohexene carbonate) (PCHC) in the terpolymer can be further increased. The resulting polymers are analyzed via ^{1}H NMR to determine the ratio between PPC and PCHC in the product (Figures S4–S8, Supporting Information). They also show narrow mass distributions ($Đ \leq 2.0$) as expected for the selective generation of terpolymers (Figures S11–S15, Supporting Information). To analyze the polymers further we used diffusion-ordered NMR spectroscopy (DOSY-NMR) measurements, where the signals of both PPC and PCHC share a diffusion coefficient (Figure S9, Supporting Information). This indicates a connection of both polymers in one molecule and therefore successful terpolymerization.

Besides the polymerization of PO, CHO, and CO_2 towards connected terpolymers we were interested in the microstructure of the polymers, since we aimed for a statistical distribution of the epoxides over the whole polymer chain. To analyze this, we measured ^{13}C NMR of the polymers and compared specifically the carbon signals of the carbonyl moiety of the synthesized terpoly-

Table 1. Polymerizations of PO/CHO/CO_2 toward statistical PPC-PCHC terpolymers.

Entry	Feed[a] PO:CHO:cat.	Dosing rate CHO [mL h^{-1}]	Time [h]	Conversion[b] PO, CHO [%]	Selectivity[c] PPC:cPC [%]	PPC:PCHC [%][c]	M_n ($Đ$) [kg mol^{-1}][d]
1	2000:190:1	0.12	7	28, 72	77:23	76:24	91.0 (1.2)
2	1000:470:1	0.12	18	81, 90	81:19	61:39	60.9 (1.8)
3	500:380:1	0.12	16	81, 89	82:18	49:51	37.2 (2.0)
4	500:430:1	0.48	5	24, 85	100:0	25:75	33.8 (1.7)
5	250:910:1	0.96	4	53, 91	100:0	14:86	99.2 (1.4)

Polymerizations in toluene, 30 bar CO_2 pressure, 25 °C, stirred at 500 rpm. [a] Feed of CHO calculated from the sum of CHO and PCHC signals in ^{1}H NMR with the sum of PO, cPC, and PPC signals as reference. [b] Calculated from the respective polymer and monomer integrals in ^{1}H NMRs. [c] Calculated from the respective (polymer) signals in ^{1}H NMRs. [d] Measured via GPC in THF relative to poly(styrene) standards.

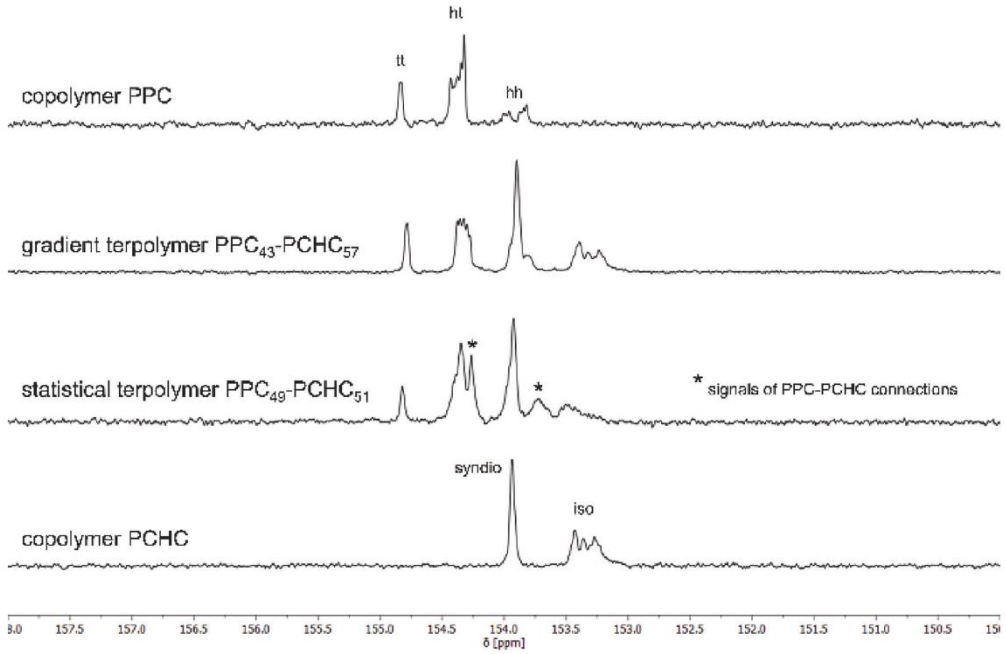

Figure 2. Carbonyl signals in the ^{13}C NMR of the pure copolymers PPC and PCHC. Compared to gradient and statistical PPC-PCHC terpolymers.

mers with pure PPC and PCHC and a gradient terpolymer synthesized via the classic one pot procedure (**Figure 2**).

In the NMR of PPC it can be distinguished between tail-to-tail (tt), head-to-tail (ht), and head-to-head (hh) connection of the PO units.[10] These three signals can be found as well in the NMRs of the terpolymers since both terpolymers don't have a strictly alternating epoxide incorporation. The tacticity of PCHC origins from the orientation of its cycle resulting in syndiotactic (syndio) or isotactic (iso) moieties.[11] In the case of both terpolymer NMRs the hh signal overlaps with the signal of syndiotactic PCHC, but only the statistical terpolymer shows the evolution of new signals (*) in the ^{13}C NMR, presumably caused by an increased number of carbonyls connecting PO and CHO with each other.

2.4. Statistical Terpolymerization of PO, LO, and CO_2

To show the versatility of the approach using a dosing system to control the microstructure we investigated LO in the statistical terpolymerization with PO and CO_2. In Table S1 (Supporting Information) these terpolymerizations are summarized. The reaction speed of LO is lower than of CHO, as indicated in Figure S1 (Supporting Information), which is why the dosing rates were reduced to avoid accumulation of LO in the reaction mixture. For the calculations of feed and conversion it must be noted, that the synthesized LO contains 92% of the *trans*-isomer. That is important since *cis*-LO is not accessible for the polymerization towards poly(limonene carbonate) (PLC) with our catalyst system and re-

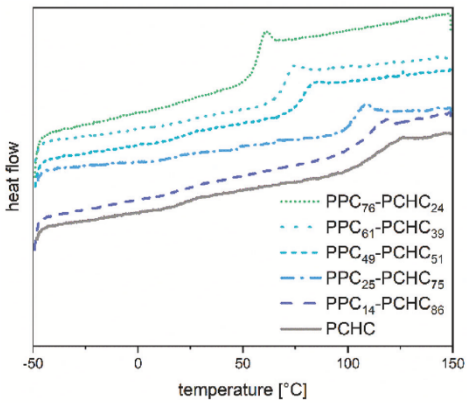

Figure 3. DSC measurements of PCHC and PPC-PCHC terpolymers with ratios in subscript.

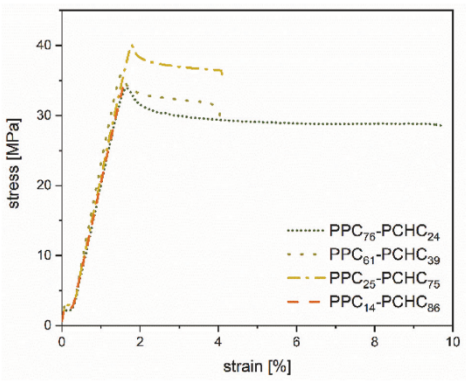

Figure 4. Tensile testing of specimen from PPC-PCHC terpolymers.

mains unreacted in the reaction solution. Via this procedure terpolymers with a tailored ratio of PPC and PLC in the final product could be synthesized. These polymers show narrow mass distributions (1.5–1.6) in gel permeation chromatography (GPC) measurements (Figures S16–S19, Supporting Information), but also carbonyl signals in ^{13}C NMR at 152–153 ppm, that origin from PPC-PLC connections in the terpolymer (Figure S10, Supporting Information). These signals indicate a successful synthesis of statistical terpolymers as explained for PPC-PCHC before.

2.5. Thermal Properties

To analyze the thermal properties of the generated polymersdifferential scanning calorimetry (DSC) and thermogravimetrcic analysis (TGA) measurements were performed and the results are summarized in Table S2 (Supporting Information). As expected the terpolymers show mixed glass transition temperatures (T_g) since both epoxides are incorporated statistically and therefore influence each other's thermal behavior. With an increasing amount of PPC in the terpolymer the T_g decreases (**Figure 3** and Figure S20, Supporting Information).

The thermal stability of the terpolymers is analyzed via TGA. Here the onset decomposition temperature (T_d) shows with increasing PPC content only a minor decrease from 293 to 262 °C for PPC-PCHC and to 244 °C for PPC-PLC (Figures S21 and S22, Supporting Information). Compared to pure PPC with a T_d of 180 to 240 °C[12] the terpolymers of PPC with PCHC show an increase in thermal stability.

2.6. Mechanical Characterization

The terpolymers were furthermore examined in tensile testing of dog bone shaped specimen. For the PPC-PCHC terpolymers an increase in elongation at break with increasing PPC content could be observed while the E-modulus remained high at over 2500 MPa (**Figure 4**). For the composition of 76:24 (PPC:PCHC) an elongation at break of 10% could be measured. In the case of PPC-PLC terpolymers this trend was not as clear. The E-moduli of 2070 to 2470 MPa for these samples were similarly high, as well as the tensile strengths of around 40 MPa. However, the elongation at break showed only minor increases up to 3% for a PPC content of 65%.

3. Conclusion

With the application of a dosing system, we were able to add one epoxide monomer in the terpolymerization of two epoxides and CO_2 into the reactor during the whole polymerization process. This way we could control the ratio of the monomers in the reaction mixture and therefore their incorporation into the terpolymer chain. Despite the major differences in reactivity of the epoxides this control over the monomer feed allowed us to synthesize statistical terpolymers with tailored ratios of the polymers in the terpolymer chain. Low polydispersities and high molecular weights show the stability of the polymerization process despite the continuous feed into the ongoing reaction. An increasing PPC content in the terpolymer led to a decreasing mixed T_g of the terpolymer, but the thermal stability remained high. An influence on the mechanical properties is given, but not as prominent as observed for the thermal behavior. With an increasing PPC content the elongation at break in tensile testing increased for the PPC-PCHC terpolymers.

Supporting Information

Supporting Information is available from the Wiley Online Library or from the author.

Acknowledgements

The authors would like to thank Andreas Schaffer and Christopher Thomas for the valuable discussions.
Open access funding enabled and organized by Projekt DEAL.

Conflict of Interest

The authors declare no conflict of interest.

Data Availability Statement

The data that support the findings of this study are available from the corresponding author upon reasonable request.

Keywords

aliphatic polycarbonates, carbon dioxide, copolymer engineering, dosing systems, statistical terpolymers

Received: March 19, 2023
Revised: April 28, 2023
Published online:

[1] S. Inoue, H. Koinuma, T. Tsuruta, *J. Polym. Sci., Part B: Polym. Lett.* **1969**, *7*, 287.
[2] Y. Xu, L. Lin, M. Xiao, S. Wang, A. T. Smith, L. Sun, Y. Meng, *Prog. Polym. Sci.* **2018**, *80*, 163.
[3] S. J. Poland, D. J. Darensbourg, *Green Chem.* **2017**, *19*, 4990.
[4] M. Cheng, D. R. Moore, J. J. Reczek, B. M. Chamberlain, E. B. Lobkovsky, G. W. Coates, *J. Am. Chem. Soc.* **2001**, *123*, 8738.
[5] M. Reiter, S. Vagin, A. Kronast, C. Jandl, B. Rieger, *Chem. Sci.* **2017**, *8*, 1876.
[6] J. Zhang, B. Farias-Mancilla, M. Destarac, U. S. Schubert, D. J. Keddie, C. Guerrero-Sanchez, S. Harrisson, *Macromol. Rapid Commun.* **2018**, *39*, 1800357.
[7] G. W. Coates, D. R. Moore, *Angew. Chem., Int. Ed.* **2004**, *43*, 6618.
[8] S. D. Allen, D. R. Moore, E. B. Lobkovsky, G. W. Coates, *J. Am. Chem. Soc.* **2002**, *124*, 14284.
[9] G. A. Luinstra, G. R. Haas, F. Molnar, V. Bernhart, R. Eberhardt, B. Rieger, *Chemistry* **2005**, *11*, 6298.
[10] D. J. Darensbourg, in *Synthetic Biodegradable Polymers* (Eds: B. Rieger, A. Künkel, G. W. Coates, R. Reichardt, E. Dinjus, T. A. Zevaco), Springer, Berlin, Heidelberg, **2012**, pp. 1–27.
[11] C. T. Cohen, C. M. Thomas, K. L. Peretti, E. B. Lobkovsky, G. W. Coates, *Dalton Trans.* **2006**, 237.
[12] O. Phillips, J. M. Schwartz, P. A. Kohl, *Polym. Degrad. Stab.* **2016**, *125*, 129.

6. Heteronuclear, monomer-selective Zn/Y catalyst combines copolymerization of epoxides and CO_2 with group-transfer polymerization of Michael-type monomers

Title: Heteronuclear, monomer-selective Zn/Y catalyst combines copolymerization of epoxides and CO_2 with group-transfer polymerization of *Michael*-type monomers

Status: Communication, published March 27, 2020

Journal: ACS Macro Letters, 9, 4, 571–575

Publisher: American Chemical Society

DOI: 10.1021/acsmacrolett.9b01025

Authors: Alina Denk‡, Sebastian Kernbichl‡, Andreas Schaffer, Moritz Kränzlein, Thomas Pehl, Bernhard Rieger*

Content

With the help of a binuclear catalyst the ring-opening copolymerization should be combined with the group transfer polymerization. Hence, a complex is synthesized with a *β*-diiminate zinc moiety to catalyze the epoxide/CO_2 copolymerization, which is connected *via* a pyridyl alcohol linker to an yttrium metallocene unit which is active in the group-transfer polymerization of *Michael*-type monomers. After mass spectrometry measurements showed the incorporation of the linking unit in poly(cyclohexene carbonate) and poly(2-vinylpyridine) individually terpolymerizations were performed either *via* sequential addition or a one pot route. Aliquot GPC analyses and solubility tests support a successful generation of block-structured polymers. Furthermore, the catalyst showed to be active also towards polymerization of 2-isopropenyl-2-oxazoline as *Michael* monomer.

‡These authors contributed equally. *A. Denk executed all the experiments and gave advice on the manuscript. S. Kernbichl had the initial idea and wrote the manuscript. A. Schaffer, M. Kränzlein and T. Pehl contributed valuable ideas and discussions. All work was carried out under the supervision of B. Rieger.

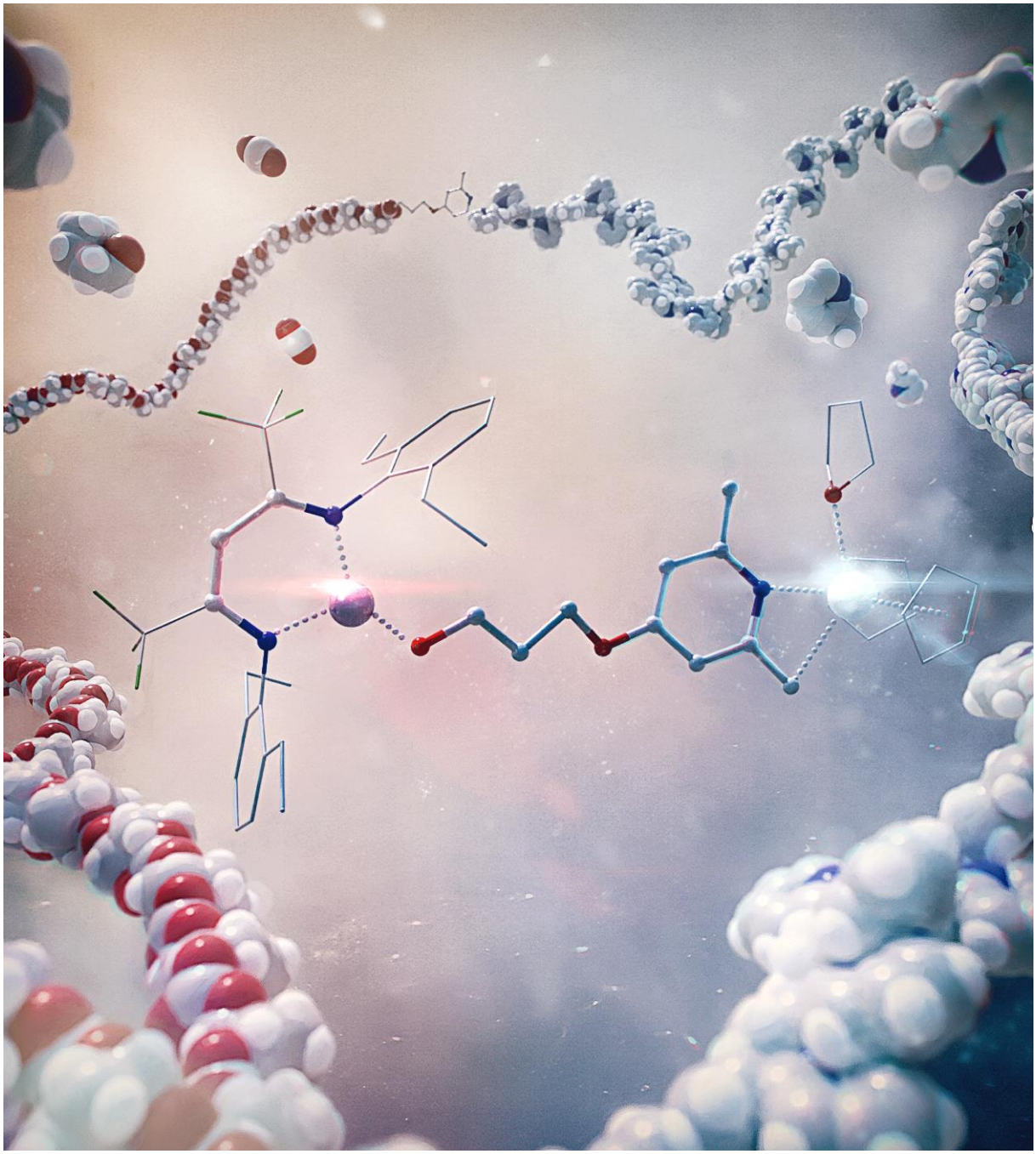

Figure 13. Cover art adopted from "Heteronuclear, monomer-selective Zn/Y catalyst combines copolymerization of epoxides and CO_2 with group-transfer polymerization of *Michael*-type monomers".[151]

ACS Macro Letters

pubs.acs.org/macroletters Letter

Heteronuclear, Monomer-Selective Zn/Y Catalyst Combines Copolymerization of Epoxides and CO_2 with Group-Transfer Polymerization of Michael-Type Monomers

Alina Denk,[†] Sebastian Kernbichl,[†] Andreas Schaffer, Moritz Kränzlein, Thomas Pehl, and Bernhard Rieger*

Cite This: *ACS Macro Lett.* 2020, 9, 571−575 Read Online

ACCESS | Metrics & More | Article Recommendations | Supporting Information

ABSTRACT: Terpolymerizations of cyclohexene oxide (CHO), CO_2, and the Michael-type monomer 2-vinylpyridine (2VP) are presented. The combination of two distinct polymerization mechanisms was enabled by the synthesis of a heterobifunctional complex (**3**). Its β-diiminate zinc moiety allows the ring-opening copolymerization of CHO and CO_2, whereas the yttrium metallocene catalyzed the rare earth metal-mediated group-transfer polymerization of the polar vinyl monomer. Both units were connected via the CH-bond activation of a pyridyl-alkoxide linker. Matrix-assisted laser desorption/ionization time-of-flight mass spectrometry (MALDI-TOF-MS) revealed the successful transfer of the linker to the end-group of the respective homopolymers poly(cyclohexene carbonate) (PCHC) and poly(2VP) (P2VP) being the prerequisite for copolymer formation. Aliquot gel-permeation chromatography (GPC) analysis and solubility behavior tests confirmed the P2VP-*block*-(*b*)-PCHC terpolymer formation via two pathways, a sequential and a one-pot procedure. Furthermore, the versatility of the method was demonstrated by introducing 2-isopropenyl-2-oxazoline (IPOx) as the second Michael-type monomer that yielded the terpolymer poly(IPOx)-*b*-PCHC.

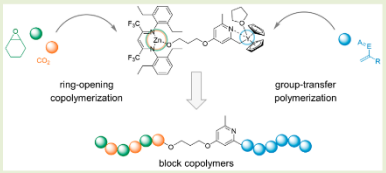

Although the ring-opening copolymerization (ROCOP) of epoxides and CO_2 was first reported 50 years ago, it remains a field of intense research.[1] The resulting aliphatic polycarbonates display attractive properties, such as biodegradability and high transparency, but the industrial demands in terms of thermal and mechanical performance have not been met yet.[2−4] The utilization of discrete, homogeneous transition metal catalysts allowed the precise synthesis of CO_2-based polymers in high activities and selectivities.[5−8] In order to improve the functionality of epoxide/CO_2-based aliphatic polycarbonates, block copolymers have been widely exploited in the last years. First, they were coupled with anhydrides to afford a novel class of polyesters.[9,10] Later, different lactones were incorporated as an additional block sequence by combining the ring-opening polymerization of lactones and the ROCOP of epoxides and CO_2.[11−20] Only a few catalysts were able to catalyze both reactions simultaneously, mainly β-diiminate zinc and dizinc phenoxide systems. Recently, our group reported the Lewis acidic BDI-Zn-N$(SiMe_3)_2$ complex **1**, which catalyzed the ROP of β-butyrolactone and the ROCOP of cyclohexene oxide and CO_2 to terpolymers in a block and statistical configuration, depending on the applied CO_2 pressure.[21]

The current study aimed to investigate the potential combination of aliphatic polycarbonates with polar polyolefins, derived from the polymerization of Michael-type monomers. The group-transfer polymerization (GTP) was initially observed by Webster et al. in 1983, where organosilicon compounds served as the initiators for the methyl methacrylate (MMA) polymerization.[22] Since then, GTP of polar monomers evolved to a valuable tool for the precise synthesis of tailor-made functional materials.[23,24] Rare-earth metal (REM) mediated GTP thereby plays an important role since high activities and the living character of the polymerization allow the synthesis of high-performance (co)polymers using monomers that range from diethyl vinylphosphonate to MMA and 2-vinylpyridine (2VP).[25−30] Currently, few studies have reported the generation of block copolymers consisting of polar polyolefins, such as PMMA and a polyester block from the ROP of a lactone.[31−34] The groups of Wang and Wu reported catalytic systems where the metal center catalyzes ROCOP of an epoxide and CO_2, and through the introduction of a second functional group, the reversible addition−fragmentation chain transfer polymerization of vinyl monomers was enabled.[35,36] Also, a Co(III) salen complex was presented that can be switched from radical polymerization to ROCOP

Received: December 30, 2019
Accepted: February 19, 2020
Published: March 27, 2020

by applying O_2 as an external stimulus.[37] But, none of these approaches combined GTP and ROCOP. Since BDI complexes are not known to catalyze the GTP of polar vinyl monomers, a heterobifunctional catalyst is required which connects two catalytically active moieties. Thereby, the zinc center would enable the coupling of the epoxide with CO_2, while the yttrium metallocene unit would precisely control the REM-GTP (Figure 1).

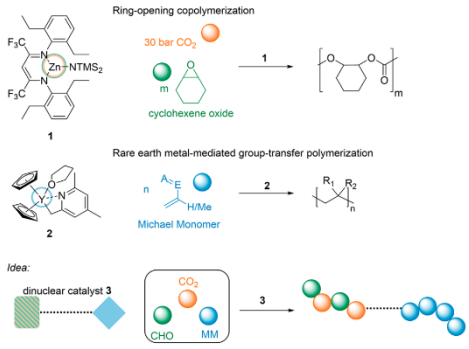

Figure 1. Top: ROCOP of CHO and CO_2 with the Lewis acidic zinc catalyst **1** to PCHC. Middle: REM-GTP of Michael-type monomers (MM) with the yttrium metallocene complex **2**. Bottom: Structure of a heteronuclear complex **3**, bearing both an yttrium and a zinc center displays the concept for the terpolymerization reaction.

Herein, we report the synthesis of a novel bifunctional catalyst **3** via the CH-bond activation of a BDI-Zn-O-pyridyl and $Cp_2Y(CH_2TMS)(thf)$. The successful end-group functionalization of the respective homopolymers, PCHC, P2VP, and PIPOx, was confirmed via MALDI-TOF MS. Catalyst **3** displayed high activity and chemoselectivity toward the ROCOP of CHO and CO_2 and the REM-GTP of 2VP and IPOx to give block copolymers using a sequential and a one-pot procedure. The resulting terpolymers were analyzed via GPC, solubility behavior, and differential scanning calorimetry (DSC).

The introduction of a suitable linking moiety was required in order to combine two different, catalytically active centers. As displayed in Scheme 1, the $-N(TMS)_2$ initiating group of **1** was successfully replaced by a pyridyl alcohol, yielding **3′**,

Scheme 1. Replacement of the Initiating Group of 1, Followed by the CH-Bond Activation of 3′ with $Cp_2Y(CH_2TMS)(thf)$, Yielding the Bifunctional Complex 3

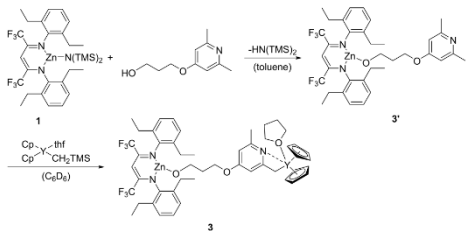

which in turn underwent a σ-bond metathesis between one adjacent methyl group and $Cp_2Y(CH_2TMS)(thf)$ and afforded the dinuclear complex **3**. The CH-activation was monitored via ^1H NMR spectroscopy and was completed after stirring for 4 h at rt (Figure S5).

The homopolymerization of the Michael-type monomer 2VP with complex **3** was performed to check the effect of the two transition metal centers on the activity of the complex in the GTP which solely proceeded at the yttrium center (Figure S7). P2VP was produced and the subsequent MALDI-MS end-group analysis of the oligomerization experiment revealed that the pyridyl moiety was linked to the polymer (Figure S8). Due to the high structural flexibility of the linking unit in **3**, the isolation of crystals for single-crystal X-ray diffraction failed. Although BDI complexes, bearing zinc alkoxide initiators, are known to catalyze the coupling of CHO and CO_2, complex **3** was tested in the copolymerization of CHO and CO_2 (Table 1, entry 1).[5] In situ attenuated total reflection infrared spectroscopy of the polymerization at 30 bar CO_2 disclosed a reaction time of 10 h (Figure S9). Compared with the already reported complex **1**, the bifunctional complex **3** was less active for the coupling of CHO and CO_2, but full conversion could still be achieved (yttrium metallocene **2** did not show conversion for the CHO/CO_2 coupling, Figure S6).[7] This prolonged reaction time could not be explained in detail, but a steric shielding of the zinc center and a competing coordination of CO_2 at the yttrium center was assumed. Electrospray ionization mass spectrometry (ESI-MS) and MALDI-MS measurements confirmed the presence of the pyridyl initiator as the polymer end-group, which was essential for the successful linking of the two planned polymer blocks (Figures S10 and S11).

Complex **3** was first tested in the sequential route with the ROCOP of CHO and CO_2 in the beginning, yielding PCHC in >99% conversion (Table 1, entry 2). Surprisingly, no P2VP formation could be observed upon adding 100 equiv of 2VP. The reason could be addressed via ^1H NMR spectroscopy by applying solely CO_2 on **3** (Figure S12). Carbon dioxide affected the dissociation of the coordinated thf molecule as well as the η^5-coordination of the Cp ligands. Moreover, the signal of the CH_2 group resulting from the CH-activation disappears, implying that the yttrium moiety was no longer bound to the pyridyl linker. GPC analysis of the PCHC block revealed a monomodal distribution, although bimodality for PCHC is well-known in literature and can be caused by catalytic traces of water that act as a chain-transfer agent.[38−41] Considering that such a chain-transfer may generate homopolymeric byproducts, the polymerizations with catalyst **3** were performed under inert conditions and freshly distilled monomers are used to prevent this side reaction. The second possibility for a sequential route starts with the homopolymerization of 2VP prior to the addition of CHO and CO_2. Indeed, conversion both to P2VP and PCHC could be observed (Table 1, entry 3). Scheme 2 presents the possible reaction pathways for the sequential route and a one-pot procedure.

In order to confirm that both polymer blocks were connected to each other and no homopolymeric byproducts were formed, an aliquot was taken before the epoxide was added. The absolute molecular weight for the P2VP block was determined by GPC analysis in DMF. A good agreement between the experimentally determined and theoretically expected M_n values indicates a high initiator efficiency of 70%. GPC analysis of the P2VP aliquot and the final

https://dx.doi.org/10.1021/acsmacrolett.9b01025
ACS Macro Lett. 2020, 9, 571−575

Table 1. Terpolymerization of CHO and CO_2 with 2VP and IPOx, Respectively, Using the Bifunctional Catalyst 3

entry	feed[a]	reaction pathway[b]	conv. A[c] [%]	M_n (A)[d] ($Đ$)[e] [kg/mol]	I[f]	conv. B[c] [%]	M_n (A-*b*-BC)[g] ($Đ$) [kg/mol]	[A]:[BC][h]
1[i]	CHO_{100}	–	–	–	–	98	28.2 (1.32)[j]	0:100
2	$2VP_{100}$:CHO_{100}	sequential	0	–	–	>99	17.5 (1.20)[j]	0:100
3	$2VP_{100}$:CHO_{100}	sequential	58	8.7 (1.16)	0.70	97	20.0 (1.25)	34:66
4	$2VP_{100}$:CHO_{200}	sequential	57	7.0 (1.33)	0.86	93	37.2 (1.37)	18:82
5	$2VP_{100}$:CHO_{100}	one pot	30	4.7[k] (1.13)	0.68	93	17.0 (1.30)	23:77
6	$IPOx_{100}$:CHO_{100}	sequential	82	14.9[k] (1.41)	0.61	99	23.0 (1.37)	50:50
7	$IPOx_{100}$:CHO_{100}	one pot	77	9.7[k] (1.56)	0.88	97	17.7 (1.40)	41:59

[a]Monomer feed of the respective monomers, [**3**] = 8.39 μmol in 1.2 mL toluene. [b]Reaction pathway according to Scheme 2. [c]Conversion determined via ^{1}H NMR spectroscopy. [d]Absolute molecular weight of block A (P2VP) determined via triple detection GPC analysis in DMF as eluent at 30 °C (dn/dc = 0.149 mL/g). [e]Polydispersity calculated from $M_{w,GPC}/M_{n,GPC}$ determined via GPC in DMF. [f]Initiator efficiency I = $M_{n,\,theo}/M_n$(A), $M_{n,\,theo}$ = eq (2VP/IPOx) × M_n (2VP/IPOx) × conversion. [g]Molecular weight of the final terpolymer determined via GPC analysis in DMF as eluent at 30 °C relative to PMMA standards. [h]Composition of the terpolymer after precipitation in pentane determined via ^{1}H NMR spectroscopy. [i]Polymerization performed in an autoclave with in situ IR monitoring. [j]Only PCHC was produced. [k]Absolute molecular weight of block A determined via ^{1}H NMR spectroscopy.

Scheme 2. Overview of the Two Possible Polymerization Pathways

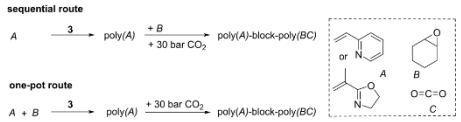

terpolymer revealed a shift of the GPC traces to lower retention times (Figure 2).

Solubility experiments were also performed. PCHC has no solubility in methanol, but the terpolymer consisting of 34% P2VP and 66% PCHC was soluble in methanol, as confirmed by ^{1}H NMR spectroscopy (Figure 2). It was also observed that the composition slightly changed to P2VP:PCHC = 41:59, owing to traces of homopolymeric PCHC. The same solubility test was conducted for an artificial polymer blend, where no PCHC was found in the methanol phase (Figure S13). Next, 200 equiv of CHO were added to the reaction mixture after successful 2VP polymerization, and again, a terpolymer was formed (Table 1, entry 4). GPC analysis confirmed the successful block formation (Figure 2). Due to the very high PCHC content, the terpolymer was not soluble in methanol any longer. The insoluble part was characterized via ^{1}H NMR, and the same P2VP:PCHC composition was found, indicating that the P2VP block was connected to the PCHC unit (homopolymeric P2VP is soluble in methanol; Figure S31). Also, for this polymerization, a slight shouldering of the GPC trace is observed that is most likely caused by homopolymeric PCHC. We were curious if the one-pot pathway also yields P2VP/PCHC terpolymers. Since CO_2 led to the decomposition of the yttrium unit, both monomers, 2VP and CHO, were mixed with **3** in the autoclave, and after stirring for 4 h, 30 bar CO_2 was applied. The conversion of 2VP decreased, probably due to the competing coordination of CHO at the yttrium moiety. Nevertheless, a terpolymer with a monomodal distribution and a dispersity of 1.30 was obtained (Table 1, entry 5). This finding demonstrates that the one-pot procedure allows the switch from the REM-GTP to the ROCOP by the addition of carbon dioxide. DSC measurements of a P2VP-*b*-PCHC terpolymer revealed a mixed glass transition temperature (T_g) of 110 °C ($T_{g,PCHC}$ = 117 °C, $T_{g,P2VP}$ = 97 °C), while thermogravimetric analysis indicated a decomposition temperature of T_{max} = 280 °C (Figures S33 and S34). In addition, IPOx as a second Michael-type monomer was selected to test the versatility of the system. ESI-MS end-group analysis of the oligomerization experiments showed the successful transfer of the pyridyl-initiating group to the PIPOx polymer (Figure S35). Terpolymerization attempts were conducted in both pathways (Table 1, entries 6 and 7), and high IPOx conversions (>77%) in high initiator efficiencies (I > 61%) resulted in PIPOx/PCHC terpolymers of equimolar composition. Two glass transitions were observed at 125 and 185 °C ($T_{g,PCHC}$ = 117 °C, $T_{g,PIPOx}$ = 174 °C; Figure S36).

In conclusion, we introduced a bifunctional complex bearing a Lewis acidic zinc moiety and an yttrium metallocene unit, linked via a pyridyl-alkoxide linker. Terpolymerizations were

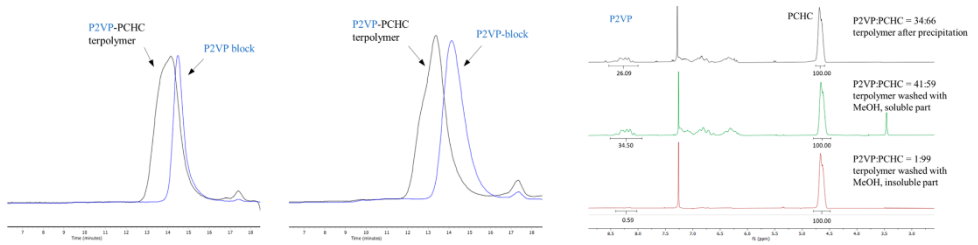

Figure 2. GPC traces. Left and middle: shift of signal from P2VP block (blue) to P2VP-PCHC terpolymer (black) for Table 1, entries 3 and 4, respectively. Right: ^{1}H NMR spectra of a P2VP-PCHC terpolymer (Table 1, entry 3) prior to (black) and after (green) washing with methanol compared with the spectrum of the insoluble part (red).

https://dx.doi.org/10.1021/acsmacrolett.9b01025
ACS Macro Lett. 2020, 9, 571−575

achieved by connecting the ROCOP of epoxides and CO_2 at the zinc center and the REM-GTP of Michael-type monomers at the yttrium side. The resulting two-block terpolymers could be obtained both via a sequential and a one-pot procedure and consist of P2VP-*b*-PCHC and PIPOx-*b*-PCHC. This combination of aliphatic polycarbonates and polar polyolefins, therefore, offers many possibilities in terms of synthetic variations and terpolymer properties that are not accessible with the respective homopolymers.

■ ASSOCIATED CONTENT

Supporting Information

The Supporting Information is available free of charge at https://pubs.acs.org/doi/10.1021/acsmacrolett.9b01025.

Detailed experimental procedures for catalyst synthesis and polymerizations, ESI-MS and MALDI-MS end-group analysis, NMRs of selected polymers, GPC, DSC, and TGA data (PDF)

■ AUTHOR INFORMATION

Corresponding Author

Bernhard Rieger − *WACKER-Chair of Macromolecular Chemistry, Catalysis Research Center, Technical University Munich 85748 Garching, Germany*; orcid.org/0000-0002-0023-884X; Phone: +49-89-289-13570; Email: rieger@tum.de; Fax: +49-89-289-13562

Authors

Alina Denk − *WACKER-Chair of Macromolecular Chemistry, Catalysis Research Center, Technical University Munich 85748 Garching, Germany*

Sebastian Kernbichl − *WACKER-Chair of Macromolecular Chemistry, Catalysis Research Center, Technical University Munich 85748 Garching, Germany*

Andreas Schaffer − *WACKER-Chair of Macromolecular Chemistry, Catalysis Research Center, Technical University Munich 85748 Garching, Germany*

Moritz Kränzlein − *WACKER-Chair of Macromolecular Chemistry, Catalysis Research Center, Technical University Munich 85748 Garching, Germany*

Thomas Pehl − *WACKER-Chair of Macromolecular Chemistry, Catalysis Research Center, Technical University Munich 85748 Garching, Germany*

Complete contact information is available at: https://pubs.acs.org/10.1021/acsmacrolett.9b01025

Author Contributions

†These authors contributed equally to this work.

Notes

The authors declare no competing financial interest.

■ REFERENCES

(1) Inoue, S.; Koinuma, H.; Tsuruta, T. Copolymerization of carbon dioxide and epoxide. *J. Polym. Sci., Part B: Polym. Lett.* **1969**, *7*, 287−292.

(2) Rieger, B.; Künkel, A.; Coates, G. W. *Synthetic Biodegradable Polymers Springer*; Berlin/Heidelberg: Germany, 2012.

(3) Lu, X. B. *Carbon Dioxide and Organometallics*; Springer International Publishing, 2015.

(4) Kozak, C. M.; Ambrose, K.; Anderson, T. S. Copolymerization of carbon dioxide and epoxides by metal coordination complexes. *Coord. Chem. Rev.* **2018**, *376*, 565−587.

(5) Cheng, M.; Lobkovsky, E. B.; Coates, G. W. Catalytic Reactions Involving C1 Feedstocks: New High-Activity Zn(II)-Based Catalysts for the Alternating Copolymerization of Carbon Dioxide and Epoxides. *J. Am. Chem. Soc.* **1998**, *120*, 11018−11019.

(6) Coates, G. W.; Moore, D. R. Discrete Metal-Based Catalysts for the Copolymerization of CO2 and Epoxides: Discovery, Reactivity, Optimization, and Mechanism. *Angew. Chem., Int. Ed.* **2004**, *43*, 6618−6639.

(7) Reiter, M.; Vagin, S.; Kronast, A.; Jandl, C.; Rieger, B. A Lewis acid [small beta]-diiminato-zinc-complex as all-rounder for co- and terpolymerisation of various epoxides with carbon dioxide. *Chem. Sci.* **2017**, *8*, 1876−1882.

(8) Kissling, S.; Lehenmeier, M. W.; Altenbuchner, P. T.; Kronast, A.; Reiter, M.; Deglmann, P.; Seemann, U. B.; Rieger, B. Dinuclear zinc catalysts with unprecedented activities for the copolymerization of cyclohexene oxide and CO_2. *Chem. Commun.* **2015**, *51*, 4579−4582.

(9) Jeske, R. C.; DiCiccio, A. M.; Coates, G. W. Alternating Copolymerization of Epoxides and Cyclic Anhydrides: An Improved Route to Aliphatic Polyesters. *J. Am. Chem. Soc.* **2007**, *129*, 11330−11331.

(10) Jeske, R. C.; Rowley, J. M.; Coates, G. W. Pre-Rate-Determining Selectivity in the Terpolymerization of Epoxides, Cyclic Anhydrides, and CO2: A One-Step Route to Diblock Copolymers. *Angew. Chem., Int. Ed.* **2008**, *47*, 6041−6044.

(11) Romain, C.; Zhu, Y.; Dingwall, P.; Paul, S.; Rzepa, H. S.; Buchard, A.; Williams, C. K. Chemoselective Polymerizations from Mixtures of Epoxide, Lactone, Anhydride, and Carbon Dioxide. *J. Am. Chem. Soc.* **2016**, *138*, 4120−4131.

(12) Wu, G.-P.; Darensbourg, D. J.; Lu, X.-B. Tandem Metal-Coordination Copolymerization and Organocatalytic Ring-Opening Polymerization via Water To Synthesize Diblock Copolymers of Styrene Oxide/CO2 and Lactide. *J. Am. Chem. Soc.* **2012**, *134*, 17739−17745.

(13) Darensbourg, D. J.; Wu, G.-P. A One-Pot Synthesis of a Triblock Copolymer from Propylene Oxide/Carbon Dioxide and Lactide: Intermediacy of Polyol Initiators. *Angew. Chem., Int. Ed.* **2013**, *52*, 10602−10606.

(14) Zhu, Y.; Romain, C.; Williams, C. K. Selective Polymerization Catalysis: Controlling the Metal Chain End Group to Prepare Block Copolyesters. *J. Am. Chem. Soc.* **2015**, *137*, 12179−12182.

(15) Hwang, Y.; Jung, J.; Ree, M.; Kim, H. Terpolymerization of CO2 with Propylene Oxide and ε-Caprolactone Using Zinc Glutarate Catalyst. *Macromolecules* **2003**, *36*, 8210−8212.

(16) Hwang, Y.; Kim, H.; Ree, M. Zinc Glutarate Catalyzed Synthesis and Biodegradability of Poly(carbonate-co-ester)s from CO_2, Propylene Oxide, and ε-Caprolactone. *Macromol. Symp.* **2005**, *224*, 227−238.

(17) Kernbichl, S.; Reiter, M.; Mock, J.; Rieger, B. Terpolymerization of β-Butyrolactone, Epoxides, and CO_2: Chemoselective CO_2-Switch and Its Impact on Kinetics and Material Properties. *Macromolecules* **2019**, *52*, 8476.

(18) Kröger, M.; Folli, C.; Walter, O.; Döring, M. Alternating Copolymerization of Carbon Dioxide and Cyclohexene Oxide and Their Terpolymerization with Lactide Catalyzed by Zinc Complexes of N. *Adv. Synth. Catal.* **2006**, *348*, 1908−1918.

(19) Romain, C.; Williams, C. K. Chemoselective Polymerization Control: From Mixed-Monomer Feedstock to Copolymers. *Angew. Chem., Int. Ed.* **2014**, *53*, 1607−1610.

(20) Paul, S.; Romain, C.; Shaw, J.; Williams, C. K. Sequence Selective Polymerization Catalysis: A New Route to ABA Block Copoly(ester-b-carbonate-b-ester). *Macromolecules* **2015**, *48*, 6047−6056.

(21) Kernbichl, S.; Reiter, M.; Adams, F.; Vagin, S.; Rieger, B. CO_2-Controlled One-Pot Synthesis of AB, ABA Block, and Statistical Terpolymers from β-Butyrolactone, Epoxides, and CO_2. *J. Am. Chem. Soc.* **2017**, *139*, 6787−6790.

(22) Webster, O. W.; Hertler, W. R.; Sogah, D. Y.; Farnham, W. B.; RajanBabu, T. V.; et al. *J. Am. Chem. Soc.* **1983**, *105*, 5706−5708.

(23) Chen, E. Y. X. Coordination Polymerization of Polar Vinyl Monomers by Single-Site Metal Catalysts. *Chem. Rev.* **2009**, *109*, 5157−5214.
(24) Soller, B. S.; Salzinger, S.; Rieger, B. Rare Earth Metal-Mediated Precision Polymerization of Vinylphosphonates and Conjugated Nitrogen-Containing Vinyl Monomers. *Chem. Rev.* **2016**, *116*, 1993−2022.
(25) Yasuda, H.; Ihara, E. Rare earth metal initiated polymerizations of polar and nonpolar monomers to give high molecular weight polymers with extremely narrow molecular weight distribution. *Macromol. Chem. Phys.* **1995**, *196*, 2417−2441.
(26) Soller, B. S.; Salzinger, S.; Jandl, C.; Pöthig, A.; Rieger, B. C−H Bond Activation by σ-Bond Metathesis as a Versatile Route toward Highly Efficient Initiators for the Catalytic Precision Polymerization of Polar Monomers. *Organometallics* **2015**, *34*, 2703−2706.
(27) Altenbuchner, P. T.; Soller, B. S.; Kissling, S.; Bachmann, T.; Kronast, A.; Vagin, S. I.; Rieger, B. Versatile 2-Methoxyethylaminobis(phenolate)yttrium Catalysts: Catalytic Precision Polymerization of Polar Monomers via Rare Earth Metal-Mediated Group Transfer Polymerization. *Macromolecules* **2014**, *47*, 7742−7749.
(28) Adams, F.; Pahl, P.; Rieger, B. Metal-Catalyzed Group-Transfer Polymerization: A Versatile Tool for Tailor-Made Functional (Co)Polymers. *Chem. - Eur. J.* **2018**, *24*, 509−518.
(29) Kaneko, H.; Nagae, H.; Tsurugi, H.; Mashima, K. End-Functionalized Polymerization of 2-Vinylpyridine through Initial C−H Bond Activation of N-Heteroaromatics and Internal Alkynes by Yttrium Ene−Diamido Complexes. *J. Am. Chem. Soc.* **2011**, *133*, 19626−19629.
(30) Wang, Q.; Chen, S.; Liang, Y.; Dong, D.; Zhang, N. Bottle-Brush Brushes: Surface-Initiated Rare Earth Metal Mediated Group Transfer Polymerization from a Poly(3-((2,6-dimethylpyridin-4-yl)-oxy)propyl methacrylate) Backbone. *Macromolecules* **2017**, *50*, 8456−8463.
(31) Kostakis, K.; Mourmouris, S.; Karanikolopoulos, G.; Pitsikalis, M.; Hadjichristidis, N. Ring-opening polymerization of lactones using zirconocene catalytic systems: Block copolymerization with methyl methacrylate. *J. Polym. Sci., Part A: Polym. Chem.* **2007**, *45*, 3524−3537.
(32) Solaro, R.; Cantoni, G.; Chiellini, E. Polymerisability of different lactones and methyl methacrylate in the presence of various organoaluminium catalysts. *Eur. Polym. J.* **1997**, *33*, 205−211.
(33) Dove, A. P.; Gibson, V. C.; Marshall, E. L.; White, A. J. P.; Williams, D. J. A well-defined magnesium enolate initiator for the living and highly syndioselective polymerisation of methylmethacrylate. *Chem. Commun.* **2002**, 1208−1209.
(34) Kajiwara, A.; Matyjaszewski, K. Formation of Block Copolymers by Transformation of Cationic Ring-Opening Polymerization to Atom Transfer Radical Polymerization (ATRP). *Macromolecules* **1998**, *31*, 3489−3493.
(35) Wang, Y.; Zhao, Y.; Ye, Y.; Peng, H.; Zhou, X.; Xie, X.; Wang, X.; Wang, F. A One-Step Route to CO2-Based Block Copolymers by Simultaneous ROCOP of CO2/Epoxides and RAFT Polymerization of Vinyl Monomers. *Angew. Chem., Int. Ed.* **2018**, *57*, 3593−3597.
(36) Zhang, Y.-Y.; Yang, G.-W.; Wu, G.-P. A Bifunctional β-Diiminate Zinc Catalyst with CO2/Epoxides Copolymerization and RAFT Polymerization Capacities for Versatile Block Copolymers Construction. *Macromolecules* **2018**, *51*, 3640−3646.
(37) Zhao, Y.; Wang, Y.; Zhou, X.; Xue, Z.; Wang, X.; Xie, X.; Poli, R. Oxygen-Triggered Switchable Polymerization for the One-Pot Synthesis of CO2-Based Block Copolymers from Monomer Mixtures. *Angew. Chem.* **2019**, *131*, 14449−14456.
(38) Nakano, K.; Kamada, T.; Nozaki, K. Selective Formation of Polycarbonate over Cyclic Carbonate: Copolymerization of Epoxides with Carbon Dioxide Catalyzed by a Cobalt(III) Complex with a Piperidinium End-Capping Arm. *Angew. Chem., Int. Ed.* **2006**, *45*, 7274−7277.
(39) Moore, D. R.; Cheng, M.; Lobkovsky, E. B.; Coates, G. W. Mechanism of the Alternating Copolymerization of Epoxides and CO2 Using β-Diiminate Zinc Catalysts: Evidence for a Bimetallic Epoxide Enchainment. *J. Am. Chem. Soc.* **2003**, *125*, 11911−11924.
(40) Kember, M. R.; Williams, C. K. Efficient Magnesium Catalysts for the Copolymerization of Epoxides and CO2; Using Water to Synthesize Polycarbonate Polyols. *J. Am. Chem. Soc.* **2012**, *134*, 15676−15679.
(41) Na, S. J.; Sujith, S.; Cyriac, A.; Kim, B. E.; Yoo, J.; Kang, Y. K.; Han, S. J.; Lee, C.; Lee, B. Y. Elucidation of the Structure of a Highly Active Catalytic System for CO2/Epoxide Copolymerization: A salen-Cobaltate Complex of an Unusual Binding Mode. *Inorg. Chem.* **2009**, *48*, 10455−10465.

https://dx.doi.org/10.1021/acsmacrolett.9b01025
ACS Macro Lett. 2020, 9, 571−575

7. Biobased Synthesis and Biodegradability of CO_2-Based Polycarbonates

Title: Biobased Synthesis and Biodegradability of CO_2-Based Polycarbonates

Status: Book chapter, published March 2, 2022

Publisher: Springer, Berlin, Heidelberg

DOI: 10.1007/12_2022_116

Authors: Alina Denk, Bernhard Rieger*

Content

The opportunities which aliphatic polycarbonates offer are not only based on their CO_2 content but have to be assessed also regarding the origin of the epoxide monomer. With a comparison of conventional and biobased synthesis routes towards the most common epoxides used for the synthesis of aliphatic polycarbonates their sustainability is explored. Besides propylene oxide and cyclohexene oxide also one of the most prominent examples for biobased epoxides, namely limonene oxide is discussed. Additionally, an interesting synthesis approach towards vegetable oil-based epoxides is covered. Looking further into the catalysis of the copolymerization of these epoxides with CO_2 the catalyst development is briefly examined. Further background is given for the mechanism behind the ring-opening copolymerization and unwanted side reactions. The diverse group of CO_2-based polycarbonates offer a wide range of properties based on the employed epoxide comonomer. Besides the aspect of a sustainable monomer basis for these monomers, another aspect of sustainability is the degradability of polymers in the environment. For the group of aliphatic polycarbonates, the research in this field is mainly focused on the compostability of poly(propylene carbonate). To classify this polymer group as a valuable unit in the uprising of sustainable polymers this aspect requires further investigation.

*A. Denk wrote the manuscript. All work was carried out under the supervision of B. Rieger.

Biobased Synthesis and Biodegradability of CO_2-based Polycarbonates

Alina Denk and Bernhard Rieger

Abstract Stimulated by the growing interest in sustainable polymers, the past few decades have seen intensive research in the field of CO_2-based polycarbonates. Within this research, the catalysts for the ring-opening copolymerization of epoxides and CO_2 developed from early heterogeneous complexes to a wide variety of homogeneous catalysts. These complexes are continuously improved to meet growing expectations regarding activity and selectivity. Simultaneously, the range of epoxide monomers has steadily expanded due to the growing interest in biobased starting materials for polymers. The potential of the resulting aliphatic polycarbonates is evident in their thermal and mechanical properties, where they exhibit a wide range from soft to brittle and from low to high glass transition temperatures. Although the biodegradability of CO_2-based polycarbonates has not yet been extensively researched, it has already been possible to gain knowledge about poly(propylene carbonate) and its compostability. The entire potential of aliphatic polycarbonates is still far from being fully discovered, and with constant development of new catalysts and monomer feedstocks, the chance of a CO_2- and biobased polymer achieving greater industrial relevance is increasing.

Keywords Biobased · Carbon dioxide · Degradation · Epoxides · Polycarbonates · Ring-opening copolymerization · Sustainability

Contents

Abbreviations

BDI	β-Diiminate
BPA-PC	bisphenol-A polycarbonate
cPC	Cyclic propylene carbonate
Đ	Polydispersity index (M_n/M_w)
ε_b	Elongation at break
E	E-modulus (or Young's modulus)
HPPO	Hydrogen peroxide propylene oxide
LO	Limonene oxide
*m*CPBA	*meta*-Chloroperoxybenzoic acid
M_n	Number-average molecular weight
M_w	Weight-average molecular weight
MTP	Methanol-to-propylene
PC	Polycarbonate
PCHC	Poly(cyclohexene carbonate)
PLC	Poly(limonene carbonate)
PO	Propylene oxide
PPC	Poly(propylene carbonate)
PPNCl	Bis(triphenylphosphine)iminium chloride
ROCOP	Ring-opening copolymerization
σ_m	Tensile strength
Salen	Salicylaldimine
TGA	Thermogravimetric analysis
TOF	Turnover frequency
TPP	Tetraphenylporphyrin
ZnGA	Zinc glutarate

1 Introduction

The successful synthesis of polycarbonates (PCs) from bisphenol A and phosgene was a milestone for the polymer industry in Germany, where large-scale production of aromatic PCs with the brand name Makrolon® was launched in 1958 by the Bayer AG (see scheme 1.1 (a)).[1] Properties like tensile strength and toughness of these thermoplastics combined with heat-resistance, flame-retardancy, transparency, and good resistance towards environmental impacts, made PCs an attractive product for application in the automotive and electronics industry.[1] Since both phosgene and bisphenol A are health hazards,[2-3] the synthesis of PCs avoiding these educts is aspired to. Furthermore, the development of novel polymers from sustainable resources is of high interest in today's research. A promising C1 building block can be found in CO_2, a non-toxic and abundant greenhouse gas. Making use of it as a monomer, the first metal-catalyzed copolymerization of CO_2 and epoxides was reported by Inoue and co-workers in 1969.[4] The alternating incorporation of CO_2 and an epoxide generates carbonate linkages, which leads to aliphatic PCs as pictured in scheme 1.1 (b).

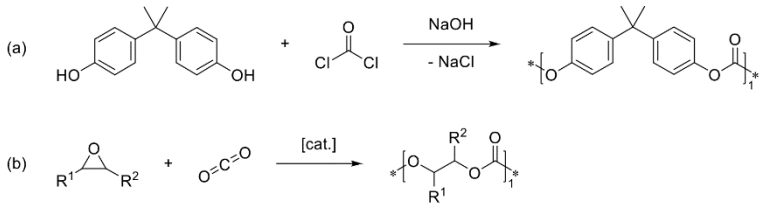

Scheme 1.1 Synthesis of (a) conventional polycarbonate from bisphenol A and phosgene and (b) aliphatic polycarbonates from epoxides and CO_2.[1, 4]

By using this building block not only can an environmentally harmful gas emitted in large quantities be used, but also alternatives to petrochemical products are investigated. The first heterogenous catalysts were further improved,[5] and over the years the focus of related research shifted towards homogenous catalysis systems. Herein, the most important complexes are based on porphyrin, salen, phenoxide or β-diiminate ligands.[6-10] Tuning the selectivity and activity of the complexes, a wide range of catalytic systems are nowadays available for the coupling of CO_2 and epoxides. Propylene oxide and cyclohexene oxide are the standard epoxy monomers for the synthesis of aliphatic PCs; however, new starting materials are constantly under research. The impact that polymer production has on the environment is not only of interest regarding the utilization of CO_2, but also in the choice of the epoxide monomer and its origin. In this chapter, we will discuss the advances that research in the fields of aliphatic PCs made in terms of monomer scope, as well as catalyst development. The focus will lie on the most prominent epoxides and their copolymerization catalysts, as well as on some less popular examples for recent developments. Furthermore, the thermal, mechanical, and degradation properties of the resulting aliphatic PCs will be discussed. The described developments will also be repeatedly analyzed regarding their sustainability.

2 Monomer synthesis

2.1 Propylene oxide

In regard to the copolymerization of epoxides and CO_2, a lot of research focuses on propylene oxide (PO) as an epoxide monomer. It has a long history as a monomer in the epoxide/CO_2 copolymerization and an even longer one in general use as a reactive chemical. The processes for PO synthesis have therefore developed over the years and have constantly been optimized, even with the growing interest in green chemistry. Two important processes for the synthesis of PO are the more traditional chlorohydrin process and the hydrogen peroxide propylene oxide (HPPO) process. In 1859, Wurtz reported the synthesis of PO from propylene chlorohydrin, setting the foundation for the chlorine route towards the epoxide.[11] Over the years, the process developed into industrial relevance using propylene and chlorine as initial reactants. The two steps in this synthesis are shown in scheme 2.2 (a). First, the chlorohydrination converts propylene into propylene chlorohydrin, which is then epoxidized using sodium hydroxide or calcium hydroxide in a saponification reaction.[12] Another pathway towards PO is the chlorine-free HPPO process. With the use of the heterogeneous titanium silicalite catalyst TS-1, propylene can be epoxidized quickly and with high selectivity (97%) towards PO (see scheme 2.2 (b)). In this case, the olefin is oxidized with hydrogen peroxide in a mixture of methanol and water as solvents. Since the main byproduct in this case is water, the synthesis is a more sustainable approach than the chlorohydrin process mentioned previously.[13]

Since both routes depend on propylene, which is usually derived from mineral oil, as a starting material, it is therefore necessary that we investigate a potential biobased synthesis of propylene. In the process towards synthesizing the olefin, most routes proceed via methanol as an intermediate. On this pathway, the hydrogenation of carbon monoxide is a well-known method for the synthesis of methanol (scheme 2.1 (1a)). Several catalytic systems have been developed for this reaction, with the most common being copper and zinc oxides supported on alumina.[14] The utilization of CO_2 instead of CO in the synthesis of methanol is even more attractive, since it offers an opportunity to take advantage of an abundant greenhouse gas (scheme 2.1 (1b)). Studies also focus on the utilization of CO_2 directly from industrial waste gas, which would allow a direct utilization instead of exhausting the pollutant.[15] With optimization of the Cu/ZnO-based catalytic system, selectivity of more than 99% towards methanol can be reached.[16] Even though the reaction with CO_2 proceeds slower than with the conventional syngas, industrial application of this pathway is possible due to the selectivity and sustainability of the reaction.[17] With the methanol building block in hand, the synthesis of propylene can proceed via methanol-to-propylene (MTP, see scheme 2.1 (2)) conversion with zeolites (e.g. ZSM-5).[18] With optimization of already existing zeolite catalysts, high activity as well as selectivity towards propylene formation can be achieved. Since this method is widely applied in industry, it will not be discussed in more detail in this work.[19-20]

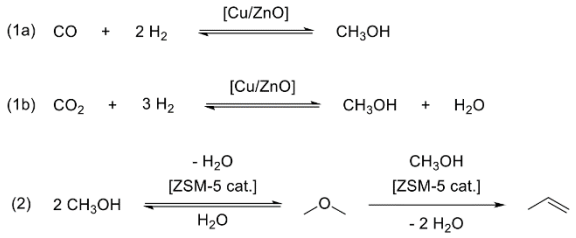

Scheme 2.1 Conversion of (1a) CO[14] or (1b) CO_2[16] to methanol and (2) the methanol-to-propylene (MTP) process[18].

In contrast to the first two processes, Liu et al. published a propylene-free approach by synthesizing PO from glycerol. In the first step, glycerol is dehydrated and hydrogenated using catalysts known in the literature, resulting in propylene glycol. With alkali-loaded silica beds as active catalysts, the group was able to convert the intermediate propylene glycol into PO (scheme 2.2 (c)). However, the yields of around 30% PO and selectivities of 70% remained moderate.[21] This makes this synthesis pathway an interesting approach in terms of sustainability, yet not industrially competitive so far.

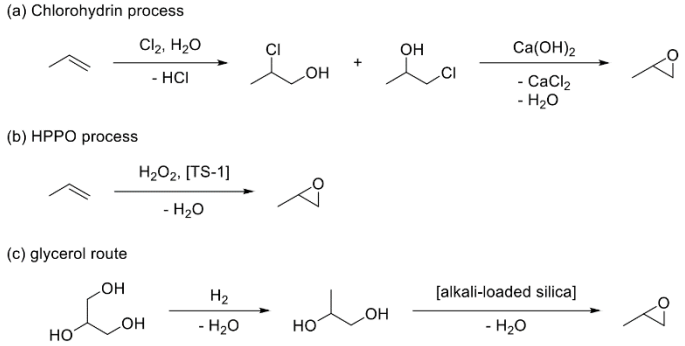

Scheme 2.2 Synthetic routes towards propylene oxide: (a) the chlorohydrin process[12], (b) propylene oxidation with hydrogen peroxide[13] and (c) hydration of glycerol[21].

2.2 Cyclohexene oxide

An intensively studied monomer for copolymerization with CO_2 is cyclohexene oxide (CHO), which is usually generated via the epoxidation of cyclohexene. However, its most common synthesis route is based on petrochemical resources, as shown in scheme 2.3 (a), where benzene, derived from crude oil, is hydrogenated towards cyclohexene.[22-23] The follow up epoxidation of cyclohexene to form CHO can be performed with various peroxides, for example hydrogen peroxide or *tert*-butyl hydroperoxide.[24-25]

From this petroleum-based route, CHO may not be the ideal "green" building block, however, another synthesis approach based on renewable resources is shown in scheme 2.3 (b).[26] Starting from plant oils without further purification, the triglycerides undergo self-metathesis to form 1,4-cyclohexadiene.[27] This intermediate can then be epoxidized, resulting in 1,2-epoxy-4-cyclohexene. The desired product CHO is then formed via hydrogenation of the remaining double bond.[26]

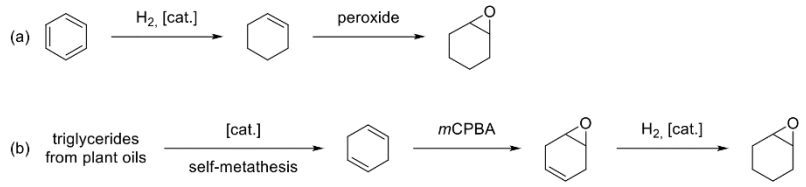

Scheme 2.3 Synthesis of cyclohexene oxide from (a) benzene[22-23] and (b) triglycerides[26-27].

2.3 Limonene oxide

When talking about plant-based feedstocks for chemicals, terpenes are probably one of the first groups of compounds to come to mind. Herein (+)-limonene is an example of an abundant monoterpene, which can be found in citrus fruits.[28] The fact that (+)-limonene can be extracted out of their peels makes it even more attractive, since those are normally considered to be waste after juice production. This makes (+)-limonene not only biobased, but also a non-food feedstock in sustainable chemistry. It is therefore only logical that this molecule is also of special interest as a potential feedstock for monomers. A 1,2-epoxidation of the double bond in the ring structure of limonene can be performed with the help of peracetic acid, resulting in a mixture of the *cis*- and *trans*-product with a ratio of 46:54 (*cis*:*trans*) (scheme 2.4 (a)).[29] Commercially available limonene oxide (LO) usually shows this ratio in the mixture of its isomers. As will be discussed later in this chapter, the most active catalysts in the copolymerization of LO and CO_2 selectively polymerize the *trans*-isomer. The groups of Greiner and Rieger therefore reported a synthesis pathway towards 1,2-LO with an increased selectivity towards the *trans*-isomer (scheme 2.4 (b)).[30] Other epoxidation methods, as for example titanium catalysts and hydrogen peroxide, are often less selective towards the 1,2-LO, and therefore produce diepoxide and other alcohol or ketone products.[31-32] In contrast to propylene as a starting material, limonene is obviously more sterically hindered and its two double bonds are making selective epoxidation crucial. An epoxide

monomer with two epoxide functionalities prone to ring opening would lead to branching in the ring-opening copolymerization instead of the aspired linear polymer.

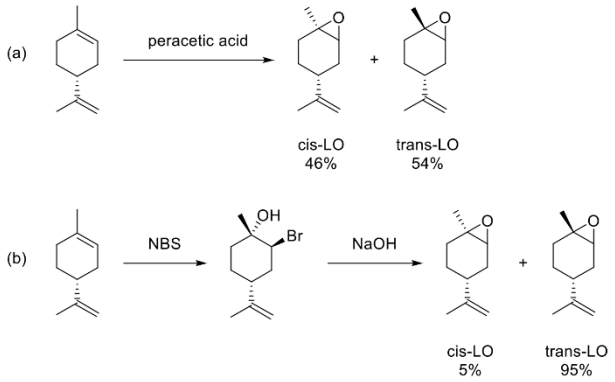

Scheme 2.4 Synthesis pathways of limonene oxide from (+)-limonene.[29-30]

2.4 Vegetable oil-based epoxides

The presence of double bonds in unsaturated vegetable oils draws attention to them as potential starting compounds for the synthesis of biobased epoxides. In 2014, Zhang et al. reported copolymerization of CO_2 with an epoxide they derived from 10-undecenoic acid. After methylation of the fatty acid, they were able to epoxidize the double bond with *meta*-chloroperoxybenzoic acid (*m*CPBA) (see scheme 2.5 (a)). The resulting epoxy methyl 10-undecenoate could then successfully be copolymerized with CO_2. The production of 10-undecenoic acid from castor oil is also interesting, since it is a non-edible oil that can be derived from the castor bean plant.[33]

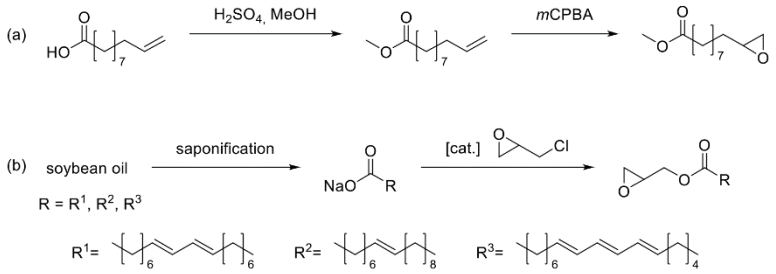

Scheme 2.5 Generation of epoxides (a) from 10-undecenoic acid[33] and (b) from soybean oil[34-35].

Another plant-based oil that is under closer examination is soybean oil, which contains multiple double bonds in its fatty acid chains. For the synthesis of epoxides from this triglyceride, two possible routes can be conceived: (1) the epoxidation of double bonds in the fatty acid chains, or (2) the addition of a terminal epoxide function via reaction with epichlorohydrin as shown in scheme 2.5 (b). The first pathway results in epoxides that show a high steric bulk at the oxirane function due to the long chain ends connected to it. With this steric hindrance, the activity of these compounds might be lowered, which makes them less attractive for industrial polymer synthesis. A terminal epoxide functionality as obtained via the second route could reduce this problem. Li and co-workers therefore saponified the soybean oil triglycerides followed by epoxide functionalization with epichlorohydrin.[34-35] However, in this case the plant oil is extracted from soybeans, which means that the production of the resulting epoxide would be in competition with food cultivation.[36]

3 Polymerization

3.1 Catalysts

Copolymerization of epoxides and CO_2 was a milestone in the synthesis of PCs. In 1969, Inoue et al. applied a catalytic system based on diethyl zinc and water to PO and CO_2, resulting in successful copolymerization of the two compounds.[4] Based on this work, interest in catalysis of ring-opening copolymerization grew in the scientific community. The group of Soga tested several aliphatic dicarboxylic acids in combination with $Zn(OH)_2$ towards their activity in the polymerization of PO and CO_2. The system of $Zn(OH)_2$ with glutaric acid turned out to be the most promising.[37] The mechanism behind this heterogenous and air-stable catalyst was investigated years later by Rieger et al. It could be shown that zinc dicarboxylates work via a bimetallic pathway. The interaction of two adjacent metal centers on the surface of the catalyst allows the alternating insertion of PO and CO_2 into the polymer chain. Furthermore, this work showed the importance of the distance between the interacting zinc centers, which directly influences the activity of the catalyst in the polymerization reaction.[5]

While the heterogenous catalyst zinc glutarate (ZnGA) is a standard system applied in industry for the copolymerization of PO and CO_2, the focus of research in the field of copolymerization catalysis progressed towards homogeneous catalysts. These offer the opportunity to vary the catalyst structure in different areas. With specific structure variations, the characteristics of a catalyst can be tuned, for example in terms of activity and selectivity. The aluminum porphyrin complex ((TPP)AlCl/$EtPh_3PBr$, see fig. 3.1) synthesized by the group of Inoue in 1985 allowed them to copolymerize CO_2 with multiple epoxides towards copolymers with a low polydispersity (< 1.1). A high control over the polymerization process and the resulting molecular weight of the polymers enabled the scientists to create block copolymers with polyesters.[6] A porphyrin catalyst with chromium as the active metal center showed activity in the copolymerization of

CHO and CO_2. The polymerizations were performed in supercritical CO_2, in which the catalyst was soluble, and this resulted in polymers with molecular weights around 3,000 g·mol^{-1}.[38] In 1995, zinc phenoxide catalysts were used by Darensbourg et al. in the copolymerization of CO_2 with PO and CHO (see fig. 3.1). With these complexes, not only copolymers but also terpolymers from a mixture of both epoxides could be synthesized. The phenoxide catalysts were shown to also form the homopolymer, which is why besides the carbonate linkages also ether linkages could be observed.[7] To reduce the generation of homopolymer, the group performed experiments where the catalyst is added to the reaction after the addition of CO_2.[39]

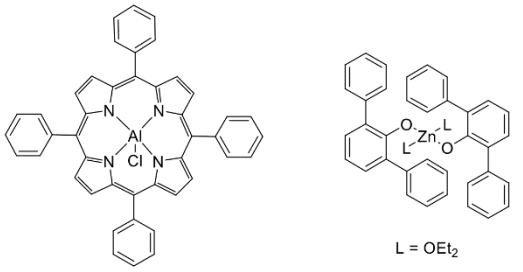

Figure 3.1 Examples of catalysts based on a porphyrin (left)[6] or a phenoxide (right)[7] ligand system.

The application of a new catalyst group should reduce the unwanted reaction towards polyether over the desired PC product. With the class of salicylaldimine (salen) complexes, it was possible to copolymerize CO_2 with CHO selectively towards an alternating PC.[40] The active centers applied in salen complexes are chromium(III), cobalt(III), and aluminum(III), and need a nucleophilic co-catalyst to enable catalysis of the copolymerization. The selectivity of the catalyst in PO/CO_2 coupling was shifted towards the formation of polymer instead of cyclic carbonate with the help of a fully conjugated backbone in the salen ligand.[41] Further variations also focused on the phenolate ring of the ligand structure. Substituents that act as electron donating groups at the aromatic ring, as for example methanolate, were shown to have a positive effect on the copolymerization of CHO with CO_2. However, the same complexes lead to an increase in cyclic propylene carbonate production for the PO/CO_2 system.[9] The initiation time of the polymerization reaction with salen catalysts was reduced by introducing the more nucleophilic azide initiating group (see fig. 3.2 (a) with R = Ph) leading to a turnover frequency (TOF) of 79.5 h^{-1}.[42] Another part of the catalytic system that is easy to modify is the exchange of the co-catalyst. Here again, it is important to match the catalytic system to the epoxide used. Bis(triphenylphosphine)iminium chloride (PPNCl) as a co-catalyst leads to a more than six-fold increase in activity (TOF = 255 h^{-1} for fig. 3.2 (a) with R = H) in CHO/CO_2 copolymerization compared to triphenylphosphine (PPh_3). In contrast, the use of PPNCl in the reaction of PO and CO_2 leads to a predominant production of the unwanted cyclic propylene carbonate over the polymer.[8] The high variability of the salen ligand was further employed by Darensbourg

and co-workers in their extensive research in the following years.[43-44] With the synthesis of a salen-based complex containing quaternary ammonium salts in the ligand structure (fig. 3.2 (b)), in 2008, the group of Lee recorded the highest TOFs (up to 26,000 h^{-1}) for the PO/CO_2 copolymerization, to the best of our knowledge, up to today.[45-46]

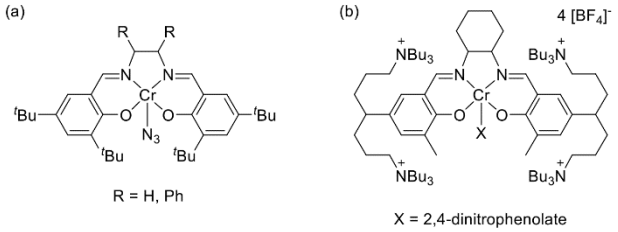

Figure 3.2 Salen catalysts from (a) Darensbourg et al.[8-9] and (b) Lee et al.[45].

The focus in this part of the chapter lies mainly on catalysts capable of copolymerizing CO_2 with PO and CHO as epoxides. When it comes to LO, however, the options of catalytic systems that can be employed are sharply decreasing. The first catalyst able to copolymerize LO and CO_2 was presented by Coates at al. in 2004.[10] It contains a β-diiminate (BDI) ligand and an acetate initiating group connected to the zinc center. The BDI ligand structure offers several different points where variations can be undertaken. The introduction of electron withdrawing substituents, as for example trifluoromethyl groups, results in an increase of catalytic activity. By optimizing the catalyst structure with ethyl and isopropyl substituents at the aromatic rings and a trifluoromethyl group at the backbone, a TOF of 37 h^{-1} could be observed (see fig. 3.3 with R^1 = Me, R^2 = ^{i}Pr, X = OAc). The group of BDI-Zn catalysts exhibits a strictly selective activity towards the copolymerization of *trans*-LO. Subsequent experiments with pure *cis*-LO and CO_2 showed no conversion of this isomer.[10] The amino-trisphenolate aluminum catalyst designed by the group of Kleij addresses this deficit (see fig. 3.3). Their complex can polymerize both isomers of LO towards PCs, which offers the opportunity to reduce the amount of unfeasible monomer feed. In contrast to the BDI-based catalysts, this complex is dependent on the interaction with co-catalysts. Kleij et al. tested PPNX (X = Cl, Br, I) for this purpose and observed that the chloride as well as the bromide species are the most efficient co-catalysts for this reaction. An exchange of the metal from Al(III) to Fe(III) resulted in an active catalyst, but it showed lower conversions of the epoxide monomer compared to the aluminum complex. The polymers produced with the aluminum catalyst from pure *cis*-LO were of moderate molecular weights (7.0–10 kg·mol^{-1}) and polydispersities (1.32–1.48).[47] However, the catalytic activity of the amino-trisphenolate aluminum complex is rather low, with a TOF of 3 h^{-1}, compared to the BDI catalyst (37 h^{-1}) mentioned before.[10, 47]

The copolymerization of CHO and CO_2 is often used as a standard reaction to compare the activity of catalysts. The first BDI-Zn complexes with isopropyl or ethyl substituents at the aromatic rings and an acetate initiating group show a TOF of 235 to 247 h^{-1} in this

reaction.[48-49] The activity could then be further increased by the introduction of electron withdrawing groups and the optimization of the substituents at the aromatic rings. This results in BDI^{CF3}-Zn-Et, a complex with ethyl substituents at the aromatic rings, which show a TOF of 4800 h^{-1}.[50] With the introduction of a bis(trimethylsilyl)amido ($N(TMS)_2$) initiation group at the zinc center, not only could the activity of the catalyst be further increased (TOF = 5520 h^{-1}), but the scope of epoxide monomers could also be extended (see fig. 3.3 with $R^1 = CF_3$, R^2 = Et, X = $N(TMS)_2$).[51] The versatile BDI^{CF3}-Zn-$N(TMS)_2$ moreover allowed the polymerization of two epoxides with CO_2 towards terpolymers. Even for the LO/CO_2 copolymerization, a major increase in activity towards a TOF of 310 h^{-1} could be observed with this catalyst. To the best of our knowledge, this is the most active catalyst for the copolymerization of LO and CO_2.

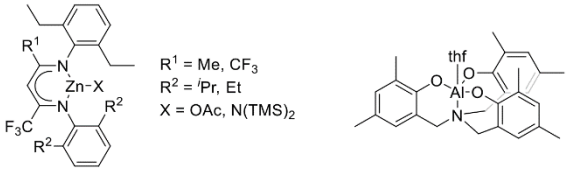

Figure 3.3 Catalysts based on the BDI-ligand structure[10, 51] (left) and the amino-trisphenolate ligand[47] (right).

Besides mononuclear complexes, dinuclear catalysts are also of high interest, since several mechanistic studies indicate a dinuclear nature of the ring-opening copolymerization mechanism.[5, 52] The group of Williams works with a broad variety of dinuclear complexes based on the reduced Robson-type structure (see fig. 3.4). With two Zn(II) centers in close proximity, the catalysts show moderate activities (25 –140 h^{-1} for CHO/CO_2) at low CO_2 pressures (1–10 bar).[53] In addition to zinc as the active center, other metals used in these complexes are Fe(III), Mg(II) and Co(III). Those show similar activities in the copolymerization of CHO and CO_2, towards poly(cyclohexene carbonate) (PCHC) ranging from 29 to 172 h^{-1} at low pressures.[54-56]

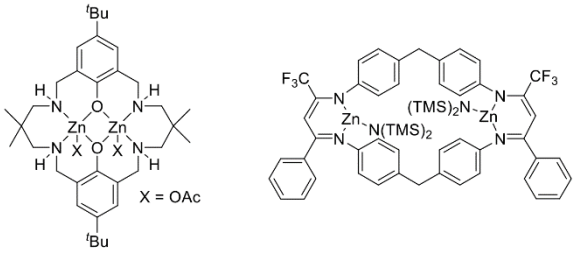

Figure 3.4 Dinuclear zinc complexes from Williams et al.[53] (left) and Rieger et al.[57] (right).

The highest activity in the copolymerization of CHO and CO_2 was reported for a dinuclear catalyst as well. The dizinc cyclic complex is based on the BDI ligand structure.

In this case the two active sites in the complex are connected via the aromatic rings in the ligand framework. The catalyst with electron-withdrawing CF_3 groups at the backbone (see fig. 3.4) reaches a TOF of up to 155,000 h^{1} at a CO_2 pressure of 30 bar. Introducing electron-withdrawing groups in the bridging ligand resulted in an almost sevenfold increase in activity compared to a similar complex with methyl instead of phenyl and CF_3 groups.[57]

A completely different approach towards PCs derived from epoxides and CO_2 via anionic polymerization is reported by Gnanou and Feng et al., who used Lewis acidic compounds. The combination of an activator for the epoxides, such as triethyl borane, and initiators, as for example PPNCl, at a CO_2 pressure of 10 bar, results in alternating copolymers. This offers a metal-free route towards the polymers, which also obviates the separation of the polymer product from any catalyst metal. In the case of the PO/CO_2 copolymerization, a combination of triethyl borane and tetrabutyl ammonium chloride (NBu_4Cl) shows the highest organocatalyst activity and a high selectivity for the synthesis of poly(propylene carbonate) (PPC, > 90%). Transferring the system to CHO as epoxide monomer the highly active triethyl borane/PPNCl-system (TOF = 600 h^{-1}) produces polymers of moderate to high molecular weights (28.3–76.4 $g \cdot mol^{-1}$).[58] A bifunctional catalyst carrying both the Lewis acidic organoboron site and the quaternary ammonium salt in one structure was published by Wu and co-workers in 2020. This catalyst exhibits a TOF of up to 4,900 h^{-1} in the copolymerization of CHO at a CO_2 pressure of 15 bar.[59]

3.2 Mechanism

The metal-catalyzed ring-opening copolymerization (ROCOP) of epoxides and CO_2 can be divided into three basic steps; initiation (1), propagation (2), and termination via chain transfer (3), as shown in scheme 3.1.[60-61] Depending on the nature of the initiating group, either an epoxide or a CO_2 molecule is inserted as the first monomer. After this step, the initiating group is attached to the end of the growing chain, while the oxygen of the monomer is coordinated to the metal center. In the propagation process, the next monomer is inserted into this metal-oxygen bond; an alternating incorporation of the two monomers is intended herein to generate the characteristic carbonate linkages. However, a possible side-reaction is the consecutive incorporation of epoxide into the growing polymer chain leading to ether instead of carbonate linkages. This can often be avoided by adjusting the reaction temperature and CO_2 pressure, but also by tuning the catalyst system towards an unfavored incorporation of two epoxides in a row. The related sequential incorporation of two CO_2 molecules, however does not take place due to enthalpic barriers hindering the generation of a resulting dicarbonate linkage in the polymer.[60-62] Termination of a growing polymer chain is usually induced by the hydrolysis of the growing chain via the addition of alcohols or water to the reaction mixture. With chain transfer agents present in the reaction mixture, the growing chain can also be separated from the active center of the catalyst via chain transfer. This can

be an intended reaction to introduce functional end groups to the polymer chain, but also an unwanted side reaction caused by impurities in the reactants.[61]

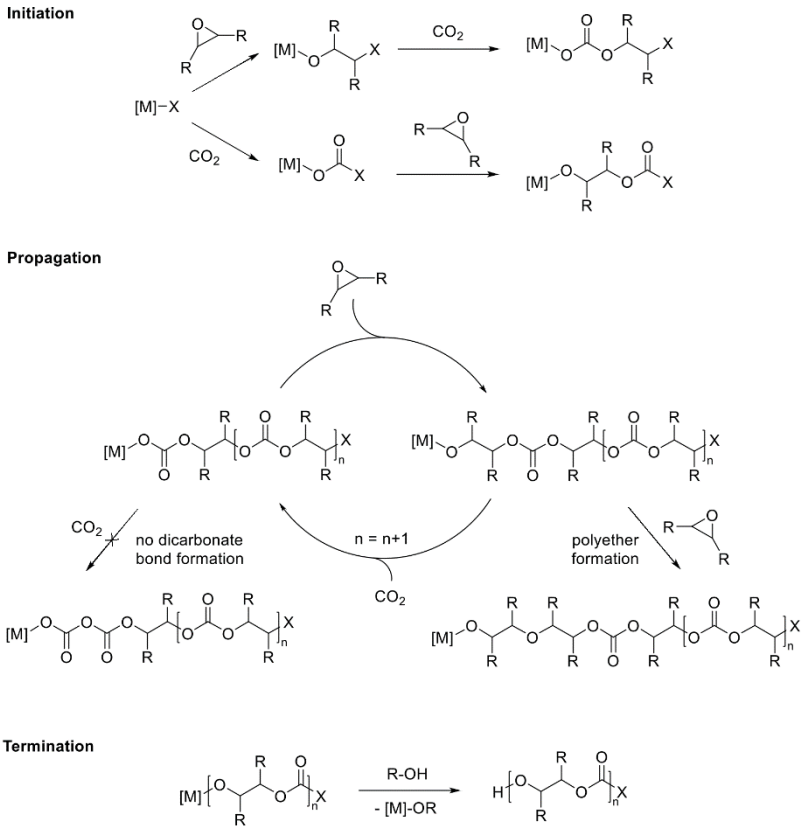

Scheme 3.1 General mechanism of the ROCOP of epoxides and CO_2.[60-61]

The generation of a cyclic carbonate byproduct via nucleophilic backbiting is in competition with the formation of PC. In the PO/CO_2 coupling, the activation energy of the cyclic carbonate product 101 kJ·mol^{-1}) is only 33 kJ·mol^{-1} higher than for the polymer product (68 kJ·mol^{-1}). This is also reflected in the PPC synthesis, where the tendency of cyclic propylene carbonate (cPC) formation via backbiting is a major challenge.[63]

4 Thermal and mechanical properties

To be able to compete against the conventional bisphenol-A polycarbonate (BPA-PC), the thermal and mechanical properties of the aliphatic PCs must be studied. For an easy comparison of the different PCs, we will focus on particular characteristics that are most commonly of interest. The glass transition temperature (T_g) and the degradation temperature (T_d) are used to characterize a polymer in view of its thermal properties. To report the degradation, it is common to use the temperature at which the sample weight is reduced by 5% ($T_{d,5\%}$). The mechanical properties can be analyzed via tensile testing, measuring the elongation of a specimen in relation to the force applied to the sample. The resulting values for the E-modulus (or Young's modulus, E), tensile strength (σ_m) and elongation at break (ε_b) will be compared in this chapter. However, as always, in the discussion of thermal and mechanical properties it is essential to be careful when comparing values from different research groups. The groups may have different measurement conditions, starting with sample preparation and continuing with applied rates or used solvents. We therefore tried to provide this data as an overview from the results of different groups, so that different impressions of the performing ranges of the polymers are accessible. Table 4.1 shows the thermal and mechanical properties of BPA-PC, PPC, PCHC and PLC from different publications.

Table 4.1 Mechanical and thermal properties of selected aliphatic polycarbonates.

polymer	M_n ($Đ$) ($kg \cdot mol^{-1}$)	T_g (°C)	$T_{d,5\%}$ (°C)	E (MPa)	σ_m (MPa)	ε_b (%)
BPA-PC[64]	20 – 25	149	-	2,400 ± 400	47 ± 4	40 ± 35
PPC[65-67]	50.1 – 217	44 – 47	254	831 ± 23	22 – 27	330 ± 9
PCHC[64, 68]	42 – 275	115	280	3,600 ± 100	42 ± 2	1.7 ± 0.6
PLC[30]	53.4	130	225	950	55	15

The aliphatic PCs show decomposition temperatures in a similar range, while the decomposition of PCHC into volatile compounds requires the highest temperatures of approx. 280 °C.[68] A significant difference between the PCs can be found in their T_gs. The absence of melting points in DSC measurements indicate a solely amorphous nature of the aliphatic PCs. Of all four PCs, PPC shows the lowest T_g of under 50 °C due to its flexible polymer chain.[65, 67] A decomposition temperature of PPC at approx. 240 °C, however, should be interpreted with caution. The degradation of the polymer can proceed via two mechanisms (see scheme 4.1); (i, ii) via backbiting at lower temperatures (150 – 180 °C) and (iii) via chain scission, usually at higher temperatures (> 200 °C). During the backbiting degradation of PPC, cPC is generated. This molecule has a boiling point at 240 °C. Observations of mass losses above this temperature could therefore originate from the evaporation of this decomposition product. With standard thermogravimetric analysis (TGA) methods, decomposition of PPC towards cPC at

lower temperatures cannot be detected, since the weight is only changing when the volatile cPC is evaporated.[66] In tempering experiments under air, a stability of PCHC up to 150 °C and only minor degradation at 180 °C could be determined. This allows an estimation of the processing window between 115 and 180 °C if decomposition of the polymer should be avoided. In this case, the degradation has been analyzed via gel permeation chromatography (GPC).[68] This method would also be interesting for the analysis of PPC degradation temperatures.

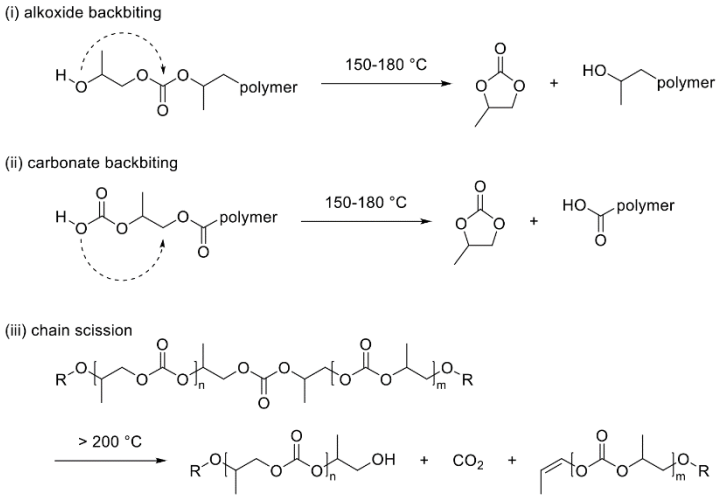

Scheme 4.1 Thermal decomposition of PPC via (i) and (ii) carbonate backbiting or (iii) chain scission.[69-70]

The low thermal stability of PPC limits industrial application of the polymer.[67] With its low T_g and E-modulus, it is furthermore not a suitable substitute for BPA-PC. The thermally more stable PCHC shows a T_g of around 115 °C and a substantially higher E-modulus (> 3,500 MPa) than PPC. However, the brittleness of PCHC with an elongation at break of only a few percent limits its application as well. The promising biobased alternative is poly(limonene carbonate) (PLC), which has the highest T_g (130 °C) of all three aliphatic PCs that is also close to the value for BPA-PC (149 °C). In tensile testing, PLC shows a moderate elongation at break of 15%, higher than the values for PCHC. But in turn, the E-modulus (950 MPa) of PLC is relatively low compared to BPA-PC (> 2,000 MPa), which results in a relatively brittle polymer as well.[30] To address the problem of brittleness, Thorat et al. synthesized a terpolymer of CO_2, PO, and CHO with a PPC content of 20%, expecting a combination of the mechanical properties of the two PCs. Unfortunately, the incorporation of PPC did not have a positive effect on the brittleness of PCHC. The resulting terpolymer showed an elongation at break of 0.7%, which is within the range of pure PCHC.[71]

The polymers based on fatty acids mentioned previously show completely different properties, not only in thermal, but also in mechanical analysis. The T_gs of the 10-undecenoic acid-based PCs synthesized by Zhang et al. are around -40 °C, which does not allow their application as thermoplastic materials, but could make them attractive polyol precursors in polymer synthesis.[33] The soybean oil-based PCs from Li and coworkers showed slightly higher T_gs of around 12 °C. Via terpolymerization with PO, they were able to produce materials with a low to moderate tensile strength (5 – 17 MPa) and a high elongation at break (250 – 430%). Even though the properties of these biobased PCs do not seem to be competitive with the examples from table 4.1, the double bonds make them interesting for post-polymerization functionalization.[34]

5 Degradation

When addressing the life cycle of polymeric materials, it is not sufficient to focus on the monomer origin. We must be aware of what happens to the product at the end of its use. With the development of CO_2-based PCs, their potential biodegradable character drew further attention. The initial conviction that all aliphatic PCs are generally biodegradable has to be clearly contradicted based on the current state of scientific research. The degradation of polymers can be roughly divided into two categories, the biological and the physical or chemical degradation. Several studies reported biological degradation experiments with PPC with the help of microorganisms or enzymes. A detailed overview of studies concerning degradation of PPC was presented by Luinstra and Borchardt.[66] While PPC is stable in water,[72] its decomposition with the help of lipases and fungi in water has been reported.[66] In another study, PPC films with molecular weights of 36 – 121 $kg \cdot mol^{-1}$ were buried in soil. After 6 months, only minor changes in the surfaces of the film could be detected. Furthermore, the observed weight loss reached only 3% in this study.[73] With the change of conditions towards standard composting at 60 °C, a visible degradation of PPC films after 3 months was found by Luinstra.[70] The thermal degradation of aliphatic PCs was already briefly addressed in the previous section. In addition, Lee et al. showed that PPC is thermally stable up to 170 °C. The group also investigated the stability of the polymer in a weathering chamber. At 63 °C, with a humidity of 50%, and irradiated with light (250 – 800 nm, 550 W/m^2), the molecular weight of the polymer decreased over three months. During this process, no cPC formation could be detected. The authors propose therefore that the degradation of PPC happened via chain scission by water due to the humidity in the weathering chamber.[72]

The pH dependency of the physical degradation of PPC was addressed by Ree and Kim et al., who showed that the decomposition is faster in a basic environment (pH 13).[74] With the help of diethyl zinc, which is also a catalyst for the PPC formation, the polymer could be degraded towards cPC at 30 °C.[75] This is also of interest, considering the catalyst residuals in the polymer product. To increase the lifetime and stability of the polymer, it might be useful to remove the catalyst residuals from the polymer product.

Besides the biodegradation properties of PPC, which was intensively studied recently, other aliphatic PCs, such as PCHC or PLC, were not thoroughly investigated in this aspect. Greiner and co-workers reported that pure PLC showed no degradation after 60 days at 60 °C in active compost. They propose the hydrophobic nature of PLC and the steric shielding of the carbonate units as explanation for its high biostability.[76] However, this feature is not necessary a disadvantage if the fields of application of these PCs request a certain stability against environmental impacts. We must be aware that when the carbonate bond is the point of degradation in the PCs, CO_2 can be set free again. This means that CO_2-based PCs are not a terminal CO_2-storage option. However, the potential beneficial uses, especially as a substitute for petroleum-based plastics, underlines the importance of these polymers.

6 Conclusions

The class of aliphatic PCs that can be synthesized from epoxides and CO_2 has become increasingly important in recent years. For this reason, a wide variety of catalysts have been developed to increase the selectivity and activity in polymer synthesis. At the same time, the monomer scope has been expanded, driven by the growing interest in biobased building blocks. The various thermal and mechanical properties exhibited by the resulting polymers can be tailored to meet specific requirements. In the future, questions will arise as to whether the PCs developed will only be used for niche products or if they are suitable for widespread use, possibly leading to less frequent demand for petroleum-based polymers.

Acknowledgement The authors would like to thank Magdalena Kleybolte for the valuable discussions on this manuscript.

References

[1] H. Domininghaus, P. Elsner, P. Eyerer, T. Hirth, *Kunststoffe: Eigenschaften und Anwendungen, Vol. 7*, Springer-Verlag Berlin Heidelberg, **2008**.
[2] M. Mehlman, *Def Sci J* **1987**, *37*, 269-279.
[3] E. Matuszczak, M. D. Komarowska, W. Debek, A. Hermanowicz, *International Journal of Endocrinology* **2019**, *2019*, 4068717.
[4] S. Inoue, H. Koinuma, T. Tsuruta, *J Polym Sci Pol Lett* **1969**, *7*, 287-292.
[5] S. Klaus, M. W. Lehenmeier, E. Herdtweck, P. Deglmann, A. K. Ott, B. Rieger, *J Am Chem Soc* **2011**, *133*, 13151-13161.
[6] T. Aida, M. Ishikawa, S. Inoue, *Macromolecules* **1986**, *19*, 8-13.
[7] D. J. Darensbourg, M. W. Holtcamp, *Macromolecules* **1995**, *28*, 7577-7579.

[8] D. J. Darensbourg, R. M. Mackiewicz, J. L. Rodgers, A. L. Phelps, *Inorg Chem* **2004**, *43*, 1831-1833.
[9] D. J. Darensbourg, R. M. Mackiewicz, A. L. Phelps, D. R. Billodeaux, *Accounts of Chemical Research* **2004**, *37*, 836-844.
[10] C. M. Byrne, S. D. Allen, E. B. Lobkovsky, G. W. Coates, *J Am Chem Soc* **2004**, *126*, 11404-11405.
[11] A. Wurtz, *Liebigs Ann Chem* **1859**, *110*, 125-128.
[12] D. L. Trent, *Kirk- Othmer Encyclopedia of Chemical Technology* **2001**.
[13] M. G. Clerici, G. Bellussi, U. Romano, *J Catal* **1991**, *129*, 159-167.
[14] H. H. Kung, *Catal Rev* **1980**, *22*, 235-259.
[15] N. Meunier, R. Chauvy, S. Mouhoubi, D. Thomas, G. De Weireld, *Renewable Energy* **2020**, *146*, 1192-1203.
[16] J. Toyir, R. Miloua, N. E. Elkadri, M. Nawdali, H. Toufik, F. Miloua, M. Saito, *Physics Procedia* **2009**, *2*, 1075-1079.
[17] F. Pontzen, W. Liebner, V. Gronemann, M. Rothaemel, B. Ahlers, *Catalysis Today* **2011**, *171*, 242-250.
[18] M. Khanmohammadi, S. Amani, A. B. Garmarudi, A. Niaei, *Chinese Journal of Catalysis* **2016**, *37*, 325-339.
[19] H. Koempel, W. Liebner, in *Studies in Surface Science and Catalysis, Vol. 167* (Eds.: F. Bellot Noronha, M. Schmal, E. Falabella Sousa-Aguiar), Elsevier, **2007**, pp. 261-267.
[20] M. Hack, U. Koss, P. König, M. Rothaemel, H.-D. Holtmann, (Ed.: MG Technologies AG), MG Technologies AG US7015369 B2, **2006**.
[21] Z. Yu, L. Xu, Y. Wei, Y. Wang, Y. He, Q. Xia, X. Zhang, Z. Liu, *Chem Commun* **2009**, 3934-3936.
[22] R. A. Benkeser, R. E. Robinson, D. M. Sauve, O. H. Thomas, *J Am Chem Soc* **1955**, *77*, 3230-3233.
[23] H. Imamura, K. Nishimura, K. Sumioki, M. Fujimoto, Y. Sakata, *Chemistry Letters* **2001**, *30*, 450-451.
[24] X. Huali, F. Yongxian, Z. Chunhui, D. Zexue, M. Enze, G. Zhonghua, L. Xiaonian, *Chemical and Biochemical Engineering Quarterly* **2008**, *22*, 25-39.
[25] G. Grigoropoulou, J. H. Clark, J. A. Elings, *Green Chem* **2003**, *5*, 1-7.
[26] M. Winkler, C. Romain, M. A. R. Meier, C. K. Williams, *Green Chem* **2015**, *17*, 300-306.
[27] R. T. Mathers, M. J. Shreve, E. Meyler, K. Damodaran, D. F. Iwig, D. J. Kelley, *Macromol Rapid Comm* **2011**, *32*, 1338-1342.
[28] I. John, K. Muthukumar, A. Arunagiri, *International Journal of Green Energy* **2017**, *14*, 599-612.
[29] F. P. Greenspan, S. M. Linder, Google Patents, **1961**.
[30] O. Hauenstein, M. Reiter, S. Agarwal, B. Rieger, A. Greiner, *Green Chem* **2016**, *18*, 760-770.
[31] A. Wróblewska, *Molecules* **2014**, *19*.
[32] M. V. Cagnoli, S. G. Casuscelli, A. M. Alvarez, J. F. Bengoa, N. G. Gallegos, N. M. Samaniego, M. E. Crivello, G. E. Ghione, C. F. Pérez, E. R. Herrero, S. G. Marchetti, *Applied Catalysis A: General* **2005**, *287*, 227-235.
[33] Y.-Y. Zhang, X.-H. Zhang, R.-J. Wei, B.-Y. Du, Z.-Q. Fan, G.-R. Qi, *RSC Advances* **2014**, *4*, 36183-36188.

[34] S. Cui, Y. Qin, Y. Li, *ACS Sustainable Chemistry & Engineering* **2017**, *5*, 9014-9022.
[35] C. Chang, Y. Qin, X. Luo, Y. Li, *Industrial Crops and Products* **2017**, *99*, 34-40.
[36] S. Cui, J. Borgemenke, Y. Qin, Z. Liu, Y. Li, in *Advances in Bioenergy, Vol. 4* (Eds.: Y. Li, X. Ge), Elsevier, **2019**, pp. 183-208.
[37] K. Soga, E. Imai, I. Hattori, *Polym J* **1981**, *13*, 407-410.
[38] S. Mang, A. I. Cooper, M. E. Colclough, N. Chauhan, A. B. Holmes, *Macromolecules* **2000**, *33*, 303-308.
[39] D. J. Darensbourg, M. W. Holtcamp, G. E. Struck, M. S. Zimmer, S. A. Niezgoda, P. Rainey, J. B. Robertson, J. D. Draper, J. H. Reibenspies, *J Am Chem Soc* **1999**, *121*, 107-116.
[40] D. J. Darensbourg, J. C. Yarbrough, *J Am Chem Soc* **2002**, *124*, 6335-6342.
[41] R. Eberhardt, M. Allmendinger, B. Rieger, *Macromol Rapid Comm* **2003**, *24*, 194-196.
[42] D. J. Darensbourg, R. M. Mackiewicz, J. L. Rodgers, C. C. Fang, D. R. Billodeaux, J. H. Reibenspies, *Inorg Chem* **2004**, *43*, 6024-6034.
[43] D. J. Darensbourg, *Chem Rev* **2007**, *107*, 2388-2410.
[44] S. J. Poland, D. J. Darensbourg, *Green Chem* **2017**, *19*, 4990-5011.
[45] S. S, J. K. Min, J. E. Seong, S. J. Na, B. Y. Lee, *Angew Chem Int Edit* **2008**, *47*, 7306-7309.
[46] S. J. Na, S. S, A. Cyriac, B. E. Kim, J. Yoo, Y. K. Kang, S. J. Han, C. Lee, B. Y. Lee, *Inorg Chem* **2009**, *48*, 10455-10465.
[47] L. Peña Carrodeguas, J. González-Fabra, F. Castro-Gómez, C. Bo, A. W. Kleij, *Chem - Eur J* **2015**, *21*, 6115-6122.
[48] M. Cheng, D. R. Moore, J. J. Reczek, B. M. Chamberlain, E. B. Lobkovsky, G. W. Coates, *J Am Chem Soc* **2001**, *123*, 8738-8749.
[49] M. Cheng, E. B. Lobkovsky, G. W. Coates, *J Am Chem Soc* **1998**, *120*, 11018-11019.
[50] M. Reiter, A. Kronast, S. Kissling, B. Rieger, *ACS Macro Letters* **2016**, *5*, 419-423.
[51] M. Reiter, S. Vagin, A. Kronast, C. Jandl, B. Rieger, *Chem Sci* **2017**, *8*, 1876-1882.
[52] D. R. Moore, M. Cheng, E. B. Lobkovsky, G. W. Coates, *J Am Chem Soc* **2003**, *125*, 11911-11924.
[53] M. R. Kember, P. D. Knight, P. T. R. Reung, C. K. Williams, *Angew Chem Int Edit* **2009**, *48*, 931-933.
[54] A. Buchard, M. R. Kember, K. G. Sandeman, C. K. Williams, *Chem Commun (Camb)* **2011**, *47*, 212-214.
[55] A. M. Chapman, C. Keyworth, M. R. Kember, A. J. J. Lennox, C. K. Williams, *ACS Catalysis* **2015**, *5*, 1581-1588.
[56] M. R. Kember, A. J. P. White, C. K. Williams, *Macromolecules* **2010**, *43*, 2291-2298.
[57] S. Kissling, M. W. Lehenmeier, P. T. Altenbuchner, A. Kronast, M. Reiter, P. Deglmann, U. B. Seemann, B. Rieger, *Chem Commun* **2015**, *51*, 4579-4582.
[58] D. Zhang, S. K. Boopathi, N. Hadjichristidis, Y. Gnanou, X. Feng, *J Am Chem Soc* **2016**, *138*, 11117-11120.

[59] G.-W. Yang, Y.-Y. Zhang, R. Xie, G.-P. Wu, *J Am Chem Soc* **2020**, *142*, 12245-12255.
[60] C. Romain, A. Thevenon, P. K. Saini, C. K. Williams, in *Carbon Dioxide and Organometallics* (Ed.: X.-B. Lu), Springer International Publishing, Cham, **2016**, pp. 101-141.
[61] D. J. Darensbourg, in *Synthetic Biodegradable Polymers* (Eds.: B. Rieger, A. Künkel, G. W. Coates, R. Reichardt, E. Dinjus, T. A. Zevaco), Springer Berlin Heidelberg, Berlin, Heidelberg, **2012**, pp. 1-27.
[62] G. W. Coates, D. R. Moore, *Angew Chem Int Edit* **2004**, *43*, 6618-6639.
[63] D. J. Darensbourg, J. C. Yarbrough, C. Ortiz, C. C. Fang, *J Am Chem Soc* **2003**, *125*, 7586-7591.
[64] C. Koning, J. Wildeson, R. Parton, B. Plum, P. Steeman, D. J. Darensbourg, *Polymer* **2001**, *42*, 3995-4004.
[65] L. Du, B. Qu, Y. Meng, Q. Zhu, *Composites Science and Technology* **2006**, *66*, 913-918.
[66] G. A. Luinstra, E. Borchardt, in *Synthetic Biodegradable Polymers* (Eds.: B. Rieger, A. Künkel, G. W. Coates, R. Reichardt, E. Dinjus, T. A. Zevaco), Springer Berlin Heidelberg, Berlin, Heidelberg, **2012**, pp. 29-48.
[67] S. Chen, M. Xiao, S. Wang, D. Han, Y. Meng, *Journal of Polymer Research* **2012**, *19*, 9800.
[68] S. Kernbichl, B. Rieger, *Polymer* **2020**, *205*, 122667.
[69] O. Phillips, J. M. Schwartz, P. A. Kohl, *Polym Degrad Stabil* **2016**, *125*, 129-139.
[70] G. A. Luinstra, *Polym Rev* **2008**, *48*, 192-219.
[71] S. D. Thorat, P. J. Phillips, V. Semenov, A. Gakh, *Journal of Applied Polymer Science* **2003**, *89*, 1163-1176.
[72] J. K. Varghese, S. J. Na, J. H. Park, D. Woo, I. Yang, B. Y. Lee, *Polym Degrad Stabil* **2010**, *95*, 1039-1044.
[73] L. C. Du, Y. Z. Meng, S. J. Wang, S. C. Tjong, *Journal of Applied Polymer Science* **2004**, *92*, 1840-1846.
[74] J. H. Jung, M. Ree, H. Kim, *Catalysis Today* **2006**, *115*, 283-287.
[75] W. Kuran, P. Górecki, *Die Makromolekulare Chemie* **1983**, *184*, 907-912.
[76] O. Hauenstein, S. Agarwal, A. Greiner, *Nature Communications* **2016**, *7*.

8. Summary

The sustainable monomer feedstock of aliphatic PCs based on CO_2 and epoxides is one reason for the high interest in these polymers. The low performance of some aliphatic PCs, however, reduces their applicability as industrially relevant material. To overcome the brittleness of PCHC, block copolymers containing PDMS were synthesized to combine the hard nature of the PC with the soft properties of a siloxane. Therefore, PDMS terminated with hydroxy groups on both chain ends was used to exchange the $N(TMS)_2$ initiating group of the BDI-Zn-$N(TMS)_2$ catalyst *in situ*. NMR monitoring of this initiating group exchange showed the expected broadening of the catalyst signals when combined with a polymeric initiating group while the generation of free $HN(TMS)_2$ from the exchange process could be observed. The copolymerization reaction proceeded fast and with high conversions of CHO. By controlling the amount of CHO added to the reaction mixture the chain length and therefore molecular weight of the block copolymer could be adjusted while the length of the PDMS block stayed the same. The successful connection of both polymer blocks was supported by DOSY NMR as the polymer-related signals shared one diffusion coefficient in contrast to a comparative measurement of a polymer blend comprising homopolymers of PCHC and PDMS, where these signals were separated. The bimodality observed in GPC measurements could be be explained by the generation of AB and BAB block structures. Due to the end group functionality of the PDMS in theory both chain ends should be able to coordinate to the active zinc center and initiate the PCHC synthesis resulting in BAB block copolymers. In reality it is possible that a fraction of the hydroxy groups does not coordinate to a zinc center and results in AB block copolymers. Additionally, to the synthesis in a small-scale experiment the stability of the reaction could be proved by upscaling it up to an 80-fold increase of epoxide monomer feed. With this large amount of polymer material in hand the block copolymers could be characterized in-depth regarding their thermal and mechanical properties. In TGA measurements a two-step decomposition could be observed, arising from the separate decomposition temperatures of PCHC at around 300 °C and PDMS at around 400 °C. Only one T_g between 110 and 120 °C was observed in DSC measurements, which belongs to PCHC. The T_g of PDMS was not intense enough to be observed in these measurements. To overcome this limitation DMA was used and from the maximum of the loss factor also the glass transition of PDMS could be determined at below -120 °C. Rheological investigations showed an increased storage modulus when PDMS is incorporated into the PC chain. An improved stability during deformation of the block copolymers compared to PCHC could be observed in multiaxial pressure tests and an improved elongation at break is measured *via* tensile testing. In general, the same trend was present in all mechanical tests: the performance improved with an increasing PDMS content, while high elastic moduli were

retained. In a phase resolved AFM analysis the mechanical character was pictured with light and dark colors, the darker the color the softer the segment. Phase separation on a nanometer scale was herein visible and with increasing amount of PDMS the ratio of dark and therefore soft segments increased as expected. This phase separation was also visible in TEM measurements. The size of the phases was not larger than 30 nm as the polymers are covalently linked with each other and could not separate more than this maximum. For a typical blend larger phases would have been expected. This small size of the phases also explained the preserved transparency of the products despite a phase separation.

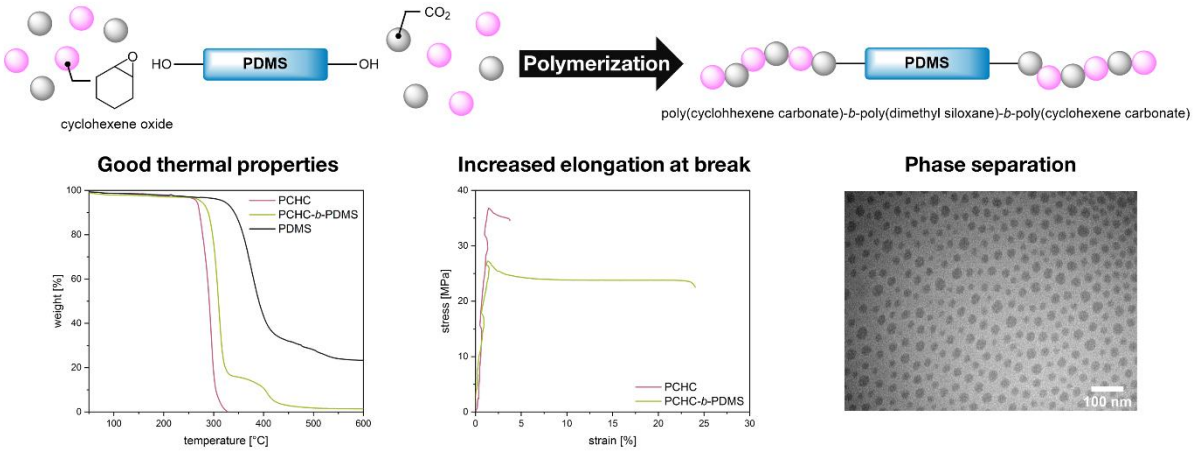

Figure 14. Table of content adopted from "The soft side of aliphatic polycarbonates: with PCHC-b-PDMS copolymers towards ductile materials".[144]

As explained earlier the BDI zinc catalyst is capable of catalyzing the terpolymerization of two epoxides with CO_2. Using this opportunity block copolymer structures can be generated *via* sequential addition of the epoxides. From a classic one pot reaction with both epoxides being present from the beginning in the reaction mixture the resulting structure is typically a gradient type as the difference in reactivity of the epoxides leads to an unsymmetrical consumption of the monomers. To synthesize completely random terpolymers a general change in the reaction setup is necessary. Instead of a one pot reaction, the catalyst was combined with the monomer, which has a lower polymerization rate, as for example PO, and was pressurized with CO_2 to start the copolymerization. Immediately the second epoxide, which is polymerizing faster, as for example CHO, was added to the reaction mixture with a rate in accordance with the consumption of the first epoxide. This way both epoxides should be incorporated at a similar rate potentially resulting a statistical terpolymer. The setup designed for this process used a glove bag to enable the storage of the monomer and the pump under an inert atmosphere. This atmosphere was further dried with phosphorus pentoxide to prevent the influence of residual moisture from degrading the polymerization catalyst. Dosing

of the second epoxide was monitored with a mass flow meter and the reactor was equipped with an *in situ* IR device. *Via* this setup the generation of product could be observed by tracking the evolution of the carbonyl signals of PPC and PCHC. They overlap at around 1750 cm^{-1} and cannot be evaluated individually. DOSY NMR measurements indicated a successful formation of terpolymers while they also ruled out the presence of separated copolymer chains. The statistical nature of the synthesized terpolymers was indicated in ^{13}C NMR measurements. Analyzing the carbonyl region of the spectra it was expected that the signals from carbonate connections between the same or different epoxides on both carbonate sides show different shifts. In comparison with spectra of pure PPC and pure PCHC as well as with a gradient type terpolymer synthesized *via* a one pot reaction showed a shift of the signals indicating an increasing amount of carbonate linkages between PO and CHO as expected for a statistical terpolymer. The variation of monomer feed by adjusting the epoxide ratio and dosing rate allowed the synthesis of statistical terpolymers with defined monomer ratios over the whole polymer chain. GPC measurements showed moderately narrow mass distributions of the terpolymers which was expected for the controlled synthesis of terpolymers. Thermal analyses with DSC showed furthermore the presence of mixed T_gs, which were decreasing with increasing PPC content. In TGA measurements a decreasing decomposition temperature was observed for the terpolymers. However, the thermal stability was still above the one of pure PPC. Mechanical analysis *via* tensile testing showed an increased elongation at break for terpolymers with a higher ratio of PPC. Finally, the variability of this approach was shown by successfully transferring the principle to LO/PO/CO_2 terpolymerization.

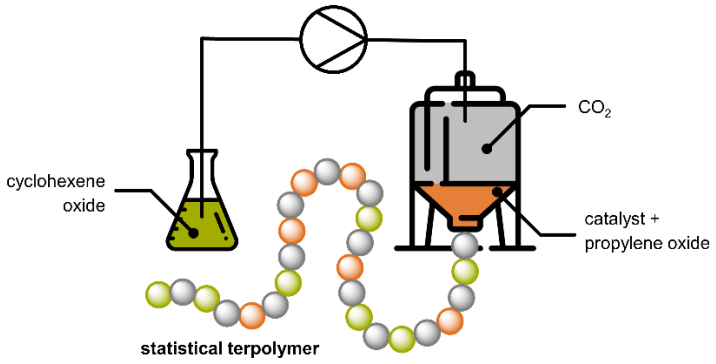

Figure 15. Table of content adopted from "Controlled synthesis of statistical polycarbonates based on epoxides and CO_2".[149]

Combining monomers into advanced copolymer structures allow the generation of novel materials with tunable properties. In case of monomers that require fundamentally different polymerization mechanisms this can be a major challenge. The combination of a ROCOP of

epoxides and CO_2 with the GTP of *Michael*-type monomers was realized *via* a binuclear catalyst system that consisted of two active metal centers. Herein, a BDI zinc moiety was used to catalyze the ROCOP and a pyridyl alcohol was introduced as initiating group with the oxygen coordinating to the zinc center. On the other side, at the pyridyl moiety an yttrium metallocene was introduced *via* C-H bond activation. In the final catalyst the pyridyl alcohol unit connected the two metal centers and was transferred to the end of a growing polymer chain in both mechanisms, ROCOP and GTP. With this complex polymerization experiments of CHO/CO_2 and 2VP were performed individually. Those experiments resulted in PCHC and P2VP with the linking unit as end group as it was confirmed by MALDI-TOF-MS measurements. To combine both mechanisms and generate the desired block copolymers the sequence turned out to be crucial. In experiments starting with the ROCOP of CHO/CO_2 the subsequent GTP of 2VP was not observed. NMR experiments of the catalyst pressurized with CO_2 indicated a decomposition of the yttrium center. Hence, the sequence of polymerization was reversed to prevent this from happening. Consequently, the synthesis of P2VP was performed in a first step followed by the addition of CHO and CO_2 after full conversion of 2VP. That way block copolymers of P2VP and PCHC were generated successfully. An alternative pathway was a one pot approach where 2VP, CHO and the catalyst were combined in the reactor and after complete 2VP consumption the reaction mixture was pressurized with CO_2 to start the copolymerization with CHO. Both routes yielded terpolymers which was supported by analysis of aliquot GPCs. Hereby, an increase in molecular weight from the P2VP block to the final block copolymer with PCHC was observed. Solubility tests furthermore indicated the successful linkage of both polymer blocks as the product turned out to be soluble in methanol, which PCHC on its own is not. Besides 2VP, the reaction was also successful with IPOx as *Michael*-type monomer showing a potential for an extended application in a broad field of monomers.

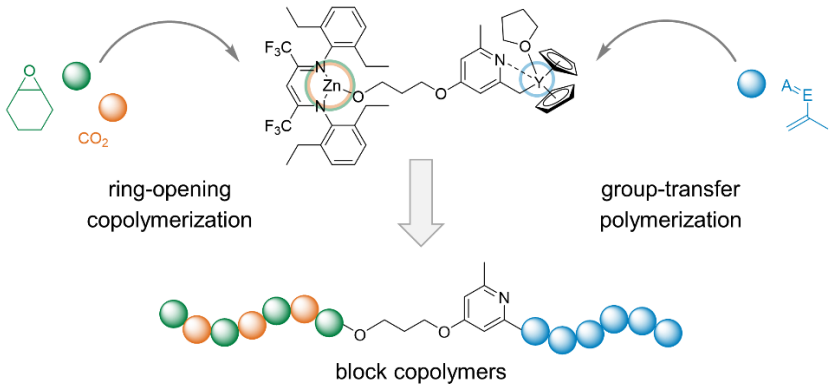

Figure 16. Table of content adopted from "Heteronuclear, monomer-selective Zn/Y catalyst combines copolymerization of epoxides and CO_2 with group-transfer polymerization of *Michael*-type monomers".[151]

9. Appendix

9.1 Supporting information: The soft side of aliphatic polycarbonates: with PCHC-*b*-PDMS copolymers towards ductile materials

The soft side of aliphatic polycarbonates: with PCHC-*b*-PDMS copolymers towards ductile materials

Alina Denk[‡], Paula Großmann[‡], Bernhard Rieger[, ‡]*

[‡]WACKER-Chair of Macromolecular Chemistry, TUM School of Natural Sciences, Catalysis Research Center, Technical University Munich, Lichtenbergstr. 4, 85748 Garching, Germany

1. General information

All reactions were carried out with standard Schlenk techniques or in gloveboxes of the company *M. Braun* under argon 4.6 (99.996%, Westfalen AG). Unless otherwise specified the used solvents were absolutized and dried. The solvents toluene and *n*-pentane were dried with a solvent purification system (SPS) MB SPS-800 from *M. Braun* and stored over appropriate molecular sieves under argon atmosphere. Commercial available chemicals were purchased from Sigma-Aldrich, ABCR, TCI Chemicals and, unless otherwise specified, used without further purification. The catalyst BDI^{CF3}-Zn-$N(TMS)_2$ (**1**) was synthesized according to procedures from literature.[1] Cyclohexene oxide was dried over CaH_2 and purified by distillation. α,ω-Hydroxy-methylene-terminated poly(dimethyl siloxane) (PDMS) was diluted in *n*-pentane, dried over CaH_2 and purified by filtration. The remaining *n*-pentane was removed under vacuum.

Nuclear magnetic resonance spectroscopy (NMR) measurements (^1H, ^{13}C, ^{29}Si, DOSY) were carried out on spectrometers AV-400 and AV-500 of the company *Bruker*. Deuterated solvents were purchased from Sigma-Aldrich and for use with substances susceptible to hydrolysis stored over molecular sieves and under argon. The chemical shifts (δ) are given in parts per million (ppm) and are calibrated to the signals of the solvents. Resonance multiplicities are abbreviated as follows: s = singlet, br s = broad singlet, m = multiplet. **In situ infrared (IR) measurements** of polymerization experiments were carried out on a *Mettler Toledo Multimax ReactIR*™ autoclave system. **Gel permeation chromatography (GPC)** experiments were carried out at a PL-GPC 50 of the company *Agilent* with $CHCl_3$ (HPLC grade, amylene stabilized) as solvent and molecular weights were calculated relative to poly(styrene) calibration standards. **Thermogravimetric analysis (TGA)** was carried out on a *TA Instruments* Q5000 with a heating rate of 10 K/min under air. **Differential scanning calorimetry (DSC)** measurements were performed on a *TA Instruments* Q2000 with a heating or cooling rate of 10K/min in non-hermetic aluminum pans. **Dynamic mechanical analysis (DMA)** measurements were performed on a DMA Q800 of the company *TA Instruments*. Specimen (30 mm × 5 mm × 1 mm) were produced via hot pressing at 160 °C. Tensile DMA measurements were performed in a temperature range from -140 °C to 0 °C with an amplitude of 1 µm and a frequency of 1 Hz and from -10 °C to 130 °C with an amplitude of 10 µm and a frequency of 1 Hz to allow precise measurements over the whole temperature range. For **tensile testing** dog bone shaped specimen (length = 50 mm, width at rejuvenation = 4.0 mm, thickness = 1.0 mm) of the polymers were prepared via hot pressing at 160 °C for 5 minutes. The measurements were carried out on a materials testing machine of the company *ZwickRoell*. The pre-force applied to the specimen was 0.1 MPa and the measurement speed

was 5 mm/min. The strain of the specimen was measured optically with a LightXtense extensometer. **Pressure tests** were performed on a materials testing machine from *Instron*. The disc shaped specimen (diameter = 60 mm, thickness = 1.6 mm) were prepared via hot pressing at 160 °C for 5 minutes and mounted in a clamp for fixation. The remaining free surface of the specimen had a diameter of 40 mm. Perpendicular to this surface a force was applied with a spherical striker of a diameter of 20 mm (with a pre-force of 1.0 N) until failure of the specimen. **Rheological measurements** of the samples were performed with a rotational rheometer ARES-G2 from TA Instruments with a plate-plate measurement geometry. The polymers were dried at 100 °C for one hour prior to hot pressing disc shaped specimen (diameter: 10 mm, thickness: 1.0 mm) at 160 °C. Oszillatoric measurements were performed at 180 °C with a strain of 1%. **Transmission electron microscopy (TEM)** was performed on a JEOL JEM 1400 plus instrument at an acceleration voltage of 120 kV. The topography and the phase contrast of the polymer samples were imaged via **Atomic force microscopy (AFM)**. The polymer specimen were cut at room temperature to examine the cross-section of the samples.

2. Synthesis procedures

α,ω-hydroxy-methylene-terminated PDMS

PDMS was synthesized according to a modified literature procedure.[2]

α,ω-Hydroxy-terminated PDMS (41.0 g, 100 mmol, 1.0 eq.) was diluted in 100 mL *n*-pentane. 1,1,4,4-Tetramethyl-2,5-dioxa-1,4-disilacyclohexane (176 mg, 400 mmol, 4.0 eq.) and 1,1,3,3-tetramethyl guanidine (TMG) (1.15 mg, 10.0 µmol, 0.01 eq.) were added to the reaction mixture and stirred at room temperature over night. Under vacuum the solvent, the unreacted 1,1,4,4-tetramethyl-2,5-dioxa-1,4-disilacyclohexane and the TMG catalyst are removed.

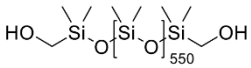

^{1}H-NMR (400 MHz, $CDCl_3$, 298 K): δ(ppm) = 3.33 (s, 4 H, CH_2), 0.14 (s, 12 H, CH_3 of end groups), 0.07 (s, 3300 H, CH_3 of chain).

PCHC synthesis from CHO and CO_2

The masses of the reactants and the reaction parameters of the polymerizations can be found in table S1. The entry numbers correlate with table 1 in the main text.

In the glovebox the catalyst **1** is dissolved in toluene, transferred into the autoclave together with cyclohexene oxide and pressurized with CO_2. In the *in situ* IR autoclave the reaction mixture is stirred (500 rpm) until the intensity of the IR signal of the polymer is not increasing anymore. In the 1.1L autoclave the reaction is stirred (500 rpm) for 30 minutes. The CO_2 pressure is then released, and the reaction mixture is diluted with wet dichloromethane to stop the reaction. The resulting product is precipitated from methanol and dried under vacuum.

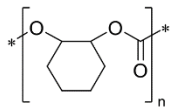

^{1}H-NMR (400 MHz, $CDCl_3$, 298 K): δ(ppm) = 4.67 (br s, 2 H, C*H*), 2.10–1.36 (m, 8 H, CH_2).

The conversion (X) of cyclohexene oxide (CHO) towards poly(cyclohexene carbonate) (PCHC) was calculated from a ^{1}H-NMR of the reaction solution before precipitation. In this calculation the integrals of the protons next to the oxygen at 3.13 ppm for CHO (I_{CHO}) and at 4.67 ppm for PCHC (I_{PCHC}) are used. The number of protons assigned to these signals is two for the monomer as well as the polymer repetition unit.

$$X_{CHO} = \frac{I_{PCHC}}{I_{CHO} + I_{PCHC}} \times 100\%$$

PCHC-*b*-PDMS synthesis from CHO and CO_2 with PDMS as chain transfer agent

The masses of the reactants and the reaction parameters of the polymerizations can be found in table S1. The entry numbers correlate with table 1 in the main text.

In the glovebox the PDMS is dissolved in 75% of the total toluene and catalyst **1** is dissolved in the remaining 25%. Both solutions are transferred into the autoclave together with cyclohexene oxide and pressurized with CO_2. In the *in situ* IR autoclave the reaction mixture is stirred (500 rpm) until the intensity of the IR signal of the polymer is not increasing anymore. In the 1.1 L autoclave the reaction is stirred (500 rpm) for 3-4 hours. The CO_2 pressure is then released, and the reaction mixture is diluted with wet dichloromethane to stop the reaction. The resulting product is precipitated from methanol and dried under vacuum.

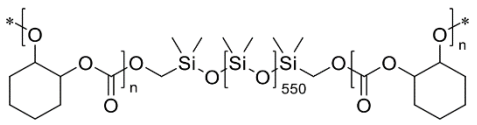

^{1}H-NMR (400 MHz, $CDCl_3$, 298 K): δ(ppm) = 4.67 (br s, 2 H, C*H*), 2.10–1.34 (m, 8 H, CH_2), 0.16 (s, 6 H, CH_3).

Due to the different reaction and autoclave sizes reaction conditions have been optimized individually. Upscaling from a 50 mL towards a 1.1 L autoclave resulted in a change in temperature from 40 to 60 °C for a sufficient reaction speed and in CO_2 pressure from 30 to 25 bar as a precaution not to reach the maximum pressure of the 1.1 L autoclave. These reaction conditions are also mentioned in table S1.

Table S1. Reactant masses and reaction parameters for the copolymerization of CHO and CO_2 with and without PDMS as chain transfer agent. Entry numbers are in accordance with entries in table 1 to 3.

entry	eq. CHO: PDMS:cat	m(CHO) [g]	m(PDMS) [g]	m(catalyst) [mg]	V(toluene) [mL]	p(CO_2) [bar]	T [°C]
1	1000:0:1	2.50	-	17.7	2.5	30	40
2	2500:0:1	90.0	-	255	200	25	60
3	1000:1:1	1.50	0.626	10.6	4.0	30	40
4	1000:1:2	1.50	0.626	21.3	4.0	30	40
5	2000:1:2	3.00	0.626	21.3	8.0	30	40
6	1500:1:1	51.7	14.4	244	150	25	60
7	2500:1:1	86.2	14.4	244	150	25	60
8	3500:1:1	121	14.4	244	200	25	60

Purification of the polymer products

All precipitated polymers are further purified for thermal and mechanical analysis. Therefore, they are dissolved in dichloromethane (5 mL/$g_{polymer}$), washed with a saturated solution of EDTA in water (3 × volume as of dichloromethane) and precipitated from methanol. The polymer is then dried under vacuum.

3. NMR spectrum of CH_2-OH end-capped PDMS

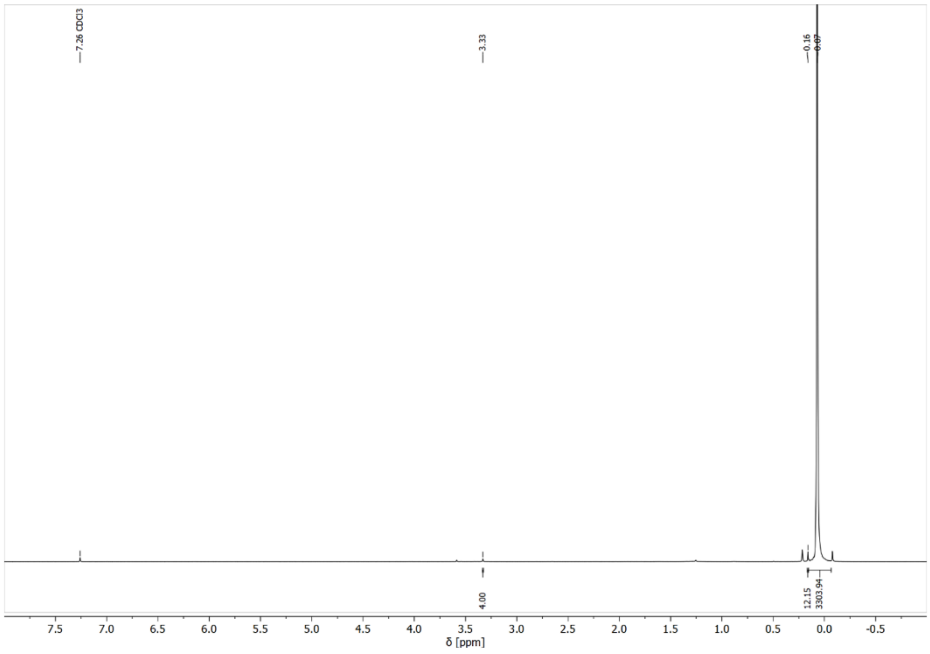

Figure S1. ^{1}H-NMR spectrum in $CDCl_3$ of the CH_2-OH end-capped PDMS.

4. NMR spectra of PDMS with catalyst

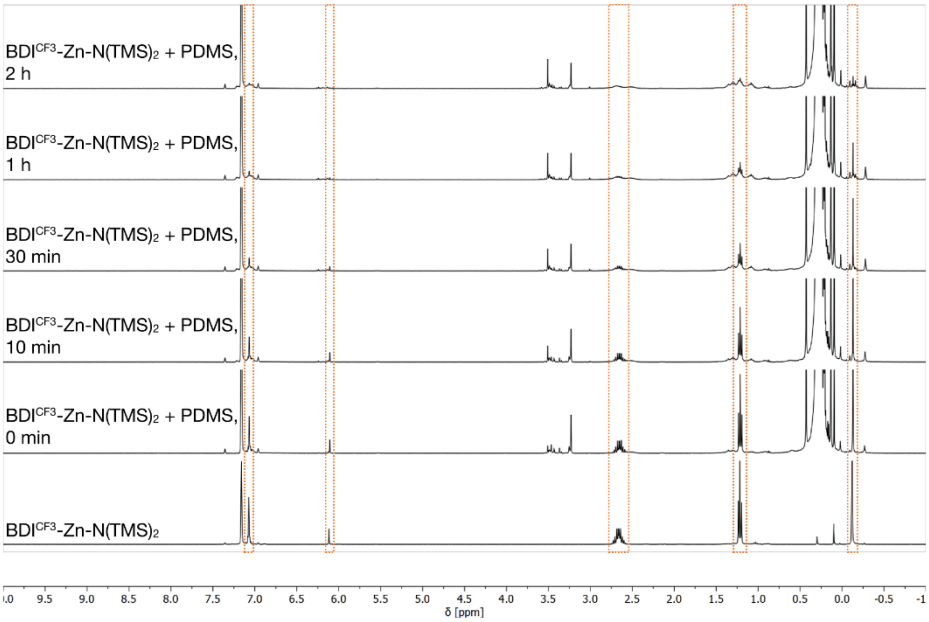

Figure S2. ^{1}H-NMR spectra in C_6D_6 of the BDI^{CF3}-Zn-N(TMS)$_2$ catalyst before and 0, 10, 30 60 and 120 min after the addition of PDMS (ratio 1:1). Decomposition upon addition of PDMS of the catalyst is visible after 10 minutes. Signals of the BDI^{CF3}-Zn-N(TMS)$_2$ catalyst are framed by orange boxes, PDMS signals are not marked.

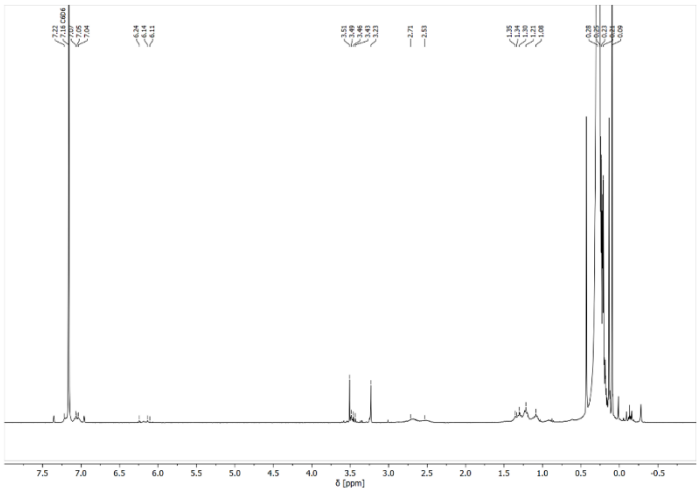

Figure S3. ^{1}H-NMR spectrum in C_6D_6 of the BDI^{CF3}-Zn-N(TMS)$_2$ catalyst 120 min after the addition of PDMS (ratio 1:1).

5. *In situ* IR measurements of the copolymerizations

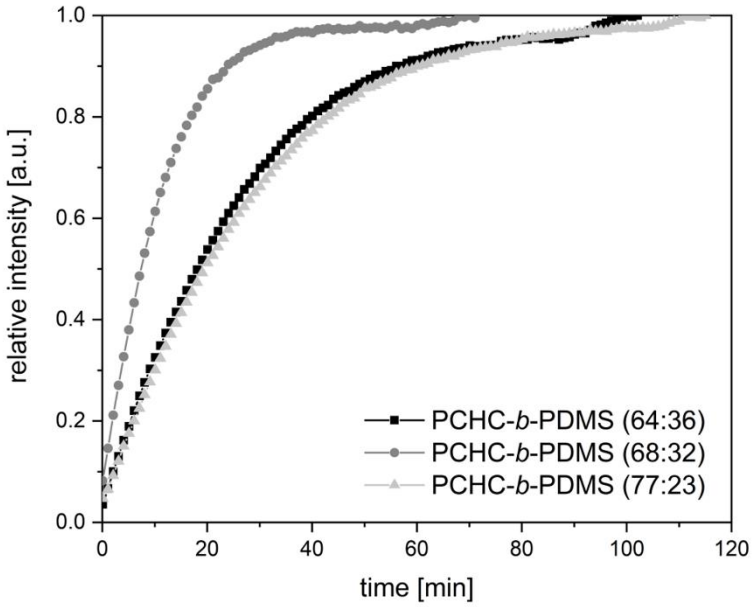

Figure S4. Intensity of the carbonyl vibration at 1750 cm^{-1} over time from *in situ* IR measurements of the copolymerizations from table 1 entry 3 to 5.

6. ^{1}H-NMR spectra of PCHC-*b*-PDMS

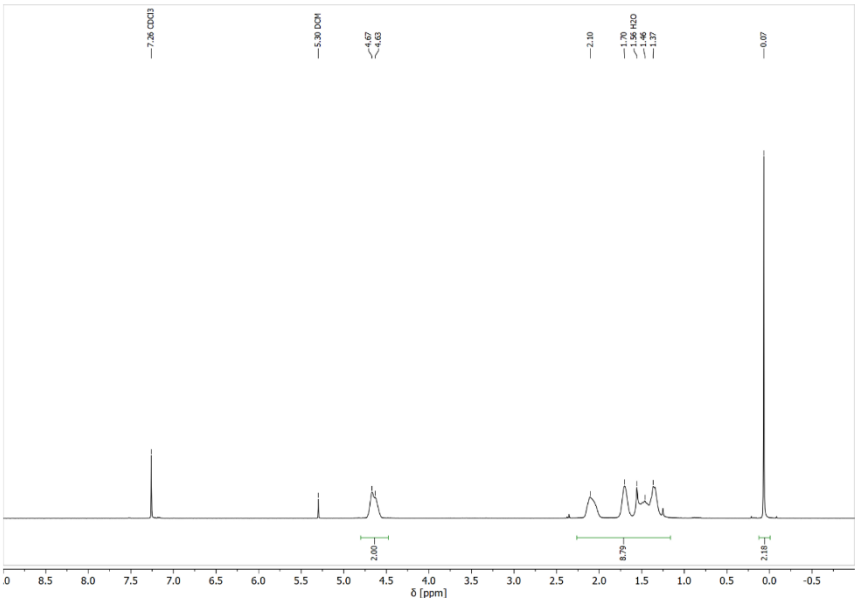

Figure S5 ^{1}H-NMR spectrum of PCHC-*b*-PDMS (table 1, entry 6), measured in $CDCl_3$.

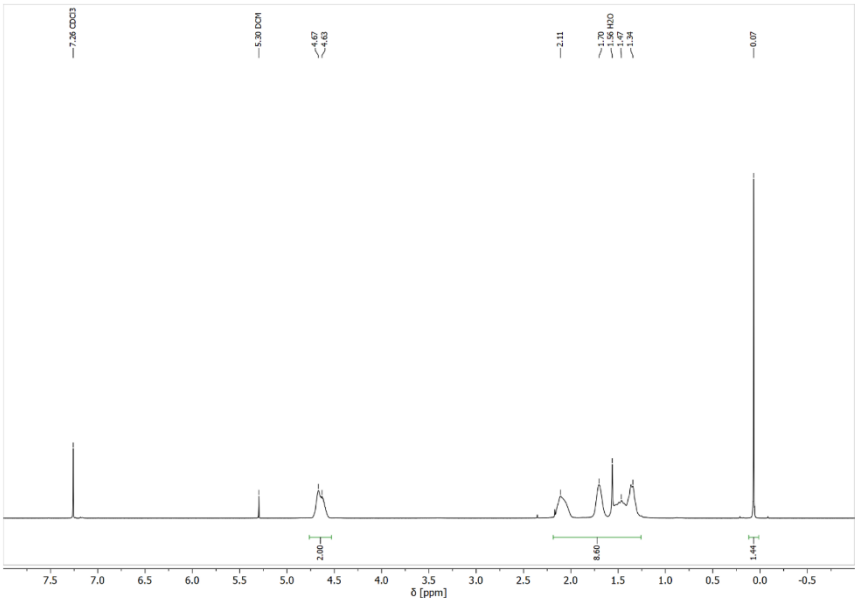

Figure S6. ^{1}H-NMR spectrum of PCHC-*b*-PDMS (table 1, entry 7), measured in $CDCl_3$.

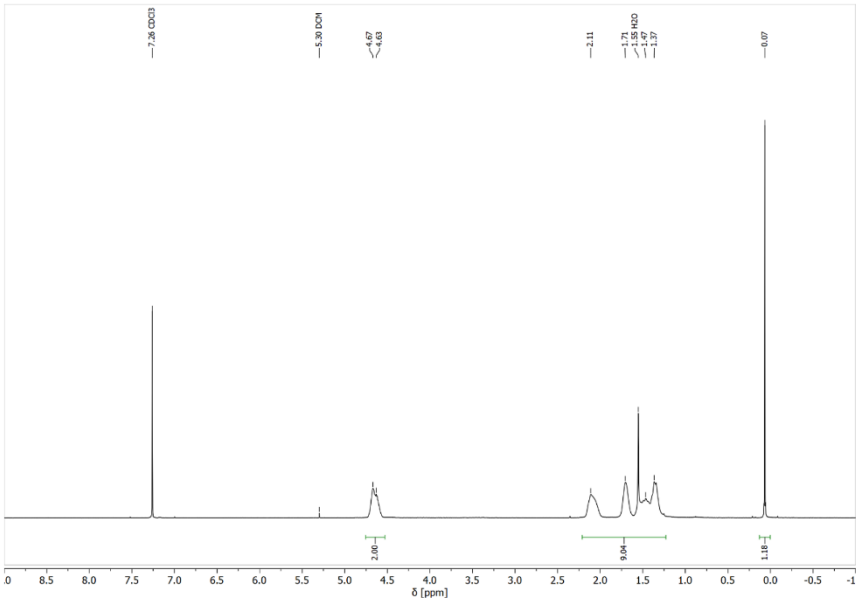

Figure S7. ^{1}H-NMR spectrum of PCHC-*b*-PDMS (table 1, entry 8), measured in $CDCl_3$.

7. GPC traces of PCHC-*b*-PDMS

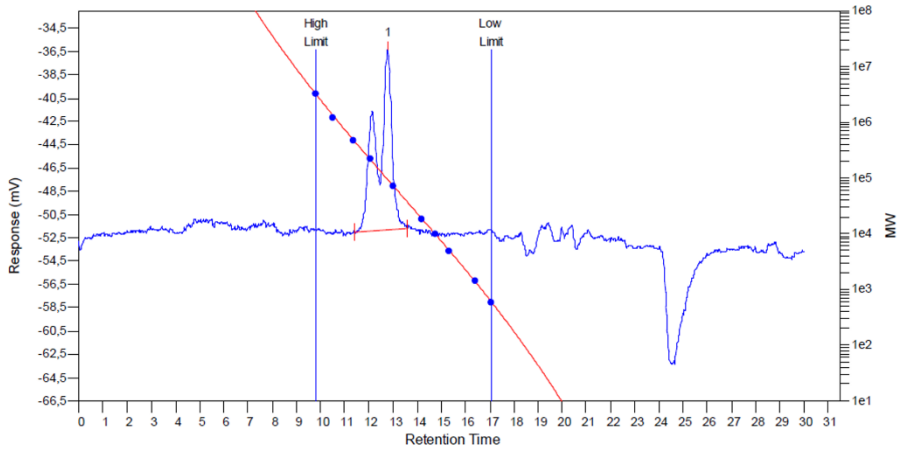

MW Averages

Peak No	Mp	Mn	Mw	Mz	Mz+1	Mv	PD
1	94439	113523	135852	162026	187474	132157	1.19669

Figure S8. GPC trace of PCHC (table 1, entry 1), measured in $CHCl_3$.

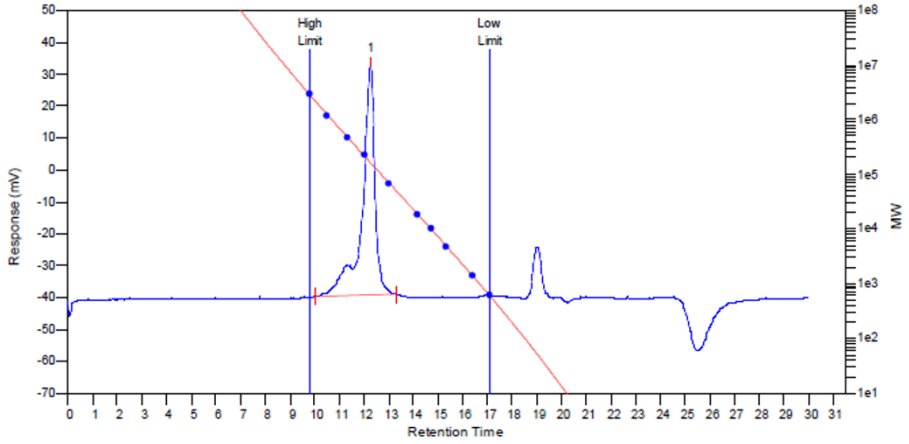

MW Averages

Peak No	Mp	Mn	Mw	Mz	Mz+1	Mv	PD
1	162714	187683	248127	396835	664440	234041	1.32205

Figure S9. GPC trace of PCHC (table 1, entry 2), measured in $CHCl_3$.

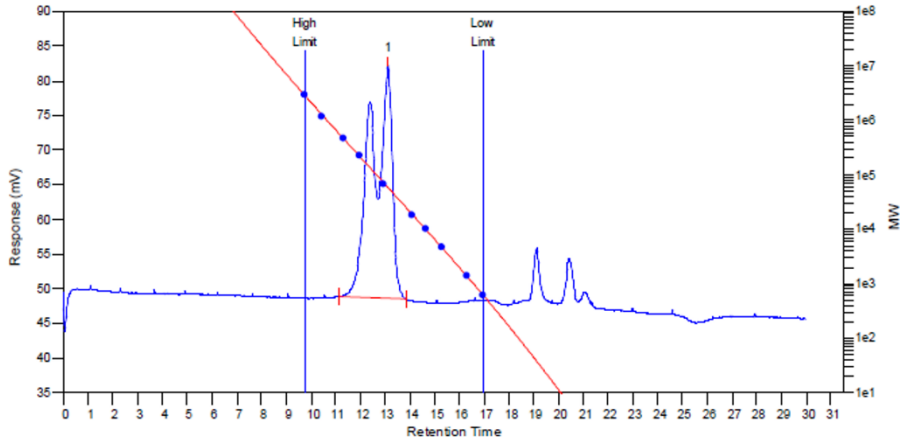

MW Averages

Peak No	Mp	Mn	Mw	Mz	Mz+1	Mv	PD
1	58143	82186	105549	136514	172506	101473	1.28427

Figure S10. GPC trace of PCHC-*b*-PDMS (table 1, entry 3), measured in $CHCl_3$.

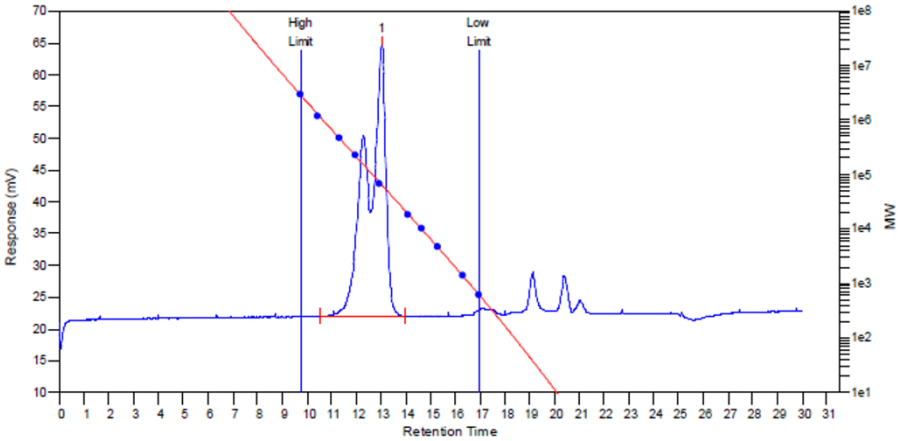

MW Averages

Peak No	Mp	Mn	Mw	Mz	Mz+1	Mv	PD
1	63995	89351	117641	165591	249576	112222	1.31662

Figure S11. GPC trace of PCHC-*b*-PDMS (table 1, entry 4), measured in $CHCl_3$.

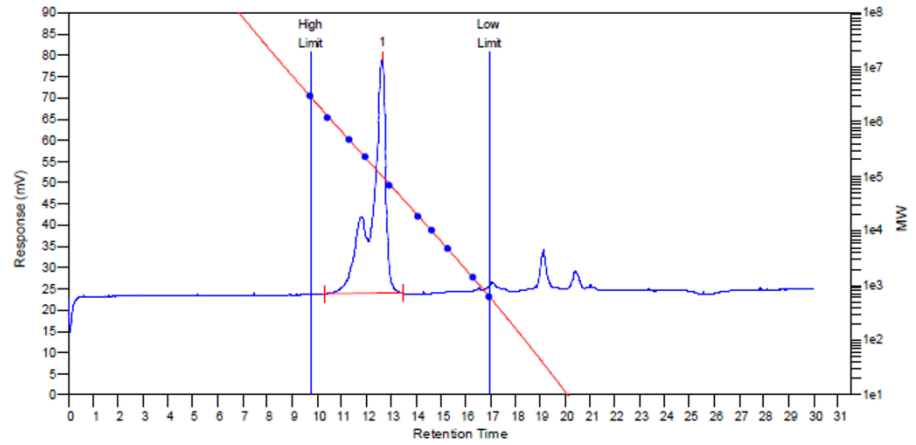

MW Averages

Peak No	Mp	Mn	Mw	Mz	Mz+1	Mv	PD
1	101368	133059	176224	257345	381326	167279	1.3244

Figure S12. GPC trace of PCHC-*b*-PDMS (table 1, entry 5), measured in $CHCl_3$.

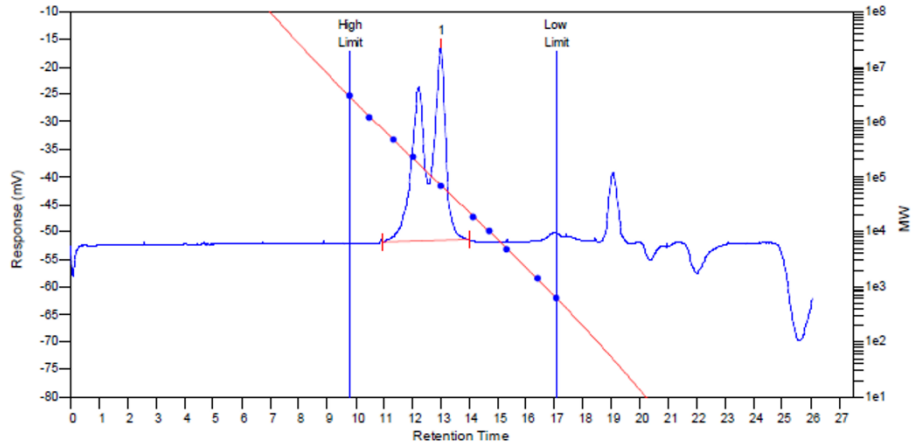

MW Averages

Peak No	Mp	Mn	Mw	Mz	Mz+1	Mv	PD
1	70671	99504	133737	180219	234173	127695	1.34404

Figure S13. GPC trace of PCHC-*b*-PDMS (table 1, entry 6), measured in $CHCl_3$.

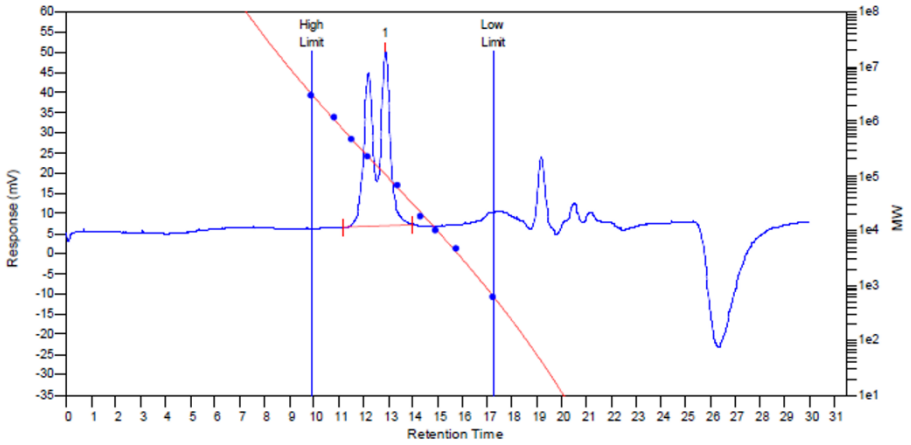

MW Averages

Peak No	Mp	Mn	Mw	Mz	Mz+1	Mv	PD
1	105407	133461	165749	202100	237156	160554	1.24193

Figure S14. GPC trace of PCHC-*b*-PDMS (table 1, entry 7), measured in $CHCl_3$.

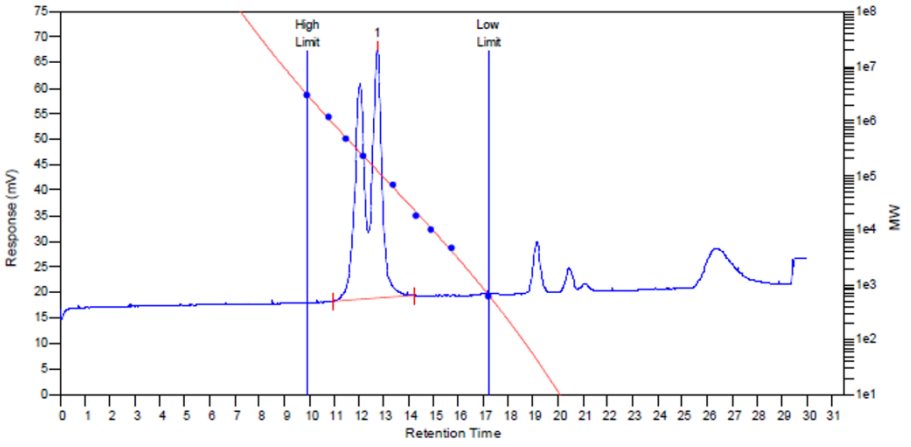

MW Averages

Peak No	Mp	Mn	Mw	Mz	Mz+1	Mv	PD
1	122152	156975	199192	246879	294526	192454	1.26894

Figure S15. GPC trace of PCHC-*b*-PDMS (table 1, entry 8), measured in $CHCl_3$.

8. DOSY-NMR spectra of PCHC-*b*-PDMS

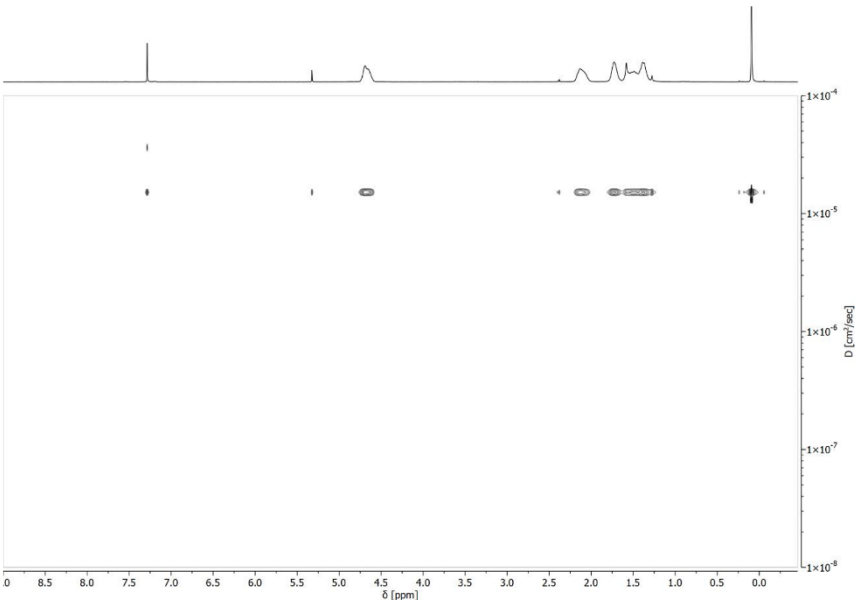

Figure S16. DOSY-NMR spectrum of PCHC-*b*-PDMS (table 1, entry 6), measured in $CDCl_3$.

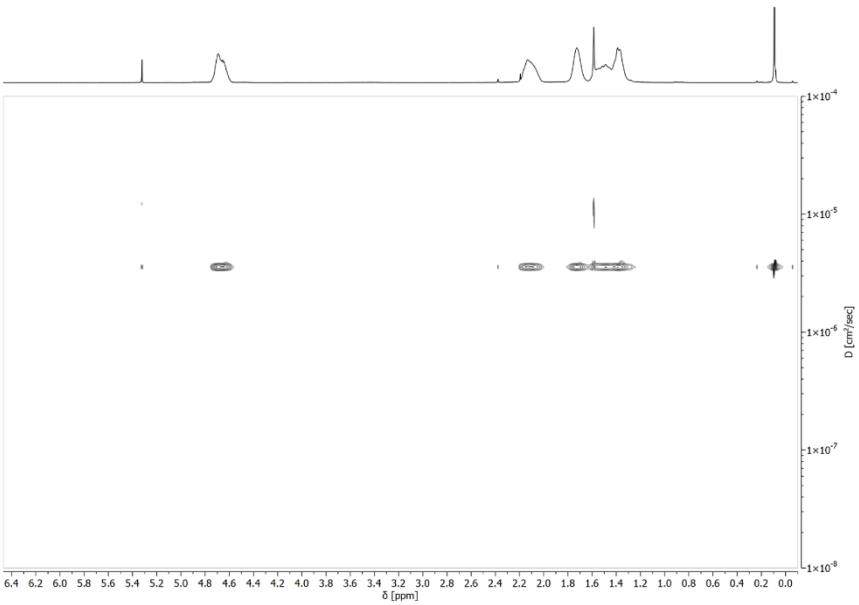

Figure S17. DOSY-NMR spectrum of PCHC-*b*-PDMS (table 1, entry 7), measured in $CDCl_3$.

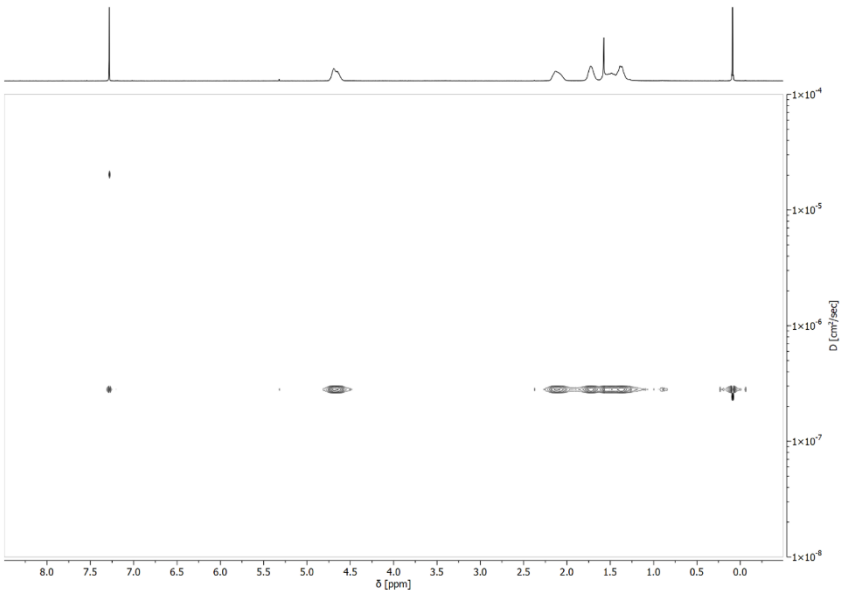

Figure S18. DOSY-NMR spectrum of PCHC-*b*-PDMS (table 1, entry 8), measured in $CDCl_3$.

9. DOSY-NMR spectrum of a PCHC/PDMS blend

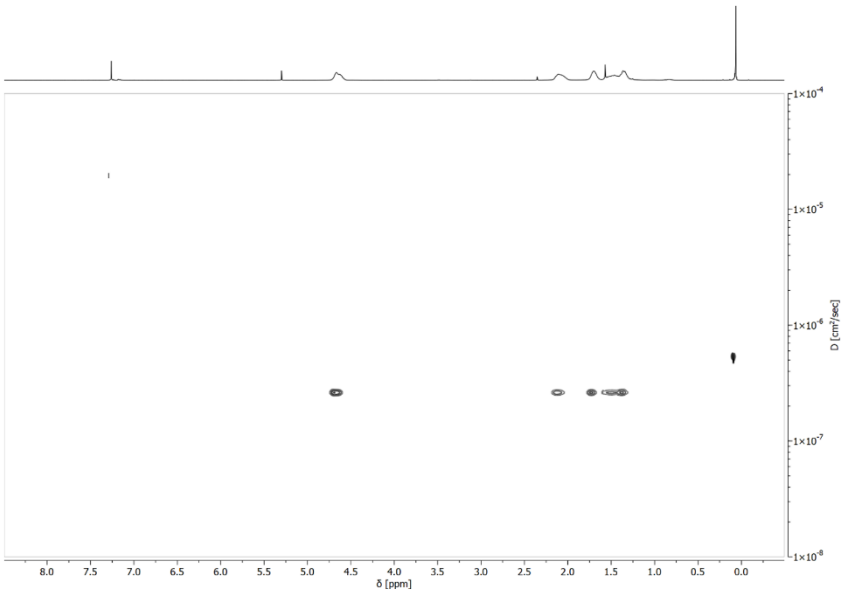

Figure S19. DOSY-NMR spectrum of a blend of PCHC (M_n = 113 kg/mol) and PDMS (M_n = 41 kg/mol), comparable to the masses of the respective blocks in the PCHC-*b*-PDMS copolymer in table 1, entry 8.

10. Thermogravimetric analysis

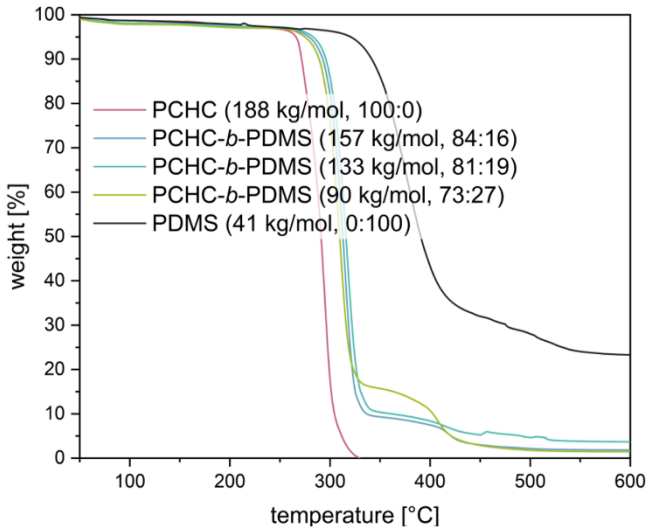

Figure S20. TGA measurements of PDMS and PCHC (table 1, entry 2) and block copolymers from PCHC and PDMS (table 1, entry 6-8).

11. Differential scanning calorimetry

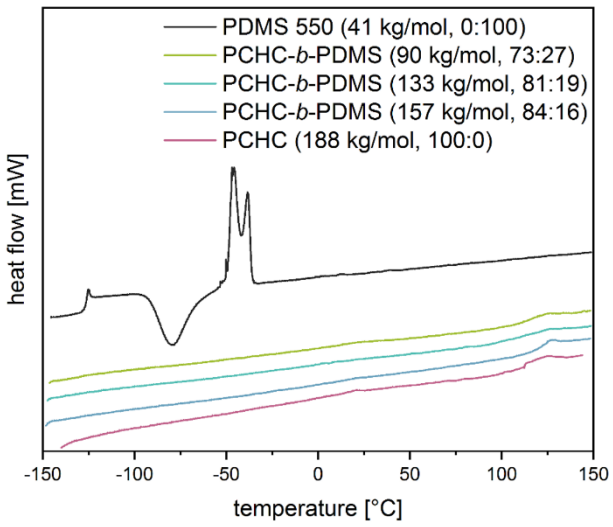

Figure S21. DSC measurements of PDMS and PCHC (table 1, entry 2) and block copolymers from PCHC and PDMS (table 1, entry 6-8).

12. Dynamic mechanical analysis

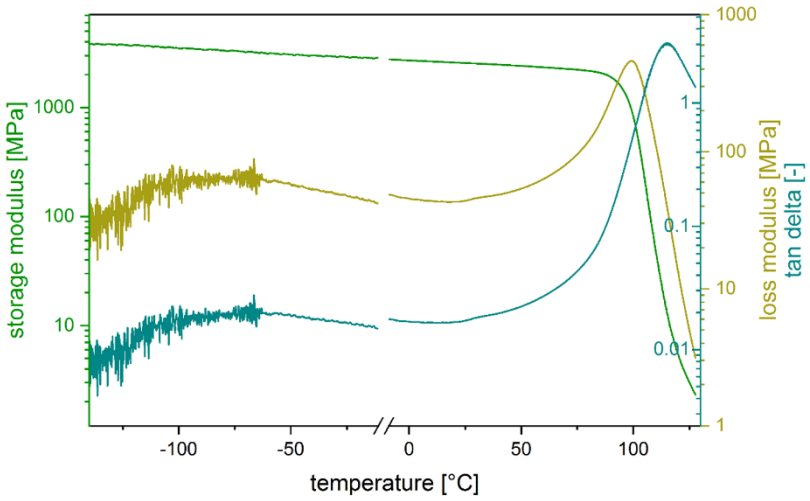

Figure S22. Dynamic mechanical analysis of PCHC (table 1, entry 2) measured with a frequency of 1 Hz and an amplitude of 1 µm at -140 to 0 °C and an amplitude of 10 µm at 0 to 130 °C. (Exemplary measurement three specimens were measured, individual values see table S2.)

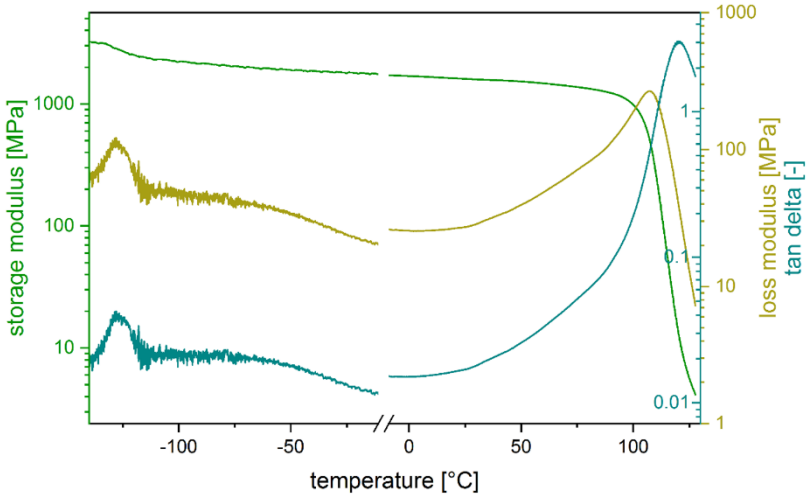

Figure S23. Dynamic mechanical analysis of PCHC-*b*-PDMS (table 1, entry 6) measured with a frequency of 1 Hz and an amplitude of 1 µm at -140 to 0 °C and an amplitude of 10 µm at 0 to 130 °C. (Exemplary measurement; three specimens were measured, individual values see table S2.)

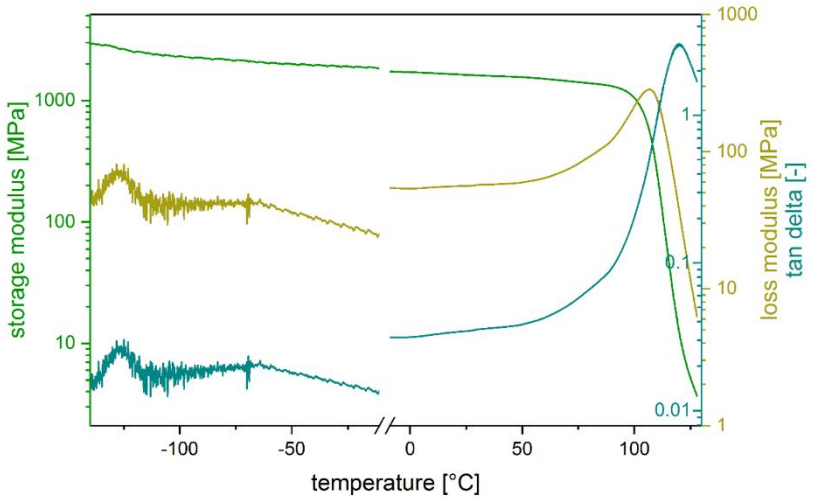

Figure S24. Dynamic mechanical analysis of PCHC-*b*-PDMS (table 1, entry 7) measured with a frequency of 1 Hz and an amplitude of 1 µm at -140 to 0 °C and an amplitude of 10 µm at 0 to 130 °C. (Exemplary measurement; three specimens were measured, individual values see table S2.)

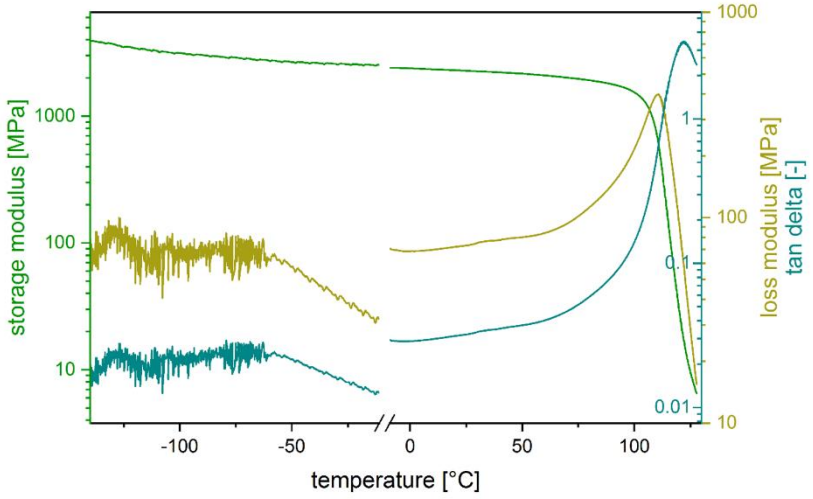

Figure S25. Dynamic mechanical analysis of PCHC-*b*-PDMS (table 1, entry 6) measured with a frequency of 1 Hz and an amplitude of 1 µm at -140 to 0 °C and an amplitude of 10 µm at 0 to 130 °C. (Exemplary measurement; three specimens were measured, individual values see table S2.)

Table S2. Data from dynamic mechanical analysis where of each polymer three specimen were measured with a frequency of 1 Hz and an amplitude of 1 µm (at -140 to 0 °C) or 10 µm (at 0 to 130 °C).

entry from table 1	sample no.	$M_{n,meas}$ [kg/mol]	$P_{n,PCHC}$ ($P_{n,total}$)[a]	PCHC: PDMS [%]	complex modulus [MPa][b]	$T_{g,tan\ \delta}$ [°C][c]
2	1	188	1324 (1324)	100:0	2507	118
	2				2286	118
	3				2589	115
6	1	99.5	412 (962)	73:27	1685	-127/119
	2				1623	-127/121
	3				1614	-127/120
7	1	133	648 (1198)	81:19	1647	-127/120
	2				1887	-126/120
	3				1711	-127/120
8	1	157	817 (1367)	84:16	2303	-127/122
	2				1838	-126/123
	3				2056	-126/122

[a] Degree of polymerization calculated as follows: $P_{n,PCHC} = (M_{n,meas} - M(PDMS_{550})) / 142$ g/mol; $P_{n,total} = P_{n,PCHC} + 550$. [b] at 20 °C. [c] from the maximum of tan delta

13. Tensile testing

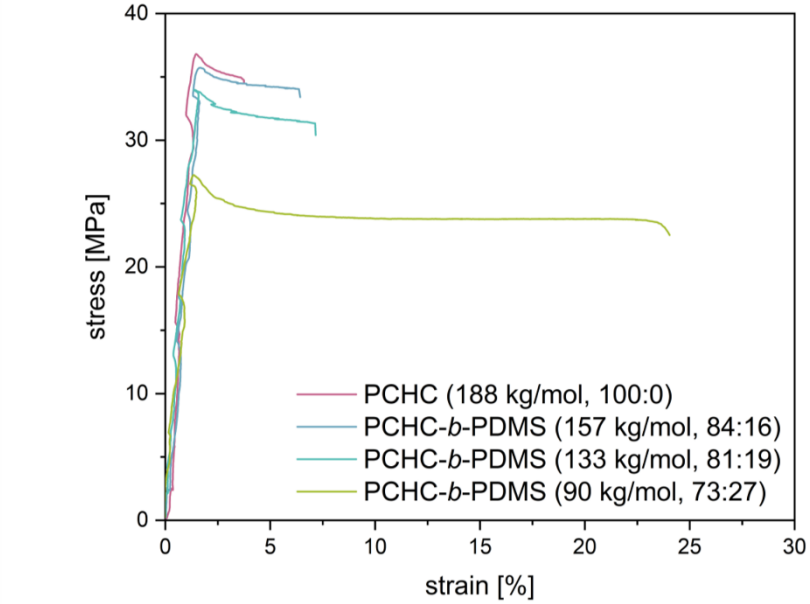

Figure 26. Stress-strain curves from tensile testing of PCHC (table 1, entry 2) and PCHC-*b*-PDMS block copolymers (table 1, entry 6-8). (Exemplary measurements; three specimens of all polymers were measured, individual values see table S3).

Table S3. Mechanical data from tensile testing, where of each polymer three specimen were measured at a rate of 5 mm/min until failure of the specimen.

entry no. from table 1	sample no.	$M_{n,meas}$ [kg/mol]	PCHC: PDMS [%]	E-modulus [MPa]	tensile strength [MPa]	elongation at break [%]
	1			2628	36.8	3.7
2	2	188	100:0	2318	33.7	1.7
	3			2517	36.6	2.3
	1			1574	27.2	24
6	2	99.5	73:27	1580	26.7	21
	3			1877	29.1	11
	1			1962	34.0	7.2
7	2	133	81:19	1984	33.1	2.6
	3			1992	34.3	2.9
	1			2155	35.7	6.4
8	2	157	84:16	1927	38.4	4.7
	3			2128	37.7	6.1

14. Pressure measurements

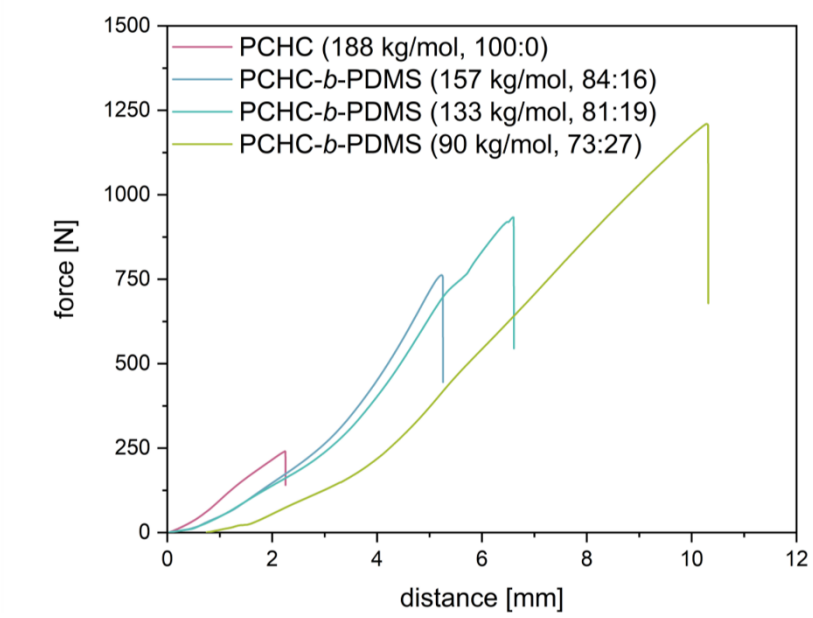

Figure S27. Pressure tests of PCHC (table 1, entry 2) and PCHC-*b*-PDMS block copolymers (table 1, entry 6-8), where force was applied to the sample until break. (Exemplary measurements; three specimens of all polymers were measured; individual values see table S4).

Table S4. Mechanical data from pressure tests where of each polymer three specimen were measured at a rate of 5 mm/min until failure of the specimen.

entry no. from table 1	sample no.	$M_{n,meas}$ [kg/mol]	PCHC: PDMS [%]	maximum force [N]	traverse path at break [mm]
2	1	188	100:0	247	3.5
	2			230	2.9
	3			240	2.3
6	1	99.5	73:27	1080	8.7
	2			913	7.7
	3			1210	10
7	1	133	81:19	933	6.6
	2			966	6.2
	3			625	4.7
8	1	157	84:16	762	5.3
	2			698	5.1
	3			1030	6.4

15. Rheology measurements

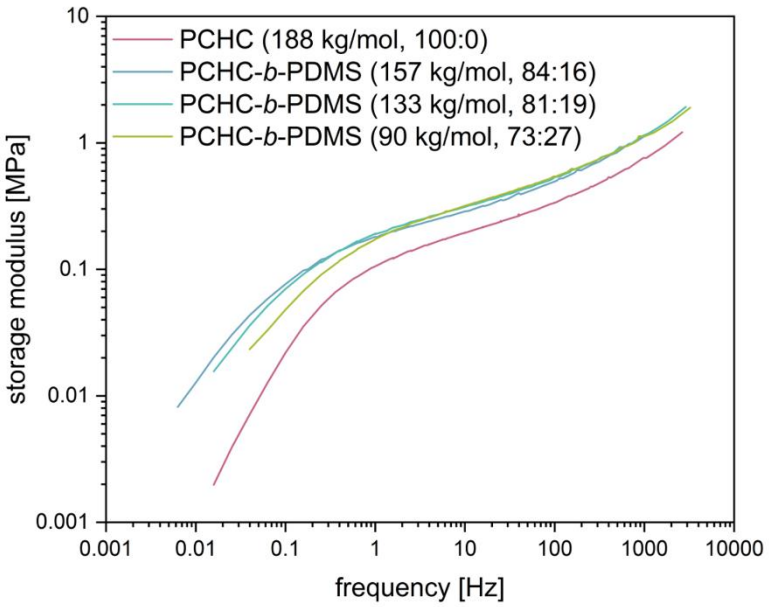

Figure S28. Master curves of the storage moduli from rheology measurements of PCHC (table 1, entry 2) and PCHC-*b*-PDMS block copolymers (table 1, entry 6-8) at 180 °C with a strain of 1%.

16. Atomic force microscopy

phase contrast: hard = light, soft = dark

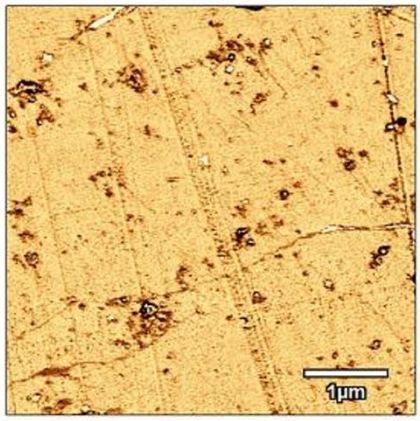

Figure S29. AFM from PCHC (table 1, entry 2) with phase resolved analysis.

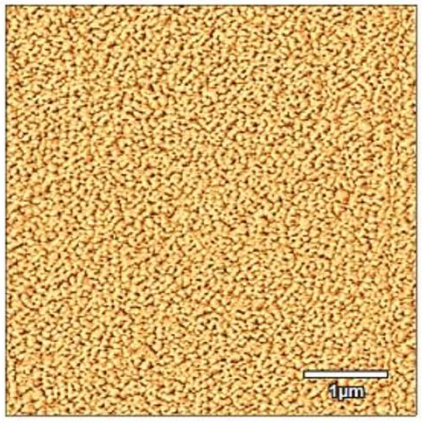

Figure S30. AFM from PCHC-*b*-PDMS (table 1, entry 6) with phase resolved analysis.

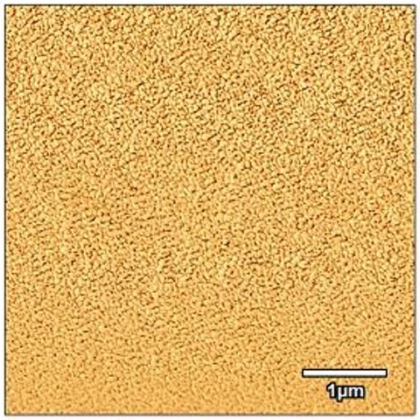

Figure S31. AFM from PCHC-*b*-PDMS (table 1, entry 7) with phase resolved analysis.

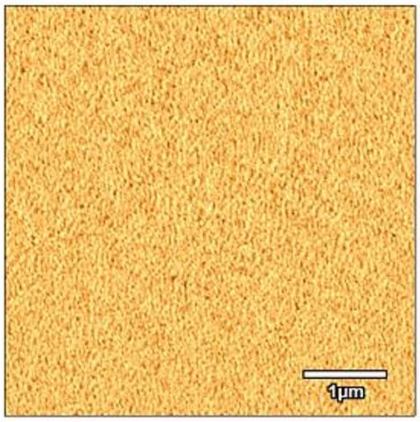

Figure S32. AFM from PCHC-*b*-PDMS (table 1, entry 8) with phase resolved analysis.

17. Transmission electron microscopy

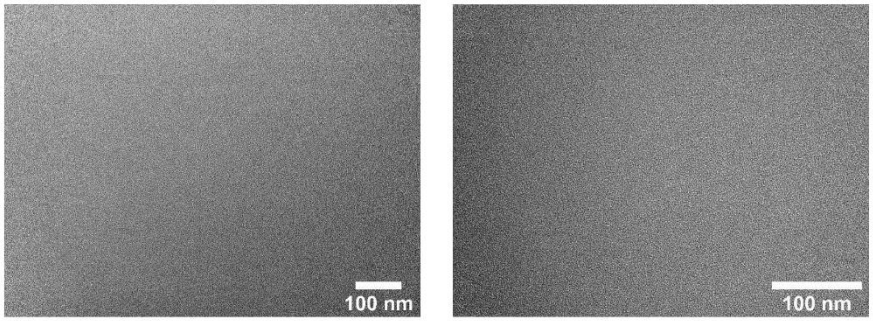

Figure S33. TEM of PCHC (table 1, entry 2).

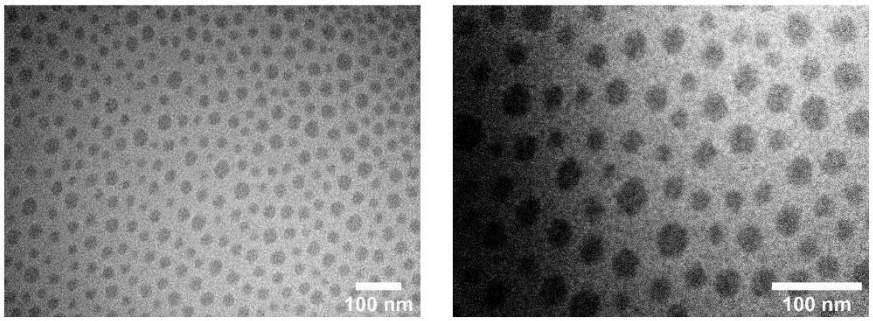

Figure S34. TEM of PCHC-*b*-PDMS (table 1, entry 6).

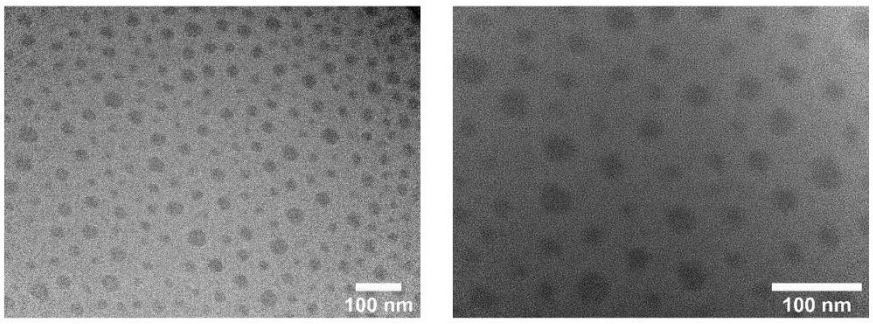

Figure S35. TEM of PCHC-*b*-PDMS (table 1, entry 7).

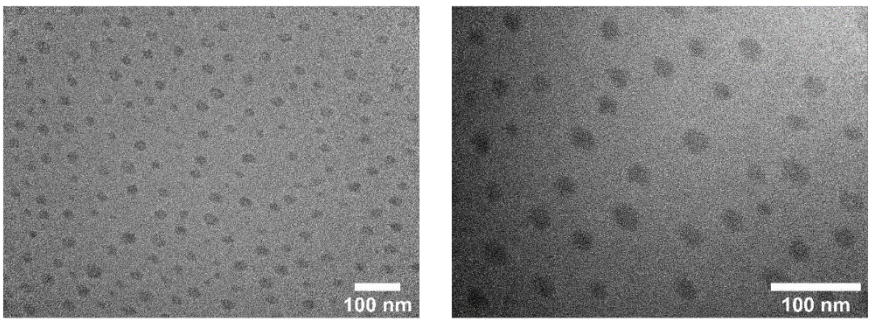

Figure S36. TEM of PCHC-*b*-PDMS (table 1, entry 8).

18. References

[1] M. Reiter, S. Vagin, A. Kronast, C. Jandl, B. Rieger, *Chemical Science* **2017**, *8*, 1876-1882.

[2] M. Reiter, A. Kronast, S. Kissling, B. Rieger, *ACS Macro Letters* **2016**, *5*, 419-423.

9.2 Supporting information: Controlled synthesis of statistical polycarbonates based on epoxides and CO_2

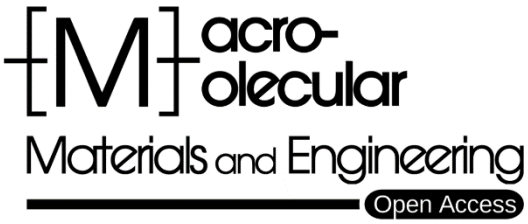

Supporting Information

for *Macromol. Mater. Eng.*, DOI 10.1002/mame.202300097

Controlled Synthesis of Statistical Polycarbonates Based on Epoxides and CO_2

*Alina Denk, Emilia Fulajtar, Carsten Troll and Bernhard Rieger**

Controlled synthesis of statistical polycarbonates based on epoxides and CO_2

Alina Denk[‡], *Emilia Fulajtar*[‡], *Carsten Troll*[‡], *Bernhard Rieger*[*, ‡]

[‡]WACKER-Chair of Macromolecular Chemistry, TUM School of Natural Sciences, Catalysis Research Center, Technical University Munich, Lichtenbergstr. 4, 85748 Garching, Germany

1. General information

All reactions were carried out with standard Schlenk techniques or in gloveboxes of the company *M. Braun* under argon 4.6 (99.996%, Westfalen AG). Unless otherwise specified the used solvents were absolutized and dried. The toluene was dried with a solvent purification system (SPS) MB SPS-800 from *M. Braun* and stored over an appropriate molecular sieve under argon atmosphere. Commercial available chemicals were purchased from Sigma-Aldrich, TCI Chemicals and, unless otherwise specified, used without further purification. The catalyst BDI^{CF3}-Zn-$N(TMS)_2$ (**cat.**) was synthesized according to procedures from literature.[1] Limonene oxide (LO) with an increased *trans*-LO content was synthesized according to literature procedures.[2] Cyclohexene oxide, propylene oxide and limonene oxide were dried over CaH_2 and purified by distillation.

Nuclear magnetic resonance spectroscopy (NMR) measurements (^1H, ^{13}C, DOSY) were carried out on spectrometers AV-400 and AV-500 cryo of the company *Bruker*. Deuterated solvents were purchased from Sigma-Aldrich and for use with substances susceptible to hydrolysis stored over molecular sieves and under argon. The chemical shifts (δ) are given in parts per million (ppm) and are calibrated to the signals of the solvents. Resonance multiplicities are abbreviated as follows: br s = broad singlet, m = multiplet. ***In situ* infrared (IR) measurements** of polymerization experiments were carried out on a *Mettler Toledo Multimax ReactIR*™ autoclave system. **Gel permeation chromatography (GPC)** experiments were carried out at a PL-GPC 50 of the company *Agilent* with THF (HPLC grade, 0.22 g/L 2,6-di-tert-butyl-4-methylphenol) as solvent and molecular weights were calculated relative to poly(styrene) calibration standards. **Differential scanning calorimetry (DSC)** measurements were performed on a *TA Instruments* Q2000 with a heating or cooling rate of 10K/min in non-hermetic aluminum pans. **Thermogravimetric analysis (TGA)** was carried out on a *TA Instruments* Q5000 with a heating rate of 10 K/min under air. For **tensile testing** dog bone shaped specimen (length = 50 mm, width at rejuvenation = 4.0 mm, thickness = 1.0 mm) of the polymers were prepared *via* hot pressing at 160 °C for 5 minutes. The measurements were carried out on a material testing machine of the company *ZwickRoell*. The pre-force applied to the specimen was 0.1 MPa and the measurement speed was 5 mm/min.

2. Synthesis procedure

In the glovebox BDI^{CF3}-Zn-$N(TMS)_2$ (cat.) is dissolved in toluene, transferred into the autoclave together with propylene oxide and pressurized with CO_2. In the *in situ* IR autoclave the reaction mixture is stirred (500 rpm) and *via* the dosing system cyclohexene oxide is added with a constant rate over the course of the whole reaction. Dosing of cyclohexene oxide is then stopped and the CO_2 pressure is released. The reaction mixture is diluted with wet dichloromethane to stop the reaction and the product is precipitated from methanol and dried under vacuum.

In further experiments limonene oxide is dosed into the reactor instead of cyclohexene oxide.

Table S1. Polymerizations of PO/LO/CO_2 towards PPC-PLC.

entry	feed[a] PO:LO:cat.	dosing rate LO [mL/h]	time [h]	conversion[b] PO, LO [%]	selectivity[c] PPC:cPC [%]	PPC:PLC [%][c]	M_n (Đ) [kg/mol][d]
1	1000:220:1	0.12	12	33, 60	77:23	65:35	101 (1.5)
2	1000:320:1	0.48	6	19, 48	78:22	49:51	50.2 (1.5)
3	500:390:1	0.24	15	50, 70	82:18	43:57	60.0 (1.6)
4	250:550:1	0.24	16	63, 54	79:21	30:70	41.5 (1.6)

Polymerizations in toluene, 30 bar CO_2 pressure, 25 °C, stirred at 500 rpm. [a] Feed of LO (92% *trans*-LO) calculated from the sum of LO and PLC signals in ^{1}H NMRs with the sum of PO, cPC and PPC signals as reference. [b] Conversion calculated from the respective polymer and monomer integrals in ^{1}H NMRs (for LO calculated according to a *trans*-LO content of 92%). [c] Calculated from the respective (polymer) signals in ^{1}H NMRs. [d] Measured *via* GPC in THF relative to poly(styrene) standards.

Purification of the polymer products

All precipitated polymers are further purified for thermal and mechanical analysis. First they are dissolved in dichloromethane (5 mL/$g_{polymer}$), then washed with a saturated solution of EDTA in water (3 × V_{DCM}) and precipitated from methanol. The polymer is then dried in vacuo.

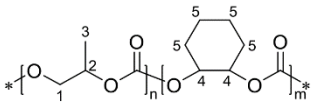

^{1}H-NMR (400 MHz, $CDCl_3$, 298 K): δ(ppm) = 4.98 (br s, 1 H, H-2), 4.65 (br s, 2 H, H-4), 4.18 (m, 2 H, H-1), 2.12-1.32 (m, 11 H, H-3 and H-5).

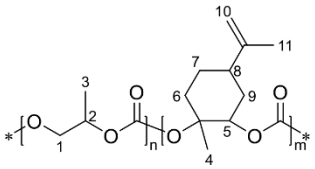

^{1}H-NMR (400 MHz, $CDCl_3$, 298 K): δ(ppm) = 4.98 (br s, 2 H, H-2 and H-5), 4.70 (br s, 1 H, H-10), 4.17 (m, 3 H, H-1 and H-10), 2.32-1.31 (m, 16 H, H-3, H-4, H-6 to H-9 and H-11).

3. *In situ* IR measurements

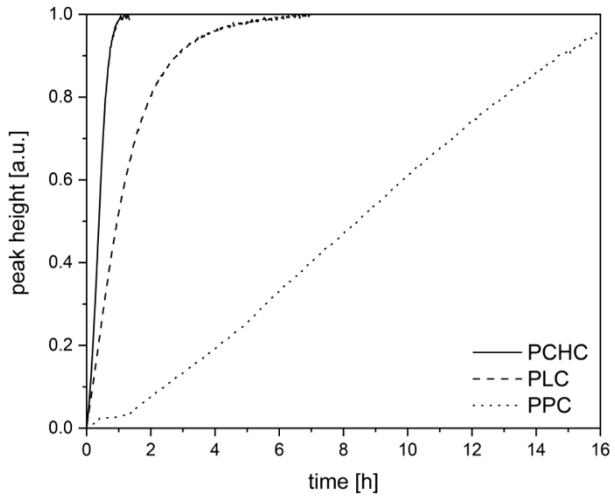

Figure S1. Intensity of the carbonyl vibration at 1750 cm^{-1} over time from *in situ* IR measurements of copolymerizations towards poly(cyclohexene carbonate) (PCHC), poly(limonene carbonate) (PLC), and poly(propylene carbonate) (PPC).

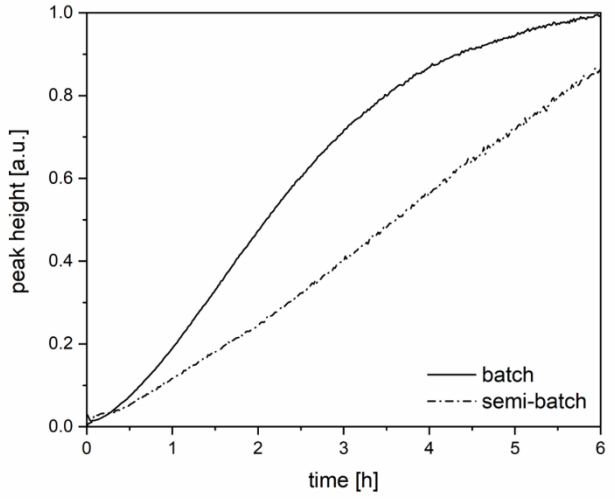

Figure S2. Intensity of the carbonyl vibration at 1750 cm^{-1} over time from *in situ* IR measurements of PO/CHO/CO_2 terpolymerizations *via* batch or semi-batch process.

4. Gradient vs. statistical terpolymer

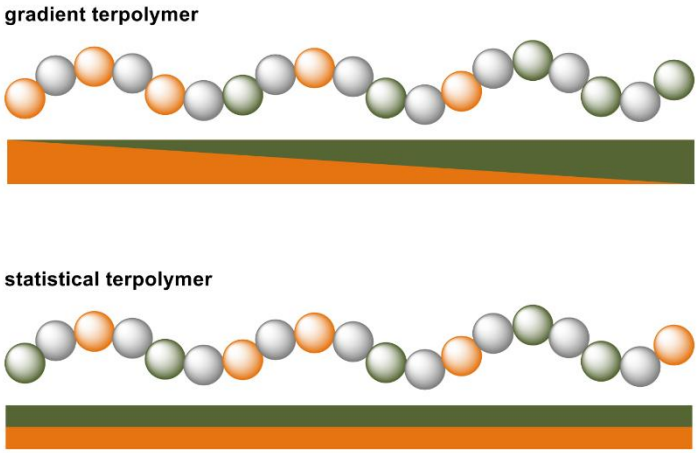

Figure S3. Schematic structure of gradient and statistical terpolymers with different monomer ratios over the whole polymer chain.

5. Back-biting mechanism

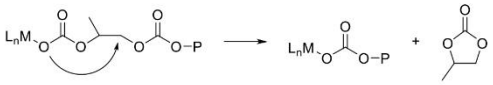

Scheme S1. Generation of the thermodynamically stable cyclic propylene carbonate (cPC) *via* back-biting during the copolymerization of PO and CO_2 (P = polymer chain).

6. NMRs

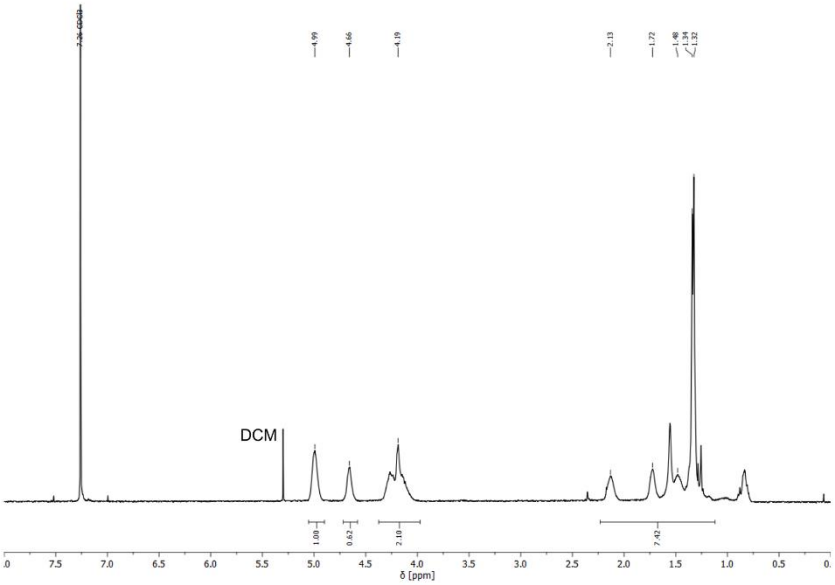

Figure S4. ^{1}H NMR of the statistical terpolymer PPC_{76}-$PCHC_{24}$ (table 1, entry 1) measured in $CDCl_3$ at 500 MHz.

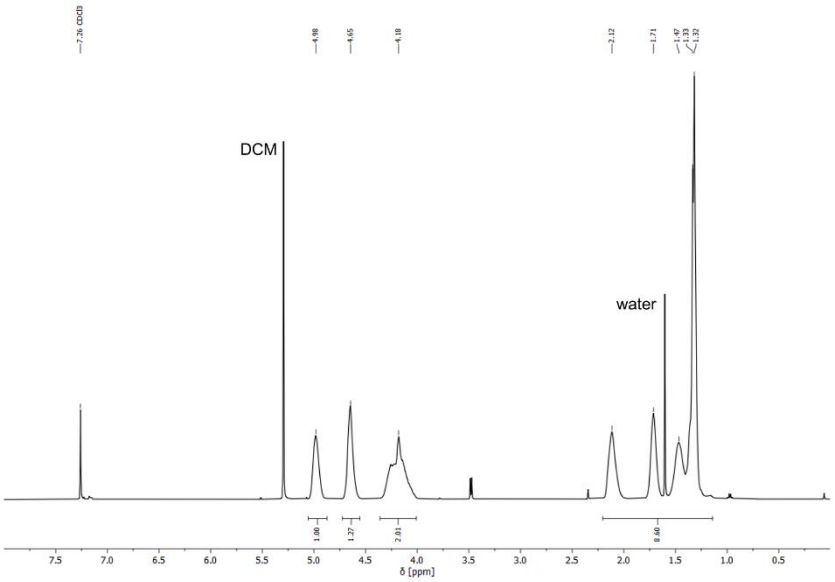

Figure S5. ^{1}H NMR of the statistical terpolymer PPC_{61}-$PCHC_{39}$ (table 1, entry 2) measured in $CDCl_3$ at 500 MHz.

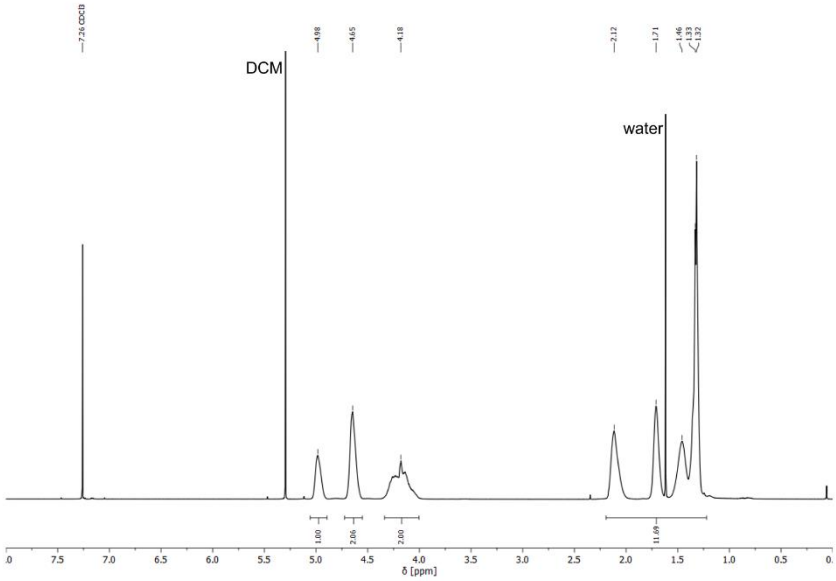

Figure S6. ^{1}H NMR of the statistical terpolymer PPC_{49}-$PCHC_{51}$ (table 1, entry 3) measured in $CDCl_3$ at 500 MHz.

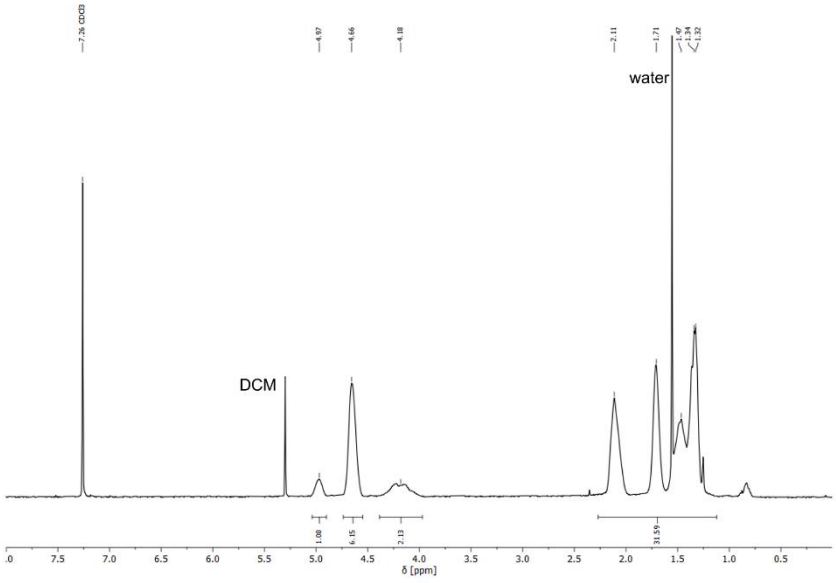

Figure S7. ^{1}H NMR of the statistical terpolymer PPC_{25}-$PCHC_{75}$ (table 1, entry 4) measured in $CDCl_3$ at 500 MHz.

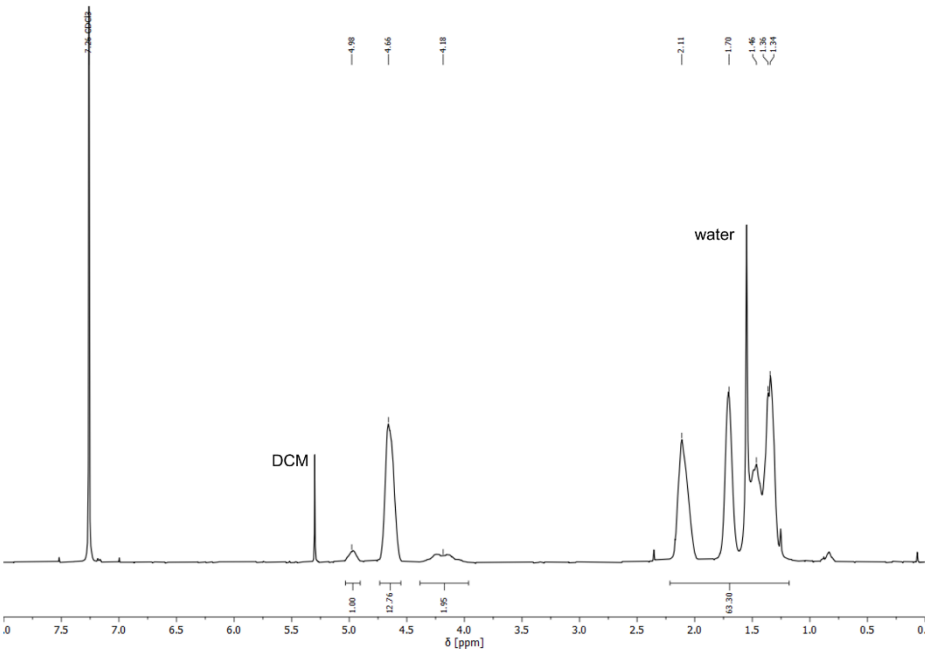

Figure S8. ^{1}H NMR of the statistical terpolymer PPC_{14}-$PCHC_{86}$ (table 1, entry 5) measured in $CDCl_3$ at 500 MHz.

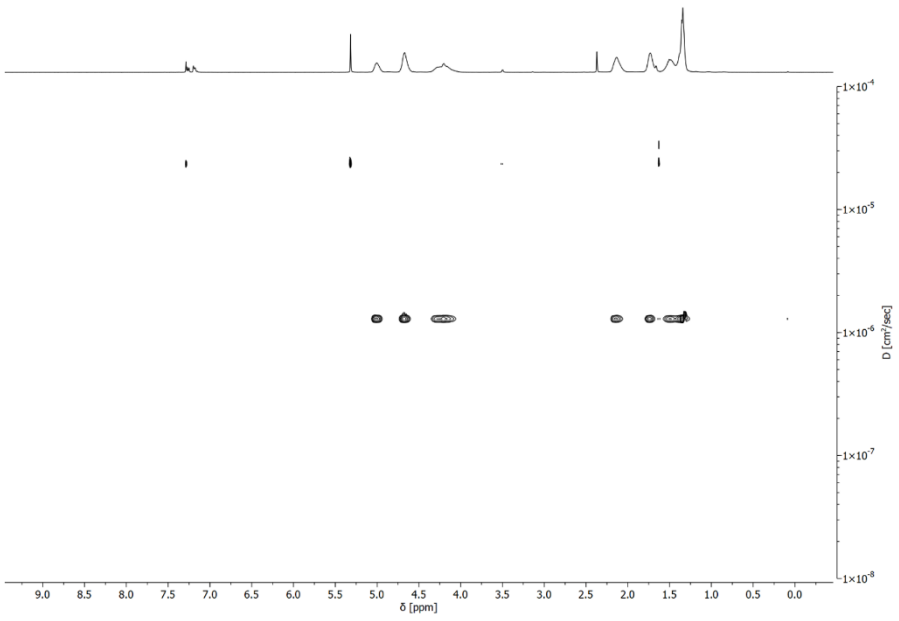

Figure S9. DOSY NMR of a PPC-PCHC terpolymer (table 1, entry 2).

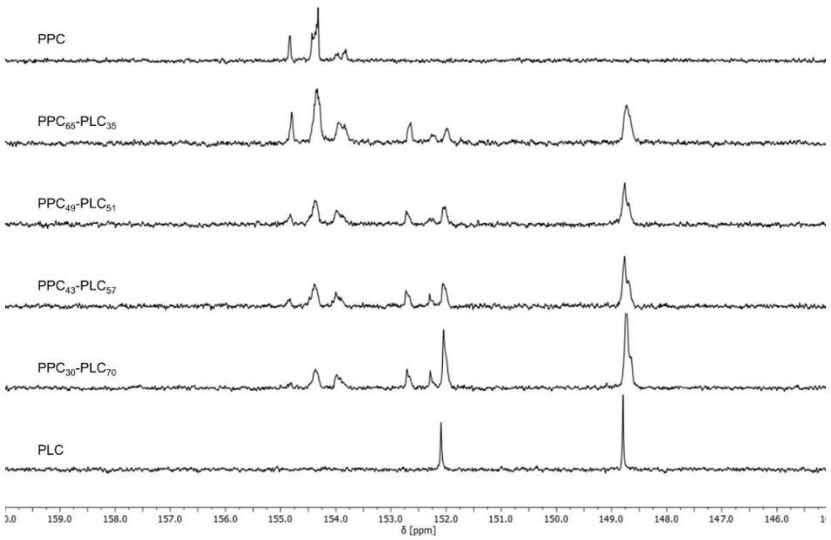

Figure S10. Carbonyl region in ^{13}C NMRs of pure PPC and PLC copolymers and PPC-PLC terpolymers.

7. GPCs

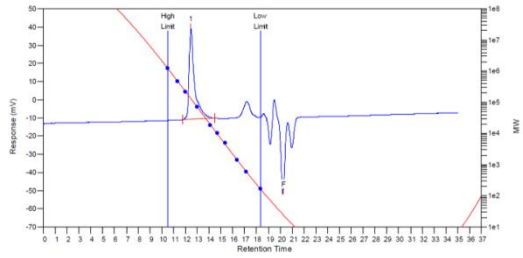

MW Averages

Peak No	Mp	Mn	Mw	Mz	Mz+1	Mv	PD
1	129761	91048	110708	123688	133019	108465	1.21593

Figure S11. GPC trace of PPC_{76}-$PCHC_{24}$, measured in THF.

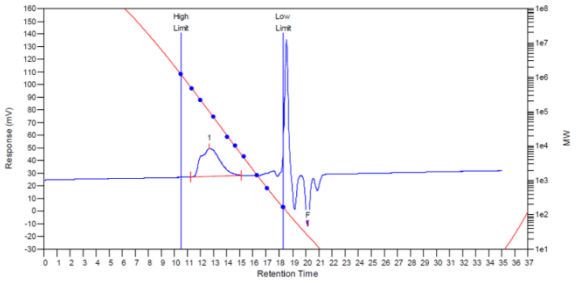

MW Averages

Peak No	Mp	Mn	Mw	Mz	Mz+1	Mv	PD
1	97957	60931	107565	157808	199903	100355	1.76536

Figure S12. GPC trace of PPC_{61}-$PCHC_{39}$, measured in THF.

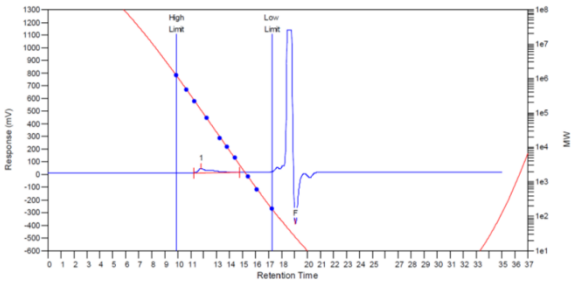

MW Averages

Peak No	Mp	Mn	Mw	Mz	Mz+1	Mv	PD
1	121591	37232	73500	103777	123132	68576	1.97411

Figure S13. GPC trace of PPC_{49}-$PCHC_{51}$, measured in THF.

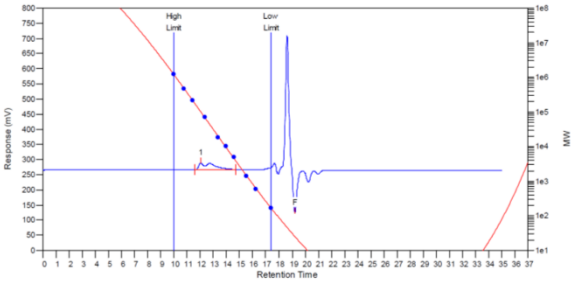

MW Averages

Peak No	Mp	Mn	Mw	Mz	Mz+1	Mv	PD
1	100320	33772	56034	76917	91960	52816	1.65919

Figure S14. GPC trace of PPC_{25}-$PCHC_{75}$, measured in THF.

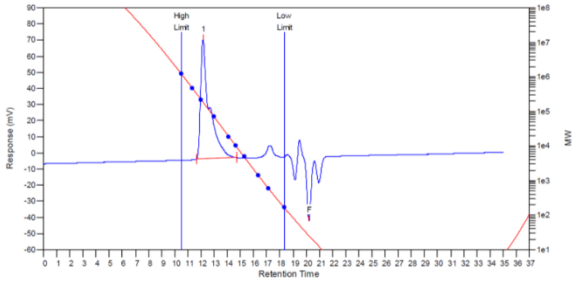

MW Averages

Peak No	Mp	Mn	Mw	Mz	Mz+1	Mv	PD
1	185147	99161	139286	167093	185235	134502	1.40464

Figure S15. GPC trace of PPC_{14}-$PCHC_{86}$, measured in THF.

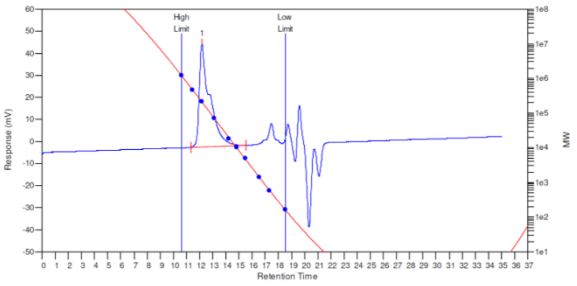

MW Averages

Peak No	Mp	Mn	Mw	Mz	Mz+1	Mv	PD
1	210880	100970	153591	190622	217331	147412	1.52115

Figure S16. GPC trace of PPC_{65}-PLC_{35}, measured in THF.

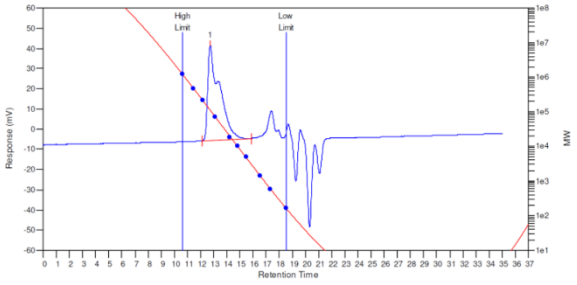

MW Averages

Peak No	Mp	Mn	Mw	Mz	Mz+1	Mv	PD
1	110033	50181	74159	93354	106851	71033	1.47783

Figure S17. GPC trace of PPC_{49}-PLC_{51}, measured in THF.

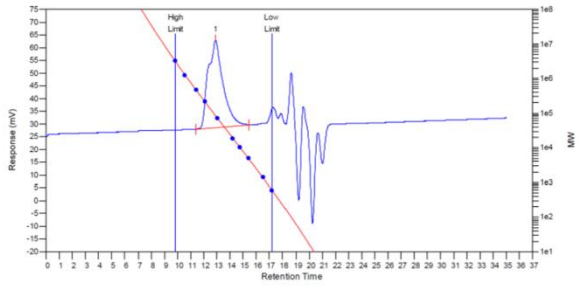

MW Averages

Peak No	Mp	Mn	Mw	Mz	Mz+1	Mv	PD
1	84138	59992	93230	125001	152663	88518	1.55404

Figure S18. GPC trace of PPC_{43}-PLC_{57}, measured in THF.

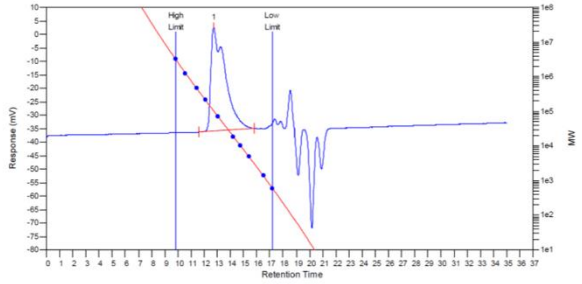

MW Averages

Peak No	Mp	Mn	Mw	Mz	Mz+1	Mv	PD
1	103704	41500	67056	87651	102883	63755	1.61581

Figure S19. GPC trace of PPC_{30}-PLC_{70}, measured in THF.

8. TGA/DSC

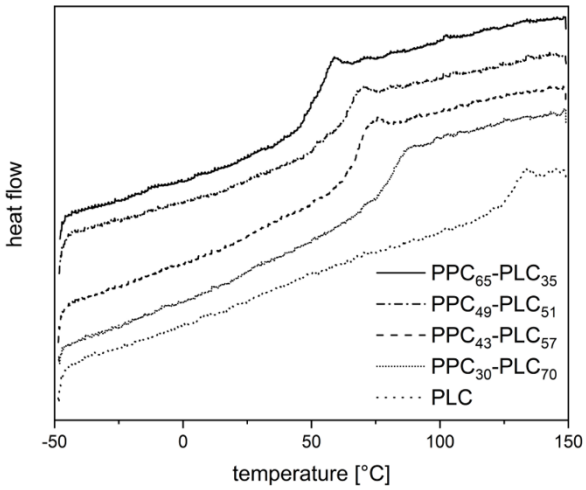

Figure S20. DSC measurements (2nd heating cycle) of PLC and PPC-PLC terpolymers with the polymer ratio in subscript.

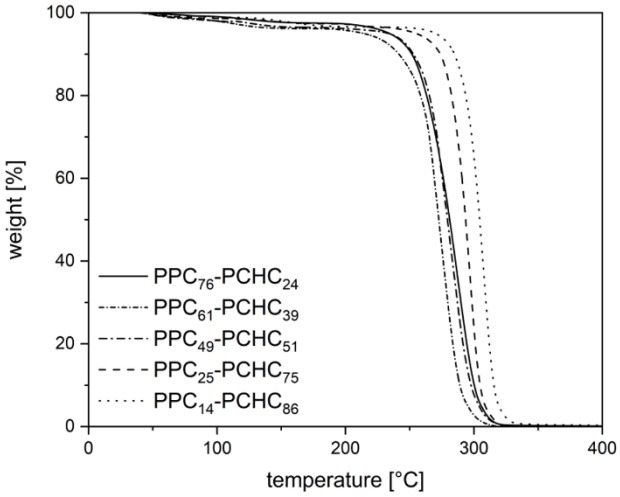

Figure S21. TGA measurements of PPC-PCHC terpolymers with the polymer ratio in subscript.

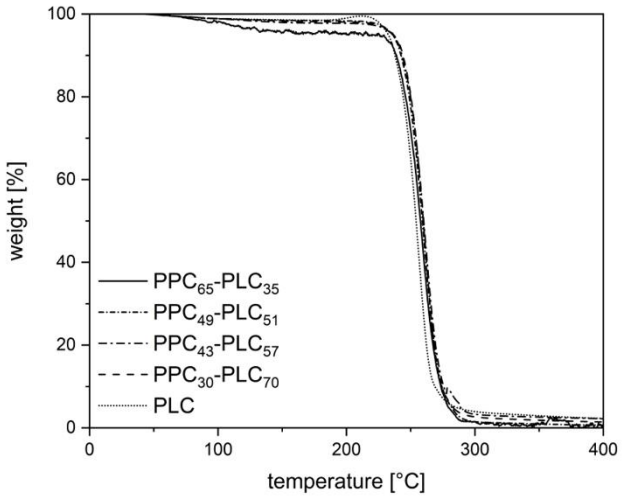

Figure S22. TGA measurements of PLC and PPC-PLC terpolymers with the polymer ratio in subscript.

Table S2. Thermal and mechanical properties of the synthesized polymers.

entry	polymer[a]	M_n (Đ) [kg/mol][b]	T_g [°C][c]	T_d [°C][d]	E-modulus [MPa][e]	tensile strength [MPa][e]	elongation at break [%][e]
1	PPC_{76}-$PCHC_{24}$	91.0 (1.2)	58	262	2520	33.9	10
2	PPC_{61}-$PCHC_{39}$	60.9 (1.8)	70	257	2830	36.5	4
3	PPC_{49}-$PCHC_{51}$	37.2 (2.0)	79	262	-	-	-
4	PPC_{25}-$PCHC_{75}$	33.8 (1.7)	105	282	2690	41.8	4
5	PPC_{14}-$PCHC_{86}$	99.2 (1.4)	110	293	2530	34.7	2
6	PPC_{65}-PLC_{35}	101 (1.5)	56	244	2470	41.6	3
7	PPC_{49}-PLC_{51}	50.2 (1.5)	66	246	2460	42.3	2
8	PPC_{43}-PLC_{57}	60.0 (1.6)	68	247	2090	36.8	2
9	PPC_{30}-PLC_{70}	41.5 (1.6)	81	248	2070	43.0	2

[a] Calculated from the respective polymer integrals in the ^{1}H NMR from the precipitated polymer products. [b] Measured *via* GPC in $CHCl_3$ relative to poly(styrene) standards. [c] Measured *via* DSC. [d] Onset decomposition temperature, measured *via* TGA. [e] Measured *via* tensile testing of dog bone shaped specimen.

9. References

[1] M. Reiter, S. Vagin, A. Kronast, C. Jandl, B. Rieger, *Chem Sci* **2017**, *8*, 1876-1882.
[2] O. Hauenstein, M. Reiter, S. Agarwal, B. Rieger, A. Greiner, *Green Chem* **2016**, *18*, 760-770.

9.3 Supporting information: Heteronuclear, monomer-selective Zn/Y catalyst combines copolymerization of epoxides and CO_2 with group-transfer polymerization of Michael-type monomers

Heteronuclear, Monomer-Selective Zn/Y Catalyst Combines Copolymerization of Epoxides and CO_2 with Group-Transfer Polymerization of Michael-Type Monomers

*Alina Denk,[†] Sebastian Kernbichl,[†] Andreas Schaffer, Moritz Kränzlein, Thomas Pehl, and Bernhard Rieger**

WACKER-Chair of Macromolecular Chemistry, Catalysis Research Center, Technical University Munich, Lichtenbergstr. 4, 85748 Garching, Germany

Content

1. Synthesis procedures

General

All reactions containing air- and/or moisture sensitive compounds were carried out under dry argon 4.6 (99.996%, *Westfalen AG*) using standard Schlenk or glovebox techniques. Toluene was dried with a solvent purification system (SPS) MB SPS-800 of the company *M. Braun* and stored over molecular sieve under argon atmosphere. Commercially available chemicals were purchased from *Sigma-Aldrich*, *ABCR, TCI Chemicals* or the central administration of materials of the Technical University of Munich and, unless otherwise specified, used without further purification. The compounds **1**,[1] 3-((2,6-dimethylpyridin-4-yl)oxy)propan-1-ol[2] and $Cp_2Y(CH_2TMS)(thf)$[3] were synthesized according to procedures from literature. Monomers were dried and purified prior to polymerization. Cyclohexene oxide was dried over NaH and purified by distillation. The monomers 2-vinylpyridine and 2-isopropenyl-2-oxazoline were dried over CaH_2 and purified by distillation. NMR-measurements (^1H, ^{13}C) were carried out on the spectrometers AV-400 and AV-500 Cryo of the company *Bruker*. Deuterated solvents were purchased from *Sigma-Aldrich* and for substances susceptible to hydrolysis stored over molecular sieves and under argon. The chemical shifts (δ) are given in parts per million (ppm) and are calibrated to the signals of the deuterated solvents. Mass spectra were carried out either on a *Varian* 500-MS with electron spray ionization (ESI) in acetonitrile using positive ionization mode at 70 eV or on a *Bruker Daltonics ultraflex TOF/TOF* with matrix assisted laser desorption ionization (MALDI). For MALDI-MS measurements the polymer sample is dissolved in dichloromethane and mixed with a saturated solution of α-cyano-4-hydroxycinnamic acid in a 0.1 vol% solution of trifluoroacetic acid in water/acetonitrile. The instrument has been calibrated with a protein standard in the same matrix as the sample prior to use. Gel permeation chromatography experiments were carried out at a PL-GPC 50 of the company *Agilent* with DMF (HPLC grade, 2.17 g/L LiBr) as solvent and PMMA calibration standards. Absolute molar masses of P2VP aliquots were determined via concentration measurement with a two-angle light scattering, viscosimetry and refractive index detection (dn/dc = 0.149 mL/g). Elemental analysis measurements were performed by the microanalytical laboratory of the Inorganic-chemical Institute of the Technical University Munich. *In situ* ATR-IR measurements were performed under argon atmosphere using a *Mettler Toledo MultiMax Pressure* system.

(1) Reiter, M.; Vagin, S.; Kronast, A.; Jandl, C.; Rieger, B., A Lewis acid β-diiminato-zinc-complex as all-rounder for co- and terpolymerisation of various epoxides with carbon dioxide. *Chemical Science* 2017, *8* (3), 1876-1882.

(2) Wang, Q.; Chen, S.; Liang, Y.; Dong, D.; Zhang, N., Bottle-Brush Brushes: Surface-Initiated Rare Earth Metal Mediated Group Transfer Polymerization from a Poly(3-((2,6-dimethylpyridin-4-yl)oxy)propyl methacrylate) Backbone. *Macromolecules* 2017, *50* (21), 8456-8463.

(3a) Hultzsch, K. C.; Voth, P.; Beckerle, K.; Spaniol, T. P.; Okuda, J., Single-Component Polymerization Catalysts for Ethylene and Styrene: Synthesis, Characterization, and Reactivity of Alkyl and Hydrido Yttrium Complexes Containing a Linked Amido−Cyclopentadienyl Ligand.

Organometallics 2000, *19* (3), 228-243; (b) Salzinger, S.; Soller, B. S.; Plikhta, A.; Seemann, U. B.; Herdtweck, E.; Rieger, B., Mechanistic Studies on Initiation and Propagation of Rare Earth Metal-Mediated Group Transfer Polymerization of Vinylphosphonates. *J Am Chem Soc* 2013, *135* (35), 13030-13040.

Synthesis of catalyst 3'

In a glovebox 52.1 mg (288 µmol, 1.0 eq.) 3-((2,6-dimethylpyridin-4-yl)oxy)propan-1-ol are dissolved in 1.0 mL toluene and a solution of 200 mg (288 µmol, 1.0 eq.) **1** in 1.0 mL toluene is added. Immediate precipitation of a light-yellow solid can be observed, which is separated from the supernatant solution by decantation. Complex **3'** in form of a light-yellow solid is dried under vacuum (yield: 61%).

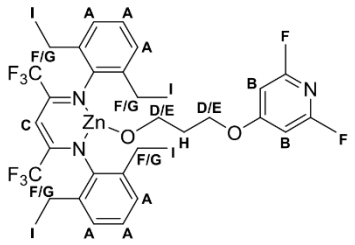

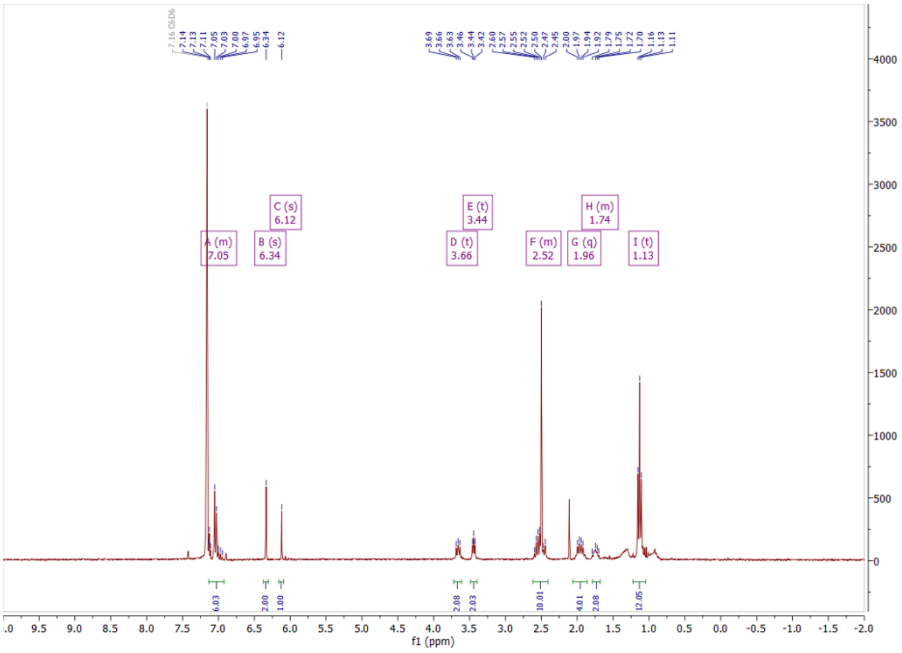

Figure S1. ^{1}H NMR spectrum of complex **3'** in benzene-d_6.

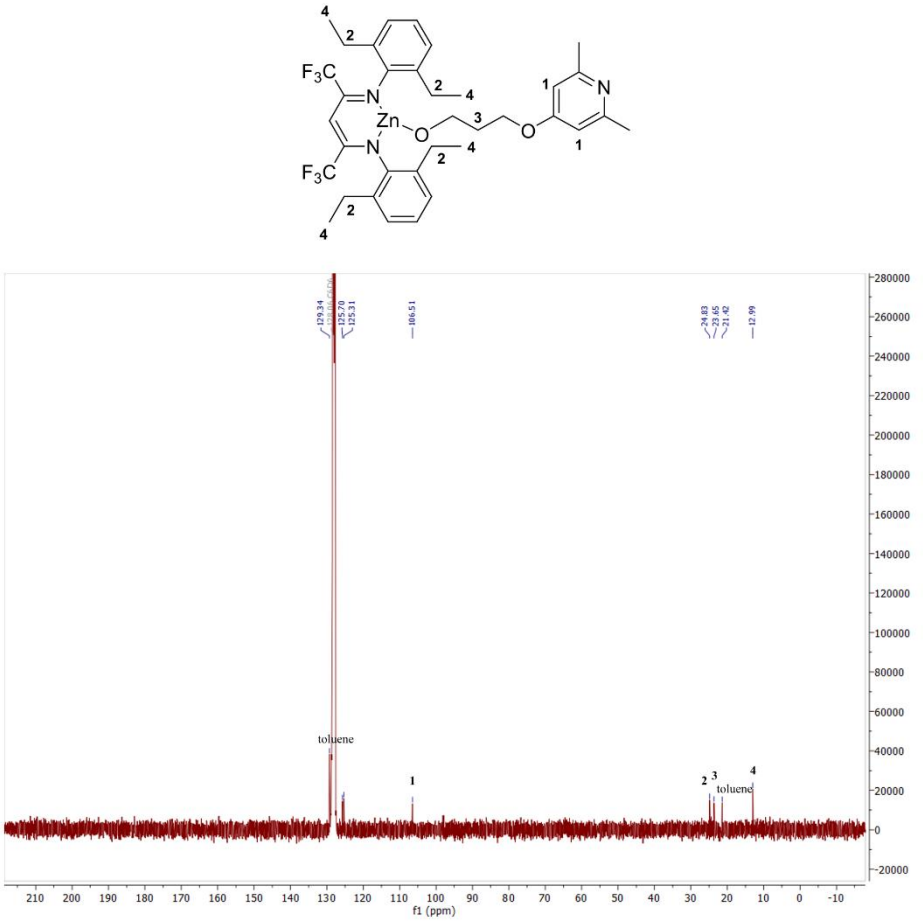

Figure S2. ^{13}C NMR spectrum of a saturated solution of complex **3'** in benzene-d_6 (due to the low solubility of the complex the signals of Pyr-C^{Ar}-Me, Pyr-C^{Ar}-O, CF_3, BDI-C^{Ar}, *C*-CF_3, *C*H-C-CF_3 and CH_2-O are not visible in the spectrum).

EA: [%] calculated: C 58.79, H 5.78, N 5.88

found: C 60.06, H 6.13, N 5.67

4

Synthesis of catalyst 3

In a vial 6.00 mg (8.39 µmol, 1.0 eq.) **3'** and 3.18 mg (8.39 µmol, 1.0 eq.) $Cp_2Y(CH_2TMS)(thf)$ are suspended in 1.2 mL toluene and stirred at room temperature for four hours. The resulting solution of the dinuclear complex **3** is used directly for a polymerization reaction.

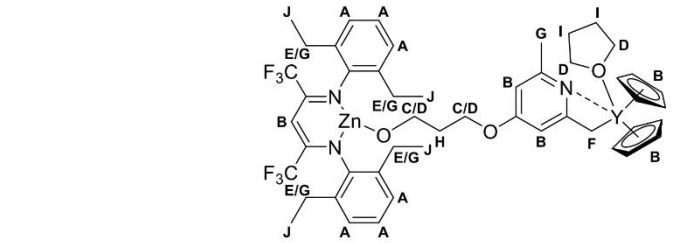

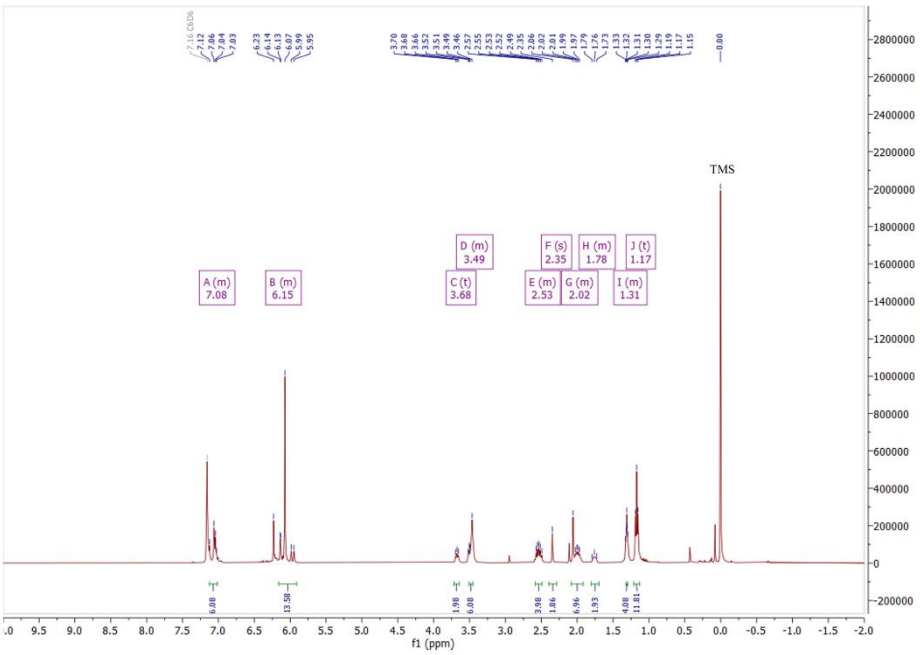

Figure S3. ^{1}H NMR spectrum of complex **3** in benzene-d_6.

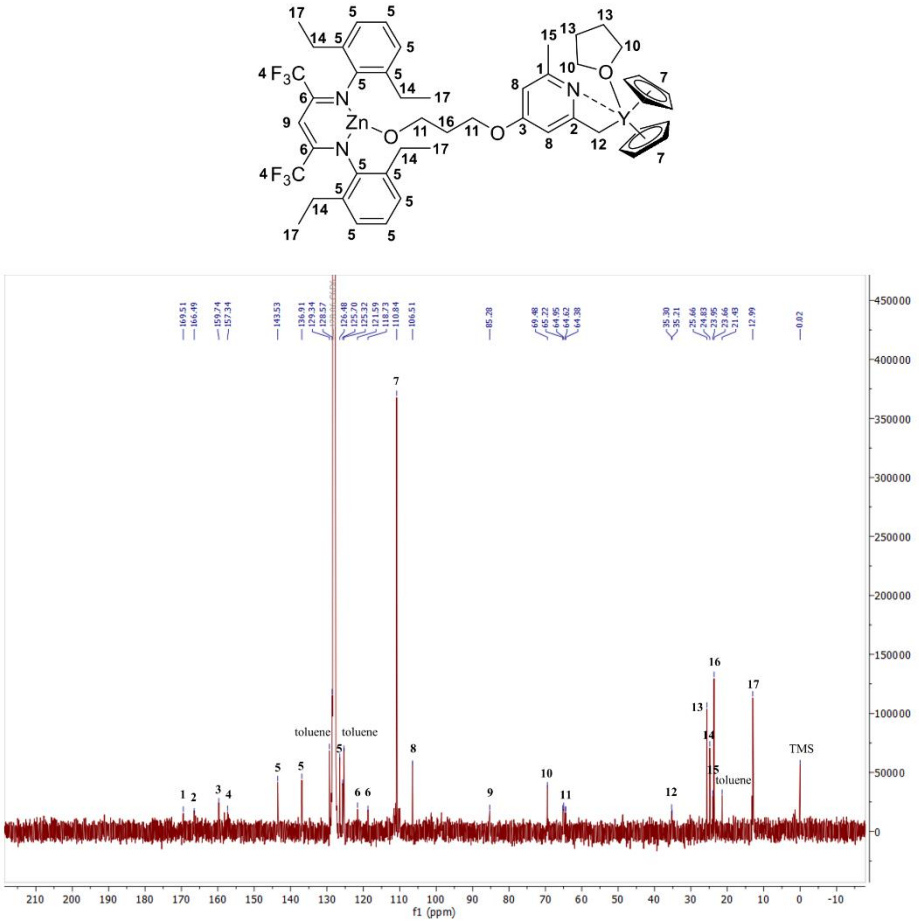

Figure S4. ^{13}C NMR spectrum of complex **3** in benzene-d_6.

EA: [%] calculated: C 58.54, H 5.82, N 4.18

found: C 57.45, H 5.48, N 4.17

6

2. NMR spectra of CH-bond activation

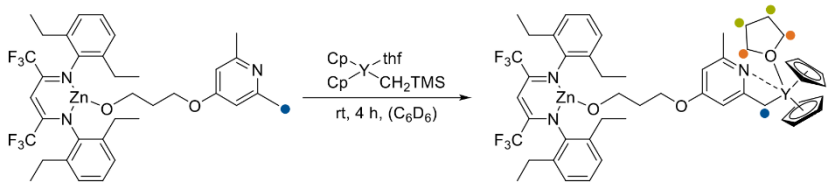

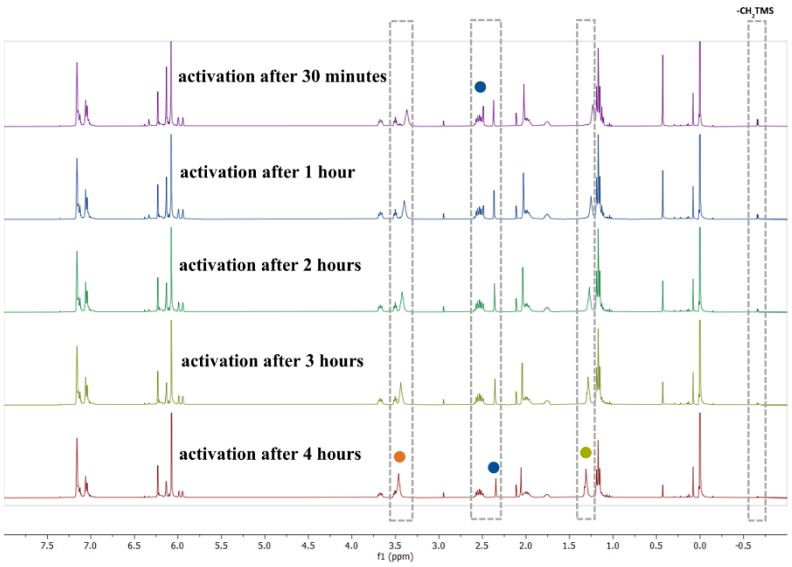

Figure S5. ^{1}H NMR spectra of the CH-bond activation of complex **3'** over four hours in benzene-d_6.

3. Mononuclear catalysts in P2VP and PCHC polymerization

$Cp_2Y(thf)(CH_2TMS)$ in the copolymerization of cyclohexene oxide/CO_2

In the glovebox 40.8 µmol (1.0 eq.) $Cp_2Y(thf)(CH_2TMS)$ are dissolved in 4.0 g toluene and transferred into a handheld autoclave together with 20.4 mmol (500 eq.) cyclohexene oxide. The reaction mixture is pressurized with 30 bar CO_2 and stirred at 40 °C. After 17 hours no generation of PCHC product could be observed.

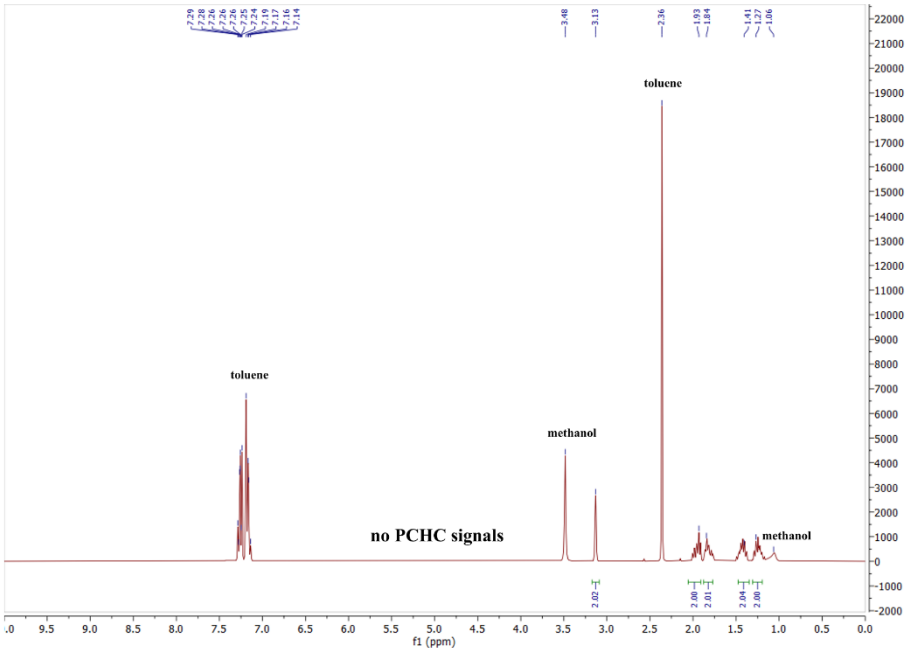

Figure S6. ^1H NMR spectrum of the reaction of CHO and CO_2 with catalyst **2** after 17 hours with no visible polymerization in benzene-d_6.

Catalyst 3' in the polymerization of 2-vinylpyridine

In a glovebox 2.80 µmol (1.0 eq.) **3'** are dissolved in 1.2 mL C_6D_6 and mixed with 280 µmol (100 eq.) 2-vinylpyridine. The reaction mixture is stirred at room temperature for five hours without observable generation of P2VP product.

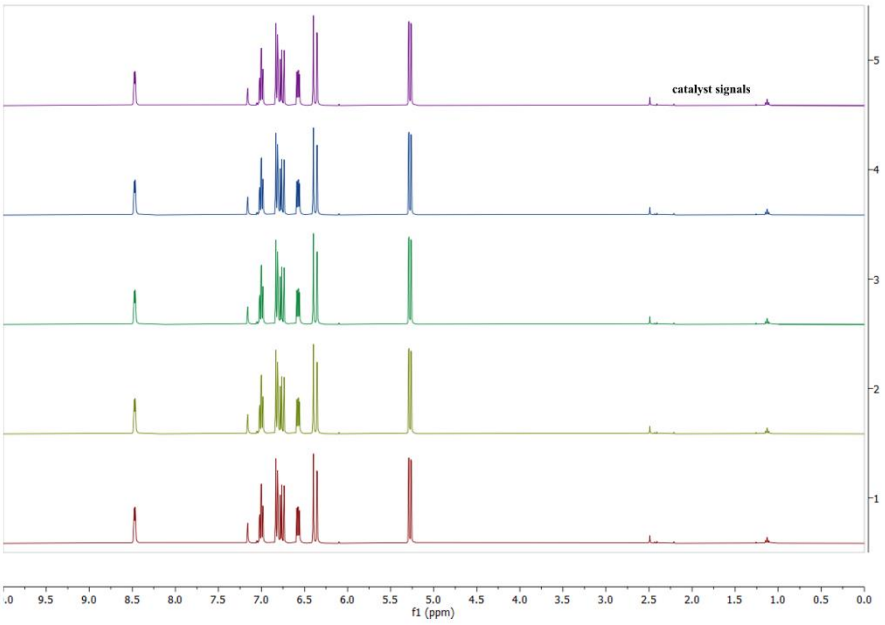

Figure S7. ^{1}H NMR spectra of the reaction of 2VP with **3'** after over five hours without polymerization in benzene-d_6.

4. MALDI-MS of oligomeric P2VP synthesized with catalyst 3

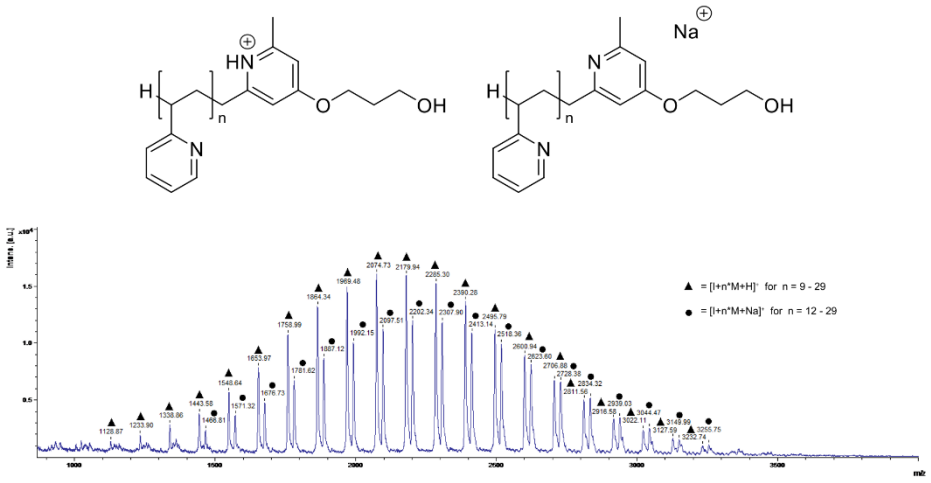

Figure S8. MALDI-MS of oligomeric P2VP synthesized with catalyst **3**.

5. Polymerization procedures

Sequential terpolymerization of cyclohexene oxide, and CO_2 with 2-vinylpyridine or 2-isopropenyl-2-oxazoline

In a glovebox 8.39 µmol (1.0 eq.) **3'** is used for the CH-bond activation with 8.39 µmol (1.0 eq.) $Cp_2Y(thf)(CH_2TMS)$ in 1.2 mL toluene. After four hours the reaction mixture is transferred into a handheld autoclave together with 2-vinylpyridine or 2-isopropenyl-2-oxazoline and stirred again for the respective time at room temperature. Cyclohexene oxide is added, the reaction mixture is pressurized with 30 bar CO_2 and stirred at 40 °C. The CO_2 pressure is released and the resulting product is precipitated from *n*-pentane and dried under vacuum.

One-pot terpolymerization of 2-vinylpyridine or 2-isopropenyl-2-oxazoline, cyclohexene oxide, and CO2

In a glovebox 8.39 µmol (1.0 eq.) **3'** is used for the CH-bond activation with 8.39 µmol (1.0 eq.) $Cp_2Y(thf)(CH_2TMS)$ in 1.2 mL toluene. After four hours the reaction mixture is transferred into a handheld autoclave together with 2-vinylpyridine or 2-isopropenyl-2-oxazoline and cyclohexene oxide and stirred at room temperature. After conversion of the Michael-type monomer, the reaction mixture is pressurized with 30 bar CO_2 and stirred at 40 °C. The CO_2 pressure is released and the resulting product is precipitated from *n*-pentane and dried under vacuum.

6. *In situ* ATR-IR spectrum of the CHO/CO_2 copolymerization with catalyst 3

In a glovebox 20.4 µmol (1.0 eq.) **1** is dissolved in 4.0 g toluene and transferred into a steel autoclave together with cyclohexene oxide. The reaction mixture is pressurized with 30 bar CO_2 and stirred at 40 °C with *in situ* IR monitoring.

In a glovebox 9.38 µmol (1.0 eq.) **3'** is used for the CH-bond activation with 9.38 µmol (1.0 eq.) $Cp_2Y(thf)(CH_2TMS)$ in 2.0 mL toluene. After four hours the reaction mixture is transferred into a steel autoclave together with cyclohexene oxide. The reaction mixture is pressurized with 30 bar CO_2 and stirred at 40 °C with *in situ* IR monitoring.

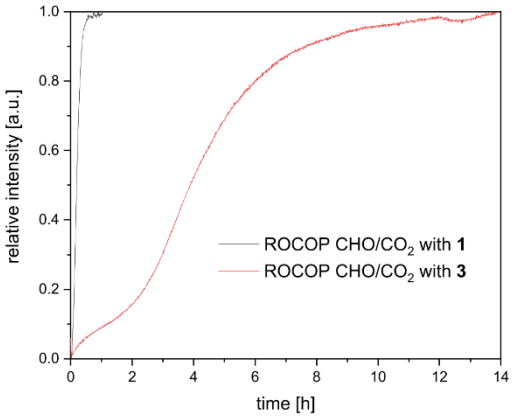

Figure S9. Relative intensity of the absorption of the C=O stretching bond in PCHC at 1750 cm^{-1} measured via *in situ* ATR-IR spectroscopy during the CHO/CO_2 copolymerization with catalysts **1** (black) and **3** (red).

7. ESI- and MALDI-MS of oligomeric PCHC synthesized with catalyst 3

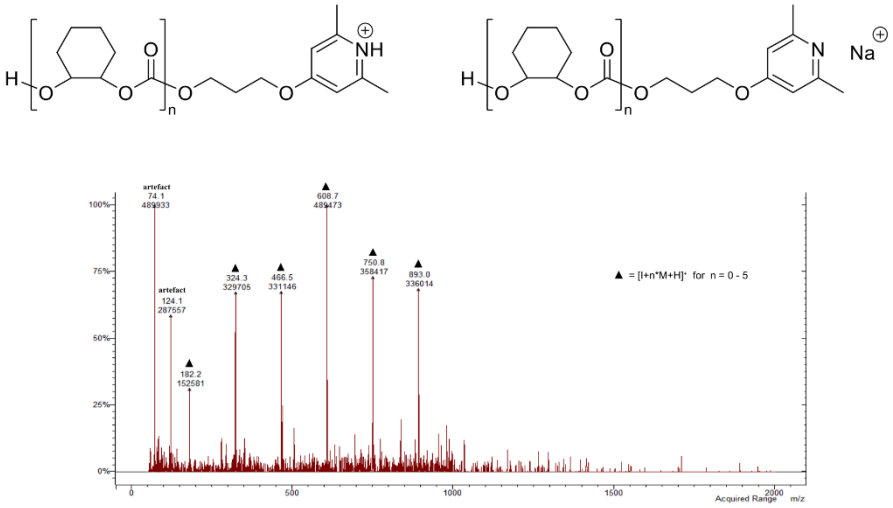

Figure S10. ESI-MS of oligomeric PCHC synthesized with catalyst **3** (signals at 74.1 and 124.1 m/z are artefacts from the spectrometer).

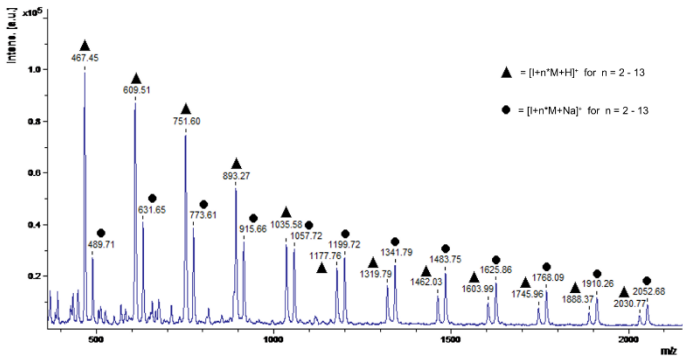

Figure S11. MALDI-MS of oligomeric PCHC synthesized with catalyst **3**.

8. NMR spectrum of catalyst 3 pressurized with CO_2

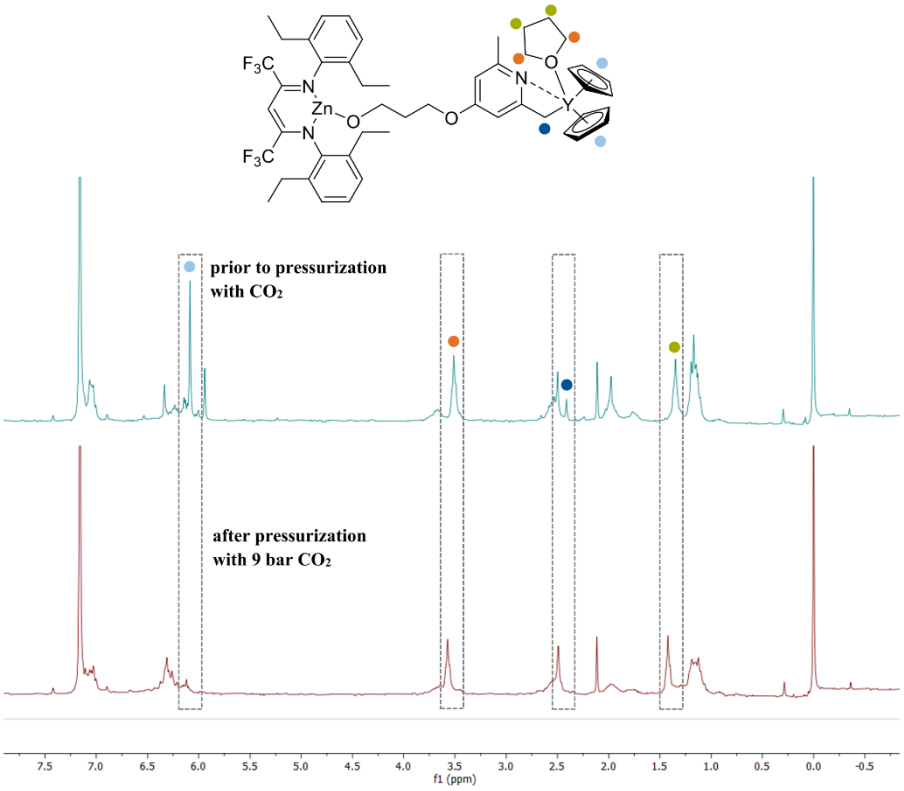

Figure S12. ^{1}H-NMR spectra of complex **3** prior and after pressurization with 9 bar CO_2 in benzene-d_6.

9. GPC traces of P2VP/PCHC and PIPOx/PCHC terpolymers

Table 1, entry 1

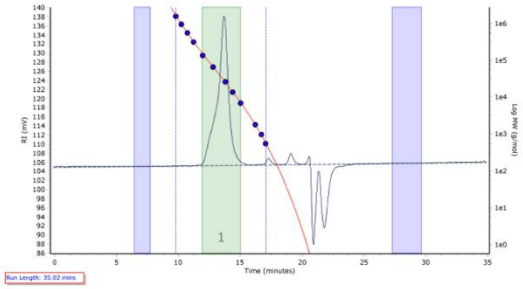

Molecular Weight Averages

Peak	Mp (g/mol)	Mn (g/mol)	Mw (g/mol)	Mz (g/mol)	Mz+1 (g/mol)	Mv (g/mol)	PD
Peak 1	27698	28225	37358	50659	67101	48409	1.324

Figure S13. GPC trace of a PCHC copolymer (table 1, entry 1).

Table 1, entry 2

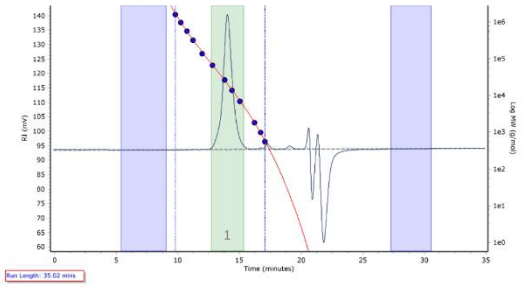

Molecular Weight Averages

Peak	Mp (g/mol)	Mn (g/mol)	Mw (g/mol)	Mz (g/mol)	Mz+1 (g/mol)	Mv (g/mol)	PD
Peak 1	20254	17495	21050	25181	30140	24511	1.203

Figure S14. GPC trace of a PCHC copolymer (table 1, entry 2).

Table 1, entry 3

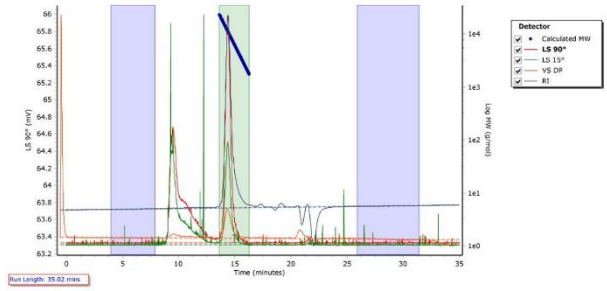

Molecular Weight Averages

Peak	Mp (g/mol)	Mn (g/mol)	Mw (g/mol)	Mz (g/mol)	Mz+1 (g/mol)	Mv (g/mol)	PD
Peak 1	11076	8743	10219	11277	12130	0	1.169

Figure S15. GPC traces of a P2VP aliquot (table 1, entry 3).

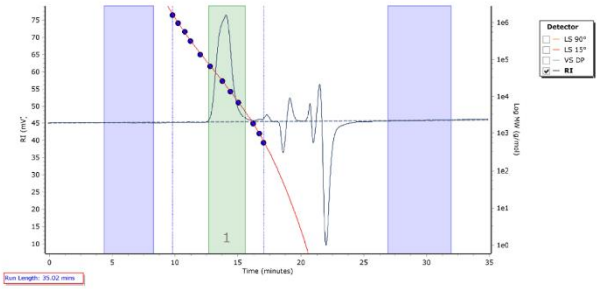

Molecular Weight Averages

Peak	Mp (g/mol)	Mn (g/mol)	Mw (g/mol)	Mz (g/mol)	Mz+1 (g/mol)	Mv (g/mol)	PD
Peak 1	19268	19975	24870	30357	35819	29543	1.245

Figure S16. GPC traces of a P2VP/PCHC terpolymer (table 1, entry 3).

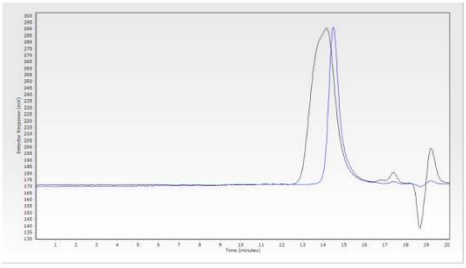

Figure S17. GPC traces (RI) of a P2VP aliquot (blue) and the corresponding P2VP/PCHC terpolymer (black, table 1, entry 3).

Table 1, entry 4

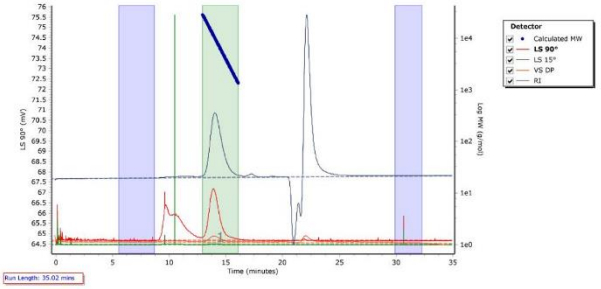

Molecular Weight Averages

Peak	Mp (g/mol)	Mn (g/mol)	Mw (g/mol)	Mz (g/mol)	Mz+1 (g/mol)	Mv (g/mol)	PD
Peak 1	10004	6976	9271	11394	13344	10460	1.329

Figure S18. GPC traces of a P2VP aliquot (table 1, entry 4).

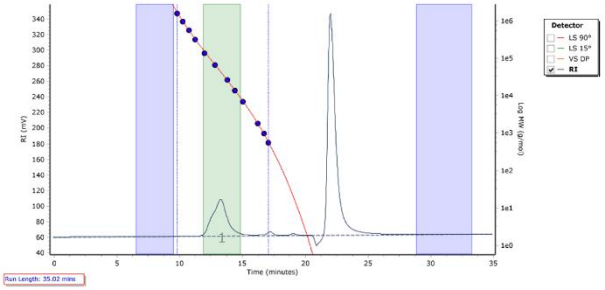

Molecular Weight Averages

Peak	Mp (g/mol)	Mn (g/mol)	Mw (g/mol)	Mz (g/mol)	Mz+1 (g/mol)	Mv (g/mol)	PD
Peak 1	42253	37153	50950	66150	81144	63919	1.371

Figure S19. GPC traces of a P2VP/PCHC terpolymer (table 1, entry 4).

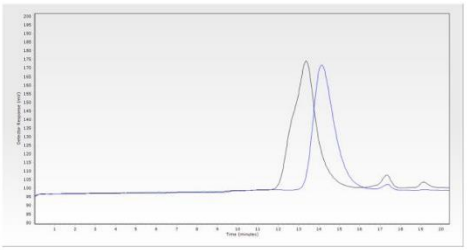

Figure S20. GPC traces (RI) of a P2VP aliquot (blue) and the corresponding P2VP/PCHC terpolymer (black, table 1, entry 4).

Table 1, entry 5

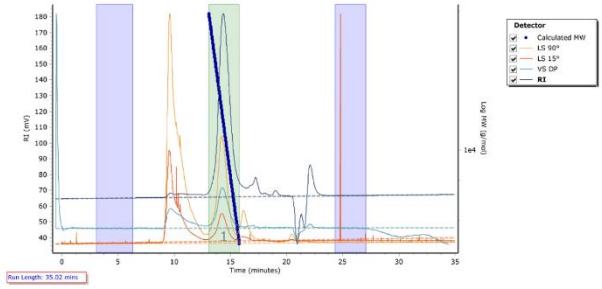

Figure S21. GPC traces of a P2VP aliquot (table 1, entry 5), the absolute molar mass was calculated via ^{1}H NMR spectroscopy.

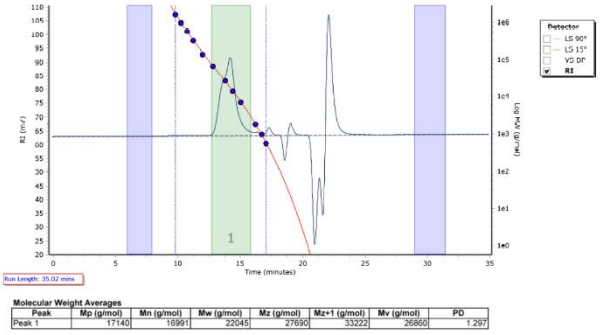

Molecular Weight Averages							
Peak	Mp (g/mol)	Mn (g/mol)	Mw (g/mol)	Mz (g/mol)	Mz+1 (g/mol)	Mv (g/mol)	PD
Peak 1	17140	16991	22045	27690	33222	26860	1.297

Figure S22. GPC traces of a P2VP/PCHC terpolymer (table 1, entry 5).

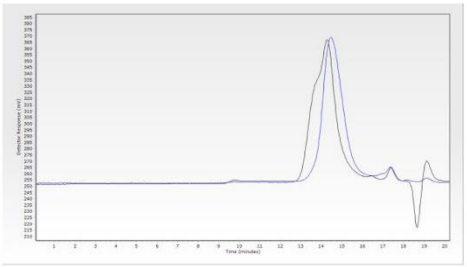

Figure S23. GPC traces (RI) of a P2VP aliquot (blue) and the corresponding P2VP/PCHC terpolymer (black, table 1, entry 5).

Table 1, entry 6

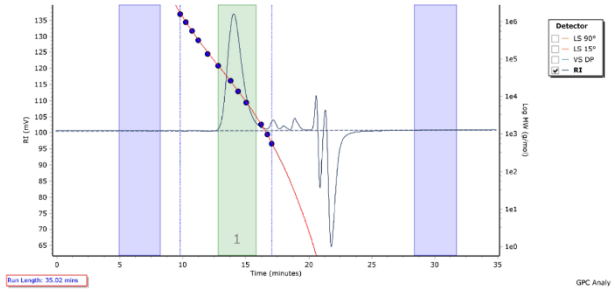

Figure S24. GPC traces of a PIPOx aliquot (table 1, entry 6), the absolute molar mass was calculated via ^{1}H NMR spectroscopy.

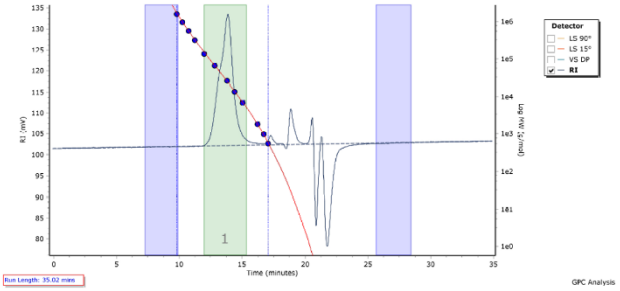

Molecular Weight Averages

Peak	Mp (g/mol)	Mn (g/mol)	Mw (g/mol)	Mz (g/mol)	Mz+1 (g/mol)	Mv (g/mol)	PD
Peak 1	23895	22995	31405	42061	54600	40346	1.366

Figure S25. GPC traces of a PIPOx/PCHC terpolymer (table 1, entry 6).

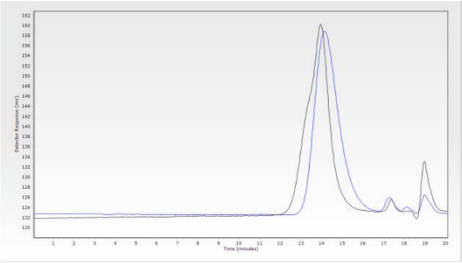

Figure S26. GPC traces (RI) of a PIPOx aliquot (blue) and the corresponding PIPOx/PCHC terpolymer (black, table 1, entry 6).

Table 1, entry 7

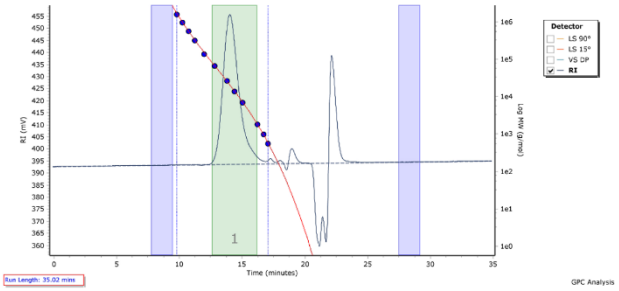

Figure S27. GPC traces of a PIPOx aliquot (table 1, entry 7), the absolute molar mass was calculated via ^{1}H NMR spectroscopy

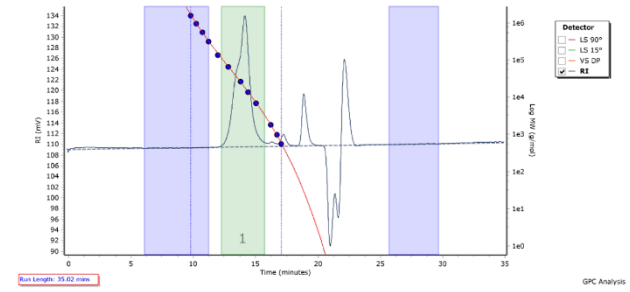

Molecular Weight Averages

Peak	Mp (g/mol)	Mn (g/mol)	Mw (g/mol)	Mz (g/mol)	Mz+1 (g/mol)	Mv (g/mol)	PD
Peak 1	18023	17657	24630	33474	43921	32047	1.395

Figure S28. GPC traces of a PIPOx/PCHC terpolymer (table 1, entry 7).

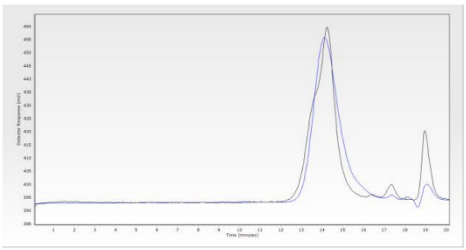

Figure S29. GPC traces (RI) of a PIPOx aliquot (blue) and the corresponding PIPOx/PCHC terpolymer (black, table 1, entry 7).

10. NMR after extraction/washing of an artificial P2VP/PCHC blend with methanol

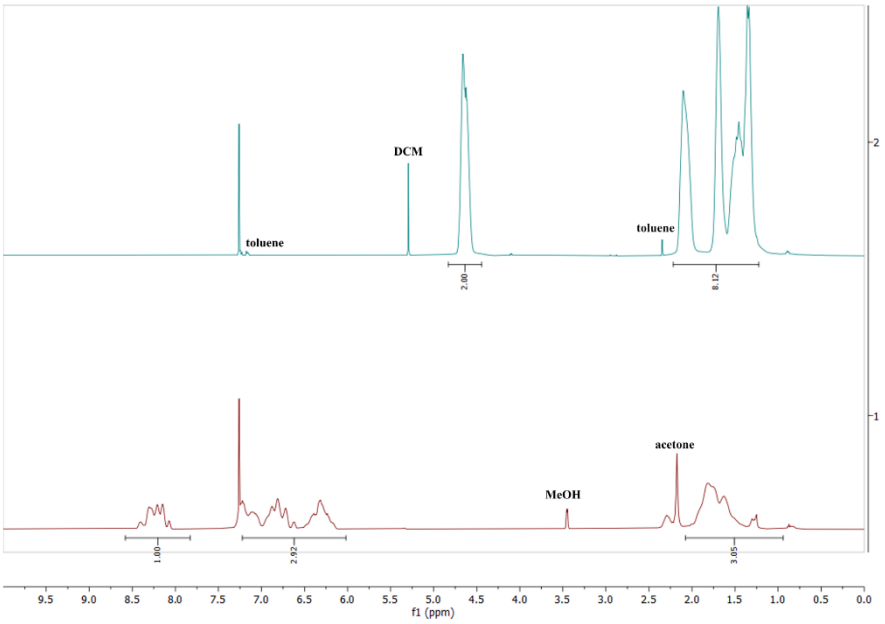

Figure S30. ^{1}H NMR spectra in chloroform-d of the methanol phase (1) and the remaining solid (2) of an artificial P2VP/PCHC blend (M_n(P2VP) = 22 kg/mol, M_n(PCHC) = 33 kg/mol) after extraction/washing with methanol.

11. NMR after extraction/washing of a P2VP/PCHC terpolymer with methanol

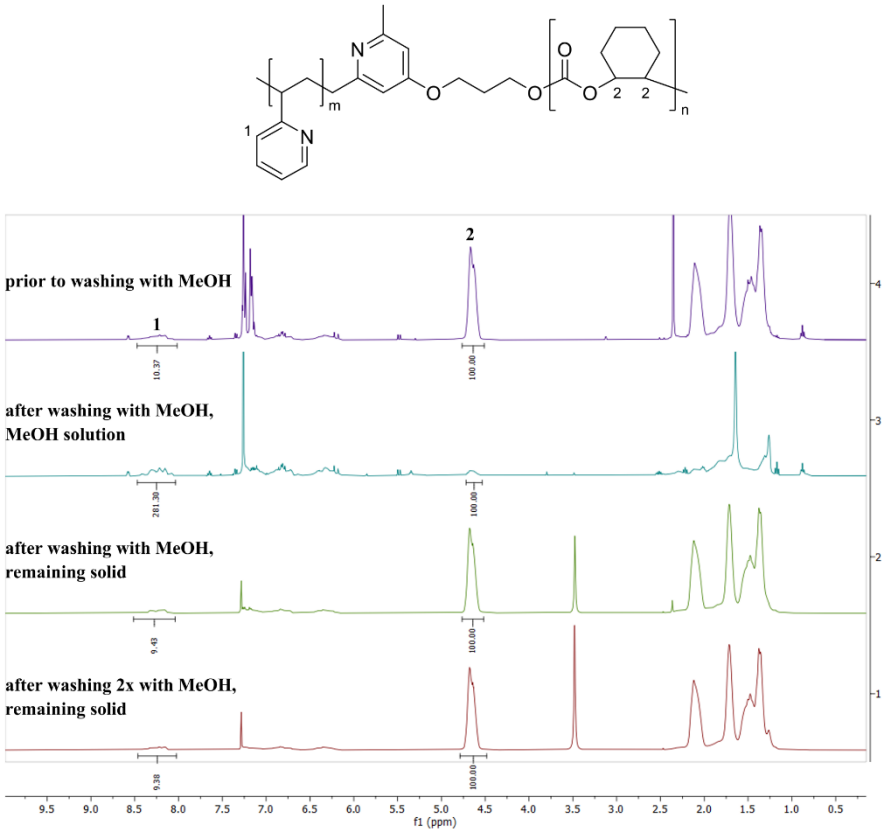

Figure S31. NMR spectra of a P2VP/PCHC terpolymer (table 1, entry 4) prior (4) and after washing with methanol (3–1) in chloroform-d.

12. GPC after extraction/washing of a P2VP/PCHC terpolymer with methanol

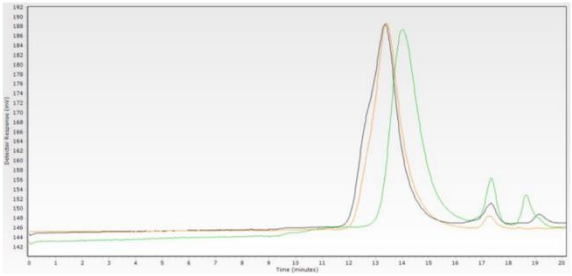

black:

Molecular Weight Averages

Peak	Mp (g/mol)	Mn (g/mol)	Mw (g/mol)	Mz (g/mol)	Mz+1 (g/mol)	Mv (g/mol)	PD
Peak 1	42253	37153	50950	66150	81144	63919	1.371

orange:

Molecular Weight Averages

Peak	Mp (g/mol)	Mn (g/mol)	Mw (g/mol)	Mz (g/mol)	Mz+1 (g/mol)	Mv (g/mol)	PD
Peak 1	40252	37096	44712	53524	62453	52193	1.205

green:

Molecular Weight Averages

Peak	Mp (g/mol)	Mn (g/mol)	Mw (g/mol)	Mz (g/mol)	Mz+1 (g/mol)	Mv (g/mol)	PD
Peak 1	22370	16163	21339	26722	31930	25948	1.32

Figure S32. GPC traces (RI) of a P2VP/PCHC terpolymer (table 1, entry 4) prior (black) and after washing with methanol (orange, remaining solid and green, methanol phase).

13. DSC Analysis of P2VP/PCHC terpolymer

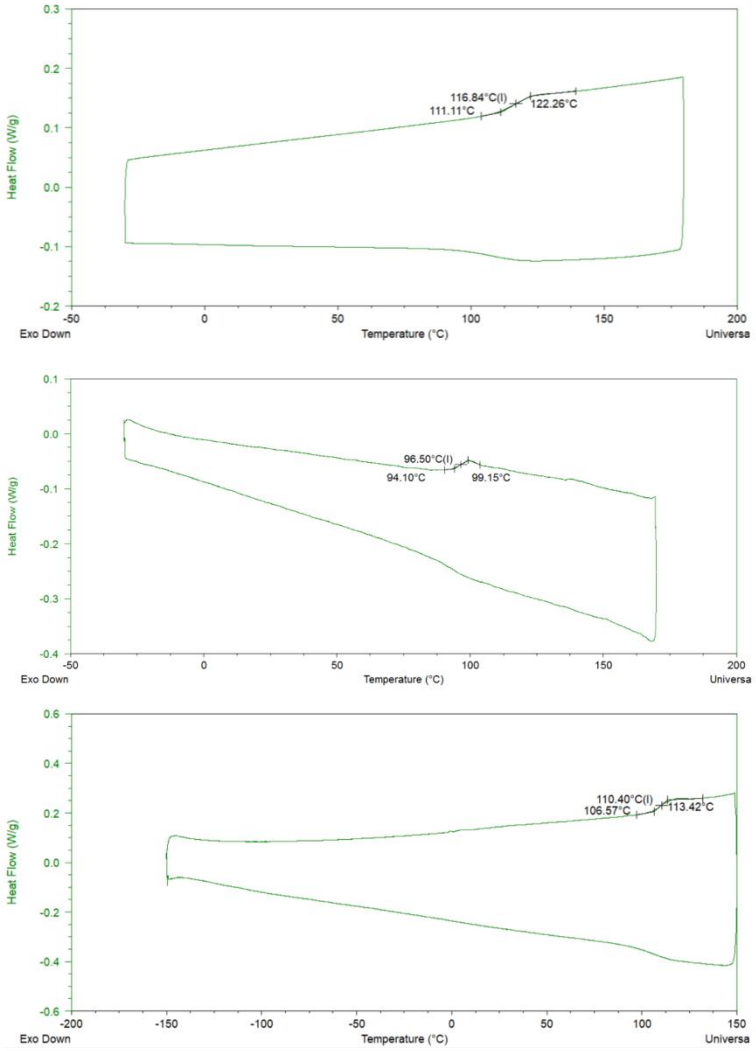

(1)

(2)

(3)

Figure S33. DSC measurement of PCHC (1), P2VP (2) and a P2VP/PCHC terpolymer (table 1, entry 3) (3).

24

14. TGA of P2VP/PCHC and PIPOx/PCHC terpolymers

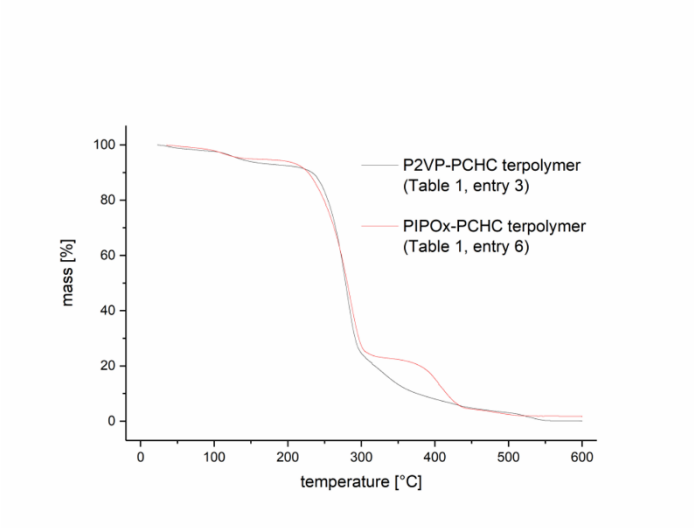

Figure S34. TGA of a P2VP/PCHC (table 1, entry 3) and a PIPOx/PCHC terpolymer (table 1, entry 6).

15. ESI-MS of oligomeric PIPOx synthesized with catalyst 3

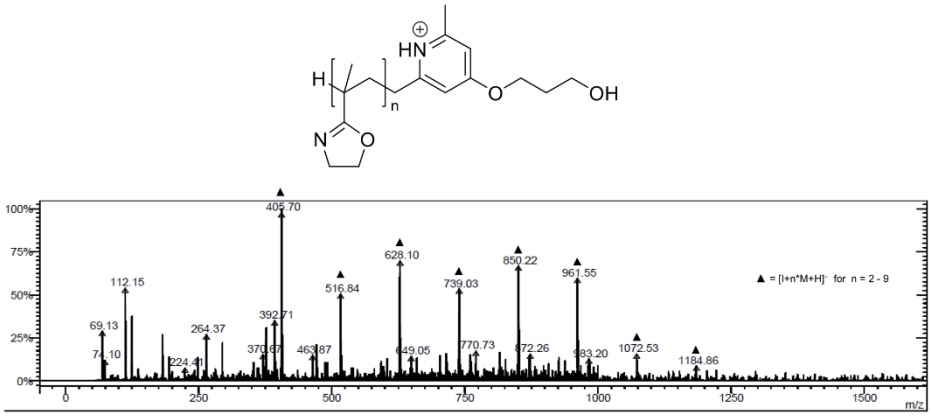

Figure S35. ESI-MS of oligomeric PIPOx synthesized with catalyst **3** (the signal at 112.15 m/z is the mass of the protonated monomer).

16. DSC Analysis of PIPOx/PCHC terpolymer

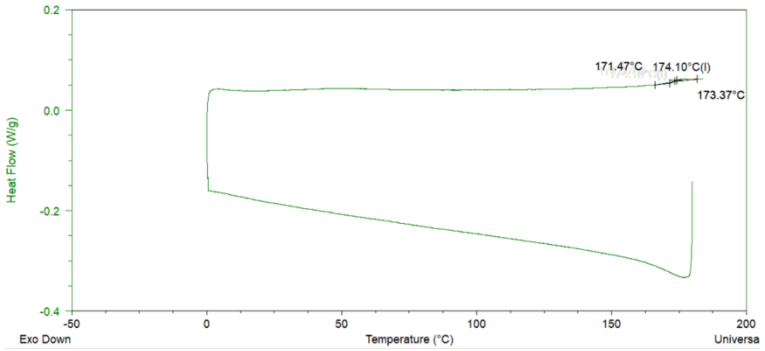

(1)

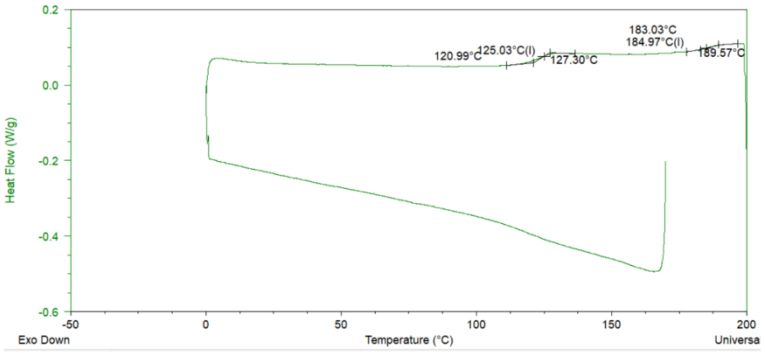

(2)

Figure S36. DSC measurement of PIPOx homopolymer (1) and of a PIPOx/PCHC terpolymer (table 1, entry 6) (2).

26

17. NMR spectra of P2VP/PCHC and PIPOx/PCHC terpolymers

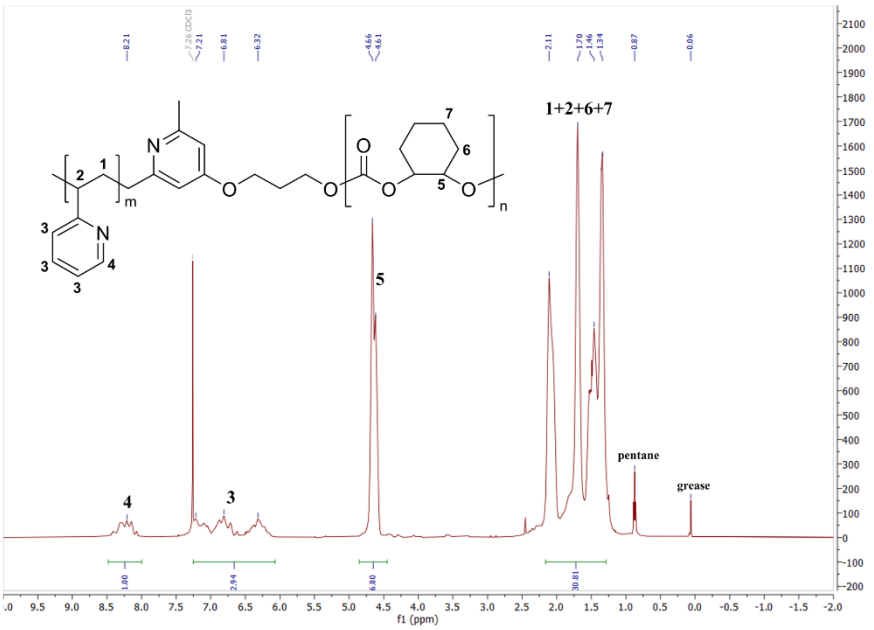

Figure S37. ^{1}H NMR spectrum of a P2VP/PCHC terpolymer (table 1, entry 5) in chloroform-d.

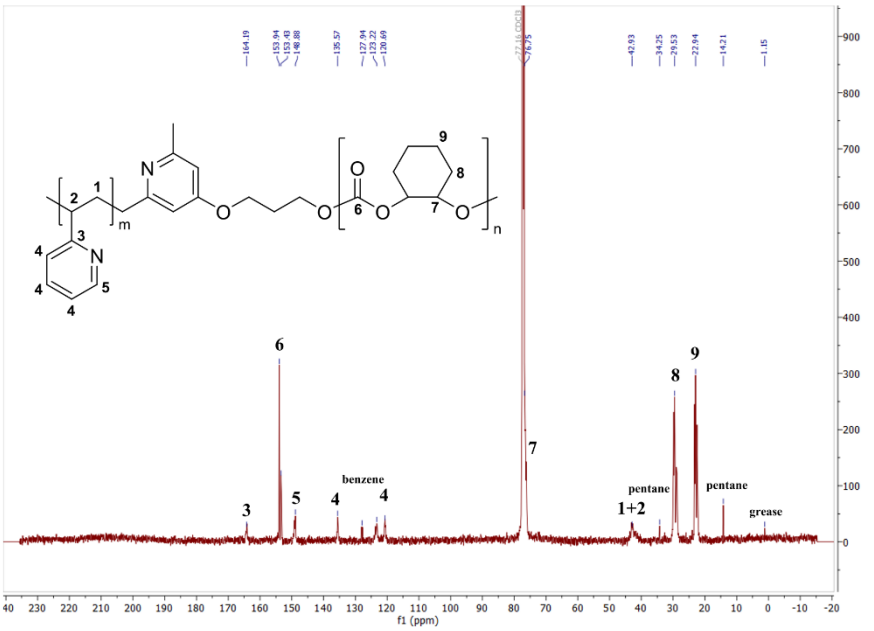

Figure S38. ^{13}C NMR spectrum of a P2VP/PCHC terpolymer (table 1, entry 5) in chloroform-d.

27

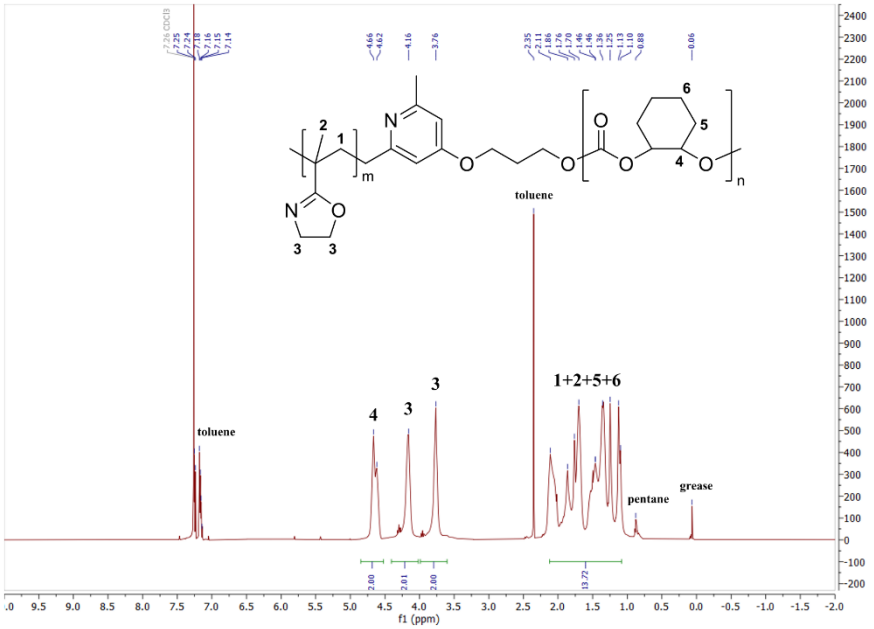

Figure S39. ^{1}H NMR spectrum of a PIPOx/PCHC terpolymer (table 1, entry 6) in chloroform-d.

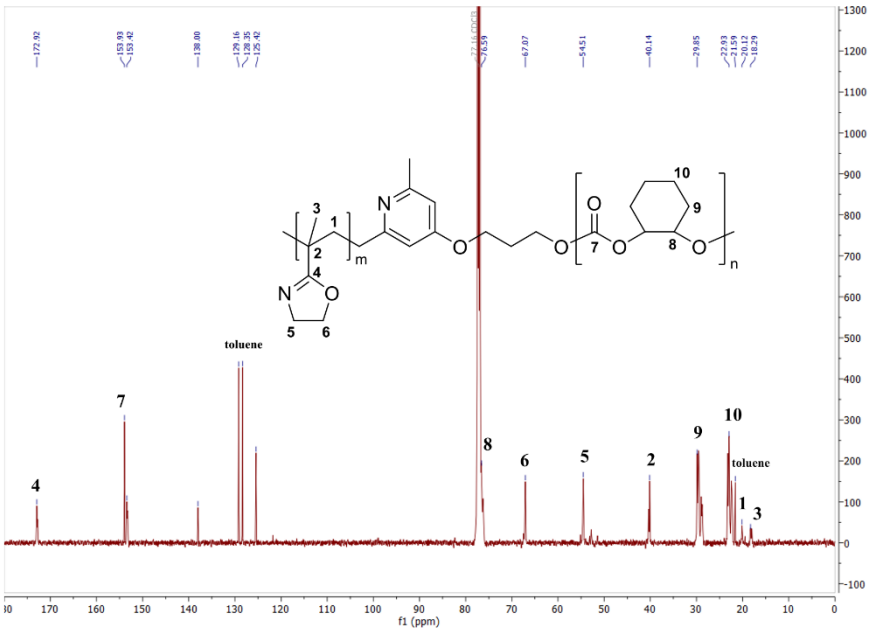

Figure S40. ^{13}C NMR spectrum of a PIPOx/PCHC terpolymer (table 1, entry 6) in chloroform-d.

9.4 List of figures

9.5 List of schemes

10. Copyright licenses

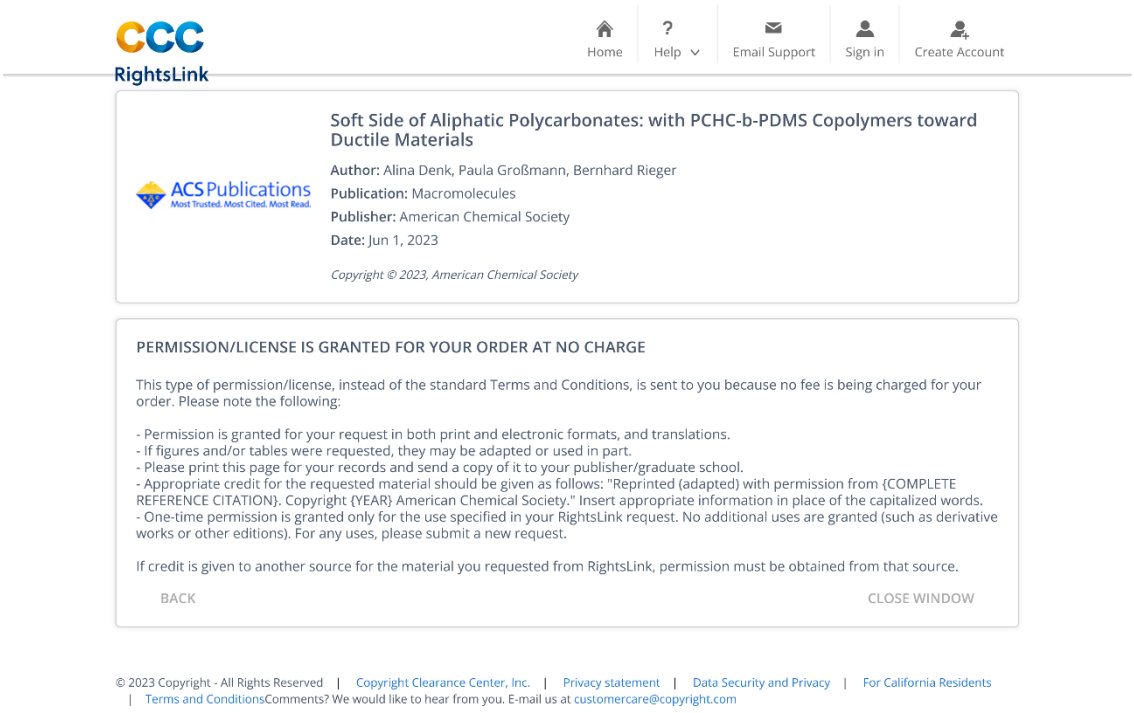

RightsLink

Home | Help | Email Support | Sign in | Create Account

ACS Publications
Most Trusted. Most Cited. Most Read.

Soft Side of Aliphatic Polycarbonates: with PCHC-b-PDMS Copolymers toward Ductile Materials

Author: Alina Denk, Paula Großmann, Bernhard Rieger
Publication: Macromolecules
Publisher: American Chemical Society
Date: Jun 1, 2023

Copyright © 2023, American Chemical Society

PERMISSION/LICENSE IS GRANTED FOR YOUR ORDER AT NO CHARGE

This type of permission/license, instead of the standard Terms and Conditions, is sent to you because no fee is being charged for your order. Please note the following:

- Permission is granted for your request in both print and electronic formats, and translations.
- If figures and/or tables were requested, they may be adapted or used in part.
- Please print this page for your records and send a copy of it to your publisher/graduate school.
- Appropriate credit for the requested material should be given as follows: "Reprinted (adapted) with permission from {COMPLETE REFERENCE CITATION}. Copyright {YEAR} American Chemical Society." Insert appropriate information in place of the capitalized words.
- One-time permission is granted only for the use specified in your RightsLink request. No additional uses are granted (such as derivative works or other editions). For any uses, please submit a new request.

If credit is given to another source for the material you requested from RightsLink, permission must be obtained from that source.

BACK CLOSE WINDOW

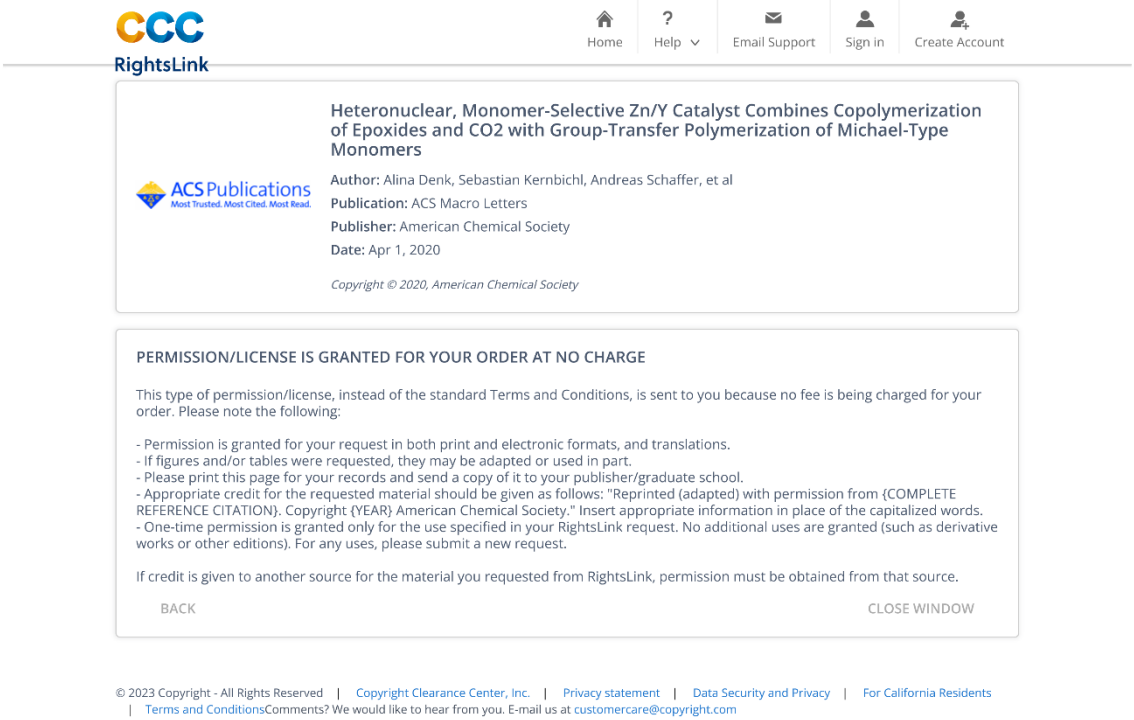

RightsLink

Home | Help | Email Support | Sign in | Create Account

ACS Publications
Most Trusted. Most Cited. Most Read.

Heteronuclear, Monomer-Selective Zn/Y Catalyst Combines Copolymerization of Epoxides and CO2 with Group-Transfer Polymerization of Michael-Type Monomers

Author: Alina Denk, Sebastian Kernbichl, Andreas Schaffer, et al
Publication: ACS Macro Letters
Publisher: American Chemical Society
Date: Apr 1, 2020

Copyright © 2020, American Chemical Society

PERMISSION/LICENSE IS GRANTED FOR YOUR ORDER AT NO CHARGE

This type of permission/license, instead of the standard Terms and Conditions, is sent to you because no fee is being charged for your order. Please note the following:

- Permission is granted for your request in both print and electronic formats, and translations.
- If figures and/or tables were requested, they may be adapted or used in part.
- Please print this page for your records and send a copy of it to your publisher/graduate school.
- Appropriate credit for the requested material should be given as follows: "Reprinted (adapted) with permission from {COMPLETE REFERENCE CITATION}. Copyright {YEAR} American Chemical Society." Insert appropriate information in place of the capitalized words.
- One-time permission is granted only for the use specified in your RightsLink request. No additional uses are granted (such as derivative works or other editions). For any uses, please submit a new request.

If credit is given to another source for the material you requested from RightsLink, permission must be obtained from that source.

BACK CLOSE WINDOW

SPRINGER NATURE LICENSE
TERMS AND CONDITIONS

Jun 24, 2023

This Agreement between Technical University Munich -- Alina Denk ("You") and Springer Nature ("Springer Nature") consists of your license details and the terms and conditions provided by Springer Nature and Copyright Clearance Center.

License Number	5575241109981
License date	Jun 24, 2023
Licensed Content Publisher	Springer Nature
Licensed Content Publication	Springer eBook
Licensed Content Title	Biobased Synthesis and Biodegradability of CO2-Based Polycarbonates
Licensed Content Author	Alina Denk, Bernhard Rieger
Licensed Content Date	Jan 1, 2022
Type of Use	Thesis/Dissertation
Requestor type	academic/university or research institute
Format	print and electronic
Portion	full article/chapter
Will you be translating?	no
Circulation/distribution	50000 or greater
Author of this Springer Nature content	yes
Title	Tunable polymer architectures for aliphatic poly(carbonates) via co- and terpolymerization of epoxides and CO2

Institution name	Technical University of Munich
Expected presentation date	Jul 2023
Requestor Location	Technical University Munich Lichtenbergstraße 4 Garching Bei München, other 85748 Germany Attn: Technical University Munich
Billing Type	Invoice
Billing Address	Technical University Munich Lichtenbergstraße 4 Garching Bei München, Germany 85748 Attn: Alina Denk
Total	0.00 EUR

Terms and Conditions

Springer Nature Customer Service Centre GmbH Terms and Conditions

The following terms and conditions ("Terms and Conditions") together with the terms specified in your [RightsLink] constitute the License ("License") between you as Licensee and Springer Nature Customer Service Centre GmbH as Licensor. By clicking 'accept' and completing the transaction for your use of the material ("Licensed Material"), you confirm your acceptance of and obligation to be bound by these Terms and Conditions.

1. Grant and Scope of License

1. 1. The Licensor grants you a personal, non-exclusive, non-transferable, non-sublicensable, revocable, world-wide License to reproduce, distribute, communicate to the public, make available, broadcast, electronically transmit or create derivative works using the Licensed Material for the purpose(s) specified in your RightsLink Licence Details only. Licenses are granted for the specific use requested in the order and for no other use, subject to these Terms and Conditions. You acknowledge and agree that the rights granted to you under this License do not include the right to modify, edit, translate, include in collective works, or create derivative works of the Licensed Material in whole or in part unless expressly stated in your RightsLink Licence Details. You may use the Licensed Material only as permitted under this Agreement and will not reproduce, distribute, display, perform, or otherwise use or exploit any Licensed Material in any way, in whole or in part, except as expressly permitted by this License.

1. 2. You may only use the Licensed Content in the manner and to the extent permitted by these Terms and Conditions, by your RightsLink Licence Details and by any applicable laws.

1. 3. A separate license may be required for any additional use of the Licensed Material, e.g. where a license has been purchased for print use only, separate

permission must be obtained for electronic re-use. Similarly, a License is only valid in the language selected and does not apply for editions in other languages unless additional translation rights have been granted separately in the License.

1. 4. Any content within the Licensed Material that is owned by third parties is expressly excluded from the License.

1. 5. Rights for additional reuses such as custom editions, computer/mobile applications, film or TV reuses and/or any other derivative rights requests require additional permission and may be subject to an additional fee. Please apply to journalpermissions@springernature.com or bookpermissions@springernature.com for these rights.

2. Reservation of Rights

Licensor reserves all rights not expressly granted to you under this License. You acknowledge and agree that nothing in this License limits or restricts Licensor's rights in or use of the Licensed Material in any way. Neither this License, nor any act, omission, or statement by Licensor or you, conveys any ownership right to you in any Licensed Material, or to any element or portion thereof. As between Licensor and you, Licensor owns and retains all right, title, and interest in and to the Licensed Material subject to the license granted in Section 1.1. Your permission to use the Licensed Material is expressly conditioned on you not impairing Licensor's or the applicable copyright owner's rights in the Licensed Material in any way.

3. Restrictions on use

3. 1. Minor editing privileges are allowed for adaptations for stylistic purposes or formatting purposes provided such alterations do not alter the original meaning or intention of the Licensed Material and the new figure(s) are still accurate and representative of the Licensed Material. Any other changes including but not limited to, cropping, adapting, and/or omitting material that affect the meaning, intention or moral rights of the author(s) are strictly prohibited.

3. 2. You must not use any Licensed Material as part of any design or trademark.

3. 3. Licensed Material may be used in Open Access Publications (OAP), but any such reuse must include a clear acknowledgment of this permission visible at the same time as the figures/tables/illustration or abstract and which must indicate that the Licensed Material is not part of the governing OA license but has been reproduced with permission. This may be indicated according to any standard referencing system but must include at a minimum 'Book/Journal title, Author, Journal Name (if applicable), Volume (if applicable), Publisher, Year, reproduced with permission from SNCSC'.

4. STM Permission Guidelines

4. 1. An alternative scope of license may apply to signatories of the STM Permissions Guidelines ("STM PG") as amended from time to time and made available at https://www.stm-assoc.org/intellectual-property/permissions/permissions-guidelines/.

4. 2. For content reuse requests that qualify for permission under the STM PG, and which may be updated from time to time, the STM PG supersede the terms and conditions contained in this License.

4. 3. If a License has been granted under the STM PG, but the STM PG no longer apply at the time of publication, further permission must be sought from the Rightsholder. Contact journalpermissions@springernature.com or bookpermissions@springernature.com for these rights.

5. Duration of License

5. 1. Unless otherwise indicated on your License, a License is valid from the date of purchase ("License Date") until the end of the relevant period in the below table:

Reuse in a medical communications project	Reuse up to distribution or time period indicated in License
Reuse in a dissertation/thesis	Lifetime of thesis
Reuse in a journal/magazine	Lifetime of journal/magazine
Reuse in a book/textbook	Lifetime of edition
Reuse on a website	1 year unless otherwise specified in the License
Reuse in a presentation/slide kit/poster	Lifetime of presentation/slide kit/poster. Note: publication whether electronic or in print of presentation/slide kit/poster may require further permission.
Reuse in conference proceedings	Lifetime of conference proceedings
Reuse in an annual report	Lifetime of annual report
Reuse in training/CME materials	Reuse up to distribution or time period indicated in License
Reuse in newsmedia	Lifetime of newsmedia
Reuse in coursepack/classroom materials	Reuse up to distribution and/or time period indicated in license

6. Acknowledgement

6. 1. The Licensor's permission must be acknowledged next to the Licensed Material in print. In electronic form, this acknowledgement must be visible at the same time as the figures/tables/illustrations or abstract and must be hyperlinked to the journal/book's homepage.

6. 2. Acknowledgement may be provided according to any standard referencing system and at a minimum should include "Author, Article/Book Title, Journal name/Book imprint, volume, page number, year, Springer Nature".

7. Reuse in a dissertation or thesis

7. 1. Where 'reuse in a dissertation/thesis' has been selected, the following terms apply: Print rights of the Version of Record are provided for; electronic rights for use only on institutional repository as defined by the Sherpa guideline (www.sherpa.ac.uk/romeo/) and only up to what is required by the awarding institution.

7. 2. For theses published under an ISBN or ISSN, separate permission is required. Please contact journalpermissions@springernature.com or bookpermissions@springernature.com for these rights.

7. 3. Authors must properly cite the published manuscript in their thesis according to current citation standards and include the following acknowledgement: '*Reproduced with permission from Springer Nature*'.

8. License Fee

You must pay the fee set forth in the License Agreement (the "License Fees"). All amounts payable by you under this License are exclusive of any sales, use, withholding, value added or similar taxes, government fees or levies or other assessments. Collection and/or remittance of such taxes to the relevant tax authority shall be the responsibility of the party who has the legal obligation to do so.

9. Warranty

9. 1. The Licensor warrants that it has, to the best of its knowledge, the rights to license reuse of the Licensed Material. **You are solely responsible for ensuring that the material you wish to license is original to the Licensor and does not carry the**

copyright of another entity or third party (as credited in the published version). If the credit line on any part of the Licensed Material indicates that it was reprinted or adapted with permission from another source, then you should seek additional permission from that source to reuse the material.

9. 2. EXCEPT FOR THE EXPRESS WARRANTY STATED HEREIN AND TO THE EXTENT PERMITTED BY APPLICABLE LAW, LICENSOR PROVIDES THE LICENSED MATERIAL "AS IS" AND MAKES NO OTHER REPRESENTATION OR WARRANTY. LICENSOR EXPRESSLY DISCLAIMS ANY LIABILITY FOR ANY CLAIM ARISING FROM OR OUT OF THE CONTENT, INCLUDING BUT NOT LIMITED TO ANY ERRORS, INACCURACIES, OMISSIONS, OR DEFECTS CONTAINED THEREIN, AND ANY IMPLIED OR EXPRESS WARRANTY AS TO MERCHANTABILITY OR FITNESS FOR A PARTICULAR PURPOSE. IN NO EVENT SHALL LICENSOR BE LIABLE TO YOU OR ANY OTHER PARTY OR ANY OTHER PERSON OR FOR ANY SPECIAL, CONSEQUENTIAL, INCIDENTAL, INDIRECT, PUNITIVE, OR EXEMPLARY DAMAGES, HOWEVER CAUSED, ARISING OUT OF OR IN CONNECTION WITH THE DOWNLOADING, VIEWING OR USE OF THE LICENSED MATERIAL REGARDLESS OF THE FORM OF ACTION, WHETHER FOR BREACH OF CONTRACT, BREACH OF WARRANTY, TORT, NEGLIGENCE, INFRINGEMENT OR OTHERWISE (INCLUDING, WITHOUT LIMITATION, DAMAGES BASED ON LOSS OF PROFITS, DATA, FILES, USE, BUSINESS OPPORTUNITY OR CLAIMS OF THIRD PARTIES), AND WHETHER OR NOT THE PARTY HAS BEEN ADVISED OF THE POSSIBILITY OF SUCH DAMAGES. THIS LIMITATION APPLIES NOTWITHSTANDING ANY FAILURE OF ESSENTIAL PURPOSE OF ANY LIMITED REMEDY PROVIDED HEREIN.

10. Termination and Cancellation

10. 1. The License and all rights granted hereunder will continue until the end of the applicable period shown in Clause 5.1 above. Thereafter, this license will be terminated and all rights granted hereunder will cease.

10. 2. Licensor reserves the right to terminate the License in the event that payment is not received in full or if you breach the terms of this License.

11. General

11. 1. The License and the rights and obligations of the parties hereto shall be construed, interpreted and determined in accordance with the laws of the Federal Republic of Germany without reference to the stipulations of the CISG (United Nations Convention on Contracts for the International Sale of Goods) or to Germany´s choice-of-law principle.

11. 2. The parties acknowledge and agree that any controversies and disputes arising out of this License shall be decided exclusively by the courts of or having jurisdiction for Heidelberg, Germany, as far as legally permissible.

11. 3. This License is solely for Licensor's and Licensee's benefit. It is not for the benefit of any other person or entity.

Questions? For questions on Copyright Clearance Center accounts or website issues please contact springernaturesupport@copyright.com or +1-855-239-3415 (toll free in the US) or +1-978-646-2777. For questions on Springer Nature licensing please visit https://www.springernature.com/gp/partners/rights-permissions-third-party-distribution

Other Conditions:

Version 1.4 - Dec 2022

11. References

[1] C. Chassenieux, D. Durand, P. Jyotishkumar, S. Thomas, in *Handbook of Biopolymer-Based Materials*, **2013**, pp. 1-6.

[2] S. C. Rasmussen, Revisiting the Early History of Synthetic Polymers: Critiques and New Insights, *Ambix* **2018**, *65*, 356-372.

[3] D. Feldman, Polymer History, *Designed Monomers and Polymers* **2008**, *11*, 1-15.

[4] L. H. Baekeland, The Synthesis, Constitution, and Uses of Bakelite, *Journal of Industrial & Engineering Chemistry* **1909**, *1*, 149-161.

[5] E. Baumann, Ueber einige Vinylverbindungen, *Liebigs Ann Chem* **1872**, *163*, 308-322.

[6] PlasticsEurope AISBL, *Plastics – the Facts 2022*, (June **2023**).

[7] H. Schnell, Polycarbonate, eine Gruppe neuartiger thermoplastischer Kunststoffe. Herstellung und Eigenschaften aromatischer Polyester der Kohlensäure, *Angew Chem* **1956**, *68*, 633-640.

[8] V. Serini, Polycarbonates, *Ullmann's Encyclopedia of Industrial Chemistry* **2000**.

[9] Covestro AG, *Managing challenging times, Roadshow Presentation*, https://www.covestro.com/en/investors/reports-and-presentations/ (June **2023**).

[10] G. Abts, T. Eckel, R. Wehrmann, Polycarbonates, *Ullmann's Encyclopedia of Industrial Chemistry* **2014**, 1-18.

[11] Covestro, "*Polycarbonate demand worldwide from 2012 to 2022, by application (in million tons)*", from https://www-statista-com.eaccess.tum.edu/statistics/750971/polycarbonate-demand-worldwide-by-application/, Statista Inc., retrieved June 24, 2023, **2018**.

[12] A. Kalair, N. Abas, M. S. Saleem, A. R. Kalair, N. Khan, Role of energy storage systems in energy transition from fossil fuels to renewables, *Energy Storage* **2021**, *3*, e135.

[13] European Bioplastics e.V., *Bioplastics market data*, https://www.european-bioplastics.org/market/ (June **2023**).

[14] J.-G. Rosenboom, R. Langer, G. Traverso, Bioplastics for a circular economy, *Nature Reviews Materials* **2022**, *7*, 117-137.

[15] A. Morschbacker, Bio-Ethanol Based Ethylene, *Polym Rev* **2009**, *49*, 79-84.

[16] T. Iwata, Biodegradable and Bio-Based Polymers: Future Prospects of Eco-Friendly Plastics, *Angew Chem Int Edit* **2015**, *54*, 3210-3215.

[17] F. P. Greenspan, S. M. Linder, Google Patents, **1961**.

[18] I. John, K. Muthukumar, A. Arunagiri, A review on the potential of citrus waste for D-Limonene, pectin, and bioethanol production, *International Journal of Green Energy* **2017**, *14*, 599-612.

[19] G. A. Luinstra, E. Borchardt, in *Synthetic Biodegradable Polymers* (Eds.: B. Rieger, A. Künkel, G. W. Coates, R. Reichardt, E. Dinjus, T. A. Zevaco), Springer Berlin Heidelberg, Berlin, Heidelberg, **2012**, pp. 29-48.

[20] J. Langanke, A. Wolf, J. Hofmann, K. Böhm, M. A. Subhani, T. E. Müller, W. Leitner, C. Gürtler, Carbon dioxide (CO2) as sustainable feedstock for polyurethane production, *Green Chem* **2014**, *16*, 1865-1870.

[21] H. Dominghaus, P. Elsner, P. Eyerer, T. Hirth, *Kunststoffe: Eigenschaften und Anwendungen, Vol. 7*, Springer-Verlag Berlin Heidelberg, **2008**.
[22] D. Freitag, G. Fengler, L. Morbitzer, Routes to New Aromatic Polycarbonates with Special Material Properties, *Angew Chem Int Edit* **1991**, *30*, 1598-1610.
[23] W. Zhou, J. Osby, Siloxane modification of polycarbonate for superior flow and impact toughness, *Polymer* **2010**, *51*, 1990-1999.
[24] M. Mehlman, Health Effects and Toxicity of Phosgene: Scientific Review, *Def Sci J* **1987**, *37*, 269-279.
[25] E. Matuszczak, M. D. Komarowska, W. Debek, A. Hermanowicz, The Impact of Bisphenol A on Fertility, Reproductive System, and Development: A Review of the Literature, *International Journal of Endocrinology* **2019**, *2019*, 4068717.
[26] B. J. P. Jansen, J. H. Kamps, E. Kung, H. Looij, L. Prada, W. J. D. Steendam, SABIC Innovative Plastics IP B.V. US7786246 B2, **2010**.
[27] H. H. Kung, Methanol synthesis, *Catal Rev* **1980**, *22*, 235-259.
[28] M. Hack, U. Koss, P. König, M. Rothaemel, H.-D. Holtmann, (Ed.: MG Technologies AG), MG Technologies AG US7015369 B2, **2006**.
[29] W. H. Carothers, F. J. V. Natta, Studies on Polymerization and Ring Formation. III. Glycol Esters of Carbonic Acid, *J Am Chem Soc* **1930**, *52*, 314-326.
[30] J. Feng, R.-X. Zhuo, X.-Z. Zhang, Construction of functional aliphatic polycarbonates for biomedical applications, *Prog Polym Sci* **2012**, *37*, 211-236.
[31] M. Dadsetan, E. M. Christenson, F. Unger, M. Ausborn, T. Kissel, A. Hiltner, J. M. Anderson, In vivo biocompatibility and biodegradation of poly(ethylene carbonate), *J Control Release* **2003**, *93*, 259-270.
[32] M. R. Kember, A. Buchard, C. K. Williams, Catalysts for CO2/epoxide copolymerisation, *Chem Commun* **2011**, *47*, 141-163.
[33] S. Inoue, H. Koinuma, T. Tsuruta, Copolymerization of carbon dioxide and epoxide, *J Polym Sci Pol Lett* **1969**, *7*, 287-292.
[34] K. Soga, E. Imai, I. Hattori, Alternating Copolymerization of CO2 and Propylene Oxide with the Catalysts Prepared from Zn(OH)2 and Various Dicarboxylic Acids, *Polym J* **1981**, *13*, 407-410.
[35] S. Klaus, M. W. Lehenmeier, E. Herdtweck, P. Deglmann, A. K. Ott, B. Rieger, Mechanistic Insights into Heterogeneous Zinc Dicarboxylates and Theoretical Considerations for CO2–Epoxide Copolymerization, *J Am Chem Soc* **2011**, *133*, 13151-13161.
[36] T. Aida, M. Ishikawa, S. Inoue, Alternating copolymerization of carbon dioxide and epoxide catalyzed by the aluminum porphyrin-quaternary organic salt or -triphenylphosphine system. Synthesis of polycarbonate with well-controlled molecular weight, *Macromolecules* **1986**, *19*, 8-13.
[37] G. A. Luinstra, G. R. Haas, F. Molnar, V. Bernhart, R. Eberhardt, B. Rieger, On the Formation of Aliphatic Polycarbonates from Epoxides with Chromium(III) and Aluminum(III) Metal–Salen Complexes, *Chem - Eur J* **2005**, *11*, 6298-6314.
[38] D. J. Darensbourg, M. W. Holtcamp, Catalytic Activity of Zinc(II) Phenoxides Which Possess Readily Accessible Coordination Sites. Copolymerization and Terpolymerization of Epoxides and Carbon Dioxide, *Macromolecules* **1995**, *28*, 7577-7579.
[39] D. J. Darensbourg, M. W. Holtcamp, G. E. Struck, M. S. Zimmer, S. A. Niezgoda, P. Rainey, J. B. Robertson, J. D. Draper, J. H. Reibenspies, Catalytic Activity of a Series of Zn(II) Phenoxides for the Copolymerization of Epoxides and Carbon Dioxide, *J Am Chem Soc* **1999**, *121*, 107-116.

[40] K. Soga, Y. Tazuke, S. Hosoda, S. Ikeda, Polymerization of propylene carbonate, *Journal of Polymer Science: Polymer Chemistry Edition* **1977**, *15*, 219-229.
[41] S. D. Allen, D. R. Moore, E. B. Lobkovsky, G. W. Coates, High-Activity, Single-Site Catalysts for the Alternating Copolymerization of CO2 and Propylene Oxide, *J Am Chem Soc* **2002**, *124*, 14284-14285.
[42] K. Nakano, T. Kamada, K. Nozaki, Selective Formation of Polycarbonate over Cyclic Carbonate: Copolymerization of Epoxides with Carbon Dioxide Catalyzed by a Cobalt(III) Complex with a Piperidinium End-Capping Arm, *Angew Chem Int Edit* **2006**, *45*, 7274-7277.
[43] W. J. Kruper, D. D. Dellar, Catalytic Formation of Cyclic Carbonates from Epoxides and CO2 with Chromium Metalloporphyrinates, *J Org Chem* **1995**, *60*, 725-727.
[44] S. Mang, A. I. Cooper, M. E. Colclough, N. Chauhan, A. B. Holmes, Copolymerization of CO2 and 1,2-Cyclohexene Oxide Using a CO2-Soluble Chromium Porphyrin Catalyst, *Macromolecules* **2000**, *33*, 303-308.
[45] T. A. Zevaco, J. Sypien, A. Janssen, O. Walter, E. Dinjus, Aluminum bisphenoxides: Promising challengers for a catalyzed copolymerization of cyclohexene oxide with CO2, *Catalysis Today* **2006**, *115*, 151-161.
[46] X.-B. Lu, L. Shi, Y.-M. Wang, R. Zhang, Y.-J. Zhang, X.-J. Peng, Z.-C. Zhang, B. Li, Design of Highly Active Binary Catalyst Systems for CO2/Epoxide Copolymerization: Polymer Selectivity, Enantioselectivity, and Stereochemistry Control, *J Am Chem Soc* **2006**, *128*, 1664-1674.
[47] D. J. Darensbourg, J. C. Yarbrough, Mechanistic Aspects of the Copolymerization Reaction of Carbon Dioxide and Epoxides, Using a Chiral Salen Chromium Chloride Catalyst, *J Am Chem Soc* **2002**, *124*, 6335-6342.
[48] R. Eberhardt, M. Allmendinger, B. Rieger, DMAP/Cr(III) Catalyst Ratio: The Decisive Factor for Poly(propylene carbonate) Formation in the Coupling of CO2 and Propylene Oxide, *Macromol Rapid Comm* **2003**, *24*, 194-196.
[49] D. J. Darensbourg, R. M. Mackiewicz, A. L. Phelps, D. R. Billodeaux, Copolymerization of CO2 and Epoxides Catalyzed by Metal Salen Complexes, *Accounts of Chemical Research* **2004**, *37*, 836-844.
[50] S. Klaus, M. W. Lehenmeier, C. E. Anderson, B. Rieger, Recent advances in CO2/epoxide copolymerization—New strategies and cooperative mechanisms, *Coordin Chem Rev* **2011**, *255*, 1460-1479.
[51] D. J. Darensbourg, R. M. Mackiewicz, J. L. Rodgers, A. L. Phelps, (Salen)CrIIIX Catalysts for the Copolymerization of Carbon Dioxide and Epoxides: Role of the Initiator and Cocatalyst, *Inorg Chem* **2004**, *43*, 1831-1833.
[52] D. J. Darensbourg, R. M. Mackiewicz, J. L. Rodgers, C. C. Fang, D. R. Billodeaux, J. H. Reibenspies, Cyclohexene Oxide/CO2 Copolymerization Catalyzed by Chromium(III) Salen Complexes and N-Methylimidazole: Effects of Varying Salen Ligand Substituents and Relative Cocatalyst Loading, *Inorg Chem* **2004**, *43*, 6024-6034.
[53] J. E. Seong, S. J. Na, A. Cyriac, B.-W. Kim, B. Y. Lee, Terpolymerizations of CO2, Propylene Oxide, and Various Epoxides Using a Cobalt(III) Complex of Salen-Type Ligand Tethered by Four Quaternary Ammonium Salts, *Macromolecules* **2010**, *43*, 903-908.
[54] S. S, J. K. Min, J. E. Seong, S. J. Na, B. Y. Lee, A Highly Active and Recyclable Catalytic System for CO2/Propylene Oxide Copolymerization, *Angew Chem Int Edit* **2008**, *47*, 7306-7309.

[55] S. J. Na, S. S, A. Cyriac, B. E. Kim, J. Yoo, Y. K. Kang, S. J. Han, C. Lee, B. Y. Lee, Elucidation of the Structure of a Highly Active Catalytic System for CO2/Epoxide Copolymerization: A salen-Cobaltate Complex of an Unusual Binding Mode, *Inorg Chem* **2009**, *48*, 10455-10465.

[56] M. Cheng, E. B. Lobkovsky, G. W. Coates, Catalytic Reactions Involving C1 Feedstocks: New High-Activity Zn(II)-Based Catalysts for the Alternating Copolymerization of Carbon Dioxide and Epoxides, *J Am Chem Soc* **1998**, *120*, 11018-11019.

[57] D. R. Moore, M. Cheng, E. B. Lobkovsky, G. W. Coates, Electronic and Steric Effects on Catalysts for CO2/Epoxide Polymerization: Subtle Modifications Resulting in Superior Activities, *Angew Chem Int Edit* **2002**, *41*, 2599-2602.

[58] M. Reiter, A. Kronast, S. Kissling, B. Rieger, In Situ Generated ABA Block Copolymers from CO2, Cyclohexene Oxide, and Poly(dimethylsiloxane)s, *ACS Macro Letters* **2016**, *5*, 419-423.

[59] M. Reiter, S. Vagin, A. Kronast, C. Jandl, B. Rieger, A Lewis acid β-diiminato-zinc-complex as all-rounder for co- and terpolymerisation of various epoxides with carbon dioxide, *Chem Sci* **2017**, *8*, 1876-1882.

[60] M. H. Chisholm, J. Gallucci, K. Phomphrai, Coordination Chemistry and Reactivity of Monomeric Alkoxides and Amides of Magnesium and Zinc Supported by the Diiminato Ligand CH(CMeNC6H3-2,6-iPr2)2. A Comparative Study, *Inorg Chem* **2002**, *41*, 2785-2794.

[61] D. R. Moore, M. Cheng, E. B. Lobkovsky, G. W. Coates, Mechanism of the Alternating Copolymerization of Epoxides and CO2 Using β-Diiminate Zinc Catalysts: Evidence for a Bimetallic Epoxide Enchainment, *J Am Chem Soc* **2003**, *125*, 11911-11924.

[62] M. Cheng, D. R. Moore, J. J. Reczek, B. M. Chamberlain, E. B. Lobkovsky, G. W. Coates, Single-Site β-Diiminate Zinc Catalysts for the Alternating Copolymerization of CO2 and Epoxides: Catalyst Synthesis and Unprecedented Polymerization Activity, *J Am Chem Soc* **2001**, *123*, 8738-8749.

[63] S. Kissling, P. T. Altenbuchner, M. W. Lehenmeier, E. Herdtweck, P. Deglmann, U. B. Seemann, B. Rieger, Mechanistic Aspects of a Highly Active Dinuclear Zinc Catalyst for the Co-polymerization of Epoxides and CO2, *Chem - Eur J* **2015**, *21*, 8148-8157.

[64] M. R. Kember, P. D. Knight, P. T. R. Reung, C. K. Williams, Highly Active Dizinc Catalyst for the Copolymerization of Carbon Dioxide and Cyclohexene Oxide at One Atmosphere Pressure, *Angew Chem Int Edit* **2009**, *48*, 931-933.

[65] A. Buchard, M. R. Kember, K. G. Sandeman, C. K. Williams, A bimetallic iron(III) catalyst for CO2/epoxide coupling, *Chem Commun (Camb)* **2011**, *47*, 212-214.

[66] A. M. Chapman, C. Keyworth, M. R. Kember, A. J. J. Lennox, C. K. Williams, Adding Value to Power Station Captured CO2: Tolerant Zn and Mg Homogeneous Catalysts for Polycarbonate Polyol Production, *ACS Catalysis* **2015**, *5*, 1581-1588.

[67] M. R. Kember, A. J. P. White, C. K. Williams, Highly Active Di- and Trimetallic Cobalt Catalysts for the Copolymerization of CHO and CO2 at Atmospheric Pressure, *Macromolecules* **2010**, *43*, 2291-2298.

[68] S. Kissling, M. W. Lehenmeier, P. T. Altenbuchner, A. Kronast, M. Reiter, P. Deglmann, U. B. Seemann, B. Rieger, Dinuclear zinc catalysts with unprecedented activities for the copolymerization of cyclohexene oxide and CO2, *Chem Commun* **2015**, *51*, 4579-4582.

[69] M. Reiter, Dissertation thesis, Technical University Munich (Munich), **2017**.
[70] C. M. Byrne, S. D. Allen, E. B. Lobkovsky, G. W. Coates, Alternating copolymerization of limonene oxide and carbon dioxide, *Journal of the American Chemical Society* **2004**, *126*, 11404-11405.
[71] C. M. Byrne, S. D. Allen, E. B. Lobkovsky, G. W. Coates, Alternating copolymerization of limonene oxide and carbon dioxide, *J Am Chem Soc* **2004**, *126*, 11404-11405.
[72] L. Peña Carrodeguas, J. González-Fabra, F. Castro-Gómez, C. Bo, A. W. Kleij, AlIII-Catalysed Formation of Poly(limonene)carbonate: DFT Analysis of the Origin of Stereoregularity, *Chem - Eur J* **2015**, *21*, 6115-6122.
[73] D. Zhang, S. K. Boopathi, N. Hadjichristidis, Y. Gnanou, X. Feng, Metal-Free Alternating Copolymerization of CO2 with Epoxides: Fulfilling "Green" Synthesis and Activity, *J Am Chem Soc* **2016**, *138*, 11117-11120.
[74] G.-W. Yang, Y.-Y. Zhang, R. Xie, G.-P. Wu, Scalable Bifunctional Organoboron Catalysts for Copolymerization of CO2 and Epoxides with Unprecedented Efficiency, *J Am Chem Soc* **2020**, *142*, 12245-12255.
[75] G. W. Coates, D. R. Moore, Discrete Metal-Based Catalysts for the Copolymerization of CO2 and Epoxides: Discovery, Reactivity, Optimization, and Mechanism, *Angew Chem Int Edit* **2004**, *43*, 6618-6639.
[76] Z. Liu, M. Torrent, K. Morokuma, Molecular Orbital Study of Zinc(II)-Catalyzed Alternating Copolymerization of Carbon Dioxide with Epoxide, *Organometallics* **2002**, *21*, 1056-1071.
[77] S. Kernbichl, B. Rieger, Aliphatic polycarbonates derived from epoxides and CO2: A comparative study of poly(cyclohexene carbonate) and poly(limonene carbonate), *Polymer* **2020**, *205*, 122667.
[78] H. Sugimoto, H. Ohtsuka, S. Inoue, Alternating copolymerization of carbon dioxide and epoxide catalyzed by an aluminum Schiff base–ammonium salt system, *J Polym Sci Pol Chem* **2005**, *43*, 4172-4186.
[79] A. Cyriac, S. H. Lee, J. K. Varghese, E. S. Park, J. H. Park, B. Y. Lee, Immortal CO2/Propylene Oxide Copolymerization: Precise Control of Molecular Weight and Architecture of Various Block Copolymers, *Macromolecules* **2010**, *43*, 7398-7401.
[80] O. Hauenstein, M. Reiter, S. Agarwal, B. Rieger, A. Greiner, Bio-based polycarbonate from limonene oxide and CO2 with high molecular weight, excellent thermal resistance, hardness and transparency, *Green Chem* **2016**, *18*, 760-770.
[81] A. Wurtz, Ueber das Aethylenoxyd, *Liebigs Ann Chem* **1859**, *110*, 125-128.
[82] D. L. Trent, Propylene Oxide, *Kirk-Othmer Encyclopedia of Chemical Technology* **2001**.
[83] M. G. Clerici, G. Bellussi, U. Romano, Synthesis of propylene oxide from propylene and hydrogen peroxide catalyzed by titanium silicalite, *J Catal* **1991**, *129*, 159-167.
[84] Q. Chen, E. J. Beckman, One-pot green synthesis of propylene oxide using in situ generated hydrogen peroxide in carbon dioxide, *Green Chem* **2008**, *10*, 934-938.
[85] N. Meunier, R. Chauvy, S. Mouhoubi, D. Thomas, G. De Weireld, Alternative production of methanol from industrial CO2, *Renewable Energy* **2020**, *146*, 1192-1203.

[86] F. Pontzen, W. Liebner, V. Gronemann, M. Rothaemel, B. Ahlers, CO2-based methanol and DME – Efficient technologies for industrial scale production, *Catalysis Today* **2011**, *171*, 242-250.
[87] J. Toyir, R. Miloua, N. E. Elkadri, M. Nawdali, H. Toufik, F. Miloua, M. Saito, Sustainable process for the production of methanol from CO2 and H2 using Cu/ZnO-based multicomponent catalyst, *Physics Procedia* **2009**, *2*, 1075-1079.
[88] M. Khanmohammadi, S. Amani, A. B. Garmarudi, A. Niaei, Methanol-to-propylene process: Perspective of the most important catalysts and their behavior, *Chinese Journal of Catalysis* **2016**, *37*, 325-339.
[89] H. Koempel, W. Liebner, in *Studies in Surface Science and Catalysis, Vol. 167* (Eds.: F. Bellot Noronha, M. Schmal, E. Falabella Sousa-Aguiar), Elsevier, **2007**, pp. 261-267.
[90] Z. Yu, L. Xu, Y. Wei, Y. Wang, Y. He, Q. Xia, X. Zhang, Z. Liu, A new route for the synthesis of propylene oxide from bio-glycerol derivated propylene glycol, *Chem Commun* **2009**, 3934-3936.
[91] R. A. Benkeser, R. E. Robinson, D. M. Sauve, O. H. Thomas, Reduction of Organic Compounds by Lithium in Low Molecular Weight Amines. I. Selective Reduction of Aromatic Hydrocarbons to Monoölefins, *J Am Chem Soc* **1955**, *77*, 3230-3233.
[92] H. Imamura, K. Nishimura, K. Sumioki, M. Fujimoto, Y. Sakata, Selective Hydrogenation of Benzene to Cyclohexadiene and Cyclohexene by Lanthanide Precipitates Obtained from Eu or Yb Metal Solutions in Liquid Ammonia, *Chemistry Letters* **2001**, *30*, 450-451.
[93] X. Huali, F. Yongxian, Z. Chunhui, D. Zexue, M. Enze, G. Zhonghua, L. Xiaonian, A review on heterogeneous solid catalysts and related catalytic mechanisms for epoxidation of olefins with H2O2, *Chemical and Biochemical Engineering Quarterly* **2008**, *22*, 25-39.
[94] G. Grigoropoulou, J. H. Clark, J. A. Elings, Recent developments on the epoxidation of alkenes using hydrogen peroxide as an oxidant, *Green Chem* **2003**, *5*, 1-7.
[95] R. T. Mathers, M. J. Shreve, E. Meyler, K. Damodaran, D. F. Iwig, D. J. Kelley, Synthesis and Polymerization of Renewable 1,3-Cyclohexadiene Using Metathesis, Isomerization, and Cascade Reactions with Late-metal Catalysts, *Macromol Rapid Comm* **2011**, *32*, 1338-1342.
[96] M. Winkler, C. Romain, M. A. R. Meier, C. K. Williams, Renewable polycarbonates and polyesters from 1,4-cyclohexadiene, *Green Chem* **2015**, *17*, 300-306.
[97] A. Wróblewska, The Epoxidation of Limonene over the TS-1 and Ti-SBA-15 Catalysts, *Molecules* **2014**, *19*.
[98] M. V. Cagnoli, S. G. Casuscelli, A. M. Alvarez, J. F. Bengoa, N. G. Gallegos, N. M. Samaniego, M. E. Crivello, G. E. Ghione, C. F. Pérez, E. R. Herrero, S. G. Marchetti, "Clean" limonene epoxidation using Ti-MCM-41 catalyst, *Applied Catalysis A: General* **2005**, *287*, 227-235.
[99] Y.-Y. Zhang, X.-H. Zhang, R.-J. Wei, B.-Y. Du, Z.-Q. Fan, G.-R. Qi, Synthesis of fully alternating polycarbonate with low Tg from carbon dioxide and bio-based fatty acid, *RSC Advances* **2014**, *4*, 36183-36188.
[100] B. Pachaly, F. Achenbach, C. Herzig, K. Mautner, WILEY-VCH, **2005**.
[101] W. Noll, Zur chemie und technologie der silicone, *Angew Chem* **1954**, *66*, 41-55.

[102] B. Pachaly, J. Weis, in *Organosilicon Chemistry III*, **1997**, pp. 478-483.
[103] O. W. Webster, W. R. Hertler, D. Y. Sogah, W. B. Farnham, T. V. RajanBabu, Group-transfer polymerization. 1. A new concept for addition polymerization with organosilicon initiators, *J Am Chem Soc* **1983**, *105*, 5706-5708.
[104] R. P. Quirk, J.-S. Kim, Mechanistic aspects of silicon-mediated polymerization (group transfer polymerization) of methyl methacrylate with ester enolate anions as nucleophilic catalysts, *J Phys Org Chem* **1995**, *8*, 242-248.
[105] P. M. Mai, A. H. E. Müller, Kinetics of group transfer polymerization of methyl methacrylate in tetrahydrofuran, 1. Effect of concentrations of catalyst and initiator on reaction rates, *Die Makromolekulare Chemie, Rapid Communications* **1987**, *8*, 99-107.
[106] O. W. Webster, in *New Synthetic Methods*, Springer Berlin Heidelberg, Berlin, Heidelberg, **2004**, pp. 1-34.
[107] S. Salzinger, B. Rieger, Rare Earth Metal-Mediated Group Transfer Polymerization of Vinylphosphonates, *Macromol Rapid Comm* **2012**, *33*, 1327-1345.
[108] H. Yasuda, H. Yamamoto, K. Yokota, S. Miyake, A. Nakamura, Synthesis of monodispersed high molecular weight polymers and isolation of an organolanthanide(III) intermediate coordinated by a penultimate poly(MMA) unit, *J Am Chem Soc* **1992**, *114*, 4908-4910.
[109] S. Collins, D. G. Ward, Group-transfer polymerization using cationic zirconocene compounds, *J Am Chem Soc* **1992**, *114*, 5460-5462.
[110] E. Y. X. Chen, Coordination Polymerization of Polar Vinyl Monomers by Single-Site Metal Catalysts, *Chem Rev* **2009**, *109*, 5157-5214.
[111] S. Collins, D. G. Ward, K. H. Suddaby, Group-Transfer Polymerization Using Metallocene Catalysts: Propagation Mechanisms and Control of Polymer Stereochemistry, *Macromolecules* **1994**, *27*, 7222-7224.
[112] U. B. Seemann, J. E. Dengler, B. Rieger, High-Molecular-Weight Poly(vinylphosphonate)s by Single-Component Living Polymerization Initiated by Rare-Earth-Metal Complexes, *Angew Chem Int Edit* **2010**, *49*, 3489-3491.
[113] P. T. Altenbuchner, B. S. Soller, S. Kissling, T. Bachmann, A. Kronast, S. I. Vagin, B. Rieger, Versatile 2-Methoxyethylaminobis(phenolate)yttrium Catalysts: Catalytic Precision Polymerization of Polar Monomers via Rare Earth Metal-Mediated Group Transfer Polymerization, *Macromolecules* **2014**, *47*, 7742-7749.
[114] A. Kronast, D. Reiter, P. T. Altenbuchner, S. I. Vagin, B. Rieger, 2-Methoxyethylamino-bis(phenolate)yttrium Catalysts for the Synthesis of Highly Isotactic Poly(2-vinylpyridine) by Rare-Earth Metal-Mediated Group Transfer Polymerization, *Macromolecules* **2016**, *49*, 6260-6267.
[115] S. Salzinger, U. B. Seemann, A. Plikhta, B. Rieger, Poly(vinylphosphonate)s Synthesized by Trivalent Cyclopentadienyl Lanthanide-Induced Group Transfer Polymerization, *Macromolecules* **2011**, *44*, 5920-5927.
[116] S. Salzinger, B. S. Soller, A. Plikhta, U. B. Seemann, E. Herdtweck, B. Rieger, Mechanistic Studies on Initiation and Propagation of Rare Earth Metal-Mediated Group Transfer Polymerization of Vinylphosphonates, *J Am Chem Soc* **2013**, *135*, 13030-13040.
[117] F. Adams, M. R. Machat, P. T. Altenbuchner, J. Ehrmaier, A. Pöthig, T. N. V. Karsili, B. Rieger, Toolbox of Nonmetallocene Lanthanides: Multifunctional Catalysts in Group-Transfer Polymerization, *Inorg Chem* **2017**, *56*, 9754-9764.

[118] F. Adams, P. Pahl, B. Rieger, Metal-Catalyzed Group-Transfer Polymerization: A Versatile Tool for Tailor-Made Functional (Co)Polymers, *Chem - Eur J* **2018**, *24*, 509-518.
[119] H. Kaneko, H. Nagae, H. Tsurugi, K. Mashima, End-Functionalized Polymerization of 2-Vinylpyridine through Initial C–H Bond Activation of N-Heteroaromatics and Internal Alkynes by Yttrium Ene–Diamido Complexes, *J Am Chem Soc* **2011**, *133*, 19626-19629.
[120] P. Pahl, C. Schwarzenböck, F. A. D. Herz, B. S. Soller, C. Jandl, B. Rieger, Core-First Synthesis of Three-Armed Star-Shaped Polymers by Rare Earth Metal-Mediated Group Transfer Polymerization, *Macromolecules* **2017**, *50*, 6569-6576.
[121] B. S. Soller, S. Salzinger, B. Rieger, Rare Earth Metal-Mediated Precision Polymerization of Vinylphosphonates and Conjugated Nitrogen-Containing Vinyl Monomers, *Chem Rev* **2016**, *116*, 1993-2022.
[122] M. M. Demir, M. Memesa, P. Castignolles, G. Wegner, PMMA/Zinc Oxide Nanocomposites Prepared by In-Situ Bulk Polymerization, *Macromol Rapid Comm* **2006**, *27*, 763-770.
[123] C. Schwarzenböck, A. Schaffer, P. Pahl, P. J. Nelson, R. Huss, B. Rieger, Precise synthesis of thermoresponsive polyvinylphosphonate-biomolecule conjugates via thiol–ene click chemistry, *Polym Chem* **2018**, *9*, 284-290.
[124] N.-G. Kang, B.-G. Kang, H.-D. Koh, M. Changez, J.-S. Lee, Block copolymers containing pyridine moieties: Precise synthesis and applications, *React Funct Polym* **2009**, *69*, 470-479.
[125] J. M. G. Cowie, V. Arrighi, *Polymers: chemistry and physics of modern materials*, CRC press, **2007**.
[126] C. Koning, J. Wildeson, R. Parton, B. Plum, P. Steeman, D. J. Darensbourg, Synthesis and physical characterization of poly(cyclohexane carbonate), synthesized from CO2 and cyclohexene oxide, *Polymer* **2001**, *42*, 3995-4004.
[127] S. Paul, C. Romain, J. Shaw, C. K. Williams, Sequence Selective Polymerization Catalysis: A New Route to ABA Block Copoly(ester-b-carbonate-b-ester), *Macromolecules* **2015**, *48*, 6047-6056.
[128] T. T. D. Chen, Y. Zhu, C. K. Williams, Pentablock Copolymer from Tetracomponent Monomer Mixture Using a Switchable Dizinc Catalyst, *Macromolecules* **2018**, *51*, 5346-5351.
[129] J. Zhang, B. Farias-Mancilla, M. Destarac, U. S. Schubert, D. J. Keddie, C. Guerrero-Sanchez, S. Harrisson, Asymmetric Copolymers: Synthesis, Properties, and Applications of Gradient and Other Partially Segregated Copolymers, *Macromol Rapid Comm* **2018**, *39*, 1800357.
[130] M. Fineman, S. D. Ross, Linear method for determining monomer reactivity ratios in copolymerization, *Journal of Polymer Science* **1950**, *5*, 259-262.
[131] N. Zhang, S. Salzinger, B. S. Soller, B. Rieger, Rare Earth Metal-Mediated Group-Transfer Polymerization: From Defined Polymer Microstructures to High-Precision Nano-Scaled Objects, *J Am Chem Soc* **2013**, *135*, 8810-8813.
[132] S. Chen, M. Xiao, S. Wang, D. Han, Y. Meng, Novel ternary block copolymerization of carbon dioxide with cyclohexene oxide and propylene oxide using zinc complex catalyst, *Journal of Polymer Research* **2012**, *19*, 9800.
[133] Y.-Y. Zhang, G.-W. Yang, G.-P. Wu, A Bifunctional β-Diiminate Zinc Catalyst with CO2/Epoxides Copolymerization and RAFT Polymerization Capacities for

Versatile Block Copolymers Construction, *Macromolecules* **2018**, *51*, 3640-3646.
[134] Y. Fan, G. Chen, J. Tanaka, T. Tateishi, l-Phe End-Capped Poly(l-lactide) as Macroinitiator for the Synthesis of Poly(l-lactide)-b-poly(l-lysine) Block Copolymer, *Biomacromolecules* **2005**, *6*, 3051-3056.
[135] D. J. Darensbourg, M. Ulusoy, O. Karroonnirum, R. R. Poland, J. H. Reibenspies, B. Çetinkaya, Highly Selective and Reactive (salan)CrCl Catalyst for the Copolymerization and Block Copolymerization of Epoxides with Carbon Dioxide, *Macromolecules* **2009**, *42*, 6992-6998.
[136] H. Yasuda, E. Ihara, Rare earth metal initiated polymerizations of polar and nonpolar monomers to give high molecular weight polymers with extremely narrow molecular weight distribution, *Macromol Chem Phys* **1995**, *196*, 2417-2441.
[137] R. Solaro, G. Cantoni, E. Chiellini, Polymerisability of different lactones and methyl methacrylate in the presence of various organoaluminium catalysts, *Eur Polym J* **1997**, *33*, 205-211.
[138] Y. Wang, Y. Zhao, Y. Ye, H. Peng, X. Zhou, X. Xie, X. Wang, F. Wang, A One-Step Route to CO2-Based Block Copolymers by Simultaneous ROCOP of CO2/Epoxides and RAFT Polymerization of Vinyl Monomers, *Angew Chem Int Edit* **2018**, *57*, 3593-3597.
[139] D. Freitag, G. Fengler, L. Morbitzer, Routes to New Aromatic Polycarbonates with Special Material Properties, *Angew. Chem. Int. Ed.* **1991**, *30*, 1598-1610.
[140] S. Kernbichl, M. Reiter, F. Adams, S. Vagin, B. Rieger, CO2-Controlled One-Pot Synthesis of AB, ABA Block, and Statistical Terpolymers from β-Butyrolactone, Epoxides, and CO2, *J Am Chem Soc* **2017**, *139*, 6787-6790.
[141] S. Kernbichl, M. Reiter, J. Mock, B. Rieger, Terpolymerization of β-Butyrolactone, Epoxides, and CO2: Chemoselective CO2-Switch and Its Impact on Kinetics and Material Properties, *Macromolecules* **2019**, *52*, 8476-8483.
[142] G. S. Sulley, G. L. Gregory, T. T. D. Chen, L. Peña Carrodeguas, G. Trott, A. Santmarti, K.-Y. Lee, N. J. Terrill, C. K. Williams, Switchable Catalysis Improves the Properties of CO2-Derived Polymers: Poly(cyclohexene carbonate-b-ε-decalactone-b-cyclohexene carbonate) Adhesives, Elastomers, and Toughened Plastics, *J Am Chem Soc* **2020**, *142*, 4367-4378.
[143] M. Owen, Why silicones behave funny, *Chem. Tech.* **1981**, *11*, 288-292.
[144] A. Denk, P. Großmann, B. Rieger, Soft Side of Aliphatic Polycarbonates: with PCHC-b-PDMS Copolymers toward Ductile Materials, *Macromolecules* **2023**, *56*, 4318-4324.
[145] Y. Wang, D. J. Darensbourg, Carbon dioxide-based functional polycarbonates: Metal catalyzed copolymerization of CO2 and epoxides, *Coord. Chem. Rev.* **2018**, *372*, 85-100.
[146] O. Hauenstein, S. Agarwal, A. Greiner, Bio-based polycarbonate as synthetic toolbox, *Nature Communications* **2016**, *7*.
[147] G. Li, Y. Qin, X. Wang, X. Zhao, F. Wang, Study on the influence of metal residue on thermal degradation of poly(cyclohexene carbonate), *J. Polym. Res.* **2011**, *18*, 1177-1183.
[148] L. Du, B. Qu, Y. Meng, Q. Zhu, Structural characterization and thermal and mechanical properties of poly(propylene carbonate)/MgAl-LDH exfoliation nanocomposite via solution intercalation, *Composites Science and Technology* **2006**, *66*, 913-918.

[149] A. Denk, E. Fulajtar, C. Troll, B. Rieger, Controlled Synthesis of Statistical Polycarbonates Based on Epoxides and CO2, *Macromolecular Materials and Engineering* **2023**, *n/a*, 2300097.
[150] A. Schaffer, M. Kränzlein, B. Rieger, Synthesis and Application of Functional Group-Bearing Pyridyl-Based Initiators in Rare Earth Metal-Mediated Group Transfer Polymerization, *Macromolecules* **2020**, *53*, 4345-4354.
[151] A. Denk, S. Kernbichl, A. Schaffer, M. Kränzlein, T. Pehl, B. Rieger, Heteronuclear, Monomer-Selective Zn/Y Catalyst Combines Copolymerization of Epoxides and CO2 with Group-Transfer Polymerization of Michael-Type Monomers, *ACS Macro Letters* **2020**, *9*, 571-575.

Tiotusen tändstickor av en trädstam
men ba' en enda sticka räcker för en skogsbrand!

("Självantänd" by Movits!)